THE APPLICATION AND EFFECTS OF VARIABLE DURATION CAMSHAFT SYSTEMS TO LIGHT DUTY DIESEL ENGINES

Tim Lancefield, Wolfson College

Doctor of Philosophy

Trinity Term 2002

ABSTRACT

The work described in this thesis was carried out to investigate the application of variable valve actuation (VVA) to light-duty diesel engines for use in passenger vehicles. The background to this was that there was little published on the subject and with advanced turbochargers, exhaust gas re-circulation systems and high pressure fuel injection systems reaching maturity it seemed likely that further enhancement of the air management in this type of engine, through VVA would receive greater interest.

The first section of this thesis discusses the external pressures on engine manufacturers, from legislation and from the customer expectations, which could be expected to influence the adoption of VVA, while looking at the criteria on which they would assess a VVA system prior to adoption.

Section two provides an overview of the effects of VVA and how they may be used to improve engine operation by highlighting the specific features of diesel engines, i.e. cold starting and compression ratio, part load fuel economy, full load torque and transient torque rise, that can be influenced by air management and what characteristics are required from the VVA system in order to provide improvements in these areas. Having identified the key features of a VVA system that would be suitable for use in light duty diesel engines section three presents a brief literature review and discusses the family of non-constant angular velocity VVA systems that were identified as having the correct characteristics and relative simplicity necessary for any system that might be made in high volume production. This section also provides a detailed analysis of one system of this type to highlight its behaviour and impact on valve train design.

Software was written to model the selected mechanism and produce the valve lift characteristics for use in simulating the engine's behaviour. Section four provides an overview of engine simulation techniques and some detail of the model constructed for this investigation. It also discusses the additional code and methodologies required to model the turbine, compressor and combustion processes, which required special treatment, and presents data to compare the behaviour of the model with the baseline of known engine behaviour.

Section five presents simulation results that show the following possible improvements: a) a 23% increase in torque, b) light part-load fuel economy improvements of 13% and c) transient rise to maximum torque times reduced from 2.3 seconds to 1.6 seconds. It also discusses the features of engine operation with VVA that provide the potential for these improvements in engine operation, quantifies the benefits that might be expected at a large number of operating conditions and discusses the interactions between the VVA and other systems such as the turbo-charger and EGR system.

Section six presents conclusions which beside the enumeration of the potential benefits and description of the key effects of VVA, highlights the need for test data to verify the extent to which the benefits can be realised in real engines and suggests areas for future research.

RADCLIFFE SCIENCE LIBRARY OXFORD
14 APR 2003

ACKNOWLEDGEMENTS

Many thanks are due to my supervisor Dr. Richard Stone for his invaluable guidance, advice and particularly for his support and encouragement during the course of this piece of work. Thanks are also owed to Dr Richard Osborne, of the Ford Motor Company and to Dr Les Smith of MIRA for the provision of the data necessary to establish and correlate the simulation models used.

Finally, thanks are owed to my colleagues at Mechadyne for their continued understanding and support and to the Company for the financial support required to allow this work to be completed.

ABBREVIATIONS

ABDC	After BDC
AFR	Air to fuel ratio.
ATDC	After TDC
BBDC	Before BDC
BDC	Bottom Dead Centre: The crank position when the piston is at its lowest position in the cylinder
BMEP/bmep	Brake mean effective pressure.
BSFC/bsfc	Brake specific fuel consumption
BTDC	Before TDC
CARB	The California Air Resources Board: A state run organisation that defines and enforces legislation on emissions from internal combustion engines in California.
CO	Carbon monoxide.
CO_2	Carbon dioxode.
CR	Compression ratio.
DOHC	Double over-head camshafts. Engine configuration with a separate camshaft for the intake and exhaust valves, where these camshafts are mounted in the cylinder head.
ECE	The Economic Commission for Europe
ECR	Effective compression ratio, defined from intake valve closing to top dead centre rather than from bottom dead centre to top dead centre as with the conventional compression ratio.
EGR	Exhaust gas re-circulation: The process of diverting some of the exhaust gases from the exhaust system into the intake manifold, under certain operating conditions to control engine emissions.
EIVC	Early intake valve closing. A valve timing strategy used to control engine load without throttling

EPA	The Environmental Protection Agency: An American Government organisation that defines and enforces legislation on matters relating to the protection of the environment.
EU	The European Union.
EVA	Term commonly used to describe direct acting electromagnetic valve actuation systems.
EVC	Exhaust Valve Closing: The crank angle at which the exhaust valve closes.
EVO	Exhaust Valve Opening: The crank angle at which the exhaust valve opens.
FMEP/fmep	Friction mean effective pressure. (Has positive values, such that imep-bmep=fmep)
HC	Unburned Hydrocarbon compounds found in internal combustion engine exhaust gases.
HCCI	Homogenous Charge Compression Ignition.
HLA	Hydraulic lash adjuster: removes the clearances between the cam, cam follower and valve stem.
IMEP/imep	Indicated mean effective pressure.
Internal EGR	The retention of exhaust gases inside the engine under certain circumstances to control emissions.
ISFC/isfc	Indicated specific fuel consumption.
IVC	Intake Valve Closing: The crank angle at which the intake valve closes.
IVO	Intake Valve Opening: The crank angle at which the intake valve opens.
LIVC	Late Intake Valve Closing; A valve timing strategy for controlling engine load without throttling
MAP	Manifold Absolute Pressure: The absolute pressure in the intake manifold.
NO_x	Oxides of Nitrogen formed under the action of high pressures and temperatures during combustion in internal combustion engines and contained in the exhaust gases.

OBD	On Board Diagnostics: Equipment or software to monitor the behaviour of emissions critical systems on a vehicle. Systems to perform this function are required by legislation.
PID/pid	Proportional, integral and derivative controller. Uses different P, I and D gains to multiply the error, integral of error and differential of error, respectively to calculate controller corrective output.
PM	Particulate matter – solid emissions from the combustion process.
PMEP/pmep	Pumping mean effective pressure. Calculated either from EVO to IVC or from BDC to BDC (+ve quantities represent positive work output during these intervals)
P_{max}	The maximum cylinder pressure, commonly used as a description of the maximum pressure the engine structure can reliably tolerate.
rack	Term used by some parts of the industry to describe the control input position of the variable inlet nozzles in VGTs
SOHC	Single over-head camshaft. Engine configuration with a single camshaft for the intake and exhaust valves, where the camshaft is mounted in the cylinder head.
SOC	Start of combustion.
SOI	Start of injection.
TDC	Top Dead Centre: The crank position when the piston is at its highest position in the cylinder
TDC(o)	TDC overlap, close to EVC and IVO.
TDC(f)	TDC firing.
VHT	Valve Head Throttling: A valve lift control strategy for controlling engine load without conventional throttling.
VGT	Variable geometry turbine: a turbine with variable inlet nozzle area and angle.
VNT	Alternative acronym for VGT
VVA	Variable valve actuation: A generic name for any method of controlling the opening and closing timings or lift characteristics of the valves of an internal combustion engine.

VVT	Variable valve timing: A less frequently used name equivalent to VVA.

LIST OF TABLES

Number	*Description*	*Page*
Table 1.3.1	Emissions Limits for gasoline powered passenger cars in the European Union (Knibb 1998)	4
Table 1.3.2	Emissions Limits for diesel powered passenger cars in the European Union (Pethers 1997)	5
Table 3.3.1.1	Typical dimensions for prototype single-slider non-constant velocity VVA systems	50
Table 5.1	Correspondence between VVA setting number, ramp bottom and ramp top valve timings, °after TDC(f) (Ramp heights 0.1mm opening and 0.2mm closing)	128
Table 5.1.3.1	Summary of imep values, resultant improvements over standard and the intake VVA settings optimised to achieve them, with standard exhaust valve timings	142
Table 5.1.4.1	Summary of imep values, resultant improvements over standard and the optimised intake and exhaust VVA settings used to achieve them	158
Table 5.3.1.2.1	Summary of controller characteristics	178

LIST OF FIGURES

Number	Description	Page
Figure 2.1.1	Typical valve timing for a standard gasoline engine	11
Figure 2.1.2	Improved valve timings for: a) Idle and b) Low part load	11
Figure 2.2.1	Valve timing for a standard diesel engine, (left), and improved idle (right) (Ramp top timings 0.1mm lift opening and 0.2 mm closing)	12
Figure 2.2.2	Improved diesel valve timings for low speed high load (left) and high speed high load (right.)	13
Figure 2.3.1	The key features of a cam profile.	13
Figure 2.3.2	The effect of cam duration on valve acceleration.	14
Figure 2.3.3	A family of cam acceleration diagrams for constant duration.	16
Figure 2.3.4	The effect of cam duration on cam curvature for a cam with roller follower. (Cam profiles as per *figure 2.3.3.*)	16
Figure 2.4.1.1	Effect of intake valve closing timing on effective compression ratio. (Lancefield *et al*, 2000)	20
Figure 2.4.4.1	Typical fixed valve timings (left) optimised low speed torque (right.) (Lancefield *et al*, 2000) (Ramp top timings 0.1mm lift opening and 0.2 mm closing)	23
Figure 3.1.2.1	Taxonomy of variable valve timing systems (Lancefield 1999)	29
Figure 3.1.4.1	Schematic of the mechanisms used to control the motion of un-constrained cam lobes.	32
Figure 3.1.4.2	Lost motion cam lobes with improved damping. (Beier *et al* 1994)	33
Figure 3.1.5.1	Gear mechanism for imposing cyclic motion onto a rotating shaft . (Ma, 1981)	36
Figure 3.1.5.2	Alternative method of actuating the epicyclic . (Phoenix and Phoenix 1991)	36
Figure 3.1.5.3	Link mechanism for generating cyclic speed fluctuations . (Mitchell, 1980)	37
Figure 3.1.5.4	Link mechanism as applied to a Yamaha motorcycle engine . (Scott and Yamaguchi, 1980)	38
Figure 3.1.5.5	Scotch yoke mechanism for generating cyclic speed fluctuations . (Frost, 1986)	38
Figure 3.1.5.6	Roller in slot "slider mechanism" for generating cyclic speed fluctuations . (Mitchell, 1978)	39

Figure 3.1.5.7	Double slider mechanism for generating cyclic speed fluctuations . (Parker and Kendrick, 1974)	40
Figure 3.1.5.8	The Rover VVC system with two double mechanisms one at each end of the head. Rear only shown. (Parker, 1994)	42
Figure 3.1.5.9	Four mechanism coupling. (Frost, 1987)	43
Figure 3.1.5.10	Standard cam drive arrangement (left) and the modified layout allowing drive shaft movement pivoted about the input gear centre. (Lancefield *et al* 2000)	44
Figure 3.1.5.11	A typical cam section "cam shell" (left) and its installation in a cylinder head (right.) (Lancefield *et al* 1993 and 2000)	45
Figure 3.2.1.1	Slider mechanism. (Lancefield *et al*, 1993)	46
Figure 3.2.1.2	Relative phase between a cam section and the drive shaft for differing drive shaft positions.	47
Figure 3.2.1.3	Mechanism phasing and typical result on the intake cam of a gasoline engine (top) and on intake and exhaust cams of a diesel engine (bottom).	47
Figure 3.3.1.1	Main features of the later Mitchell variable duration VVA mechanism (Lancefield *et al*, 1993)	49
Figure 3.3.2.1	The triangle that governs the operation of the device superimposed on a section through the mechanism	51
Figure 3.3.2.1.1	Angular velocity of the cam shell relative to the drive shaft ($\dot{C}$ - $\dot{D}$) for a variety of engine speeds at 3mm drive shaft eccentricity, for the geometry of System 1 in table 3.3.1.1.	54
Figure 3.3.2.1.2	Absolute angular velocity of the cam shell for ±1mm, ±2mm and ±3mm, drive shaft eccentricities at 5000 rpm engine speed, for the geometry of System 1 in table 3.3.1.1.	54
Figure 3.3.2.1.3	Absolute angular acceleration of the cam shell for a variety of drive shaft eccentricities and engine speeds, for the geometry of System 1 in *table 3.3.1.1.*	55
Figure 3.3.2.2.1	Geometry of a direct acting follower and cam.	55
Figure 3.4.1	The five fundamental valve train layouts. (Jacques, 1997)	57
Figure 3.4.2	Typical, modern direct acting tappet with hydraulic lash adjuster. (Dammers, 1997)	58
Figure 3.4.1.1	The key features of a cam profile and geometry for a valve train with direct acting tappet.	59
Figure 3.4.1.2	The effects of cam lift and period on eccentricity.	60
Figure 3.4.1.3	The effect of lift (left) and cam period (right) on spring requirements.	61
Figure 3.4.1.4	The effect of acceleration ratio (positive period to negative period) on instantaneous radius of curvature.	61

Figure 3.4.2.1	The eccentricity characteristics for a family of cam periods, with variable duration VVA (left) and fixed cams (right).	63
Figure 3.4.2.2	The acceleration characteristics for a family of fixed geometry cams with the same periods as in *figure 3.4.2.3*	64
Figure 3.4.2.3	The acceleration characteristics for a family of cam periods generated with variable duration VVA with the same periods as in *figure 3.4.2.2.*	64
Figure 3.4.2.4	The acceleration characteristic for the standard period cam, as shown in *figure 3.4.2.2*, and spring capability lines at varying engine speeds	65
Figure 3.4.3.1	The acceleration and spring capability characteristics for a family of cam periods generated with variable duration VVA with the same periods as in *figure 3.4.2.2*, but with a different cam design process.	66
Figure 4.2.1.1	Overview of the major sub-systems employed in the simulation model for the prediction of the effects of VVA on light-duty diesel operation.	77
Figure 4.2.2.1.1	Common-Rail injector with profiled and multi-shot characteristics (Hummel *et al* 2000)	83
Figure 4.2.3.2.1.1	Schematic of a pulse converting exhaust system junction. (Bassett *et al*, 1999)	88
Figure 4.3.1	Engine systems overview.	92
Figure 4.3.2.2.1	The output of the built in GT-Power Wiebe based combustion model when set to use all default settings.	95
Figure 4.3.2.2.2	The output of the 2-term Wiebe based combustion model proposed by Watson *et al* (1980)	96
Figure 4.3.2.2.3	Pilot and rate shaped injection characteristics (Hummel *et al* 2000)	97
Figure 4.3.2.2.4	The 3-term Wiebe combustion correlation	98
Figure 4.3.2.2.5	The effects of the shape factors on Wiebe curve shape.	99
Figure 4.3.2.2.6	Comparison of baseline and burn rate curves generated by the developed code at 1000 (left) and 4500 rpm (right).	99
Figure 4.3.2.3.1	Variable geometry turbine schematic with inlet guide vanes closed (top) and open (bottom)	100
Figure 4.3.2.3.2	Efficiency versus pressure ratio and mass flow rate charts for the turbine at four nozzle settings (Increasing rack moving anti-clockwise from closed nozzles top right.) Raw and extrapolated data. (Basic data shown as solid data points, estimated data shown as open data points and extrapolated data in contours)	101
Figure 4.3.2.3.3	1000 rpm full load, closed nozzle turbine operating locus and raw and extrapolated efficiency contours on pressure ratio and reduced mass flow ordinates.	102
Figure4.3.2.4.1	Raw compressor data from the manufacturer showing the boundary of the data and their stall line.	103

Figure 4.3.2.4.2	Extension of the compressor maps to higher speeds, pressure ratios and mass flows.	104
Figure 4.3.2.4.3	Additional high and low speed lines and data points extending the manufacturer's data lines added to the compressor map.	105
Figure 4.3.2.4.4	Operating locus of the compressor crossing the stall line	106
Figure 4.3.2.4.5	Truncation of the compressor efficiency characteristic caused by crossing the stall line	106
Figure 4.3.2.4.6	Compressor map extensions to lower speeds and into stall.	107
Figure 4.3.2.4.7	The completed compressor efficiency map showing the three regions of extrapolated data	108
Figure 4.3.3.1.1	Comparison of the model imep and bmep results with the baseline data.	109
Figure 4.3.3.1.2	Comparison of the isfc and bsfc characteristics of the model and baseline data.	109
Figure 4.3.3.1.3	Comparison of pmep and fmep characteristics of the model and the baseline data.	110
Figure 4.3.3.1.4	Comparison of the air mass flow rates for the model and the baseline.	111
Figure 4.3.3.1.5	The effect of air flow differences on air-fuel-ratio. (Fixed fuelling.)	112
Figure 4.3.3.1.6	Volumetric efficiency referred to manifold conditions	112
Figure 4.3.3.2.1.1	Correlation of normalised burn rate curves at 1000 (top left), 2000 rpm (top right), 3000 rpm (bottom left) and 4000 rpm (bottom right).	113
Figure 4.3.3.2.1.2	Maximum cylinder pressure and its timing.	114
Figure 4.3.3.2.1.3	Variation of pmax and its timing as a function of start of combustion.	115
Figure 4.3.3.2.2.1	Cylinder heat transfer as a percentage of fuel energy at full load.	116
Figure 4.3.3.3.1.1	Target boost level and those achieved by the model.	117
Figure 4.3.3.3.1.2	Turbine power.	117
Figure 4.3.3.3.1.3	Comparison of model and baseline turbine speeds and turbine nozzle positions	118
Figure 4.3.3.3.1.4	Turbine efficiency	118
Figure 4.3.3.3.1.5	Turbine operating locus for 1000 rpm full-load on the closed nozzle rack efficiency map. Also shown is the original data from the manufacturer used to generate the map	119
Figure 4.3.3.3.1.6	Turbine inlet and outlet temperatures and temperature differentials	120

Figure 4.3.3.3.2.1	Compressor efficiency.	121
Figure 4.3.3.3.2.2	Operating locus of the compressor at 1000 rpm and the area where measured data is used (Inside solid line)	122
Figure 4.3.3.3.2.3	Average compressor operating points - increasing speed upward and to the right	122
Figure 4.3.3.3.2.4	Compressor operating loci - increasing speed upward and to the right	123
Figure 5.1.2.1	Turbine speed versus simulation cycle number	131
Figure 5.1.2.2	Air mass flow rate versus cycle number for various initial conditions	132
Figure 5.1.2.3	AFR characteristic for various initial conditions.	133
Figure 5.1.2.4	imep characteristic for AFR controlled and fixed fuelling.	133
Figure 5.1.3.1	imep as a function of intake valve closing timing over the full speed range.	134
Figure 5.1.3.2	Percentage change in imep as a function of intake valve closing timing over the full speed range.	135
Figure 5.1.3.3	Volumetric efficiency referred to ambient conditions as a function of intake valve closing timing	136
Figure 5.1.3.4	Volumetric efficiency referred to manifold conditions as a function of intake valve closing timing	136
Figure 5.1.3.5	Work from TDC overlap to start of injection.	138
Figure 5.1.3.6	Work from TDC(o) to SOI.	139
Figure 5.1.3.7	Engine mass air flow rates	139
Figure 5.1.3.8	Absolute intake manifold pressure.	140
Figure 5.1.3.9	Compressor operating points for the operating speeds (1000 rpm bottom left, trend upwards to the right with increasing speed. Nominal valve timing).	141
Figure 5.1.3.10	pmep as a function of intake valve timing and engine speed	142
Figure 5.1.4.1	Variation in imep with varying exhaust valve opening timing and optimised intake valve closing.	143
Figure 5.1.4.2	Percentage change in imep (relative to standard exhaust valve timing) with varying exhaust valve opening timing and optimised intake valve closing.	144
Figure 5.1.4.3	Percentage change in air flow with varying EVO	144
Figure 5.1.4.4	The effect of exhaust VVA on isfc at 4500 rpm	145

Figure 5.1.4.5	Changes in expansion work with varying EVO	146
Figure 5.1.4.6	Change in exhaust pumping work with varying EVO	146
Figure 5.1.4.7	Change in total work from firing TDC to Overlap TDC with changing EVO	147
Figure 5.1.4.8	Cyclic maximum, average and minimum pressures in the pipe preceding turbine entry for 1800 rpm (left) and 4500 rpm (right) plotted against exhaust valve opening timing.	148
Figure 5.1.4.9	Variation in imep with VGT nozzle rack setting at 3800 rpm (left) and at 4500 rpm (right)	149
Figure 5.1.4.10	Variation of airflow with changing turbine rack and exhaust VVA at 3800 rpm (left) and 4500 rpm (right)	150
Figure 5.1.4.11	Work distribution in the expansion and exhaust strokes at 4500 rpm	151
Figure 5.1.4.12	Pumping loops at 4500 rpm with standard early and late EVO	152
Figure 5.1.4.13	Cylinder pressure traces with early and late EVO, at 4500 rpm, showing interference between cylinders 1 and 3	153
Figure 5.1.4.14	Turbine power at 4500 rpm, with varying rack and exhaust VVA settings	154
Figure 5.1.4.15	Converged, full load, cycle averaged compressor operating points for optimised intake and exhaust VVA.(1000 rpm lower left, increasing speed moving right)	154
Figure 5.1.4.16	Engine air flow and compressor efficiency at 4500 rpm for varying rack and exhaust VVA settings.	155
Figure 5.1.4.17	Percentage change in imep with 10% increased turbine mass flow capacity(left) and 10% increase in turbine and compressor mass flow capacities (right) for a range of VGT settings and exhaust VVA settings, at 4500 rpm	155
Figure 5.1.4.18	Full-load imep curves with optimised intake VVA, optimised intake and exhaust VVA and optimised intake and exhaust VVA with 110% scaled compressor.	158
Figure 5.2.4.1	The effects of VGT setting on bmep and bsfc (left) and air flow, afr and pmep (BDC to BDC) (right) with 10mg/stroke fuelling, no EGR and standard valve timings	162
Figure 5.2.4.2	The effects of intake and exhaust VVA on bmep (left) and bsfc (right) with fully closed VGT setting and 10 mg/stroke fuelling	163
Figure 5.2.4.3	Effects of intake VVA setting on bmep (left) and bsfc (right) at various VGT settings.(Zero EGR)	163
Figure 5.2.5.1	VGT settings required to produce specified EGR levels for a range of EGR valve effective diameters. 2000 rpm with 10 mg/stroke fuelling, standard valve timings	165
Figure 5.2.5.2	isfc at specified EGR levels for a range of EGR valve effective diameters. 2000 rpm with 10 mg/stroke fuelling, standard valve timings. (VGT nozzle settings as per figure 5.2.5.1)	165
Figure 5.2.5.3	The VGT settings taken for 5mg/stroke (left) and 10mg /stroke fuelling (right) with exhaust VVA setting 3	166

exhaust VVA setting 3

Figure 5.2.5.4 The effects of exhaust VVA on bmep (left) and the work done on the piston (right) at 10mg /stroke fuelling, 10% egr and standard intake valve timing 167

Figure 5.2.5.5 Work done between TDC(f) and BDC and BDC and TDC(o), (left) and changes in these values relative to intake VVA setting 4 (standard) (right) for 5mg/stroke (top) and 10mg/stroke fuelling (bottom) 168

Figure 5.2.5.6 Work done between TDC(o) and BDC and BDC and TDC(f), (left) and changes in these values relative to intake VVA setting 4 (standard) (right) for 5mg/stroke (top) and 10mg/stroke fuelling (bottom) 169

Figure 5.2.5.7 Changes in work done in the two half cycles TDC(f) to TDC(o) and TDC(o) to TDC(f) and the full cycle relative to intake VVA setting 4 (standard) for 5mg/stroke (left) and 10mg/stroke fuelling (right) 170

Figure 5.2.5.8 Indicated, friction and resulting work output for 5mg/stroke (left) and 10mg/stroke fuelling (right) 170

Figure 5.2.5.9 Changes in bmep (left) and bsfc (right) versus intake VVA setting, with exhaust VVA setting 3, 5mg/stroke fuelling at three EGR rates. 171

Figure 5.2.5.10 Changes in bmep (left) and bsfc (right) versus intake VVA setting, with exhaust VVA setting 3, 10mg/stroke fuelling at three EGR rates. 171

Figure 5.2.5.11 Percentage change in isfc from standard, for varying fuelling, EGR and intake VVA settings (Exhaust VVA setting 3) 172

Figure 5.2.5.12 bsfc values for 5 mg/stroke and 10 mg/stroke at 2000 rpm and the three EGR rates, with varying intake VVA and exhaust VVA setting 3 173

Figure 5.3.1.1.1 Combustion characteristic map in the fuelling - EGR space. (Arrows point to the data used when measured data was not available) 176

Figure 5.3.1.2.1 Time based controller characteristics used with the standard valve timing. (The first 4.8 seconds is used to stabilise the low load operating condition) 179

Figure 5.3.2.1 Transient VGT setting as a function of engine cycle number for the standard valve timings 180

Figure 5.3.2.2 Transient torque rise with standard valve timing 181

Figure 5.3.2.3 Transient EGR-fuelling operating locus with standard valve timing 182

Figure 5.3.2.4 Cycle based response of the EGR orifice diameter and percentage, VGT setting, air flow and torque with standard valve timing 182

Figure 5.3.3.1 Time series of VVA controllers. t = 4.8 s (end of cycle 80) is the start of the transient 184

Figure 5.3.3.2 Transient torque rise with and without VVA 185

Figure 5.3.3.3 Increase in torque levels when using VVA compared to those with fixed standard valve timings. 185

Figure 5.3.3.4	Air flows with fixed standard valve timing and VVA	186
Figure 5.3.3.5	Turbine and compressor efficiencies for standard fixed valve timing and with VVA	187
Figure 5.3.3.6	Volumetric efficiency and valve timing settings (4 is standard)	187
Figure 5.3.3.7	Mean torque available to accelerate the turbo-charger and percentage greater torque available with VVA	188
Figure 5.3.3.8	VGT settings and boost pressure during the transient.	189
Figure 5.3.4.1	Time series characteristics of the "twice speed" and step controllers applied to the VVA (left) and EGR systems (right)	190
Figure 5.3.4.2	The effect of faster VVA controllers on torque rise	190
Figure 5.3.4.3	The effect of faster EGR valve controllers on torque rise	191
Figure 7.1.1.2.1	Ideal air standard Atkinson cycle (Stone, 1992-3)	209

TABLE OF CONTENTS

1 INTRODUCTION 1

1.1 OBJECTIVES OF THIS STUDY 1

1.2 GENERAL 1

1.3 FACTORS DRIVING ADOPTION OF VARIABLE VALVE ACTUATION 3
1.3.1 Legislation 3
1.3.2 Customer expectation 6
1.3.3 Vehicle manufacturers' economics 7

2 OVERVIEW OF ENGINE VALVE TIMING 10

2.1 GASOLINE ENGINE VALVE TIMING 11

2.2 DIESEL ENGINE VALVE TIMING 12

2.3 ENGINE DESIGN BENEFITS FROM VVA 13

2.4 POTENTIAL BENEFITS OF VVA APPLIED TO DIESEL ENGINES 17
2.4.1 Improved cold starting / reduction of compression ratio 19
2.4.2 Emissions and fuel economy 20
2.4.3 Increased power 22
2.4.4 Increased low speed torque 22
2.4.5 Improved turbocharger transient response 24

2.5 CONCLUSIONS 25

3 VVA MECHANISM SELECTION FOR DIESEL ENGINES 26

3.1 LITERATURE SURVEY, CLASSIFICATION OF VVA SYSTEMS AND SELECTION OF TARGET SYSTEM 27
3.1.1 General 28
3.1.2 A taxonomy of variable valve timing systems 29
3.1.3 Non-constant velocity camshaft systems: 31
3.1.4 Un-constrained non-constant velocity systems 31
3.1.5 Constrained non-constant velocity mechanisms 35
3.1.6 Design overview of the application of a constrained non-constant velocity VVA mechanism 44

3.2 CHARACTERISTICS OF THE SELECTED VVA MECHANISM 46
3.2.1 Valve lift characteristics with the selected VVA mechanism 46

3.3 ANALYSIS OF THE SELECTED VVA MECHANISM 49
3.3.1 Description of the mechanism and its critical features 49
3.3.2 Analysis and dynamics 51
3.3.2.1 Raven's method to analyse the rotary motion of the camshells 51
3.3.2.2 Extension of Raven's method to give valve acceleration 55

3.4 VALVE TRAIN IMPLICATIONS 57
3.4.1 Cam follower, cam curvature and spring design for fixed valve train 59
3.4.2 Cam follower, cam curvature and spring design with non-constant velocity VVA systems 63
3.4.3 Cam profile design for operation with variable duration VVA 66

3.5 CONCLUSIONS 67

4 ENGINE PERFORMANCE PREDICTION 68

4.1 THE DEVELOPMENT OF ENGINE SIMULATION 69
4.1.1 Introduction 69
4.1.2 Simple models 70
4.1.2.1Quasi-steady methods: 70
4.1.2.2Filling and emptying methods: 70
4.1.3 Wave action methods. 71
4.1.3.1Method of characteristics 72
4.1.3.2Lax Wendroff method 72
4.1.3.3Finite difference methods 73
4.1.4 3-Dimensional methods: 74

4.2 1-D CODE BUILDING BLOCKS 76
4.2.1 Fluid flow 77
4.2.1.1 Pipe friction or pressure losses 78
4.2.1.2 Heat transfer 78
4.2.1.3 Junctions 78
4.2.1.4 Orifices and valves 79
4.2.2 In-cylinder models 80
4.2.2.1 Combustion 81
4.2.2.2 Heat transfer 83
4.2.2.3 Emissions 85
4.2.3 Mechanical systems 86
4.2.3.1 Friction 86
4.2.3.2 Turbines and compressors 87

4.3 CALIBRATION OF THE BASELINE MODEL 91
4.3.1 Description of the engine 92
4.3.2 Description of the model 93
4.3.2.1 VVA modelling 94
4.3.2.2 Combustion 95
4.3.2.3 Turbine maps 100
4.3.2.4 Compressor maps 103
4.3.3 Comparison of model operating characteristics and baseline data 108
4.3.3.1 Overall engine performance 109
4.3.3.2 Combustion and cylinder heat transfer 113
4.3.3.3 The turbo-charger 116
4.3.3.4 Discussion of the overall model predictions 124

4.3.4 CONCLUSIONS 126

5 SIMULATION OF THE EFFECTS OF VVA APPLIED TO A DIESEL ENGINE 128

5.1 STEADY STATE FULL LOAD OPERATION 129
5.1.1 Additions and changes to the model 129
5.1.2 Model convergence with fixed fuelling and AFR controlled fuelling 130
5.1.3 Intake VVA 134
5.1.4 Intake and exhaust VVA 143

5.2 PART LOAD OPERATION 159
5.2.1 Preparation of the model 159
5.2.2 Part load operating priorities 161
5.2.3 Control strategies 161
5.2.4 Interaction of Intake and exhaust VVA with the VGT, without EGR at 2000 rpm 162
5.2.5 Interaction of Intake and exhaust VVA with Variable Geometry Turbine and EGR at 2000 rpm 164

5.3 TRANSIENT OPERATION 175
5.3.1 Changes to the model 175
5.3.1.1 Combustion 176
5.3.1.2 Controller operation and characteristics 177
5.3.2 Behaviour with standard valve timing 180
5.3.3 Comparison of standard valve timing and VVA performance 183
5.3.4 Sensitivity to controller speed 189

5.4 CONCLUSIONS 193

6 CONCLUSIONS AND FUTURE WORK 195

6.1 CONCLUSIONS 195
6.1.1 Drivers for the adoption of VVA in light-duty diesel engines 195
6.1.2 Necessary features for VVA in diesel engines 196
6.1.3 Creation and correlation of the simulation model. 197
6.1.4 Predicted engine performance improvements 199
6.1.4.1 Full load torque 199
6.1.4.2 Part load fuel economy 201
6.1.4.3 Transient torque rise 203

6.2 FUTURE WORK 204

7 APPENDICES

7.1 APPENDIX 1 208
7.1.1 Miller and Atkinson Cycles 208
7.1.1.1 Miller cycle 208
7.1.1.2 Atkinson cycle 209

7.2 APPENDIX II 210
7.2.1 Simulation error band estimation 210
7.2.1.1 Pipe flows 210
7.2.1.2 Orifice flows 211
7.2.1.3 Combustion and cylinder heat transfer 211
7.2.1.4 Turbine and compressor operation 212
7.2.1.5 Full system errors 212

8 REFERENCES / BIBLIOGRAPHY 214

1 INTRODUCTION

1.1 OBJECTIVES OF THIS STUDY

Earlier work, (Lancefield, 1999) was carried out to investigate the field of Variable Valve Actuation, ("VVA") through a literature search. As part of this exercise the devices were classified by type and their ability to improve engine out emissions, fuel economy and power and torque density, was assessed. This work highlighted that, whilst a great deal had been written about the application of VVA to gasoline engines, and the subject was well understood, very little appeared to be known or had been published about the effects of VVA on turbo-charged light-duty diesel engines.

This report builds on this earlier work by investigating the effects of a specific VVA mechanism, selected for its applicability to light-duty diesel engines during the classification exercise.

Specific areas of work are the analysis of the valve train dynamics associated with the use of this mechanism and their impact on valve train design and the investigation of the improvements that can be achieved in part load fuel economy, full load torque and transient torque rise rate by its use in an engine of typical modern design.

1.2 GENERAL

Conventionally four stroke internal combustion engines have had fixed geometry valve train systems operating their valves. In most cases, particularly for automotive use, the basic motion of the valves is prescribed by the design of the camshaft. The conventional camshaft is effectively a single entity that rotates at half engine speed and in fixed phase relative to the crankshaft.

The individual valves are controlled, directly or indirectly, by cam lobes of fixed shape which are part of the camshaft. Thus normally the valve opening timing, the shape of the valve lift profile relative to crank angle and the timing of the valve closing are independent of engine operating conditions.

The processes that occur in an internal combustion engine are discontinuous and timed relative to the crankshaft rather than in real time. The characteristics of these processes are affected by engine speed and required engine output.

The nature of these discontinuous processes is such that an engine with a fixed valve train system will be the product of a process to develop a valve train design that performs adequately under all circumstances, but one that will be non-optimal under most operating conditions.

This situation occurs because the engine producer has to develop engines that meet a number of conflicting requirements. These conflicts arise from the fixed valve train system and particularly from using a fixed geometry camshaft. The requirements the engine has to meet are in general terms imposed by legislation, customer expectation and cost effectiveness. The difficulties arise because a camshaft design that will provide good high speed operation will not provide good low speed operation, and similar conflicts between high and low load operation exist. Thus any fixed camshaft design is a compromise and since the vehicle manufacturers have to meet legislative requirements it is these dictates that are uppermost in the engine developers' mind. Hence other aspects of the engine operation suffer.

If the engine designer has the ability to alter the effective opening characteristics of the valves relative to the crankshaft then the engine's operation can be optimised over a larger part of its operating envelope.

Variable valve actuation systems, which allow the valve opening characteristics to be altered, have been known for many years (Bull, 1924) but until recently it has been possible to achieve the improvements required by legislation by other, less demanding means, such as: changing from carburettors and distributors to computerised engine management systems and the use of catalytic converters to treat the noxious engine emissions and convert them into less harmful forms.

The use of these modern systems has led to the situation where further gains in efficiency and reductions in the pollutants produced are now extremely difficult to achieve. This in turn has led the engine manufacturers to look closely at the use of VVA systems to produce the significant improvements in efficiency and cleanliness that will be required by future legislation.

1.3 FACTORS DRIVING ADOPTION OF VARIABLE VALVE ACTUATION

As already mentioned the factors driving the adoption of VVA fall broadly into three areas:

1. Legislative pressures.
2. Customer expectations.
3. Cost pressures.

However, in all areas of vehicle production it is cost effectiveness that dictates which solutions are implemented. Modern engines are produced to extremely well refined designs, where most, if not all, gains that can be made by improvements to the conventional componentry have been exploited. Thus further gains in performance, efficiency and cleanliness are difficult to achieve without some extra complexity. But further improvements will continue to be expected. These future improvements are likely to lead to the more widespread use of VVA.

The function of VVA is already widely understood and increasingly used on gasoline engines where the reasons for its adoption are clear. However the situation is less well understood with VVA for diesel engines. The background to what may drive the adoption of VVA for diesel engines will be discussed and contrasted with that of gasoline engines:

1.3.1 Legislation

In North America, Europe and Japan, environmental legislation of growing stringency, regional regulation and fiscal incentives increasingly influence engine performance and design. Globally, the majority of the environmental controls are imposed by four bodies: In the European Union (EU), the European Parliament sets the levels through the European Commission. The Economic Commission for Europe (ECE) provides regulations that cover a wider range of countries; European EU and non-EU members, the former Soviet Block countries and Asian countries. But, unlike the other bodies whose regulations are incorporated in the relevant country's legislation, the ECE sets standards which are adopted to varying extents by its members. In the USA, the Environmental Protection Agency (EPA) sets Federal Legislation whilst the California Air Resources Board (CARB) covers California, which generally sets more stringent emissions levels than the EPA. In Japan the levels are set by the Ministry of Transport.

The emissions performance levels set by the various legislative bodies are reviewed regularly and increase in stringency as new emissions control technologies are developed. Although the emissions limits and the test procedures vary in detail, the stringency levels of US Federal, European Union and Japanese legislated limits are now broadly equivalent. However, regional priorities vary: this is particularly the case for the improvement of fuel economy which is receiving increasing priority in Western Europe and Japan but much less in the USA where fuel is cheaper. Thus in Europe and Japan, fuel economy is an increasingly influential factor in engine design while in the USA, exhaust emissions control remains the principal preoccupation.

To put the increasing stringency of the legislation into a quantitative framework it is instructive to note that current European legislated emissions levels, for gasoline engines, represent about 2% of 1971 levels and if current proposals are enacted, by 2005 they are expected to be about 1% of 1971 (Knibb 1998). See *table 1.3.1.*

Directive	**Year**	**CO**	**HC**	**HC+NOx**	**NOx**	**Units**
70/220/EEC	1970	152.00	10.1			g/test
74/290/EEC	1974	122.00	8.6			"
77/102/EEC	1977	122.00	8.6		14.0	"
78/665/EEC	1978	99.00	7.6		11.9	"
83/351/EEC	1983	76.00		22.0		"
88/76/EEC	1988	30.00		8.0		"
89/458/EEC	1989	19.00		5.0		"
91/44/EEC – Euro 1	1992	2.72		0.97		g/km
94/12/EC - Euro II	1996	2.20		0.50		"
Euro III	2000	(*)2.3		0.15		"
Euro IV	2005	1.00		0.08		"
Euro V	2010?	?	?	?	?	?

CO = Carbon monoxide, HC = Unburned hydrocarbons, NOx = Oxides of Nitrogen

(*) Change of cold start test procedure

Table 1.3.1. Emissions Limits for gasoline powered passenger cars in the European Union, (Knibb 1998)

The ability of VVA to enhance environmentally related vehicle performance makes it a useful tool in meeting the progressively more demanding objectives mandated by environmental legislation. In addition to lowering emissions, it has the capability to improve fuel consumption and engine output, which enhances its attractiveness and increases the likelihood of its adoption. This is in contrast with most other emissions control systems, which are only able to positively affect one aspect of engine operations whilst making other aspects worse. e.g. Catalysts. VVA can positively affect all aspects of engine operation.

As already stated the pressures that are driving the adoption of VVA in gasoline engines are well known, but this is not the case concerning the application of VVA to diesel engines. The pressures on the diesel engine manufacturer and user are similar to those on the gasoline engine manufacturer, but the extent to which they are significant in driving the adoption of VVA is rather less clear.

Directive	Title	Year	CO	HC+NOx	HC	NOx	PM	Units
96 EC, 94/12/EC	Euro II	1997	1.0	0.7 (0.9)	-	N/A	0.08(0.1)	g/km
2000EC*	Euro III	2000	0.6	0.56	-	0.5	0.05	"
2005EC	Euro IV	2005	0.5	0.3	-	0.25	0.025	"
78/665/EEC	Euro V	2010?	???	??	?	??	??	"

CO = Carbon monoxide, HC = Unburned hydrocarbons, NOx = Oxides of Nitrogen, PM = Particulate Matter

(*) Change of cold start test procedure

Table 1.3.2. Emissions limits for diesel powered passenger cars in the European Union, (Pethers 1997)

The emissions and fuel consumption legislation applicable to diesel engines is formulated by the same bodies as that for the gasoline engines. But there are significant differences in the emphasis of the legislation. See *table 1.3.2.* The nature of the diesel cycle is such that the emissions from the engine are of different types and in different quantities from those emitted by a gasoline engine.

It can be seen from the above and *table 1.3.1* that diesel engines are allowed to emit more NOx than their gasoline counterparts, but produce considerably less CO. Both of these are characteristic features of the diesel cycle, normally running lean, with excess oxygen, and thus

producing little CO, but with very high cylinder temperatures and pressures producing conditions for dissociation and forming NO_x.

What is not clear at present is the extent to which the addition of VVA can influence the emissions from diesel engines, but it can be shown that lowered cylinder temperatures and pressures can be achieved, which should lead to a reduction in the amounts of NO_x formed.

Perhaps the most significant emissions concern for the diesel engine is that of particulate matter. It has recently been hypothesised that diesel exhaust particulates may be carcinogenic and, although there appears to be no clear proof of this, methods for its reduction are being sought, either by reducing the amount formed or by trapping and chemically altering it after production.

1.3.2 Customer expectation

In the three major markets for automotive engines, Europe, the USA and Japan, the consumers are becoming increasingly sophisticated. They are also becoming increasingly environmentally aware.

The desire to have vehicles that have more features, utility and convenience has led to increases in overall vehicle weights, but the owners are demanding ever higher levels of performance in terms of acceleration and top speed. In general, these are at odds with improved fuel economy, unless the engines, or the engine - transmission combinations, can be made with higher specific output and torque characteristics as well as increased efficiency.

It is widely known that diesel engines exhibit significantly higher levels of low speed torque and exceptional fuel economy in comparison with gasoline engines. However, there are two areas where the operation of the diesel engine is perceived as inferior to a gasoline engine. Maximum rating and transient acceleration.

At maximum rating *i.e.* high speed maximum power, the diesel engine has a disadvantage in relation to gasoline engines. The reasons for this are primarily related to peak cylinder pressure limitations and combustion systems that limit maximum speed to perhaps 5000 rpm, with maximum power at perhaps 4400 rpm. A typical modern European gasoline engine will produce maximum power at 5500 rpm, or higher and continue to produce useful torque up to 6500 rpm,

producing a very different driving feel. Diesel engines for passenger vehicles would benefit from an increase of maximum power and VVA is one of the options able to produce this effect.

Since most modern, light duty diesel engines are turbocharged the rate at which the turbine is able to accelerate limits the rate at which engine torque can be increased, leading to a perceived "turbo lag." Various methods of improving transient acceleration are under investigation, including electrically assisted devices, variable geometry turbines and VVA, but, of these VVA is the only device that is able to influence turbo lag, significantly increase specific torque and power whilst simultaneously improving fuel economy and emissions.

1.3.3 Vehicle manufacturers' economics

The automotive industry is extremely cost sensitive and at first sight the added complexity of VVA might be thought to increase overall cost unacceptably. However, this need not be the case for a number of general reasons that apply to both gasoline and diesel engines:

Fuel economy is a high priority for the vehicle manufacturers as future legislation will force them to reduce both individual vehicle and overall fleet fuel consumption. The penalty for not meeting the legislative demands is simply not being able to sell cars. There is also an increasing ecological awareness amongst the public and this is influencing their purchasing trends. Whilst neither of these factors has a strict cash value the vehicle manufacturers do in general ascribe a cash value to demonstrable reductions in fuel consumption. The amount varies by manufacturer, according to the mix of vehicle sizes and costs and the geographical disposition of the markets in which they are sold, but on this basis improvements in fuel economy can partially pay for extra systems such as VVA.

The extra cost of a VVA system can be offset against prime material costs by making engines with fewer cylinders and of smaller displacement as VVA can increase the specific output and torque of engines.

The use of physically smaller engines has other, less obvious, advantages for the vehicle manufacturer: Smaller engines allow increased cabin space without increase of vehicle size and reduced engine weight allows extra features without increased vehicle weight.

The total cost of an engine to the producer does not just amount to the cost of manufacture. Of major concern is warranty cost for unreliable parts. An example of a system that is being increasingly substituted by VVA in gasoline engines, for this reason, is the exhaust gas re-circulation (EGR) system. These systems divert exhaust gases from the exhaust system into the intake manifold, to control part load emissions. The nature of the gases that these systems carry makes them comparatively unreliable leading to substantial warranty costs to the vehicle manufacturer. The replacement of the conventional EGR system by VVA, implementing internal EGR, provides the potential for reduction of warranty costs and cost offset against the cost of the VVA system, which in some cases may even fully fund the VVA.

Similar cost offsets can be achieved if the size or complexity of the catalyst and after-treatment systems can be reduced. This is likely to become increasingly important as precious metals such at platinum and rhodium become increasingly rare.

Modern legislation for vehicles also stipulates that all systems that are critical to the emissions characteristics of the engine are monitored for correct operation by on board diagnostics (OBD) systems. Certain of the engine systems, EGR systems in particular, are very difficult and costly to monitor because of the indirect measuring systems required. When VVA is substituted for the EGR system, since the VVA system has a closed loop control system with a simple feedback sensor, its correct operation is easily monitored with a system that is already present. This again represents a financial benefit which can be offset against the cost of the VVA system if a specific sensor can be removed and substituted by the VVA sensor.

This combination of improved fuel economy, reduced material costs, lower warranty costs, ease of diagnosis and higher specific output is making the adoption of VVA increasingly attractive to the engine manufacturer. All of these factors apply to gasoline engines, but the picture is not so clear with diesel engines.

Current knowledge seems to indicate that there are a number of potential opportunities for cost offset of VVA in the diesel engine, but they are not as clear cut as for the gasoline engine. They might be found in the removal of glow plugs in certain warmer regions as VVA can improve cold starting, and in the potential to use conventional turbochargers rather than variable nozzle or variable geometry turbines because VVA can redistribute the energy in the engine. Electrically

assisted turbochargers are being investigated for improving transient acceleration and these may also offer the opportunity for some cost offset for VVA.

There may also be benefits associated with weight and size reduction from increased specific rating and reduced cylinder pressures and temperatures.

Modern diesel engines use very high levels of EGR, but because of the limited valve overlap, dictated by the high compression ratios, this has to be implemented externally. Also because of the very high levels of EGR, worthwhile benefits can be gained from cooling the EGR, using a heat exchanger. Using conventional valve train systems this must be done outside the engine. So there is currently no opportunity for substitution of this function.

However, there may be opportunities for the partial substitution of, or cost reduction of, some systems that form part of the exhaust system. Some modern diesel engines are being fitted with lean "De-NO_x" catalysts and are likely, in the future, to be fitted with particulate traps. It is possible that in future VVA may be able to influence the operation of diesel engines to an extent where significant cost reductions can be achieved on these external systems, particularly through facilitating advanced combustion systems such as homogeneous charge compression ignition (HCCI).

These (currently) limited opportunities for cost offset perhaps make it less likely that this factor will influence the adoption of VVA on already relatively expensive engines. The main drivers to the adoption of VVA on diesel engines will be improved part load fuel economy, increased specific output and improved low speed transient drivability.

2 OVERVIEW OF ENGINE VALVE TIMING

In order to understand how VVA may affect engine operation it is necessary to be able to contrast the valve timings possible with VVA with those used in modern engines with fixed valve timing. This early discussion will cover both gasoline and diesel engines, but will be confined to engines for light duty passenger vehicles. This distinction is made because these types of engine typically operate over very wide speed and load ranges and thus force the heaviest compromises on an engine with fixed valve timing. (It should also be mentioned that in terms of the effects available on engine performance there are strong analogies between variable geometry intake manifolds and VVA, but variable intake manifolds cannot influence part load economy or emissions and thus VVA is a more influential device.)

There are a number of ways in which engine valve timing can be displayed, using various different crank positions as the reference for the four valve timing points, and timings can be quoted over a range of ± 360° or over a 720° range. Also some engine manufacturers quote timings at significant lift, 0.2 to 0.3 mm, to allow for valve train wind up, particularly in pushrod engines and those fitted with hydraulic lash compensation devices. This can lead to discrepancies when comparing quoted valve timing angles. However, probably the clearest and most widely used notation for valve timings is demonstrated below, (Heywood, 1988 - 1), (Lancefield *et al*, 1993) and (Stein *et al*, 1995), and to avoid confusion, throughout this document, unless otherwise stated, valve timing figures are quoted at the top of the quietening ramps.

In the method used here, the valve timings are quoted relative to overlap TDC for IVO and EVC, and relative to two BDC timings for EVO and IVC. The use of firing TDC as the 0° reference for the 720° cycle leads to EVO being quoted relative to the first BDC and IVC relative to the second. The timings illustrated in *figure 2.1.1* are quoted as, EO=52° BBDC, EC=4° ATDC, IVO=4° BTDC and IC=52° ABDC.

With this definition of valve angles, under some circumstances with VVA negative angles can result, e.g. If EVC is before TDC, IVO is after TDC or IVC is before BDC then the numbers will be quoted as negative. All valve timings in this work will be defined using this convention unless otherwise explicitly stated.

2.1 GASOLINE ENGINE VALVE TIMING

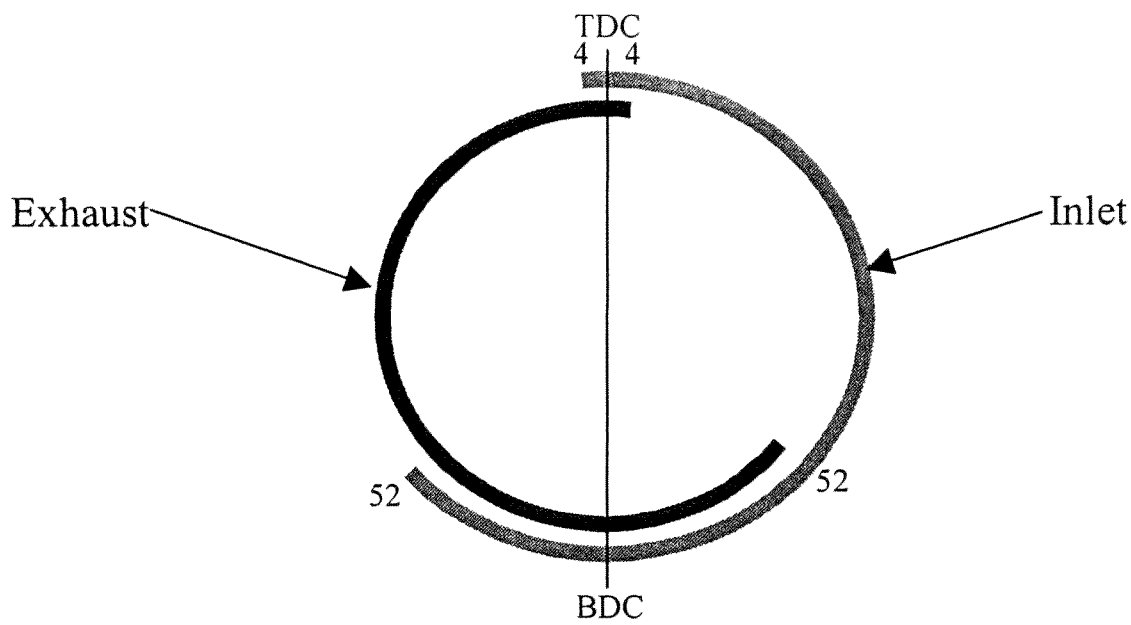


Figure 2.1.1 Typical valve timing for a standard gasoline engine

The timings shown in *figure 2.1.1*, above are for a mature European gasoline engine. (Lancefield *et al*, 1993). This engine had been developed for European and North American use and particularly to meet legislative requirements in the North American region. It was usually used with an automatic gearbox and torque converter. In this operating environment the engine needed to offer good emissions, a robust idle and good low speed torque. These are characterised by small overlap, 8°, (the sum of EVC and IVO), relatively late EVO and early IVC. Under normal usage this engine was very competent, but not outstanding in any way. The compromises forced by fixed valve timing are evident when these timings are contrasted with those generated using VVA to improve specific operating conditions on this same engine. (Lancefield *et al*, 1993). The engine in question was fitted with intake cam duration control and a coarse exhaust cam indexing system. *Figure 2.1.2* shows improved valve timings resulting from testing.

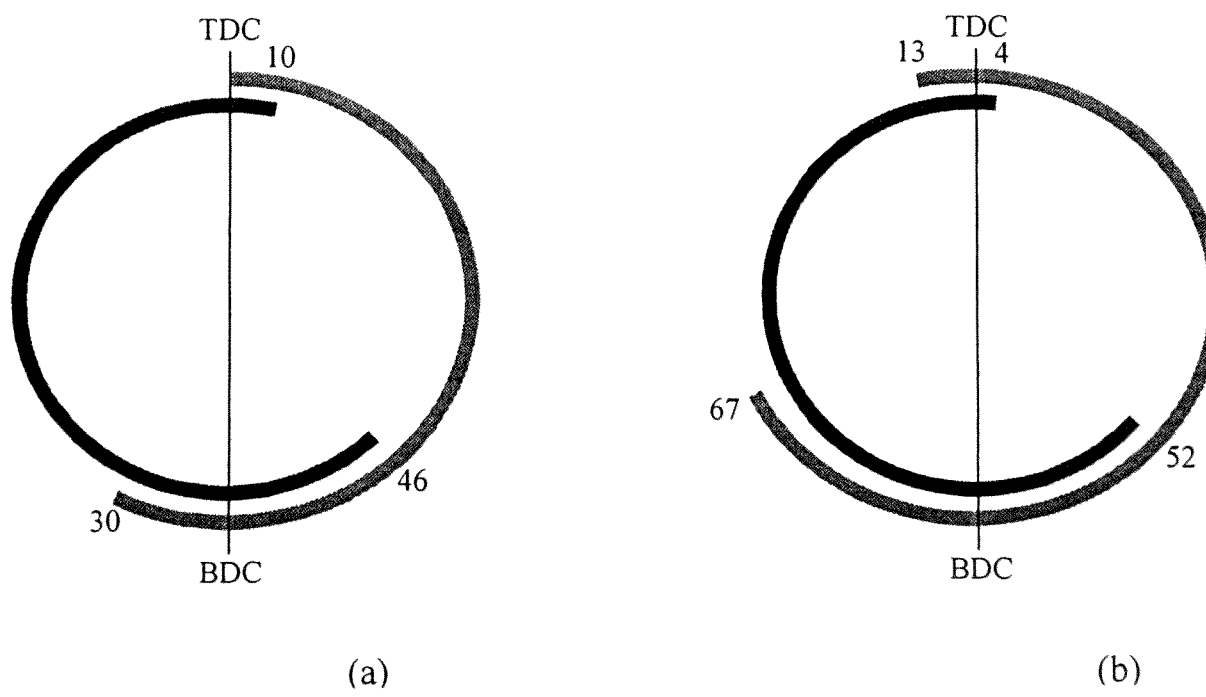


Figure 2.1.2. Improved valve timings for: a) Idle and b) Low part load.

2.2 DIESEL ENGINE VALVE TIMING

The timings shown in *figure 2.2.1a*, below are for a current production European turbocharged and inter-cooled diesel engine. (Lancefield *et al*, 2000). This engine had been developed primarily for European use and particularly to meet the legislative requirements of Euro III. It would usually be used with an automatic gearbox and torque converter. In this operating environment the engine must offer good emissions, low fuel consumption, a robust idle and good low speed torque.

The features to notice are: The valve to piston clearance problems caused by the high compression ratio are characterised by the conservative intake opening timing. The requirement for good low load economy is illustrated by the relatively late EVO to maximise expansion work. IVC is the usual compromise between good low speed and high speed torque, but it should be noted that the use of a turbocharger reduces the extent of this compromise as very high volumetric efficiencies can be maintained across the speed range even with relatively early IVC. The ways in which improvements can be achieved by the use of VVA on this engine are evident when the timings of *figure 2.2.1a* below, are contrasted with those found using VVA to improve specific operating conditions, in *figures 2.2.1b, 2.2.2a and 2.2.2b* (Lancefield *et al*, 2000).

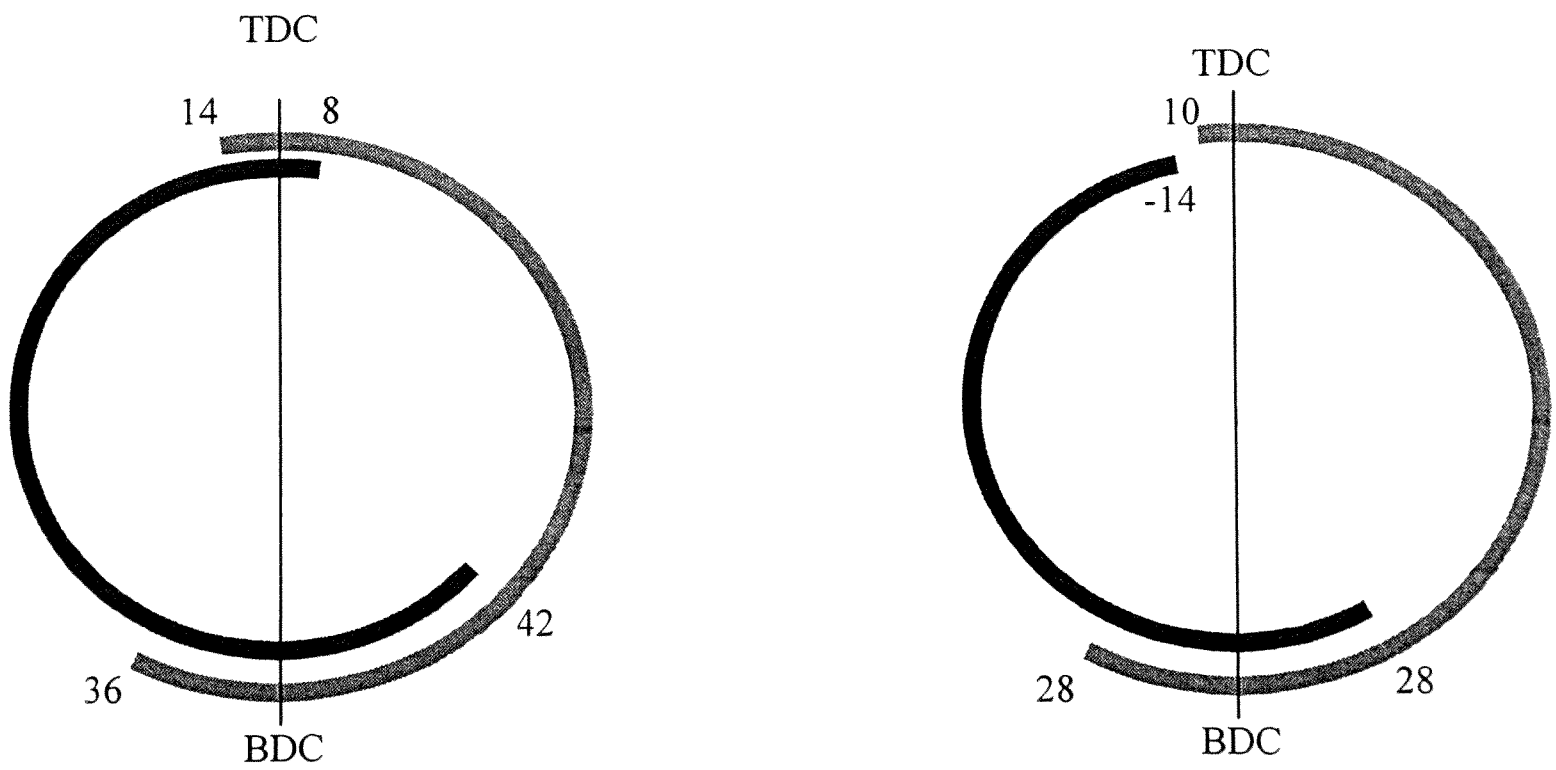


Figure 2.2.1 Valve timing for a standard diesel engine, (left), and improved idle (right) (Ramp top timings 0.1mm lift opening and 0.2 mm closing)

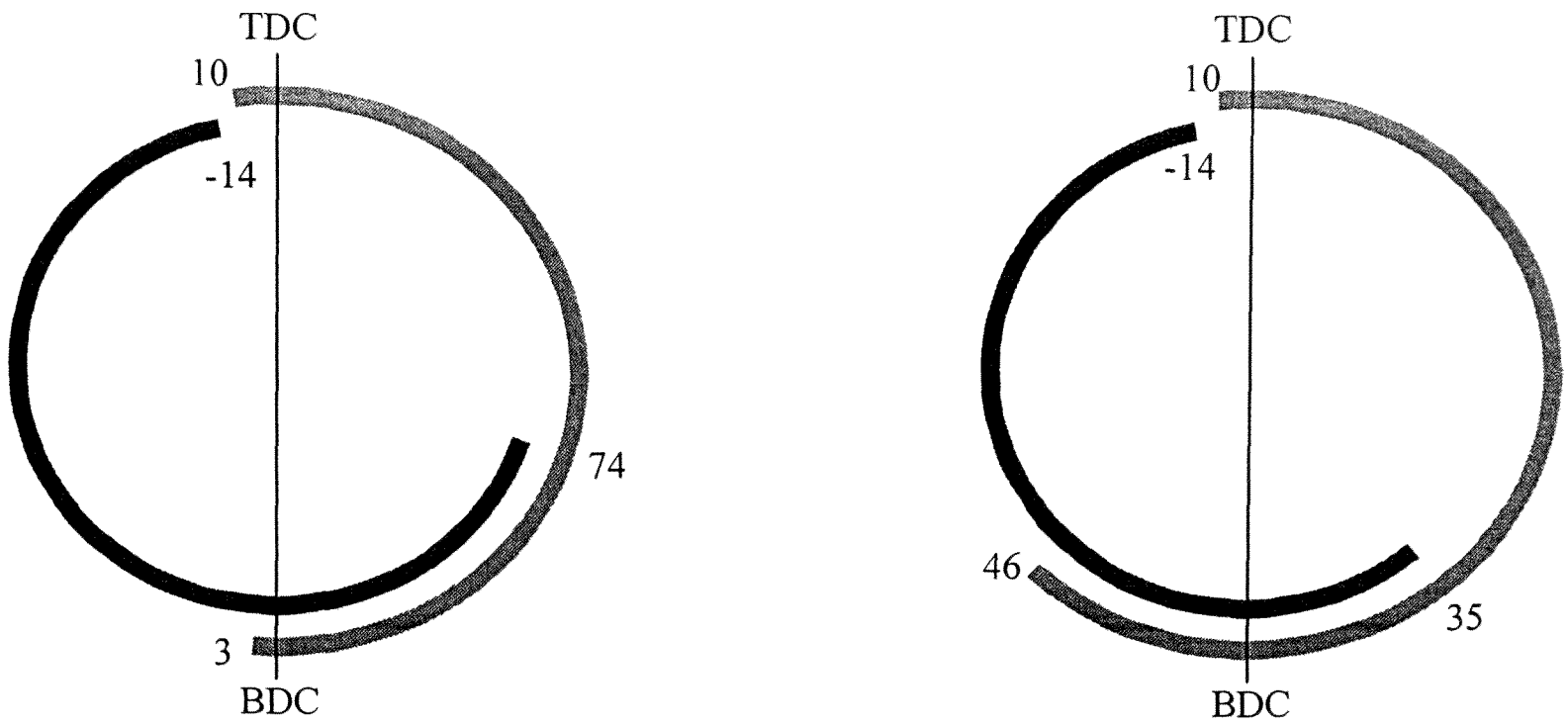


Figure 2.2.2 Improved diesel valve timings for low speed high load (left) and high speed high load (right.)

2.3 ENGINE DESIGN BENEFITS FROM VVA

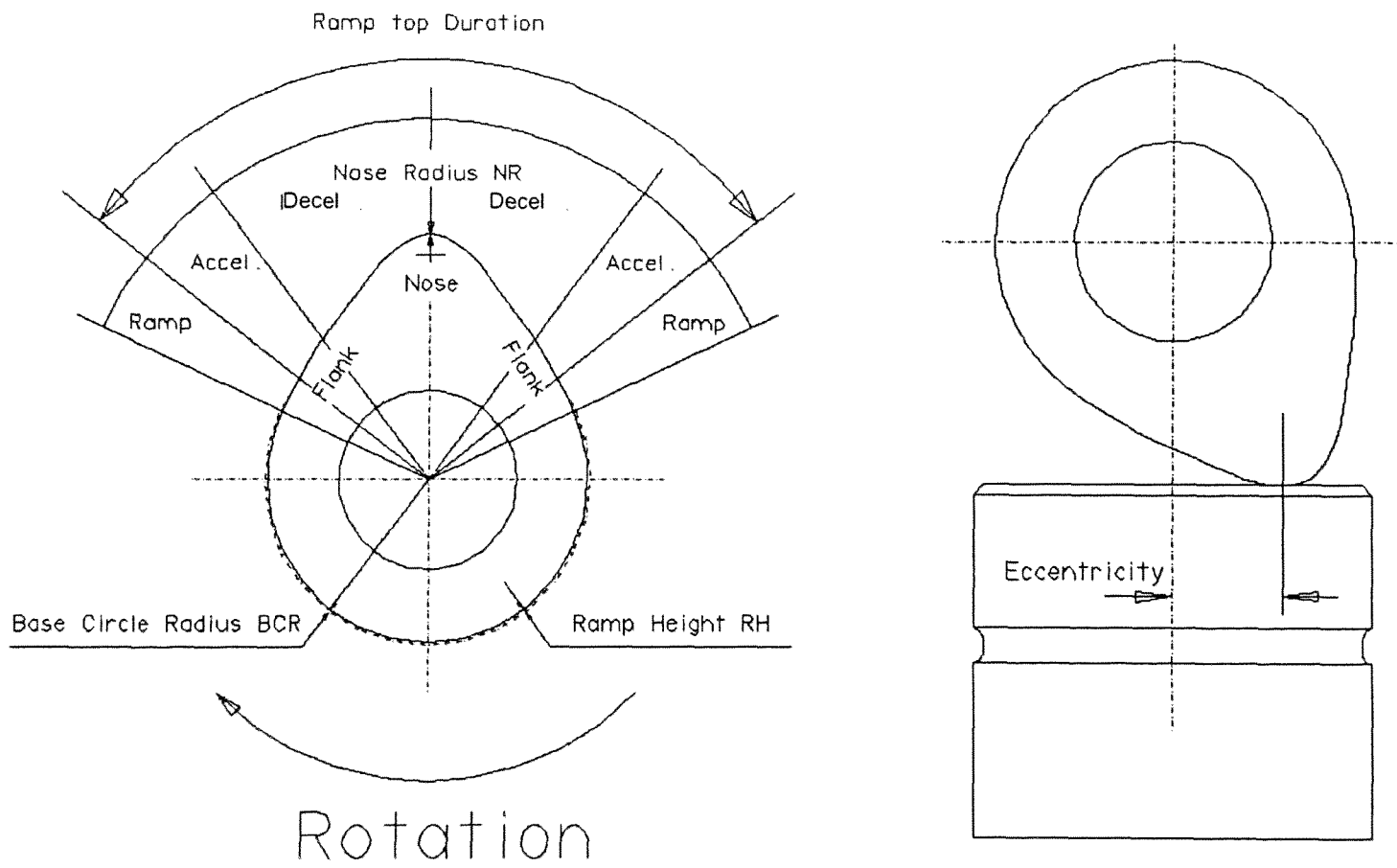


Figure 2.3.1. The key features of a cam profile.

A detailed discussion of cam and valve train design is outside the scope of this document, and the reader is referred to (Heath, 1988) and (Hollingworth and Hodges, 1991) for descriptions of modern cam design methods. Despite it being inappropriate to go into too much detail on the

subject, there are certain aspects of cam design that can be influenced to advantage if a valve train is designed from the outset to incorporate VVA.

Taking for granted that appropriate valve motion for desired engine function is achievable, the key areas of concern in any valve train design are, durability, cost of manufacture and friction.

Durability: The major threats to cam durability are contact stresses and lubrication. VVA can have small effects on the lubrication, (Heath, 1988), but the major effect is in controlling contact stresses (Heath, 1988). Most current VVA strategies and devices encourage the use of longer duration cams than would be possible without VVA . The implication of this is that, in general, the valve accelerations at any given engine speed are lowered. *Figure 2.3.2* shows the effect of cam duration on maximum acceleration for cam designs that have the same spring requirement. Since contact forces between the cam and its follower are a direct function of valve acceleration and spring forces, longer duration cams have lowered accelerations and therefore lower stress levels.

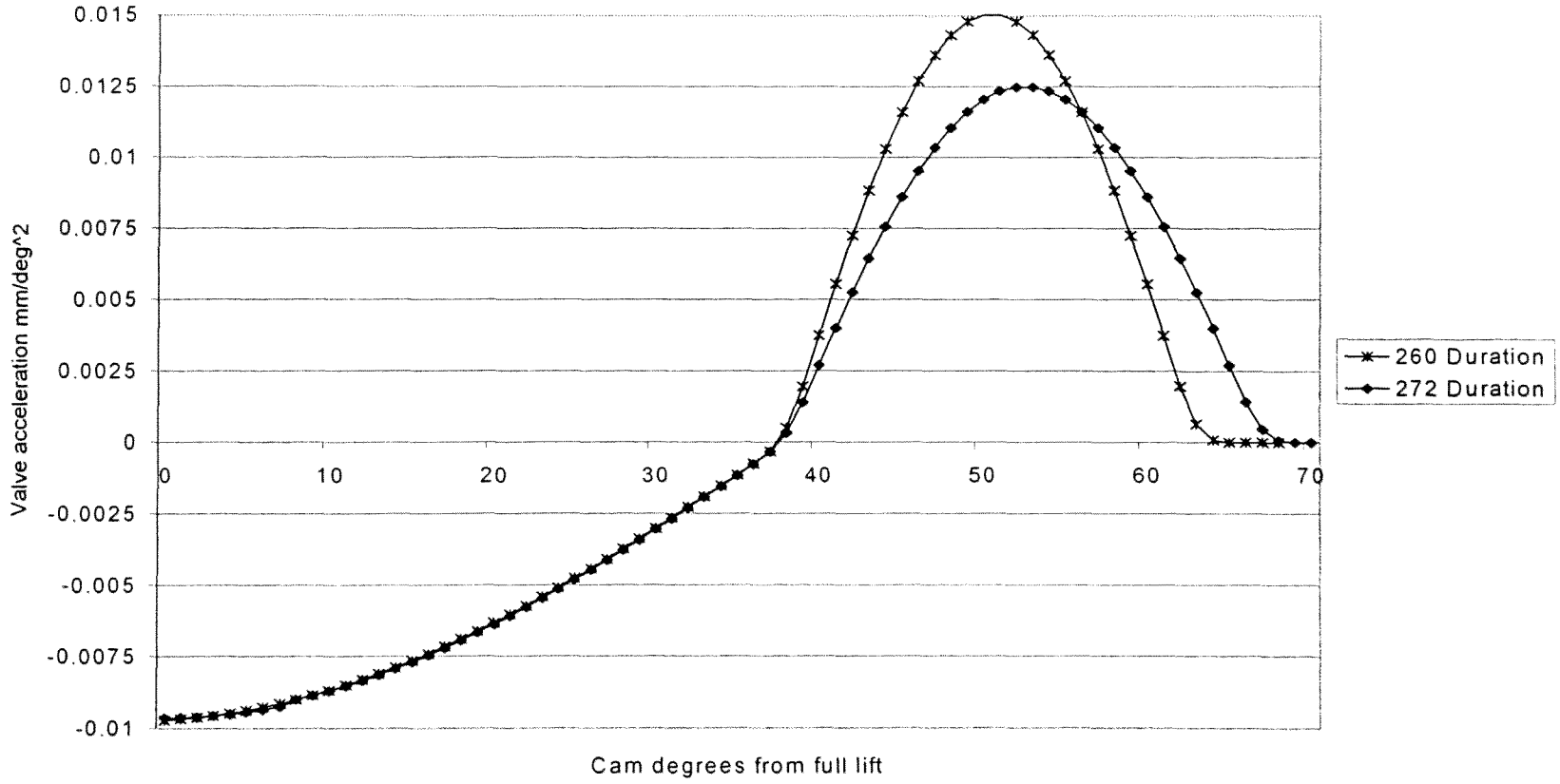


Figure 2.3.2. The effect of cam duration on valve acceleration.

In addition to the lowering of the contact forces longer duration cams have larger radii of curvature in the most vulnerable areas, particularly over the nose of a cam designed to operate a direct attack follower and on the flanks of cams for use in roller follower applications. This again contributes to a lowering of the contact (Hertzian) stresses in the cam.

Cost: As with all manufactured articles, the cost of a camshaft is made up of:

1. Material costs

2. Manufacturing costs (the most significant are labour and investment costs)

As indicated above VVA has the ability to reduce the stresses in the cam, by reducing valve accelerations. This reduction in stress levels can in some cases allow the use of a cheaper, lower specification material.

Probably more significant is the control of cam flank curvature in roller follower applications: Modern automotive valve train systems use relatively short period, high lift cams. In applications where these shorter cam periods are used in conjunction with roller followers, concave cam flanks can result. The radius of curvature of these concave regions determines the radius of grinding wheel that can be used to manufacture the cams. The smaller the negative radius the more expensive the process as grinding wheel life is a function of its diameter. The more often the wheel needs to be changed the higher the cost. In some cases the radius is so small that a belt grinder is used. Belt durability is not good, again leading to higher costs.

The longer duration cams possible with VVA allow the acceleration curve of the cam to be altered to make the cam flanks with a large positive radius rather than the small negative radius of the normal short duration profile. *Figure 2.3.3* shows a family of acceleration diagrams of common duration, but differing maximum positive accelerations.(These would also have slightly different spring requirements) *Figure 2.3.4* shows the curvature characteristics resulting from these differing acceleration diagrams. This shows that for the highest positive acceleration a small negative radius results and as the maximum acceleration is reduced so the minimum negative radius becomes larger until the flank curvature remains positive. It can be seen from this that increasing the period of the cam, by allowing reduced maximum acceleration, can allow control of flank radius.

Friction: The friction levels in a valve train are a function of valve acceleration, both directly and indirectly: Directly, the friction is determined by the forces in the system, which are the sum of the acceleration forces and the spring forces. However, since the spring design is a function of maximum valve acceleration, the spring force is also influenced by the design of the cam. Since

the use of VVA can produce lower maximum valve accelerations, by allowing the use of longer duration cams, softer springs and therefore reduced overall friction levels are possible.

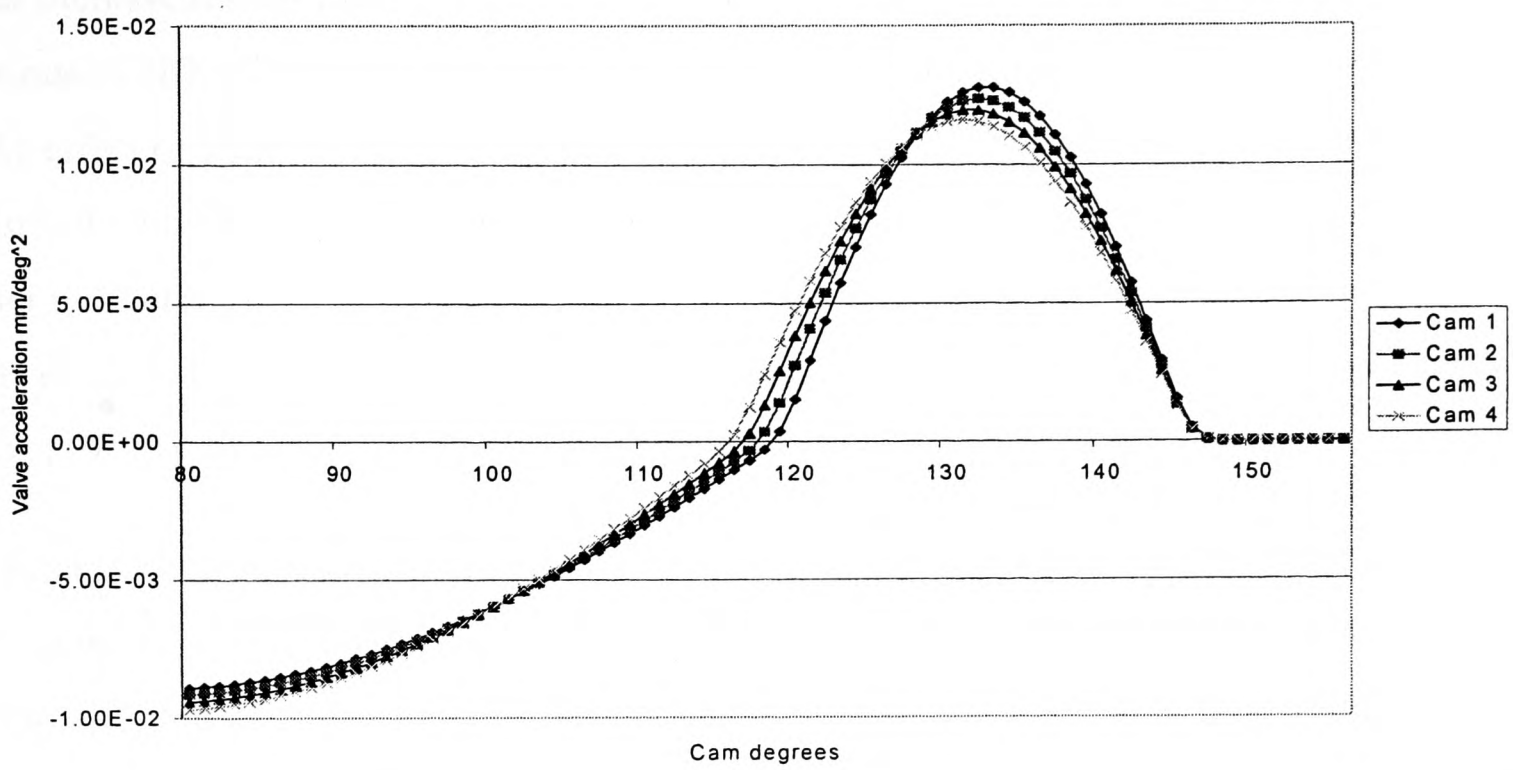


Figure 2.3.3. A family of cam acceleration diagrams for constant duration.

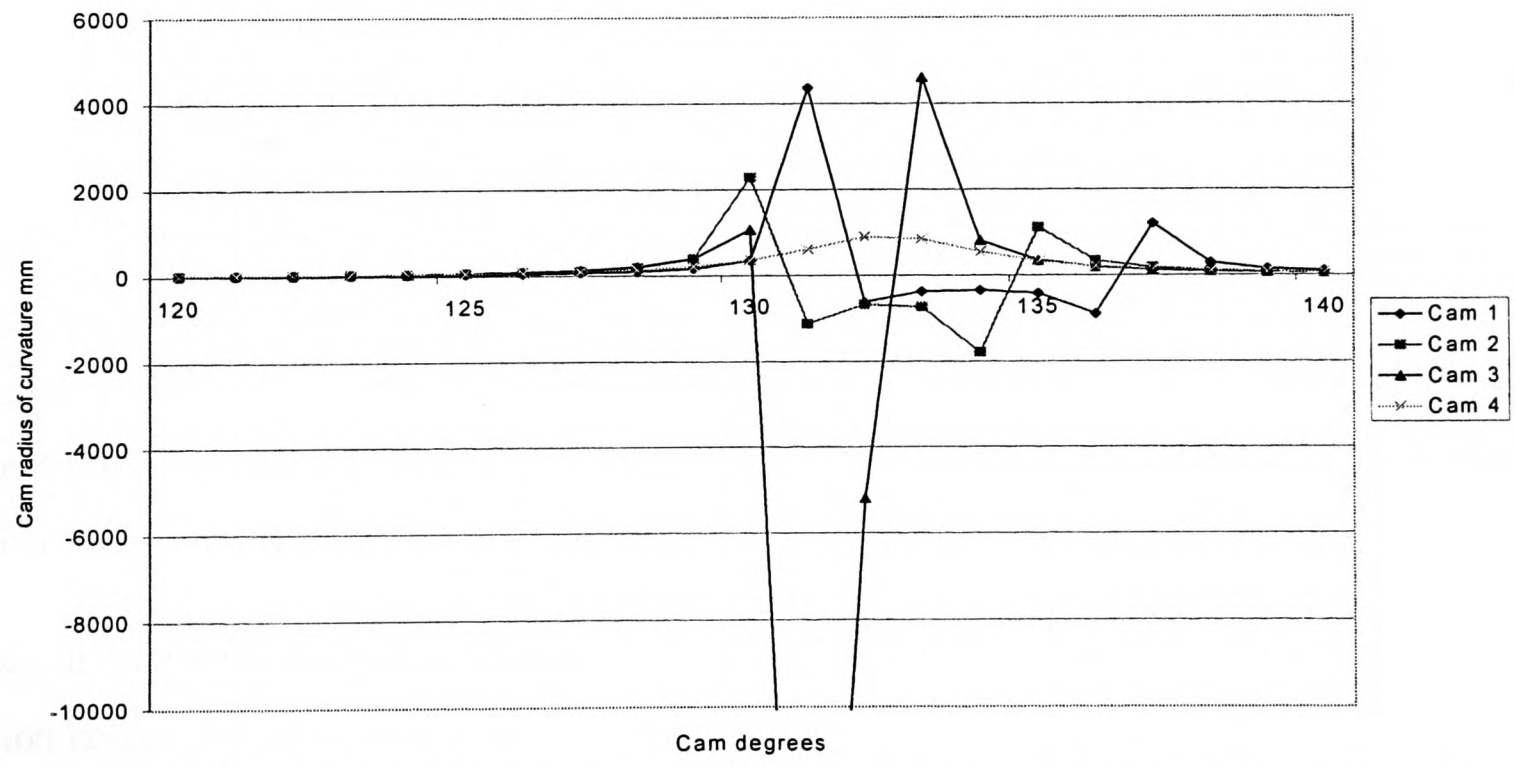


Figure 2.3.4 The effect of cam duration on cam curvature for a cam with roller follower. (Cam profiles as per *figure 2.3.3.*)

There are also more subtle issues associated with cam eccentricity and its impact on valve train component size, which are outside the scope of this section, but are discussed in section ***3.4.2***.

2.4 POTENTIAL BENEFITS OF VVA APPLIED TO DIESEL ENGINES

Over the last few years there have been a number of significant changes to diesel engine systems. There has been large scale adoption of turbo-charging followed by the addition of inter-cooling to further increase ratings and more recently the introduction of EGR systems to help control emissions of NO_x, (Horrocks and Robertson, 1996). The addition of turbo-charging to engines has the effect of blurring many of the effects of variable valve timing. This is particularly so with the current widespread use of wastegate systems to limit boost pressures (which allow the use of smaller turbochargers to produce high levels of boost at lower engine speeds), but most of all the effects of valve timing are masked with variable nozzle turbines (VNT) or variable geometry turbines (VGT) which are becoming increasingly widespread. (Anon, 1999)

This discussion will be confined to light duty turbo-charged diesel engines for automotive applications (as they form the majority of diesel engines produced) and will concentrate on the potential of variable valve timing to affect normal engine functions and to this extent systems for enhanced engine braking, which although they are strictly VVA systems, will not be discussed beyond offering some references for the interested reader: (Hu *et al*, 1997) and (Meistrick, 1993)

There is a distinct contrast between the large amount of literature published on the application and effects of VVA in gasoline engines and the limited amount available on diesel engines. It seems likely that this is because, with the high compression ratios common in light duty diesels, only devices that alter cam duration are suitable and these are necessarily more complex and invasive of engine design than the simple phasers currently widely used in gasoline engines. Most of the references deal with truck engines or bigger, but these are used to illustrate features that apply to light duty engines as well.

Diesel, or compression ignition engines operate on a different principle from a gasoline or spark ignition engine and as a consequence have a number of significant design differences. Gasoline engines run throttled, diesels normally operate turbo-charged and un-throttled whilst gasoline engines have compression ratios between 8 and 10 ratios lower than the 18:1 to 22:1 range typical of light duty diesels.

These design differences impose fundamentally different requirements on the valve train design and the functionality required of a VVA system applied to a diesel. They also dictate that some of the ways in which VVA can affect engine operation are different to those for a gasoline engine.

The fact that diesel engines have very high compression ratios means that they have very little clearance between the piston and the cylinder head face and valves when the piston is at TDC. This dictates that the valves can have little or no lift at overlap TDC. The first consequence of this is that the valve opening periods are relatively short, leading to relatively highly stressed valve trains. (A factor contributing to the widespread introduction of 4-valve layouts in modern diesel engines.)

The second consequence is that any VVA system employed can only alter IVO and EVC very marginally otherwise valve to piston contact or negative overlap and undesirable valve closed piston motion can occur. This leaves only EVO and IVC available for the useful application of VVA. Fortunately these two valve timings can have significant effects on engine operation, but to achieve changes in EVO and IVC without affecting EVC and IVO requires VVA systems that can alter the open period of the valves, not just the phasing of a fixed open period relative to the crank. As already mentioned very little work has been published about the use of VVA in diesel engines, which is thought to be mainly a consequence of a perceived lack of appropriate VVA systems, but may also be partly due to the major advances in diesel injection systems that have occurred in the last five years. The introduction of very high pressure common rail, unit injector and hydraulically amplified injection systems have had a significant impact on the performance and emissions characteristics of diesel engines, which may have reduced, or deferred, the need for VVA. There is a paucity of published investigative work both in simulation and hardware and thus the benefits of VVA in diesel engines are less well understood than those in gasoline engines.

Despite the apparent lack of work in this area, the potential for the application of VVA to light duty diesel engines has been recognised, and benefits identified include: improved starting or the option of using a lower compression ratio, flattening and raising of the torque curve, improved fuel economy and emissions (Stone and Kwan, 1985).

2.4.1 Improved cold starting / reduction of compression ratio

The major reason for the very high geometric, or nominal, compression ratio in modern diesel engines is that they need to be able to start at very low temperatures, typically down to –25° C and even lower for military vehicles. This requires the nominal compression ratio to be several ratios higher than would be required for the engine to run normally once started and warmed up. If the nominal compression ratio is made low enough for good normal operation, these effects produce cranking cylinder temperatures and pressures that are sufficiently low to make very low temperature starting difficult, if not impossible.

Cold starting quality is strongly influenced by the air temperature in the cylinder at the end of the compression stroke and is a function of compression ratio and intake valve closing timing. Since fixed intake valve closing timing is usually significantly after BDC, in order to benefit from charge dynamic effects at higher engine speeds, at cranking speeds some of the air is pumped out of the cylinder. Also under cranking conditions the compression process is relatively slow, so heat loss from the charge to the cylinder, piston and cylinder head can be significant. The reduced trapped mass and increased heat transfer reduce compression temperatures. Advancing IVC towards BDC increases the trapped mass and compression work and therefore compression temperature. Holmer and Haggh, (1969) report that on a truck engine a change of IVC from 44° to 23° after BDC allowed a reduction of compression ratio from 17:1 to 15:1 with the same starting performance at –18°C.

Figure 2.4.1.1 shows the effect of intake valve closing on the effective compression ratio ("ECR") of an engine. (Effective compression ratio, defined from intake valve closing to top dead centre rather than from bottom dead centre to top dead centre as with the conventional compression ratio.) In this case the engine has a nominal compression ratio of 20:1 and IVC at 58° after BDC. Advancing IVC to 25° after BDC increases the ECR by 3 ratios. (Similarly retarding IVC reduces ECR, which may be significant for hot-restart in hybrid vehicles.)

The nominal compression ratios in diesel engines are often higher than required for best economy to ensure reliable starting, to such an extent that the thermodynamic gains are outweighed by the reduction in mechanical efficiency (Stone and Kwan, 1989). The use of VVA to increase the ECR allows the nominal compression ratio of the engine to be reduced, which not only maintains or improves cold starting, but also has implications to output.

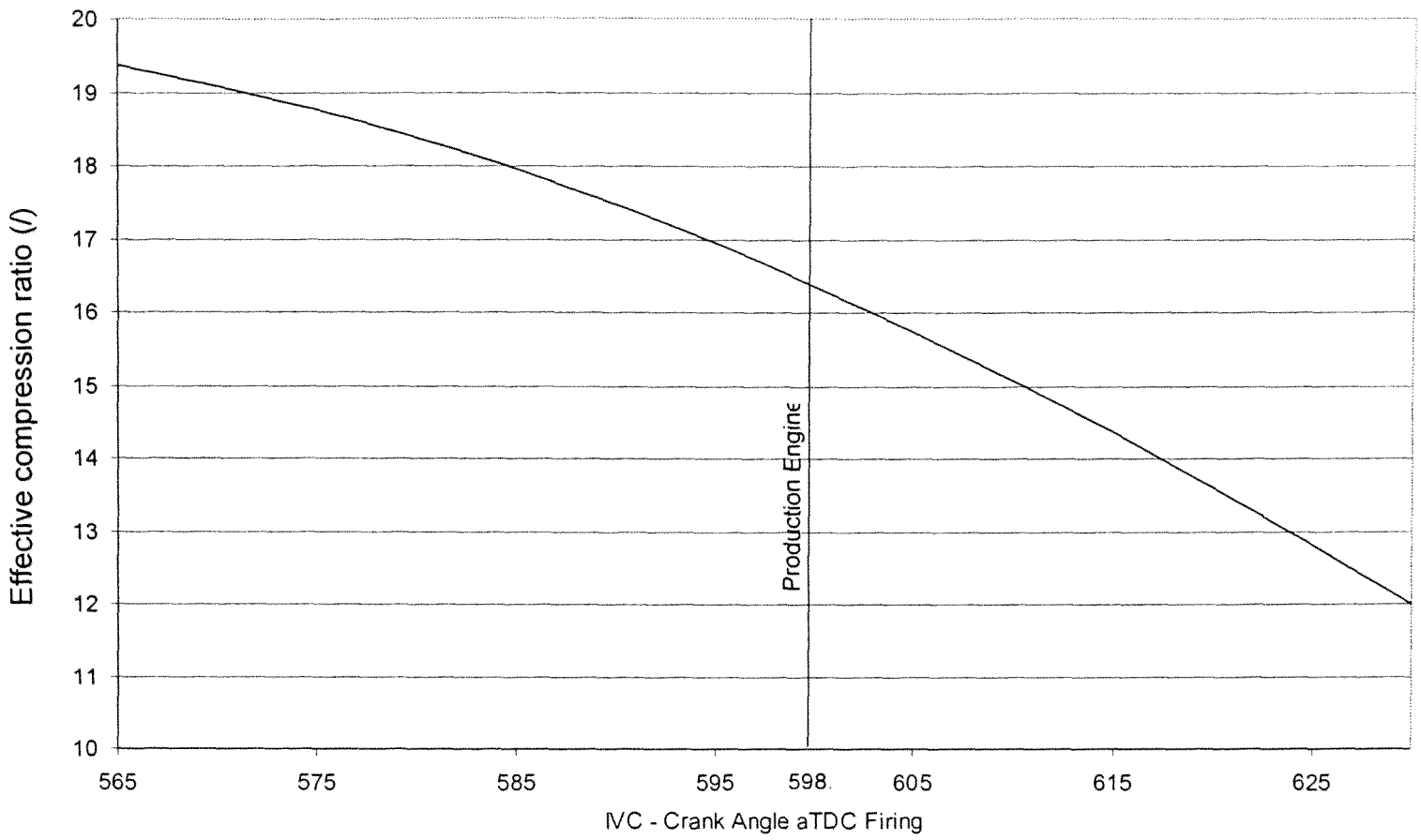


Figure 2.4.1.1 Effect of intake valve closing timing on effective compression ratio (Lancefield *et al*, 2000).

It is not uncommon for modern diesel engines to have upper cylinder pressure limits imposed by structural limitations. The reduction of the nominal compression ratio allows maintained output levels with lower peak cylinder pressures (Watson and Janota, 1982), or increased output for a similar peak cylinder pressure.

2.4.2 Emissions and fuel economy

Under light load operating conditions the engine has little or no boost from the turbocharger and is running effectively as a naturally aspirated engine. As there is little or no overlap, only EVO and IVC are available to alter engine operation. As with gasoline engines, the optimisation of EVO is a trade off between extra expansion work and increased blow down pumping work. There is also the added complication of its interaction with the turbine. However, because diesel engines always run un-throttled, at very low loads they actually trap larger masses of air than they need to produce low power outputs. Thus despite the requirement to run lean, there is an opportunity to reduce the trapped mass by closing the intake valve later than would be normal. This can increase fuel efficiency by using a pseudo Atkinson cycle, but taking advantage of reduced effective compression ratio, rather than over-expanding as with the Miller cycle (Heywood, 1988 -2). See Appendix 1

Bazari and French, (1993) concluded that the relationship between intake valve timing and emissions on turbo-charged diesels was "not well known" and that most effort had been devoted to increasing volumetric efficiency, particularly in relation to IVC. However, they do report that on the engine investigated either advancing or retarding the intake valve closing timing, from its nominal fixed timing, reduced NO_x and BSFC, whilst HC, particulates and smoke all increased, particularly at high loads. This can be explained by the reduction in trapped mass leading to lower cylinder temperature and air-fuel ratio. The reduction of temperature and reduced equivalence ratio were responsible for the reduced NO_x, whilst the improved economy arose from reduced pumping work, from reduced mass flow, and reduced friction from the lower cylinder pressures.

In addition to the light load effects EVO timing has on expansion work and blow down pumping work, (both of which affect fuel economy) it also has the ability to affect output through its interaction with the turbine: it has been shown, (Lancefield *et al*, 2000) that at 1000 rpm full load, advancing exhaust opening from 42° to 96° before BDC, with all other timings held constant, increased full load torque at low engine speeds, by 13%. This was associated with an increase in BSFC of 3% with constant air-fuel ratio. From this, it would appear that if no increase in torque were taken a fuel economy gain should be expected. (Full-load fuel economy is not a high priority and increased output would probably be taken rather than the economy improvement.) This piece of work, carried out on an engine with a waste-gate controlled turbo-charger, did not produce any part load fuel economy figures.

As with gasoline engines, exhaust gas recirculation (EGR), is an important method for reducing the formation of NO_x in diesel engines, but because diesel engines operate with lean mixtures (more oxygen in the exhaust gases) and much higher cylinder pressures than gasoline engines they produce more NO_x and therefore require higher levels of EGR[1] to compensate. (Kohketsu, *et al*, 1997, Itoyama, *et al*, 1997 and Yamada, *et al*, 1998).

([1] It should be noted that modern light duty diesel engines use very high levels of EGR, in some cases more than 60% by mass (Horrocks and Robertson, 1996), but the systems currently employed are exclusively external and increasingly these systems require throttled intake systems to induce sufficient mass flow. Also, because they are using such high levels of EGR they are increasingly being fitted with EGR coolers to reduce bulk cylinder temperature at the end of the induction stroke.)

To implement internal EGR using some form of VVA system, it has been proposed that the intake valve could be opened for a short period during the exhaust stroke (Benajes, *et al*, 1996). This causes EGR to be forced into the intake system, to be induced during the subsequent intake stroke. However, since exhaust fouling of the intake ports has been identified as a problem, (Leonard *et al*, 1993), it may be that a similar approach, but opening the exhaust valve briefly during the intake stroke, might achieve the same result without any intake port fouling. However, neither of these strategies can be achieved with simple VVA systems.

2.4.3 Increased power

To increase engine output requires either high speed torque to be improved, if the engine speed range is limited, or the torque to be maintained and the speed range to be extended. Since the upper speed limit of a modern diesel engine is usually imposed by combustion speed limitations there appears to be little opportunity to extend the speed range using VVA.

However, since VVA can allow an engine to operate with a lower nominal compression ratio, the BMEP can theoretically be increased, (by increasing the boost levels) within the same maximum cylinder pressure limitations (Watson and Janota, 1982). Zappa and Franca (1979) investigated using VVA to reduce the effective compression ratio of an engine in order to be able to increase the output through operating on the Miller cycle. Stone and Kwan (1985) suggest that raising and flattening the torque curve, of a diesel engine, should be possible with variable valve timing. This would result in increased power.

2.4.4 Increased low speed torque

There are two circumstances to consider here, very low speed where the mass flow through the engine is insufficient to allow the turbocharger to produce any significant boost and when the turbocharger is producing boost. When the engine is operating at full load the driver is demanding as much torque as the engine can produce. Thus the task of the VVA system is to maximise torque, and efficiency is a lesser concern.

Without boost , the engine is essentially naturally aspirated, and since the lack of overlap effectively isolates any exhaust system activity from the intake, volumetric efficiency and thus the torque is controlled by IVC. Therefore, optimisation of volumetric efficiency would take account of the (limited) pressure wave and momentum flux effects in the intake manifold. This

would normally require the VVA system to progressively advance IVC as speed decreases. Under this operating condition, EVO is the usual compromise between expansion work and exhaust blow down work.

When boost is available the picture is more complex. Torque is still strongly affected by volumetric efficiency, but when boost is available, useful work, that increases the torque output, is available from the induction stroke as well. Thus, IVC, through maximising volumetric efficiency, and EVO, through its interaction with the turbine, both play a part in maximising torque. As would be expected, the control exerted by intake closing is by maximising volumetric efficiency referred to manifold conditions. Exhaust opening optimises expansion work and blow down pumping work as usual, but it also controls the energy supply to the turbine, which in turn influences boost pressure and thence torque through work done in the induction stroke. *Figure 2.4.4.1* contrasts valve timings for a typical modern diesel engine with fixed valve timings with those optimised for improved low speed torque.

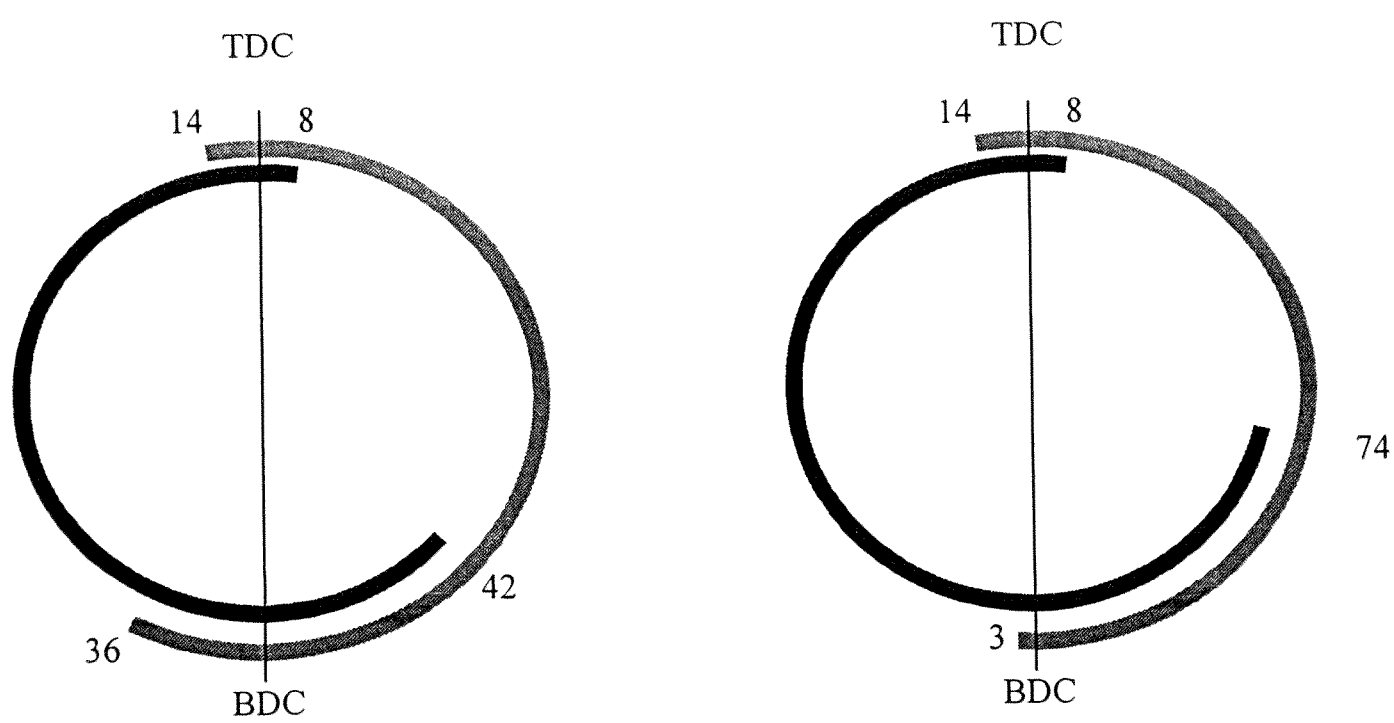


Figure 2.4.4.1 Typical fixed valve timings (left) optimised low speed torque (right.) (Lancefield et al, 2000) (Ramp top timings 0.1mm lift opening and 0.2 mm closing)

Results from a simulation based investigation of a VVA application to a current production light duty diesel, indicate that at low engine speeds advancing EVO from the standard timing can increase torque substantially (Lancefield *et al*, 2000). At 1600 rpm full load, torque was improved by 9% by advancing EVO from 42° to 96° BBDC. When IVC and EVO timings were both optimised at the same speed full load torque was improved by 15%, by advancing EVO

from 42° to 74° BBDC and IVC from 36° to 3° ABDC. In both cases the air-fuel ratio was held constant.

It can be seen from these data that the additional energy supplied to the turbine by opening the exhaust valve earlier is very significant in boosting output. In non-steady state operation this could be used to achieve other improvements:

2.4.5 Improved turbocharger transient response

There is little literature investigating this area. Charlton *et al* (1991) investigated the effects of variable valve overlap control on load rejection in a constant speed generating set (750 kW Paxman Valenta 6RP200). This study showed that maximising the mass flow through the engine as quickly as possible after the load application improved load rejection and built up boost pressure most quickly. Increasing overlap had this effect in the configuration simulated. High speed, light duty automotive engines cannot use this technique, but control of EVO and IVC can similarly influence the energy supply to the turbine.

With modern engine management systems, at full load, diesel engines run with lower limiting AFR control to prevent the generation of visible smoke. Therefore, under "tip-in" (rapidly increasing load) transient operation the rate at which engine torque can rise is dictated by the rate at which air flow increases. If turbo-lag is appreciable the resulting slow rate of torque rise can cause drivability problems. Altering IVC to maximise volumetric efficiency and EVO to produce maximum turbine output, upon recognition of tip-in transients, can make extra mass flow and turbine energy available to accelerate the turbocharger more rapidly than without variable valve timing.

Variable geometry turbines are becoming increasingly widely used and are also able to influence the energy flow to the turbine: increasing gas jet velocities by restricting the orifice areas in the nozzle ring of the turbine. This can be used to provide a good turbine "match" to the engine across a large part of its operating range and also offer transient response improvements, but there are pumping work repercussions of closing down the nozzles. However, to date, there appears not to have been any public debate about the impact of this on fuel economy or transient operation.

2.5 CONCLUSIONS

In summary, it seems that if suitable VVA characteristics can be implemented, taking into account the limitations imposed by the design fundamentals of diesel engines, then VVA is able to improve the operation of diesel engines in a number of ways:

1. Increased valve train design flexibility to allow reduced cost of manufacture, improved reliability or function and reduced valve train friction and space requirements.

2. Improved cold starting and/or potential for reduced compression ratio.

3. Improved fuel economy and perhaps emissions.

4. Increased power.

5. Increased low speed torque.

6. Improved transient torque rise.

However, from the lack of literature available on the subject it can be concluded that the application of VVA to diesel engines is far from well understood. One likely impediment to the generation of data to improve this understanding is very simple low cost, VVA systems do not exist for diesel engines. But, in order to investigate the benefits, even through simulation, some knowledge of the behaviour of the VVA system is necessary. Therefore, in order to increase the knowledge in this area two main activities are necessary:

1. Review the available VVA systems, assess their suitability for application to diesel engines and select a target system to investigate.

2. On the basis of the characteristics of the selected VVA system investigate the potential for improving the operation of light duty diesel engines.

Subsequent sections of this document address these activities, with chapter 3 covering the selection and characteristics of a suitable VVA system, whilst chapter 5 presents results from the investigation, through simulation, of the application of this system to a modern 4 cylinder diesel engine.

3 VVA MECHANISM SELECTION FOR DIESEL ENGINES

As has already been mentioned the design of the light duty diesel engine, and in particular the high compression ratio typically used, requires that special care is taken to avoid valve to piston contact around overlap TDC when designing even a standard valve train for these engines. For VVA the implication of this constraint is that increases in valve overlap are not feasible.

Analysis of the requirements of VVA for diesel engines indicates that both advance and retard of EVO and IVC may be necessary to realise the full potential for improvement in engine operation. Advancing EVO and retarding IVC are possible with conventional camshaft phasing devices, but negative overlap and unwanted residuals result. However, retarding EVO and advancing IVC would both lead to an increase in valve lift at overlap TDC and any significant movement would be precluded by valve to piston contact. This essentially renders phasing of the camshafts impractical. Therefore, the most fundamental characteristic of a VVA system for diesel engines is that it can change the duration of the valve open period.

Having identified the necessary operating characteristic of a VVA system for diesel engines, the major factor that needs to be considered in the selection of a suitable candidate system for performance investigation, is the cost of implementation to the engine manufacturer. This is a composite of engineering (design) costs, piece costs, cost of investment in production equipment and warranty costs. Balancing these to find an optimum is difficult, but key features are minimal change to the engine design, low piece costs, high reliability, use of familiar looking parts made of known materials, by known processes and finally relative simplicity.

The next section of this report deals with the classification of VVA systems in general and then concentrates on those that, according to the above criteria, could be considered suitable candidates for application to diesel engines. From these a target system is selected for further investigation.

3.1 LITERATURE SURVEY, CLASSIFICATION OF VVA SYSTEMS AND SELECTION OF TARGET SYSTEM

Variable valve timing as a method of altering the characteristic of an engine has been understood for many years (Bull, 1924) but until recently it had been possible to achieve the required improvements in performance, economy and emissions by other, less demanding means, such as:

1. Changing from carburettors and distributors or distributor type diesel pumps to computerised control systems.
2. The use of catalytic converters to treat the noxious engine emissions and convert them into less harmful forms.
3. Improved materials, e.g. piston materials that allow reduced top ring land heights with consequent reduction in emissions from crevice volumes.
4. Improved manufacturing methods, providing economical methods for machining materials that were previously too difficult to use, such as parent metal cylinders bores in aluminium blocks and fibre reinforced aluminium combustion chamber roofs for diesel engines.

Concurrently, analytical techniques and diagnostic instrumentation improved, leading to greater awareness of the factors that affect engine operation, particularly in the area of combustion. These led to design advances such as the 4 valve pent roof combustion chamber which has both combustion and valve train advantages. (Lancefield *et al*, 1995)

However, the problem associated with well developed, mature, products is that further improvements become incremental, small and difficult to achieve. This is now true of automotive internal combustion engines. To make the gains in performance, emissions and efficiency that will be required to meet the future legislative and customer demands, alternative technologies will be needed. The flexibility of variable valve timing systems and their ability to affect all aspects of engine operation make them suitable for helping to meet the anticipated legislative and customer demands.

3.1.1 General

There have been several notable review papers, attempting to classify the large variety of VVA systems that have been proposed, patented, and built in either prototype or serial production forms (Gray, 1988), (Dresner and Barkan, 1989), (Ahmad and Theobald, 1989) and (Stone and Kwan, 1989).

Others, (Stojek and Swoirok, 1984), (Ma, 1988)and (Demelbauer-Ebner *et al*, 1991), have sought to highlight particular features of the effects of VVA on engine operation, either through the evaluation of a single variable, such as overlap, or the effects on a single output, such as fuel economy or torque.

A third group have investigated the strategies for the wider use of VVA to improve all aspects of engine operation (Asmus, 1991), (Oehling *et al*, 1995).

In the fourteen years since the earliest of these papers was published, the technology of VVA has advanced, new systems have been invented and some have gone into serial production (although it is interesting to note that with two exceptions, all of the more recently produced systems fall into the simplest category of device and are similar in function to those that were in production when the above papers were produced). As part of this work, it is proposed to bring the classification of VVA devices up to date and extend it to cover other devices that have effects analogous to VVA. This is done using the approach proposed by Stone and Kwan (1989):

3.1.2 A taxonomy of variable valve timing systems

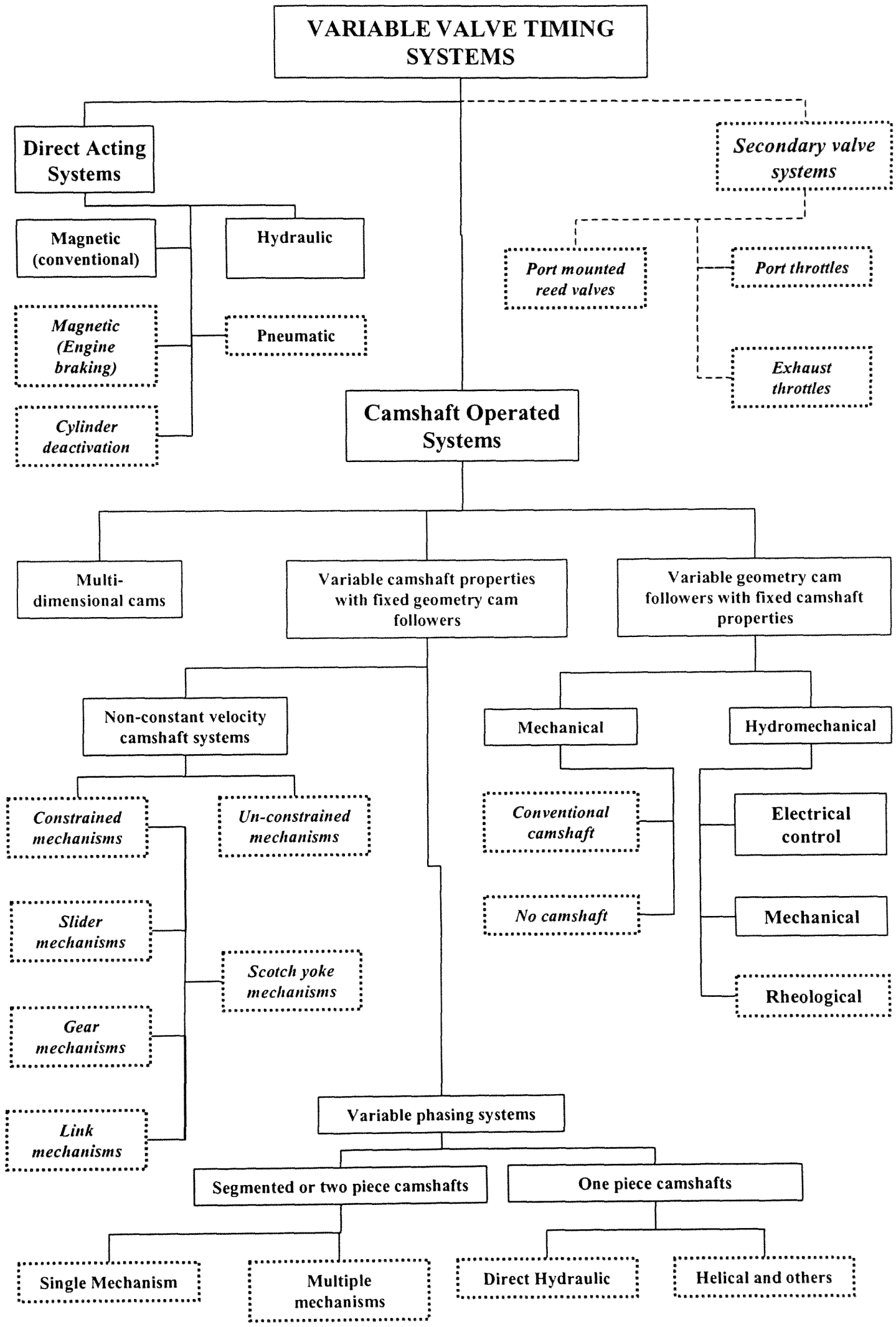


Figure 3.1.2.1 Taxonomy of variable valve timing systems (Lancefield 1999)

Figure 3.1.2.1 illustrates in diagrammatic form the basic classifications of VVA systems proposed by Stone and Kwan, (1989), with extensions (*in italics in dotted boxes*) to cover new types of devices that fall within the original classifications and an additional grouping of devices that have some of the functions of VVA, such as secondary valve systems.

In Lancefield (1999) there is a detailed discussion of systems representative of each of the boxes in the taxonomy to highlight their particular technical and commercial strengths and weaknesses. Also included are drawings of many of the systems.

In general the devices mentioned are considered to have the potential to run as prototypes (if this has not actually been done) and are therefore of interest. This judgement alone reduces the number of individual devices to be covered dramatically as many that have been proposed, particularly in patents, and even some that have been investigated as prototypes, have so many weaknesses that they cannot be considered practical. These weaknesses are typically in the areas of stressing, either through dynamic or shock loading, although complexity, cost, durability and physical size and weight rule out many systems.

When seeking systems specifically for diesel engines, consideration of the necessary operating characteristic of allowing variable valve open period simply allows systems such as "Variable phasing systems" (Lancefield, 1999 – Section 4.4.2.3.1) and "Secondary valve systems" (Lancefield, 1999 – Section 4.3) to be discounted from further consideration.

"Multi-dimensional cams" can also be discounted for technical reasons as the practical range of authority over valve open period is insufficient (Lancefield, 1999 – Section 4.4.2.1).

It is important to recognise at this point that this exercise is concerned with the conventional operation of diesel engines with stratified combustion, which , in general terms, requires maximised valve head air flow. Thus the systems classified as "Variable geometry cam and followers with fixed camshaft properties" (Lancefield, 1999 – Section 4.4.2.2) which typically reduce lift at the same time as reducing valve open period, can be removed from the list of candidate systems because valve lift reduction is undesirable. These systems are also relatively complex and probably would not have acceptable costs of application for this type of use. (It should be noted that the recently launched BMW "ValveTronic" system is of this major

classification, sub-classifications "Mechanical" and "Conventional camshaft." It is used for valve head throttling of a gasoline engine to provide significant improvements in fuel economy.)

Commercial constraints are the major reason for discounting the "Direct acting systems" (Lancefield, 1999 – Section 4.4.1). Whilst these types of system offer great flexibility of operation, they are perceived to be extremely expensive on all levels: design costs and piece costs are high, reliability is not yet fully demonstrated, the parts look unfamiliar and use unusual materials and manufacturing processes and they lack simplicity.

The unsuitability of the above VVA systems leaves only non-constant velocity camshaft systems:

3.1.3 Non-constant velocity camshaft systems:

These fall broadly into two groups, those that allow the cam lobes some freedom to move relative to the main shaft of the camshaft, under the influence of the valve spring loads, here referred to as *un-constrained mechanisms and* those that use mechanisms to impose a cyclically varying speed on the conventional rotation of the cam lobes and retain control of the cam lobe motions throughout each revolution, here referred to as *constrained mechanisms*.

3.1.4 Un-constrained non-constant velocity systems

For reasons explained later in this section this classification of VVA system can also be removed from the list of candidate systems for diesel engines, but a limited discussion is included because it is known that devices of this type were intensively developed, but later abandoned, by VW. The interested reader is referred to Lancefield (1999 – Section 4.4.2.3.2.2) which provides a detailed explanation of these devices

In principle the devices covered by this classification are elegant and simple, in that they allow the forces generated within the valve train to influence the valve motion. They are compact since the mechanisms are completely contained within the space allowed for the standard camshaft and they can operate without any external control, although several mechanisms proposed do have external control.

Paulmier (1974) arguably used the simplest approach, fitting very soft valve springs and allowing the follower to lose contact with the cam lobe and rejoin with it as dynamics dictate. Whilst such

a system is able to demonstrate the effects of increased time area under the valve lift curve it cannot reduce valve open period and is totally impractical from the noise and durability points of view.

More practical approaches have been proposed and typically these are intended to shorten the periods the valves are held open at low speeds. This is achieved by allowing the cam lobes some rotary freedom relative to the shaft on which they are mounted and using the valve spring forces to retard and then advance the cam lobes to change their effective duration. If completely un-constrained a cam lobe will retard when attempting to open the valve and advance when closing the valve. In their simplest form these devices allow the cam lobes to retard and advance perhaps 15° cam, providing a 60° crank range in duration, before they reach some form of limiting stop. If simple mechanical dead stops were used, then impact loadings and excessive noise would result.

The relatively practical systems in the public domain seek to overcome the problems associated with impact by using spring and damper mechanisms to control the motion of the cam lobes. *Figure 3.1.4.1* shows a generalised model of these systems.

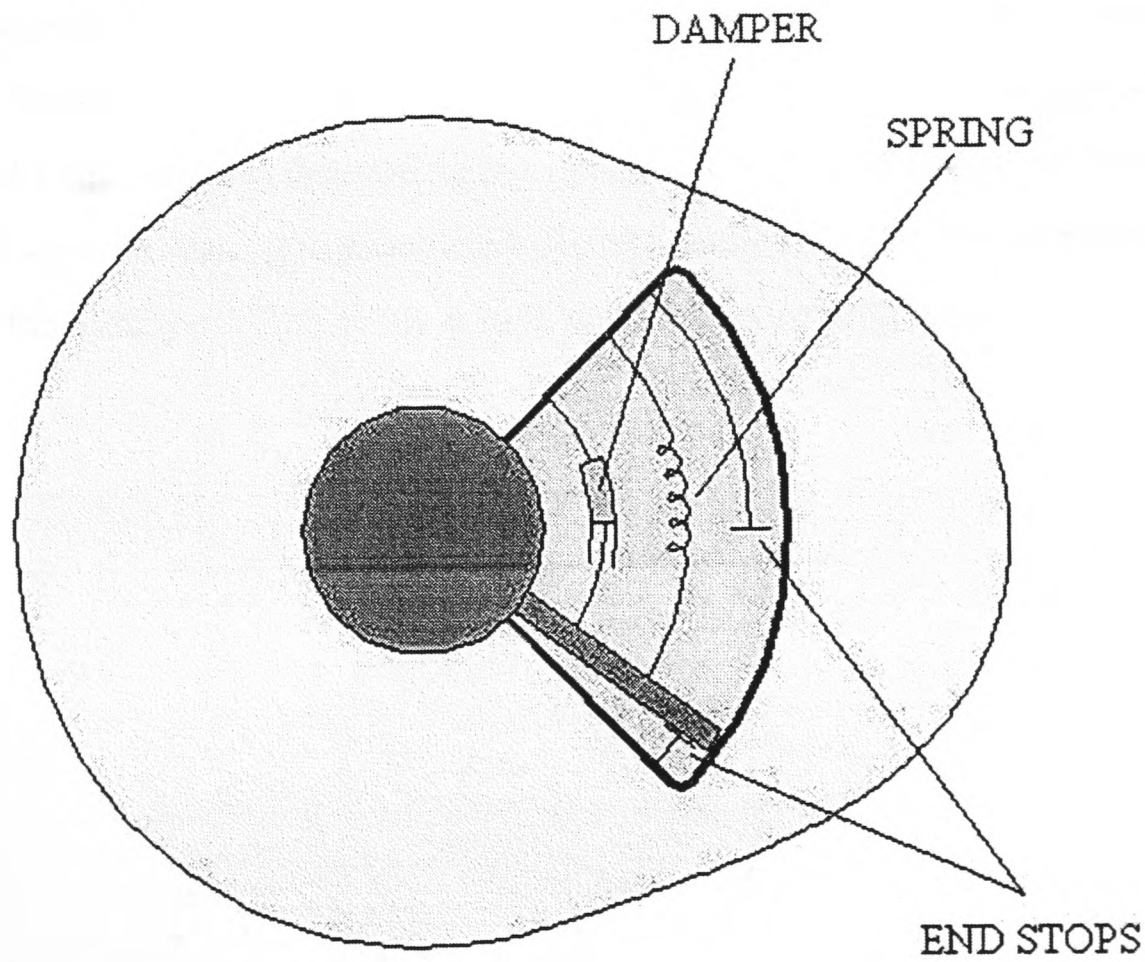


Figure 3.1.4.1. Schematic of the mechanisms used to control the motion of un-constrained cam lobes.

The natural characteristic of this type of device is for the duration to extend with increasing speed. Asymmetric damping characteristics alter the effects on opening and closing timings, and if the cam lobe is to return to its nominal position between lift cycles a spring is required.

This natural characteristic is not altogether satisfactory, as a low speed retardation of intake opening can introduce unwanted residuals through negative overlap. However retarding of intake closing with increasing engine speed is desirable. Similar conflicts arise in application to the exhaust camshaft of a diesel engine since EVC is constrained and the natural characteristic is not necessarily correct for EVO. This implies that to get the best from this type of VVA system an external control system to modulate duration and camshaft phasers would be needed to modify the characteristic for use with diesel engines.

Volkswagen AG have been active with this type of VVA system for a number of years. A patent by Krüger (1984) shows the simplest forms of the device, using just dead stops and an alternative with a simple rotary vane type damper. Later work (Beier *et al*, 1994) shows the introduction of rotary dampers of a more advanced form than the earlier work, see *figure 3.1.4.2*. Neither of these pieces of work appears to include an external control system, so they are relying on the natural characteristic of the stops and dampers. Krüger (1984) shows that without dampers the valve opening is fixed by the stop and the closing is a dynamic function of engine speed, with valve closing retarding with increasing engine speed. He also shows that the addition of a bi-directional damper extends the duration of the event at each end with increasing speed.

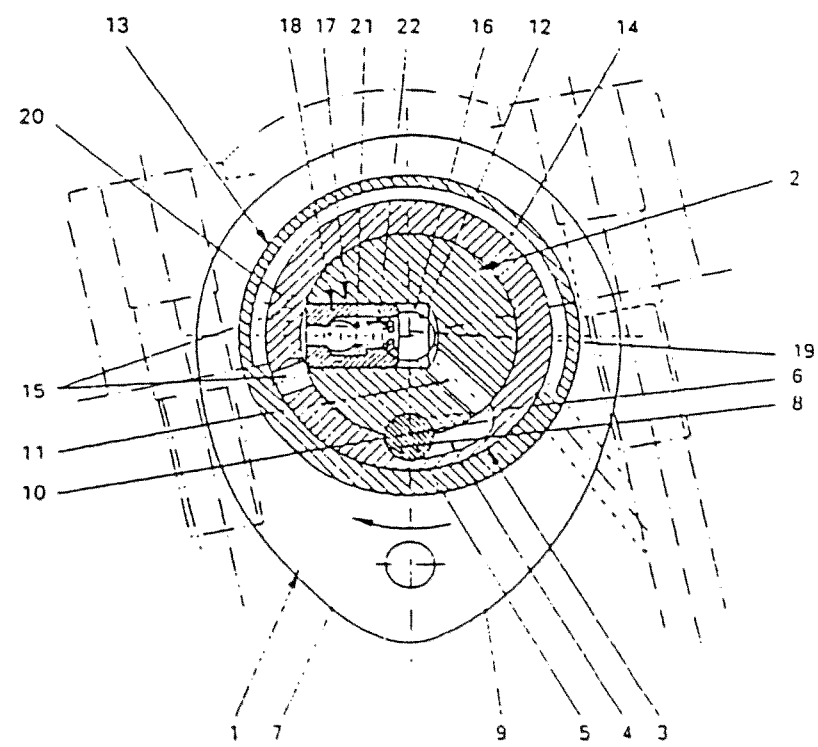


Figure 3.1.4.2. Lost motion cam lobes with improved damping. (Beier *et al* 1994)

A derivative of this type of system called "Flino" by Volkswagen was reputed to be entering production (Williams, 1997) in the new "Beetle" that is being manufactured in Mexico. For the rumours to have reached this level it is clear that: extensive prototype running has been carried out with the Flino system, benefits are available and it is durable. However, tight tolerances needed in its manufacture appear to have caused problems in terms of cost and repeatability, as will be discussed further later, and it now seems unlikely that the system will be put into production.

The Flino system relied on the natural characteristics of the internal springs and dampers to control its behaviour as a function of engine speed only. But Frost (1992) and Frost and Lancefield (1996) proposed systems that could be externally controlled to constrain the duration change symmetrically or otherwise.

Neither of the Frost systems was implemented in hardware, but they were extensively analysed and it was concluded that the problems associated with implementing springs and damper arrangements with appropriate rates was such that even with the axial implementation proposed (Frost 1992), they would be too expensive to make and the project was discontinued.

It is this latter point that is the major concern with devices of this type. It is clear that VW have addressed the problems - at least at a prototype level. Inspection of the diagram in *figure 3.1.4.2* show that the oil flows for the dampers pass through drillings that meet at the surfaces of the shaft and tube. To prevent significant oil flows along the axis of the shaft/tube, as required for the dampers to work properly, needs a very tight fit between the two. This is difficult to achieve since it needs to be so in several regions along the length of the camshaft. Variations in fit and damper characteristic from cam lobe to lobe will contribute to varying cylinder filling. As with many of the VVA systems utilising hydraulic functions, oil rheology will also affect system behaviour and dirt may also cause problems.

Therefore, whilst this type of device is apparently simple, and is very attractive because it is essentially a "drop-in" device with low design and investment costs, practical matters associated with control of tolerances appear to make the device itself too expensive and/or unreliable to implement. This leaves only constrained non-constant velocity mechanisms for further consideration:

3.1.5 Constrained non-constant velocity mechanisms

There is a large number of mechanisms that can impose a cyclically varying angular velocity onto the conventional rotation of a shaft. Bickford, (1926) deals with mechanisms for intermittent motion, some of which could be used for applications such as this. Fuenmayor *et al* (1982) discuss four bar link mechanisms for this use, whilst Freudenstein *et al* (1988) and rather later Wampler (1993) deal with the more general issues of synthesis and analysis of variable valve timing systems.

Practical experience with many devices in this type and the available literature seem to point to four classifications of mechanism for this particular type of VVA system:

1. Gear based mechanisms – *gear mechanisms*
2. Four bar link mechanisms with pin jointed linkages – *link mechanisms*
3. *Scotch yoke mechanisms*
4. Four bar link with sliding element - *slider mechanisms*

Gear mechanisms: Many devices of this type have been reported in the literature. Roe (1972) used an epicyclic gear train with a modulating input. Both Ma (1981), *figure 3.1.5.1*, and Phoenix and Phoenix (1991), *figure 3.1.5.2*, used the same underlying principle, but Ma used a small pulley driven by the cam drive chain/belt, at a multiple of crank speed, to cycle the annulus of the epicyclic, whilst the Phoenix system integrated a mechanism adjacent to the camshaft to cycle the epicyclic in the same way.

These inventors use the reduction ratios available from these types of device in different ways. Roe used the annulus as the drive to the cam, with the planet carrier driven from the crank and the modulating input applied to the sun wheel. Ma shows the drive from the crank to the sun wheel, the output to the cam from the planet carrier and the modulating input to the annulus, whilst the Phoenix system used the annulus as the drive to the cam, with the driven sun wheel from the crank and the modulating input applied to the planet carrier. Dependent upon the ratios of the epicyclic it may be possible to implement the 2:1 reduction from crank to camshaft in the device, with a 1:1 drive from the crank. This would have the potential for reduced complexity and perhaps reduced engine height. Roe mentions this factor and Ma appears to have taken advantage of it, but Phoenix does not appear to have addressed this matter.

It is also worth mentioning that these devices do not always have symmetrical output characteristics. A detailed discussion of this is unnecessary at this point, but an analysis of the geometry of the systems applying the modulating input will highlight the cause of the asymmetry.

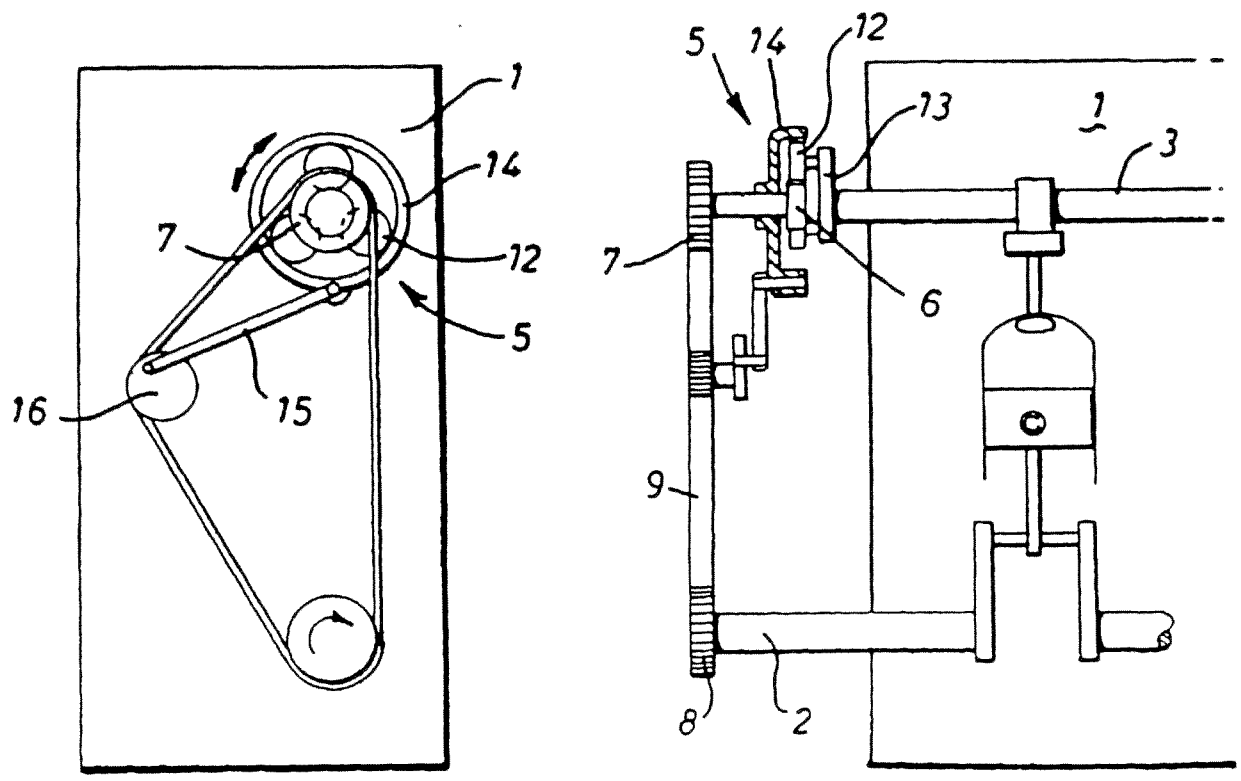


Figure 3.1.5.1. Gear mechanism for imposing cyclic motion onto a rotating shaft . (Ma, 1981)

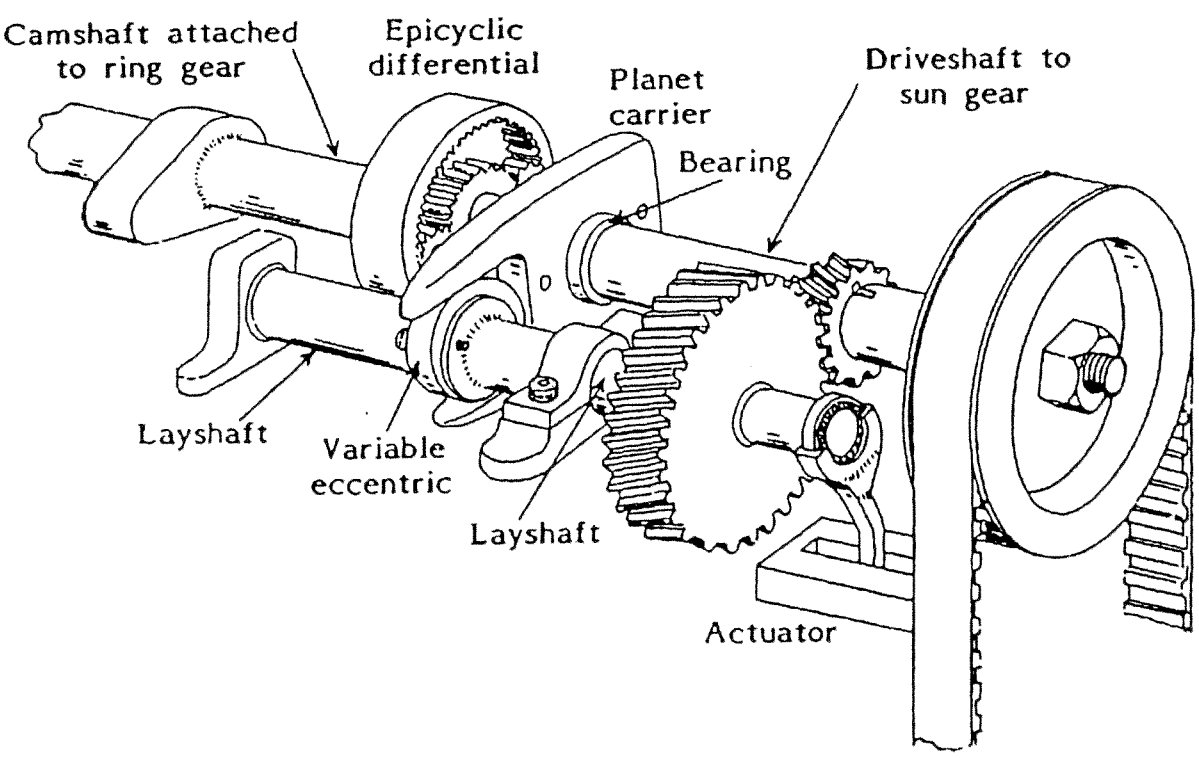


Figure 3.1.5.2. Alternative method of actuating the epicyclic . (Phoenix and Phoenix 1991)

Link mechanisms: Despite the work of Fuenmayor *et al* (1982), Mitchell (1980) appears to be the only one to have done extensive work on applying this type of mechanism, *figure 3.1.5.3*. It was

implemented on a single overhead camshaft Yamaha motorcycle engine, as reported by Scott and Yamaguchi (1980) and is shown in this form in *figure 3.1.5.4.*

To operate a mechanism of this type the drive shaft is moved eccentric to the camshaft centreline, to generate a cyclic speed variation during each rotation of the shaft. This can pose difficulties with the drive arrangement, particularly with belt and chain drives, where these movements will usually cause changes to the length of the tight and slack runs of the belt or chain, and thus necessitate the use of tensioners with unusually large operating ranges and faster jack up and leak down characteristics than would normally be required. (Certain configurations of belt and chain drives can remove this problem, but gear drives appear to offer the best solution to this problem Lancefield *et al,* 2000). All drive arrangements also have the possibility of small phase changes.

Like certain of the epicyclic devices, mentioned above, slightly asymmetric characteristics result from the use of these devices.

28 26 17

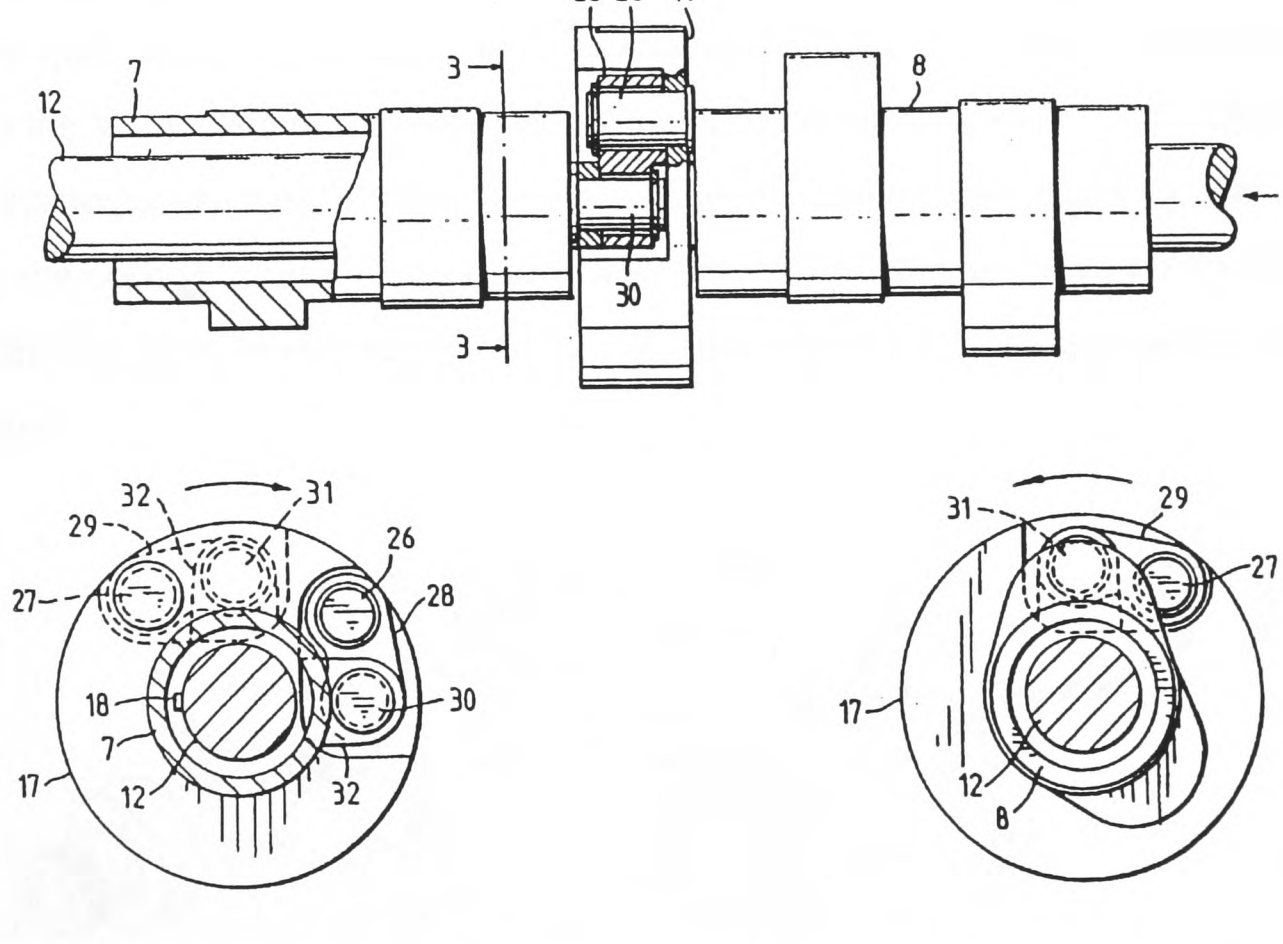


Figure 3.1.5.3. Link mechanism for generating cyclic speed fluctuations (Mitchell, 1980).

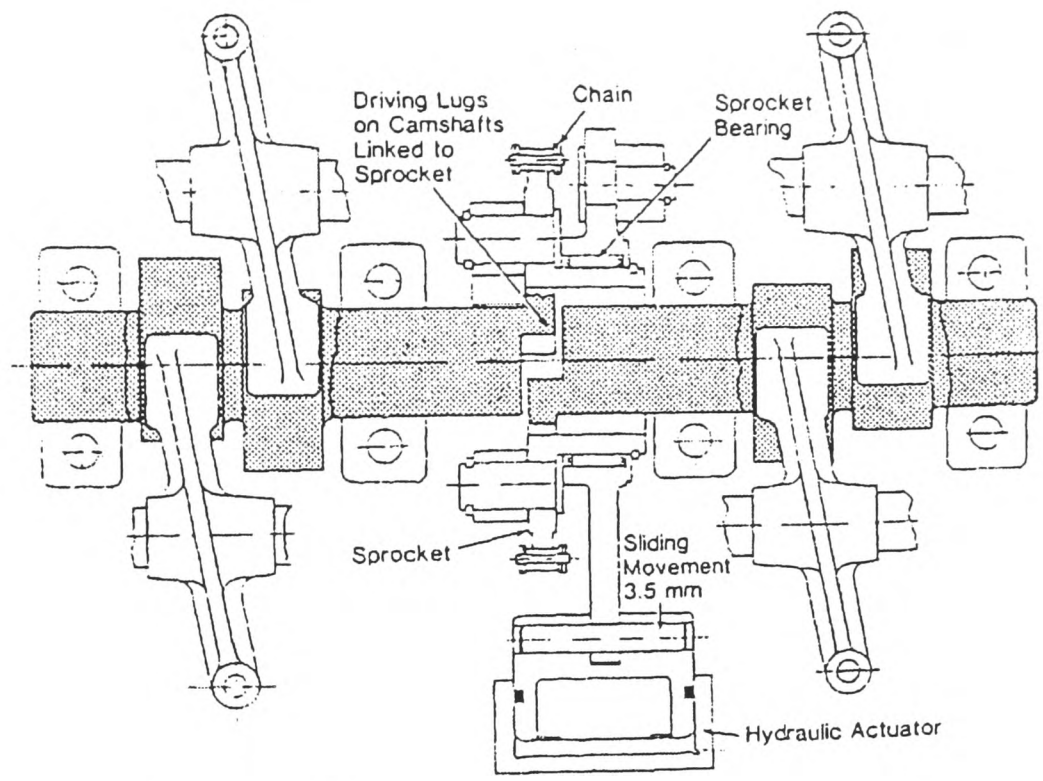


Figure 3.1.5.4. Link mechanism as applied to a Yamaha motorcycle engine (Scott and Yamaguchi, 1980).

Scotch yoke mechanisms: Frost (1986 and 1987) appears to be the only inventor to have used this type of mechanism specifically to generate a symmetrical motion. In the device disclosed in the earlier patent application he uses a pair of mechanisms 180° apart and back to back, one driving the output to the VVA system, the other driving a balance weight, *figure 3.1.5.5.* The later application discloses four mechanisms all packaged together in a single coupling. The coupling is moved from the outside to provide the eccentricity for the oscillations and therefore it does not require the drive shaft to be moved, *figure 3.1.5.9.* The reasons for these approaches will be discussed later.

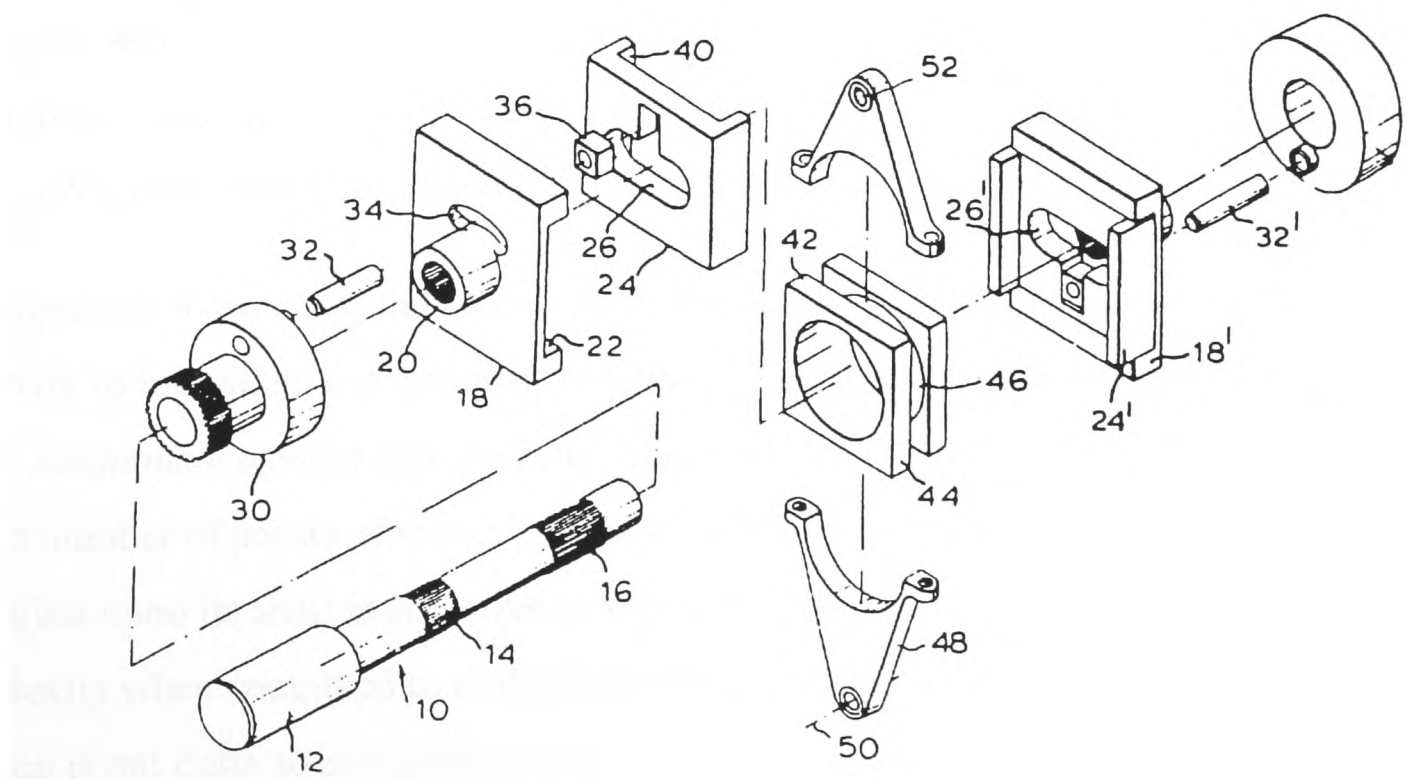


Figure 3.1.5.5. Scotch yoke mechanism for generating cyclic speed fluctuations (Frost, 1986).

Slider mechanisms: This type of mechanism appears to be the most popular with designers. These mechanisms typically comprise a four bar linkage, with a sliding/rolling element. Mitchell (1978), *figure 3.1.5.6*, shows an example with a roller in a slot. Again this type of mechanism requires that the drive shaft be moved to create the oscillating motion.

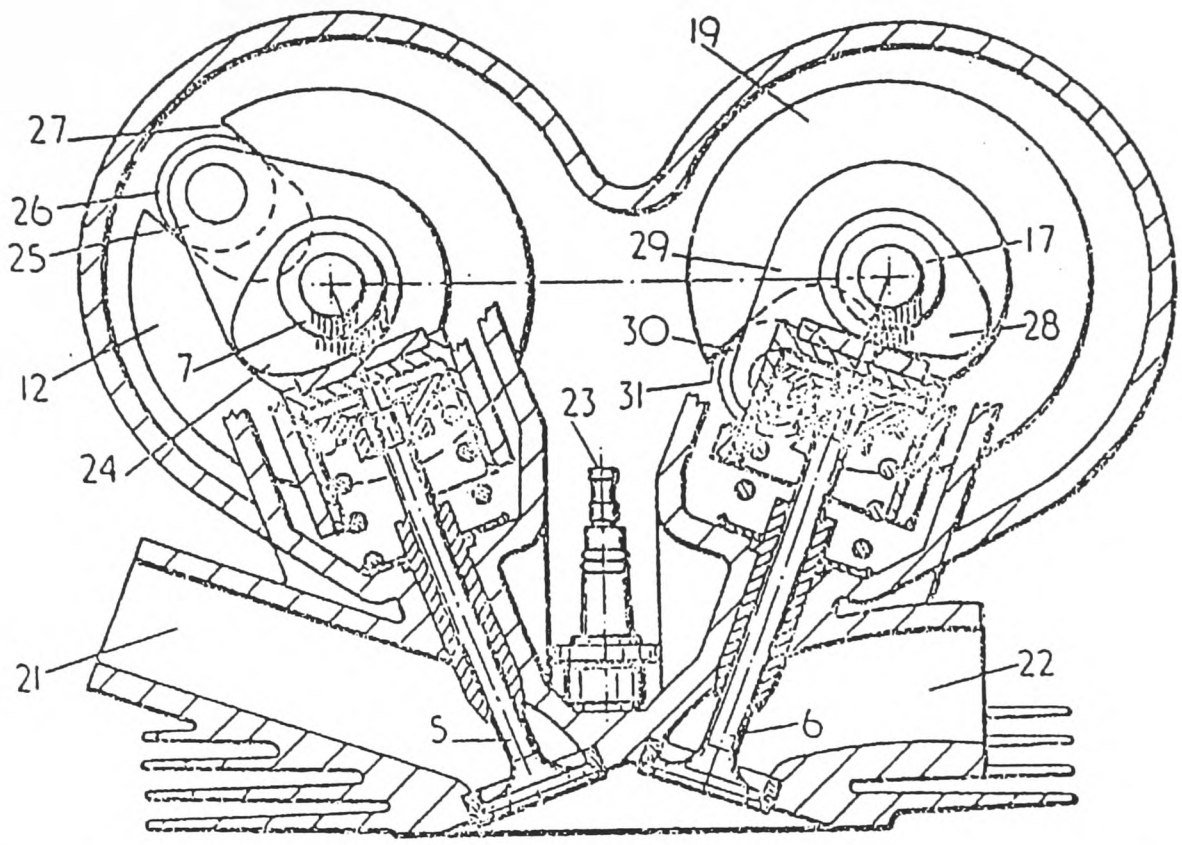


Figure 3.1.5.6. Roller in slot "slider mechanism" for generating cyclic speed fluctuations (Mitchell, 1978).

Associated Engineering, as discussed by Parker and Kendrick, (1974), used a double slider mechanism to overcome the problem associated with the requirement to move the drive shaft. See *figure 3.1.5.7.* More recently, Unisia, one of the component manufacturing companies associated with Nissan, used a similar double slider mechanism in the system they offered (Hara, 1993), but, unlike the Rover VVC system, which was based on the Associated Engineering design (Whitely, 1995), the Unisia offering has not been put into production.

It is important to note that the mechanisms discussed above can be applied to the whole camshaft, to individual cam lobes or to groups of cam lobes. Here the former will be termed *single mechanism devices* and the latter *multiple mechanism devices*. This distinction is important from a number of points of view. The use of a single mechanism to change the duration of all cam lobes upon its shaft is attractive as it should offer: lower cost, improved packaging and lower complexity when compared to multiple devices distributed along the camshaft. However the position is not quite so straightforward:

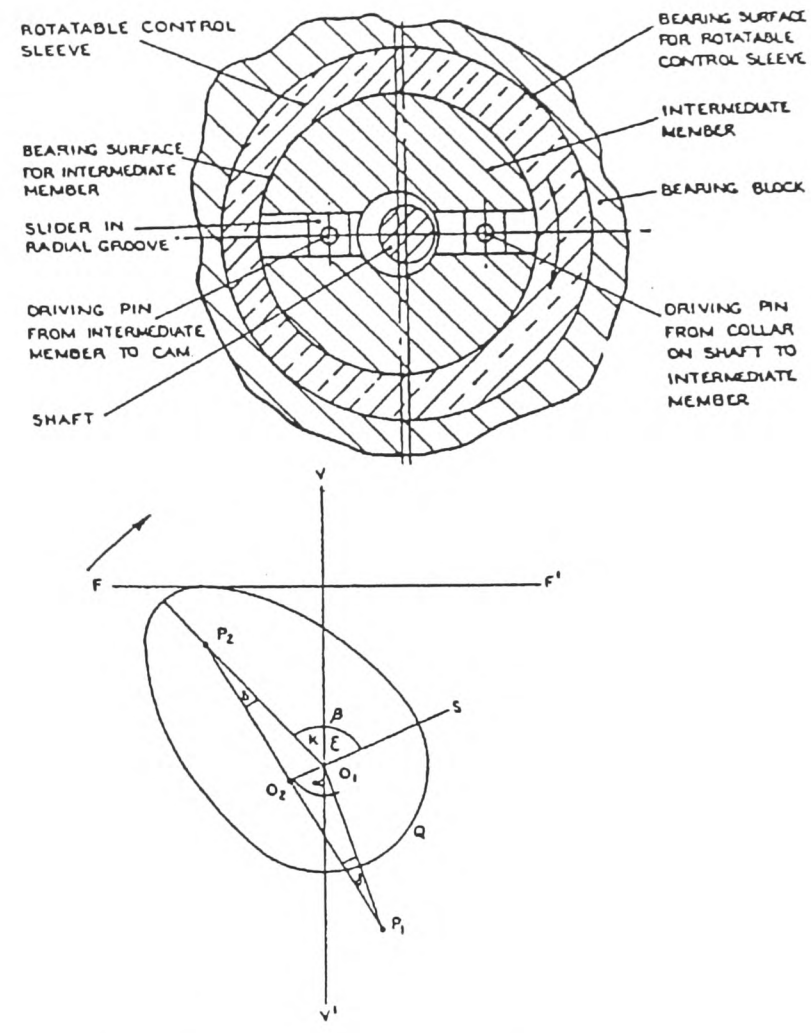


Figure 3.1.5.7. Double slider mechanism for generating cyclic speed fluctuations (Parker and Kendrick, 1974).

Single mechanism devices. There are practical difficulties that limit the usefulness of this type of system, but it is worth covering their operation to highlight why the difficulties arise.

The use of this type of system dictates that the mechanism forms part of the cam-drive arrangement and numerous mechanisms have been proposed, a number of which have been discussed in general terms above. The systems proposed by Roe (1972), Ma (1981), and Phoenix and Phoenix (1991) used an epicyclic gear train with a modulating input, whilst the system from Frost (1986) used a scotch yoke mechanism. The problem with these devices is that they are required to produce one oscillation per cylinder per camshaft revolution. This means that for an in-line four cylinder engine (which is the only practical configuration for this type of mechanism) the mechanism runs at twice engine speed. The angular accelerations and the resulting forces within the mechanisms produce high levels of friction and very highly stressed components.

As already mentioned above, several of the candidate mechanisms for this type of application have asymmetric characteristics. It was this feature that led Frost (1986) to the use of a scotch

yoke mechanism so that rotary balance weights could be properly employed. The use of a second mechanism to generate the 180° out of phase drive simply for a balance weight and the inherently high friction of a scotch yoke simply exacerbated the problem with friction.

The mechanism proposed by Frost (1986) and shown in *figure 3.1.5.5*, was built as a prototype and tested to provide (unpublished) data on both internal forces and engine operation. The forces in the control system were of the order of kilo-newtons, and durability was a concern, and although no improvements in fuel economy could be measured because of the high friction, indirect indicators such as manifold vacuum and spark timing provided evidence of the effects of reduced overlap on idle and increased overlap on part load residuals.

This combination of problems with high friction and large internal forces whilst obtaining encouraging indirect indicators from the Ma system led Frost (1986), who was working with Ma, to revert to the multiple mechanism approach. Ma (1988) concluded that the friction penalty associated with these types of device may be such that any fuel economy benefit derived from the improved engine thermodynamics would be exceeded by the energy absorbed by the VVA mechanism.

Multiple mechanism devices: To achieve a useful result from this type of device requires that the camshaft be divided into sections, one per cylinder, and that each section is driven by a mechanism that produces one complete oscillation per rotation of that cam shaft section (Lancefield *et al*, 1993). All of the mechanisms covered by the generic discussions above are capable of performing this function, but the practicality of finding space for the mechanisms tends to rule out the epicyclic gear approach. Running engines have been produced using the link type mechanisms (Scott and Yamaguchi, 1980), scotch yoke mechanisms (un-published work by Frost), and most commonly slider type mechanisms (Griffiths and Mistry 1988, Hara (1993), Lancefield *et al* (1993) and the Rover VVC system as reported by Whitely (1995)). The devices reported by Griffiths and Mistry and Lancefield *et al* are single slider mechanisms with moving drive shafts, whilst those reported by Hara and Whitely are double slider mechanisms with fixed drive shafts.

The disposition of the mechanisms along the camshaft, as a whole, vary from system to system, but space is the constraint that dictates the design.

The system reported by Lancefield *et al* (1993) used six mechanisms, each mounted at the front of its cam section, above the cylinder head bolts. The Jaguar cylinder head for this project was specially designed and manufactured to allow this configuration. The installation was also aided by the generous proportions of this older engine design.

The Rover VVC system did not have the luxury of a special cylinder head or adequate space for a similar solution and consequently used a different configuration: this design used two double slider mechanisms at each end of the cylinder head to minimise the impact on the cylinder head design Parker (1992 and 1994). The rear two mechanisms operated cam sections 3 and 4, with 3 driven by a shaft passing through cam section 4 connecting it to the rear-most mechanism. The drive to the rear two mechanisms was from the back of the exhaust camshaft. The front mechanisms operated cam sections 1 and 2 and were a mirror image of the rear, except being driven in the normal way from the crank. *Figure 3.1.5.8.*

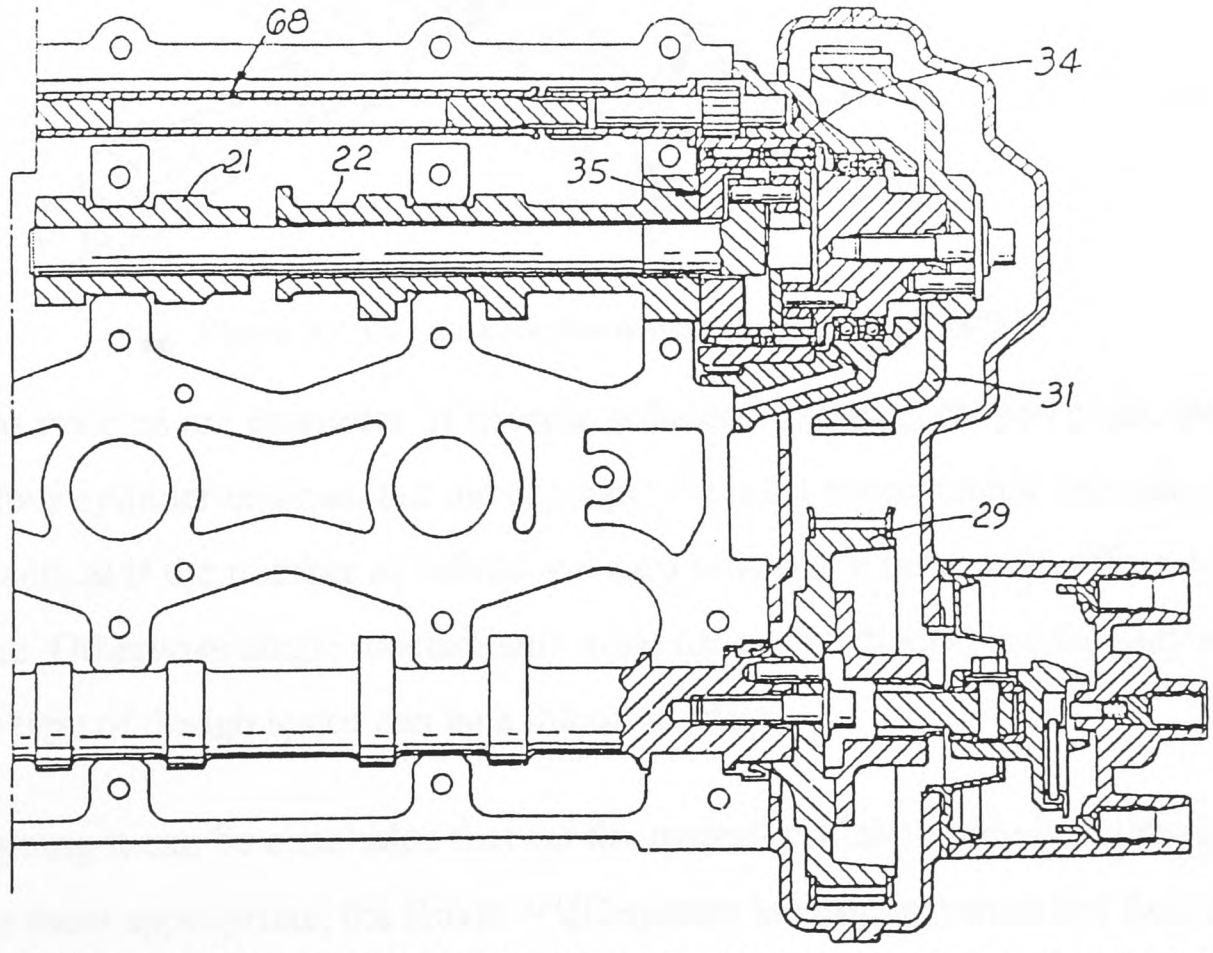


Figure 3.1.5.8. The Rover VVC system with two double mechanisms one at each end of the head. Rear only shown (Parker, 1994)

Frost (1987) discloses a single coupling with four separate mechanisms contained within it, *figure 3.1.5.9.* The coupling is central to the engine and drives cam sections 2 and 3 directly, whilst cam sections 1 and 4 are driven by shafts passing through cam sections 2 and 3 respectively. This design pre-dates the Rover system in this design feature.

It is also interesting in that it uses a scotch yoke arrangement to produce the cyclic speed fluctuations, but employs gears on the shafts and racks inside the scotch yokes to convert this motion from linear to rotary. A key feature of this system is that it relies on being able to produce a drive to the mechanism at the centre of the engine, something that was common on motorcycles, but has not found favour with conventional engine designers and has now become uncommon even on motorcycles.

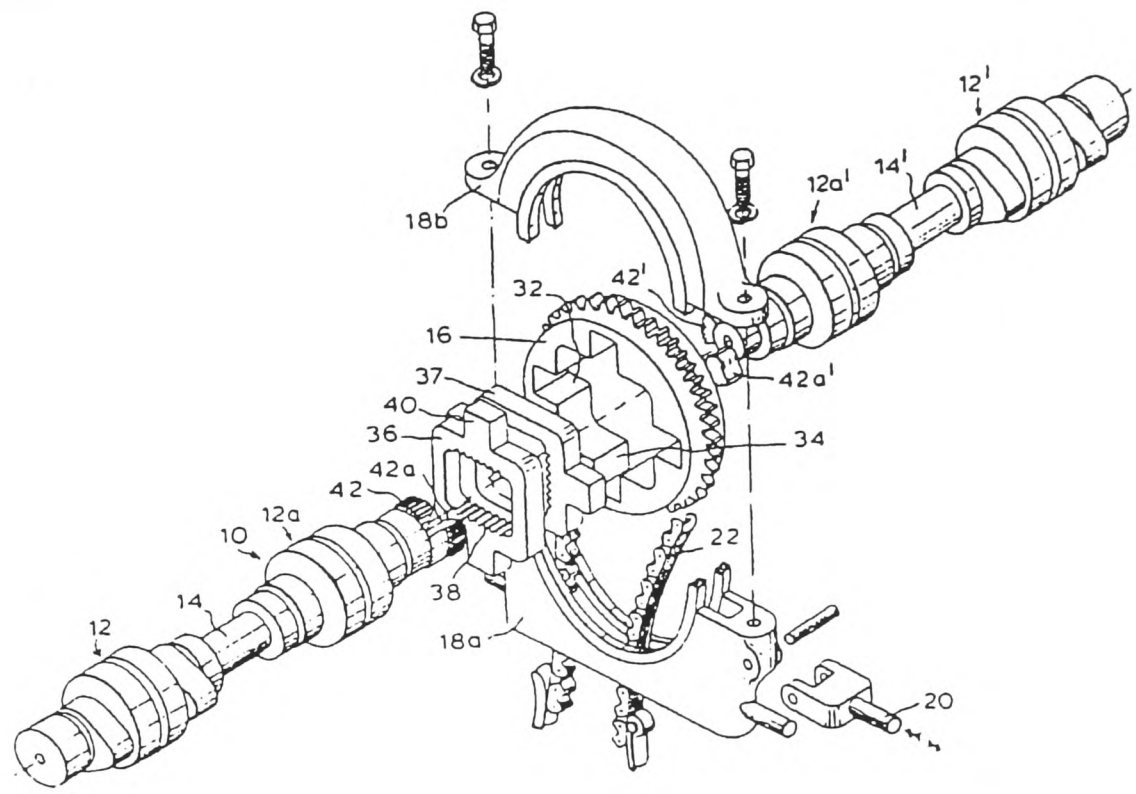


Figure 3.1.5.9. Four mechanism coupling. (Frost, 1987)

These later two systems are examples of specific solutions to particular problems. Both are only applicable to four cylinder engines, but the concept of double mechanisms between pairs of cylinders is practical if the number of valves and cam follower arrangement afford the designer sufficient space. Otherwise single mechanisms (one for each cylinder) are the only solution and even with this type of design space can be a major problem.

From the foregoing it can be concluded that for the majority of applications multiple mechanism designs are the most appropriate, the Rover VVC system having demonstrated function, and in some form, acceptable cost of implementation. However, designs other than that used by Rover are feasible and to illustrate the reasoning behind the selection of the configuration to be used for the performance investigation, the design process for one such application will be outlined:

3.1.6 Design overview of the application of a constrained non-constant velocity VVA mechanism

Although the VVC system was put into production, it has been subject to reliability problems in the field, with wear of the pins and drive blocks the major concern. To maintain an acceptable package size, the double slider mechanisms used in the VVC are of necessity small, leading to highly stressed components with a tendency to wear. To overcome this problem it is necessary to increase the sizes of the components sufficiently to avoid wear problems. But the size of suitably loaded components is such that it precludes double slider mechanisms and as a result the best configuration is multiple single slider mechanisms with a moveable drive shaft with its attendant cam drive problems.

Since it was known from testing of prototypes (Lancefield *et al* 1993) that these larger single mechanisms were strong and durable it was necessary to seek cam drive layouts that did not have problems with changes in chain or belt run lengths. Investigation of a large number of potential cam drive configurations led to one utilising gear drives to the camshafts that allowed the moving drive shafts to rotate around an input drive gear, introducing a helpful phase shift and maintaining drive integrity without any need for tensioners or like adjusting systems.

Figure 3.1.5.10 shows the standard cam drive arrangement for one engine investigated (left) and the modified layout allowing drive shaft movement pivoted about the input gear centre (right).

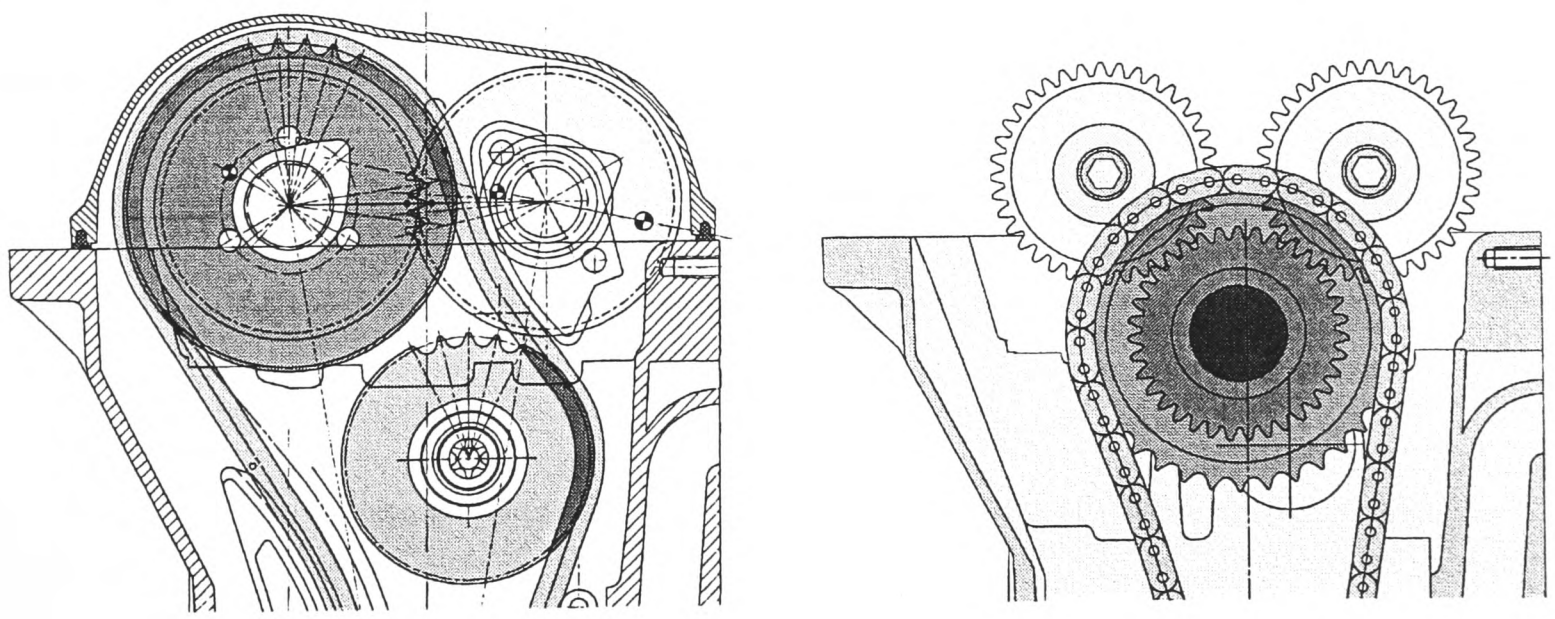


Figure 3.1.5.10 Standard cam drive arrangement (left) and the modified layout allowing drive shaft movement pivoted about the input gear centre (Lancefield *et al* 2000).

An earlier design for a gasoline engine also introduced the concept of placing the mechanisms between pairs of valves in 4-valve engines. This has the advantage that the mechanisms are not competing for space with cam bearings, but their central position precludes their use with direct

acting tappets. *Figure 3.1.5.11* shows a typical cam section "cam shell" (left) and its installation in a cylinder head (right). Although this central mechanism is limited to some form of roller finger follower or roller rocker type of valve train design this was not considered to be too great a limitation as many new engines were (and still are) being designed with these types of valve train in order to reduce valve train friction.

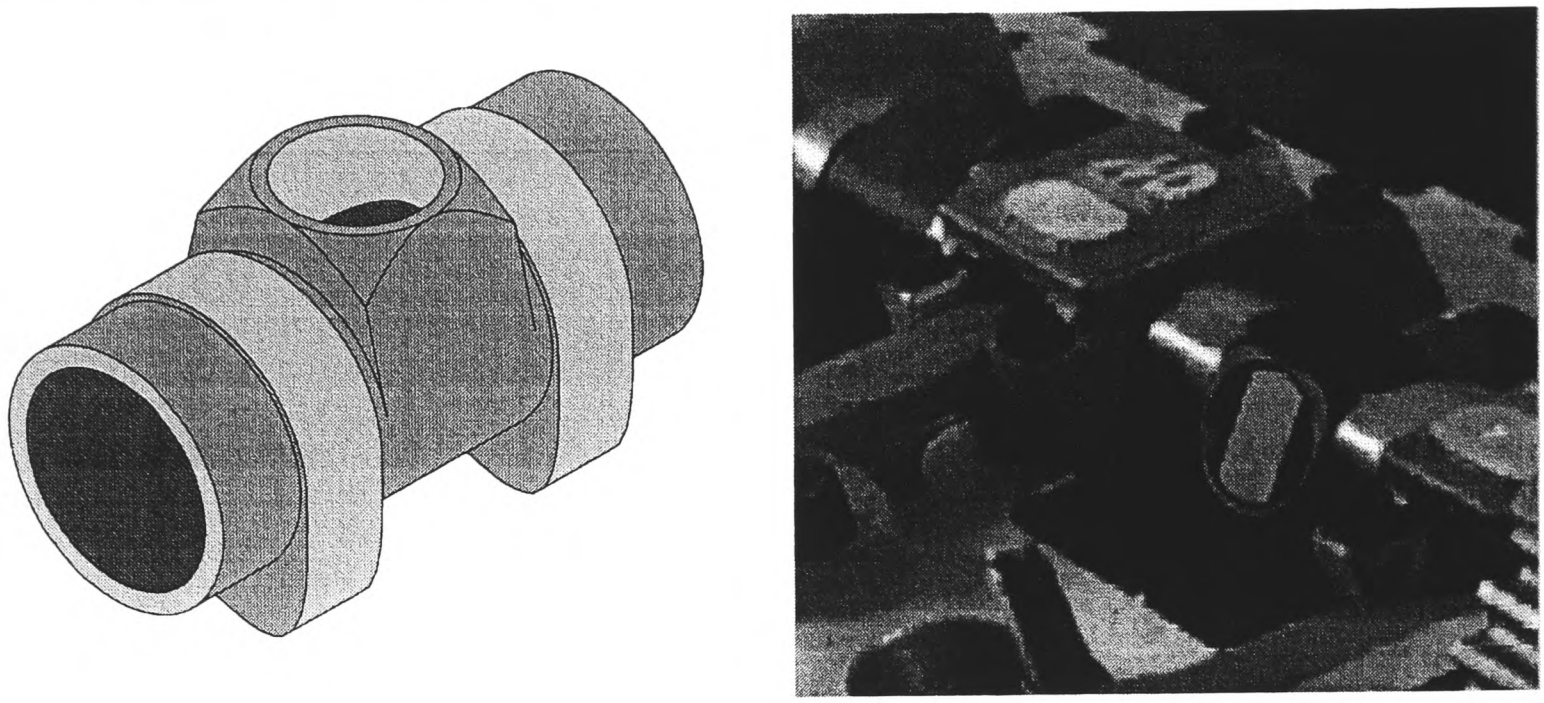


Figure 3.1.5.11 A typical cam section "cam shell" (left) and its installation in a cylinder head (right) (Lancefield *et al* 1993 and 2000).

Having established that multiple-mechanism single-slider designs were practical for application to both gasoline and diesel engines this type of mechanism was selected for investigation of the influence of VVA on light duty diesel engines. However, an understanding of the exact nature of the valve lift curves that result from its application was needed:

3.2 CHARACTERISTICS OF THE SELECTED VVA MECHANISM

This section of the report discusses the following:

1. Valve lift characteristics of this type of VVA mechanism and how it may be applied to both gasoline and light duty diesel engines.
2. The detailed kinematics of the mechanism and how valve train operation with this type of VVA system can be analysed.
3. How the use of this VVA system can improve valve train characteristics.

(It should be noted that, despite four types of *constrained non-constant velocity camshaft systems* being discussed individually in section 3.1.5, their characteristics are sufficiently similar that the detailed discussion of the selected slider type will adequately illustrate them all.)

3.2.1 Valve lift characteristics with the selected VVA mechanism

As mentioned above, the mechanism, *figure 3.2.1.1,* produces a cyclically varying rotary motion superimposed on the normal half engine speed rotation of the cam sections. It can be seen from inspecting *figure 3.2.1.1* that the phase angle "A," between the cam shell and the drive shaft alternates in direction. *Figure 3.2.1.2* quantifies this for several drive shaft positions.

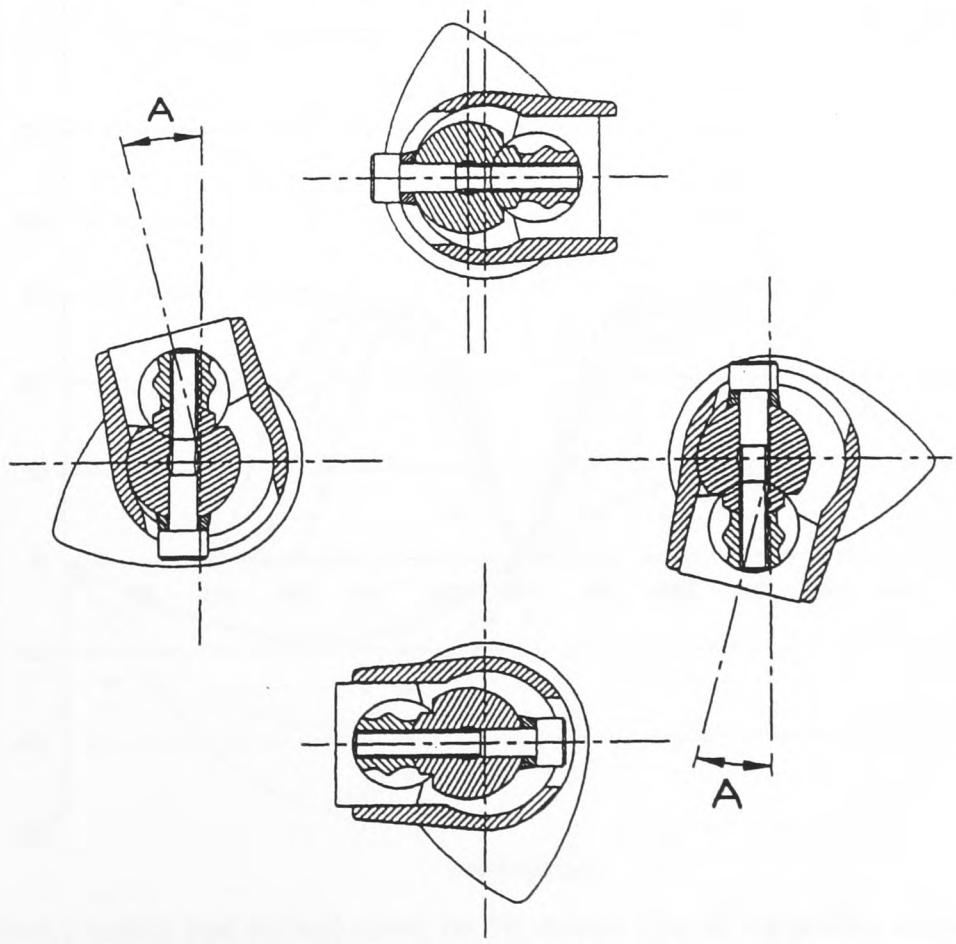


Figure 3.2.1.1. Slider mechanism. (Lancefield *et al*, 1993)

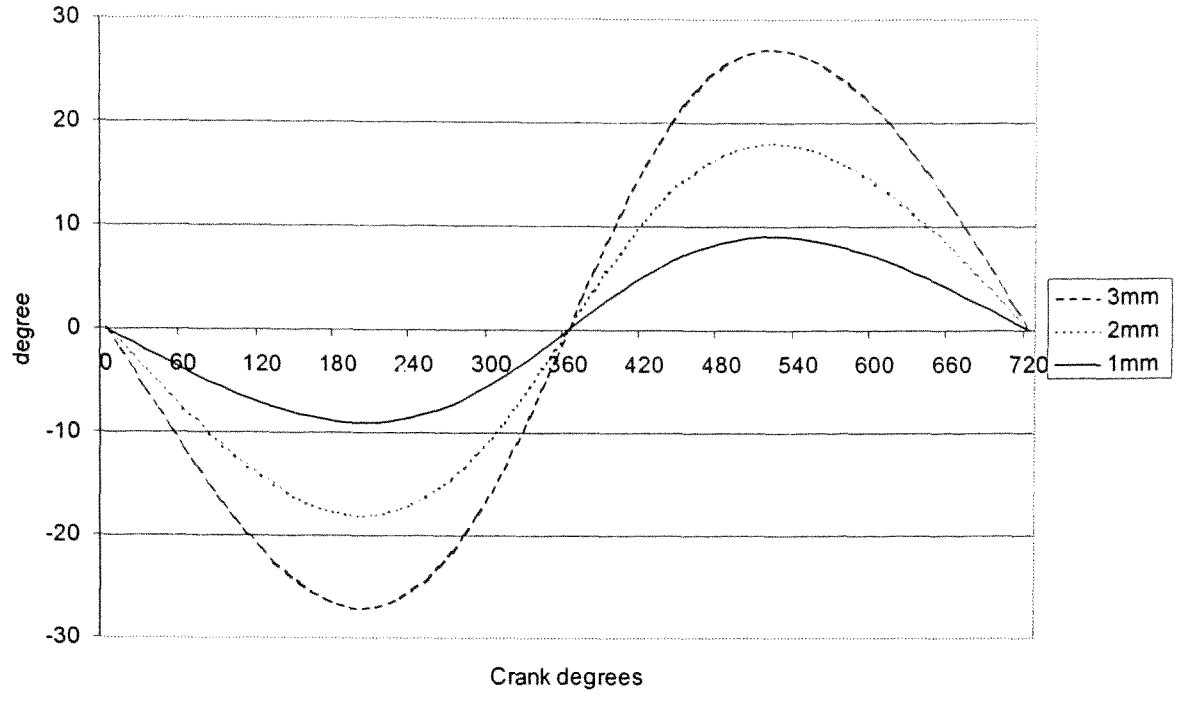


Figure 3.2.1.2. Relative phase between a cam section and the drive shaft for differing drive shaft positions.

Figures 3.2.1.3 show how the cyclically varying phase might be set relative to the valve lift diagrams of a gasoline intake cam (top) and both intake and exhaust cams on a diesel engine (bottom). The resulting effective cam profiles are also shown.

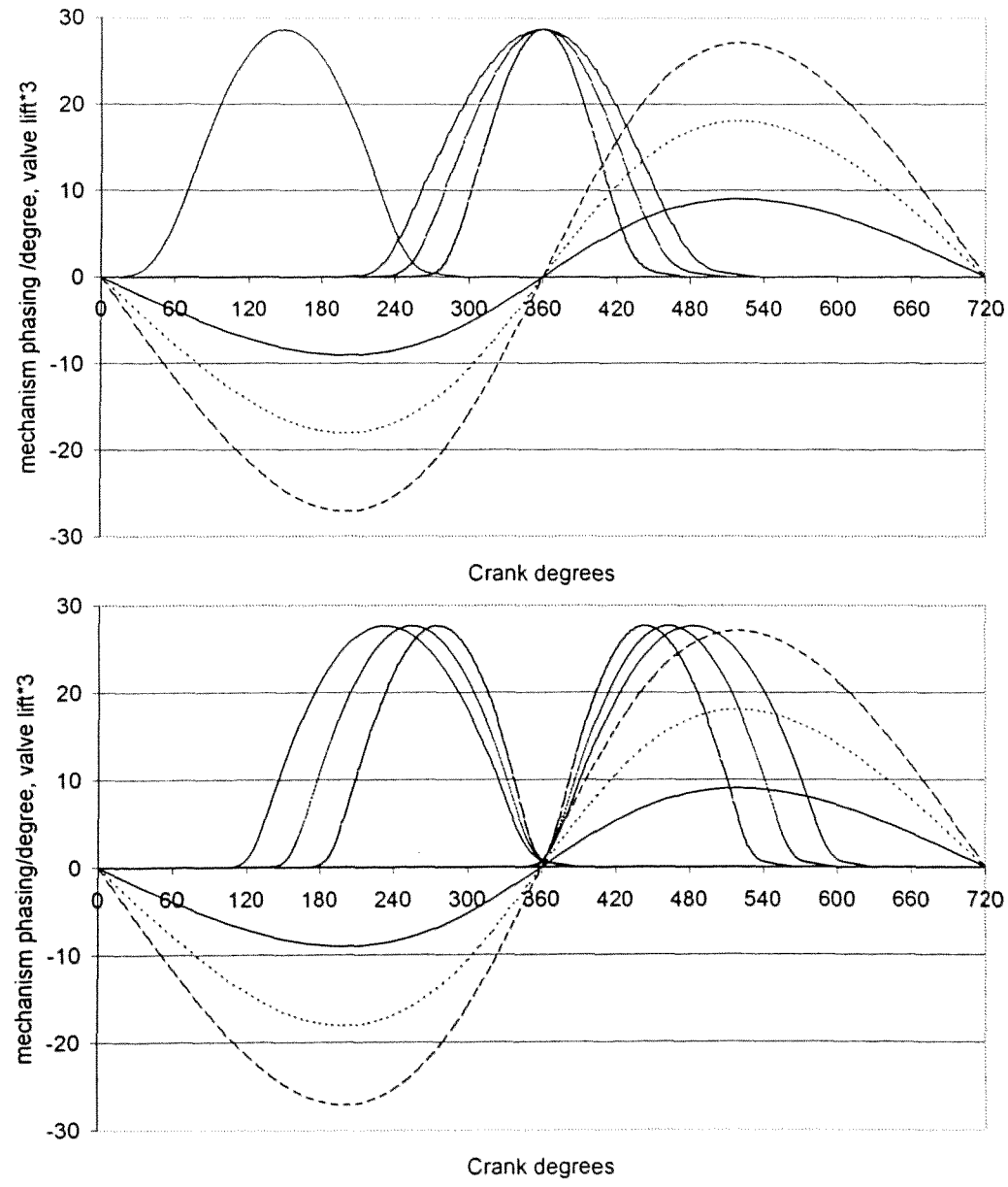


Figure 3.2.1.3. Mechanism phasing and typical result on the intake cam of a gasoline engine (top) and on intake and exhaust cams of a diesel engine (bottom).

The fact that the cross over point (change from advance to retard) of the mechanism can be positioned anywhere in the valve lift cycle means that this type of system has the ability to control duration and leave any arbitrary point on the lift curve at its standard timing. It can be seen from *figure 3.2.1.3 (bottom)* that the system can provide the required characteristics for operation with diesel engines: valve to piston contact can be avoided whilst EVO and IVC can be varied over substantial ranges for cam open periods both greater and smaller than the standard cam profile.

Thus it can be seen that the basic behaviour of this type of system is correctly matched to the requirements of diesel engine VVA, but further analysis is needed to understand the kinematics of the device and their impact on valve train design and operation:

3.3 ANALYSIS OF THE SELECTED VVA MECHANISM

3.3.1 Description of the mechanism and its critical features

The moveable drive-shaft is driven at half crankshaft speed. This shaft in turn drives through a drive "pin" attached to its side and a drive "block" which fits around the drive "pin" and runs in the side bore of the camshaft section or "shell", *figure 3.3.1.1*.

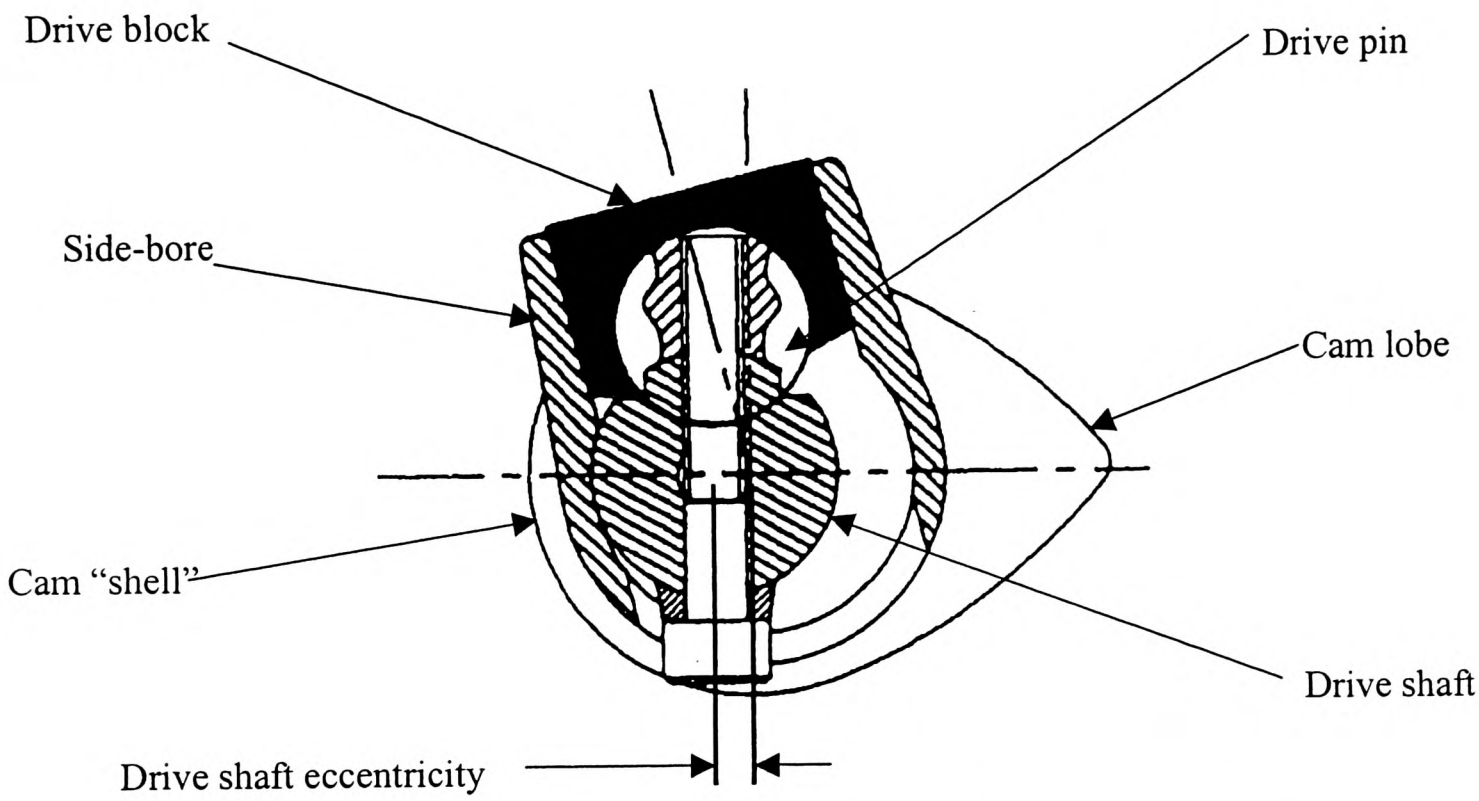


Figure 3.3.1.1. Main features of the later Mitchell variable duration VVA mechanism (Lancefield *et al*, 1993)

To generate the varying angular velocity the drive shaft is moved eccentric from the centreline of the cam shells, which remain fixed in their normal position. The greater the eccentricity the greater the effect on the cam period. Reversing the direction of the eccentricity will alter the sign of the change in period, allowing both increases and decreases of effective period to be achieved. The introduction of a generalised x-y motion of the eccentricity provides the opportunity to produce what amounts to a general shift in phasing of the camshaft as well as the period control.

It is apparent from *figure 3.3.1.1* that a number of geometric features that strongly affect the system behaviour are fixed at the time of design, but there are conflicts between them:

1. The angle between the cam lobe(s) and the side bore (This takes into account the valve train geometry and is determined to achieve the correct effects on the valve timing.)

2. The diameter of the drive shaft (Shaft torsional stiffness and mechanism range are in conflict over this dimension.)
3. The diameter of the bore through the cam shell (Increasing it allows greater drive shaft eccentricity but it also forces 4. (below), to be increased, which reduces the effectiveness of the increased eccentricity.)
4. The distance from the drive shaft centre to the centre of the drive pin (minimising this increases the mechanism range.)

Point 1. above is defined by the valve train geometry and what point on the valve lift curve is required to be unchanged, but the relationship between the other dimensions mentioned is more complex. Simplistically, the greater the eccentricity in relation to the distance from the drive shaft centre to the drive pin centre the greater the angular variation available from the mechanism. However, practical constraints such as mechanism bearing areas, drive shaft torsional stiffness and how the drive pin is attached to the side of the drive shaft strongly affect this relationship. Increasing the drive shaft diameter, to increase stiffness, has the effect of increasing the distance from the drive shaft centre to drive pin centre. Thus to restore the range a greater eccentricity is required. This in combination with the increase in shaft diameter necessitates a larger diameter through the cam shell. But this increases the minimum radius that the mechanism side-bore can utilise again reducing the range of the mechanism. From this it can be seen that careful optimisation of the dimensions is needed to arrive at design solutions with adequate range and stiffness. Typical dimensions for systems that have been run in prototype form are:

System 1		System 2	
Drive shaft diameter	21mm	Drive shaft diameter	19.7mm
Distance from drive shaft centre to drive pin centre	15mm	Distance from drive shaft centre to drive pin centre	12.75 mm
Maximum eccentricity	±3mm	Maximum eccentricity	±3 mm
Maximum range (crank)	±23°	Maximum range (crank)	±27.2°

Table 3.3.1.1 Typical dimensions for prototype single-slider non-constant velocity VVA systems

3.3.2 Analysis and dynamics

Figure 3.3.2.1 shows the triangle that governs the operation of this device superimposed on a section through the mechanism with the variables ***D*** the drive shaft angle, ***C*** the cam shell output angle, ***x*** the drive shaft eccentricity, ***r*** the radius from the drive shaft centre to the centre of the drive pin and ***R***, the distance from the centre of rotation of the cam shell to the centre of the drive pin.

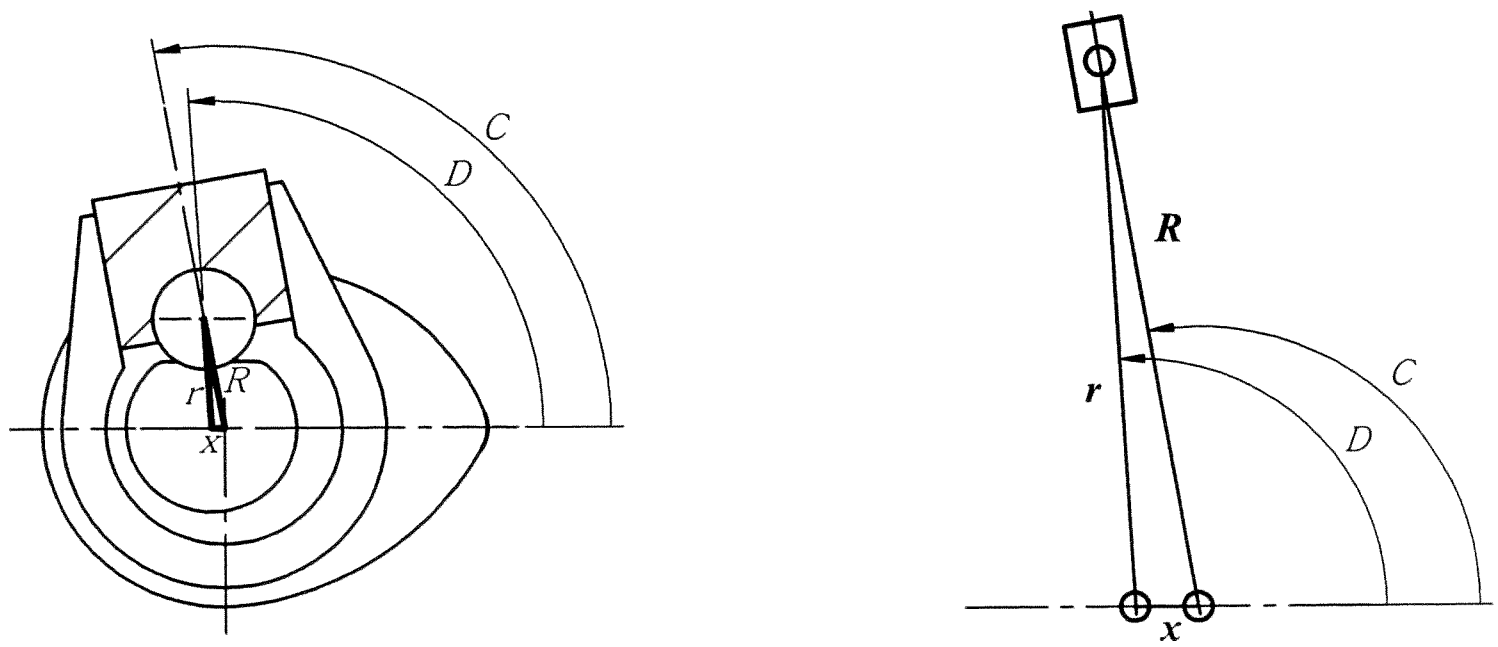


Figure 3.3.2.1 The triangle that governs the operation of the device superimposed on a section through the mechanism (left) and conventional representation as "quick return" slider type mechanism (right).

The variables and geometry described above are used in the following "Ravens method" analysis of the mechanism's behaviour

3.3.2.1 Raven's method to analyse the rotary motion of the camshells

Raven's Method uses complex numbers to represent vectors :

A unit vector can be defined as the complex number $e^{j\theta}(= \cos\theta + j\sin\theta)$

and scaled with magnitude r $re^{j\theta}(= r(\cos\theta + j\sin\theta))$

the time differential of the unit vector is $(\frac{d(e^{j\theta})}{dt} =)$ $\dot{\theta}je^{j\theta}(= \dot{\theta}j(\cos\theta + j\sin\theta))$

Using the above results and applying them to the triangle ***r-R-x*** shown in *figure 3.3.2.1*:

In vector notation this triangle can be represented by :

$$\underset{\rightarrow}{x} + \underset{\rightarrow}{r} = \underset{\rightarrow}{R} \quad \text{----} \quad (1)$$

In complex notation (x is defined as real)

$$x + re^{jD} = Re^{jC} \quad \text{----} \quad (2)$$

Taking the first differential and noting that $\dot{x} = 0$ for constant settings (In general it will change slowly in comparison with the mechanism dynamics)

$$\dot{r}e^{jD} + r\dot{D}je^{jD} = \dot{R}e^{jC} + R\dot{C}je^{jC} \quad \text{----} \quad (3)$$

Expanding and noting that $\dot{r} = 0$ (as it is a mechanical design feature)

$$jr\dot{D}(\cos D + j\sin D) = \dot{R}(\cos C + j\sin C) + jR\dot{C}(\cos C + j\sin C)$$

expanding and collecting terms

$$jr\dot{D}\cos D - r\dot{D}\sin D = \dot{R}\cos C + j\dot{R}\sin C + jR\dot{C}\cos C - R\dot{C}\sin C$$

Splitting into real and imaginary parts

Real part

$$-r\dot{D}\sin D = \dot{R}\cos C - R\dot{C}\sin C \quad \text{----} \quad (4)$$

Imaginary part

$$r\dot{D}\cos D = \dot{R}\sin C + R\dot{C}\cos C \quad \text{----} \quad (5)$$

From (5)

$$\dot{R} = \frac{r\dot{D}\cos D - R\dot{C}\cos C}{\sin C} \quad \text{----} \quad (6)$$

Substituting (6) into (4) gives :

$$-r\dot{D}\sin D = \cos C\left(\frac{r\dot{D}\cos D - R\dot{C}\cos C}{\sin C}\right) - R\dot{C}\sin C$$

$$-r\dot{D}\sin D\sin C = \cos C(r\dot{D}\cos D - R\dot{C}\cos c) - R\dot{C}\sin^2 \mathrm{C}$$

$$-r\dot{D}(\sin D\sin C + \cos D\cos C) = -R\dot{C}\cos^2 C - R\dot{C}\sin^2 C$$

and thus

$$-R\dot{C} = -r\dot{D}(\cos D\cos C + \sin D\sin C)$$

$$\dot{C} = \frac{r}{R}\dot{D}(\cos D\cos C + \sin D\sin C)$$

hence :

$$\dot{C} = \frac{r}{R}\dot{D}\cos(D - C) \quad \text{----} \quad (7)$$

From (4) :

$$\dot{C} = \frac{\dot{R}\cos C + r\dot{D}\sin D}{R\sin C} \quad \text{----} \quad (8)$$

Substituting (8) into (5) gives :

$$r\dot{D}\cos D = \dot{R}\sin C + R\cos C(\frac{\dot{R}\cos C + r\dot{D}\sin D}{R\sin C})$$

$$rR\dot{D}\cos D\sin C = R\dot{R}\sin^2 C + R\dot{R}\cos^2 C + rR\dot{D}\cos C\sin D$$

$$r\dot{D}\cos D\sin C = \dot{R} + r\dot{D}\cos C\sin D$$

$$\dot{R} = r\dot{D}\cos D\sin C - r\dot{D}\cos C\sin D$$

hence :

$$\dot{R} = -r\dot{D}(\sin(D-C)) \quad \text{----} \quad (9)$$

Differentiating (3) again and noting that $\dot{r} = 0$

$$rj(\ddot{D}e^{jD} + j\dot{D}^2e^{jD}) = (\ddot{R}e^{jC} + \dot{R}\dot{C}je^{jC}) + j(\dot{R}\dot{C}e^{jC} + R\ddot{C}e^{jC} + R\dot{C}^2je^{jC})$$

Expanding and assuming $\ddot{D} = 0$ i.e the engine speed is constant

$$-r\dot{D}^2(\cos D + j\sin D) = \ddot{R}(\cos C + j\sin C) + \dot{R}\dot{C}j(\cos C + j\sin C) + \dot{R}\dot{C}j(\cos C + j\sin C)$$
$$+ R\ddot{C}j(\cos C + j\sin C) - R\dot{C}^2(\cos C + j\sin C)$$

Taking real and imaginary parts

real $$-r\dot{D}^2\cos D = \ddot{R}\cos C - 2\dot{R}\dot{C}\sin C - R\ddot{C}\sin C - R\dot{C}^2\cos C \quad \text{----} \quad (10)$$

imaginary $$-r\dot{D}^2\sin D = \ddot{R}\sin C + 2\dot{R}\dot{C}\cos C + R\ddot{C}\cos C - R\dot{C}^2\sin C \quad \text{----} \quad (11)$$

from (10) $$\ddot{R} = \frac{2\dot{R}\dot{C}\sin C + R\ddot{C}\sin C + R\dot{C}^2\cos C - r\dot{D}^2\cos D}{\cos C} \quad \text{----} \quad (12)$$

Substituting(12) into (11) and multiplying by cos$C$

$$-r\dot{D}^2\sin D\cos C = 2\dot{R}\dot{C}\sin^2 C + R\ddot{C}\sin^2 C + R\dot{C}^2\cos C\sin C$$
$$-r\dot{D}^2\cos D\sin C + 2\dot{R}\dot{C}\cos^2 C$$
$$+ R\ddot{C}\cos^2 C - R\dot{C}^2\cos C\sin C$$

$$-r\dot{D}^2\sin D\cos C = 2\dot{R}\dot{C}(\sin^2 C + \cos^2 C) + R\ddot{C}(\sin^2 C + \cos^2 C) - r\dot{D}^2\cos D\sin C$$

$$r\dot{D}^2(\cos D\sin C - \sin D\cos C) = 2\dot{R}\dot{C} + R\ddot{C}$$

hence :

$$\ddot{C} = -\frac{2\dot{R}\dot{C} + r\dot{D}^2\sin(D-C)}{R} \quad \text{----} \quad (13)$$

As will be seen later the key results for calculating valve motion are (7) for $\dot{C}$ and (13) for $\ddot{C}$ as these allow calculation of valve velocity and acceleration from valve lift data. The method could be extended to calculate the "jerk" term as the derivative of acceleration, but numerical differentiation of the acceleration values calculated from the above results produces adequate

results. (It should be noted that if repeated numerical differentiation of position data is used numerical noise usually renders the jerk values useless.)

Figures 3.3.2.1.1,2,3 show the angular velocity of the cam shell relative to the drive shaft, the absolute angular velocity of the cam shell and the absolute angular acceleration of the cam shell for a variety of drive shaft eccentricities and engine speeds, for the geometry of System 1 in *table 3.3.1.1.* The slightly asymmetric characteristic of the mechanism is apparent from these charts.

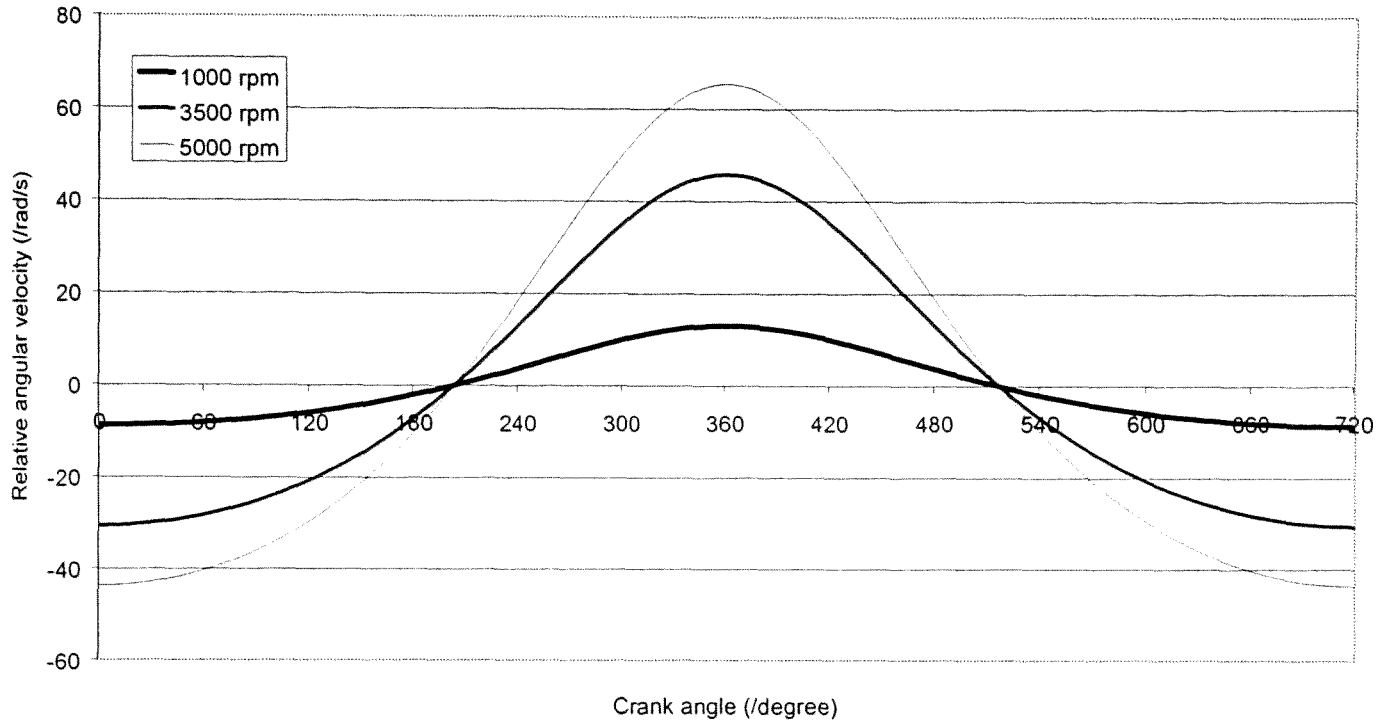


Figure 3.3.2.1.1 Angular velocity of the cam shell relative to the drive shaft ($\dot{C}$ - $\dot{D}$) for a variety of engine speeds at 3mm drive shaft eccentricity, for the geometry of System 1 in *table 3.3.1.1.*

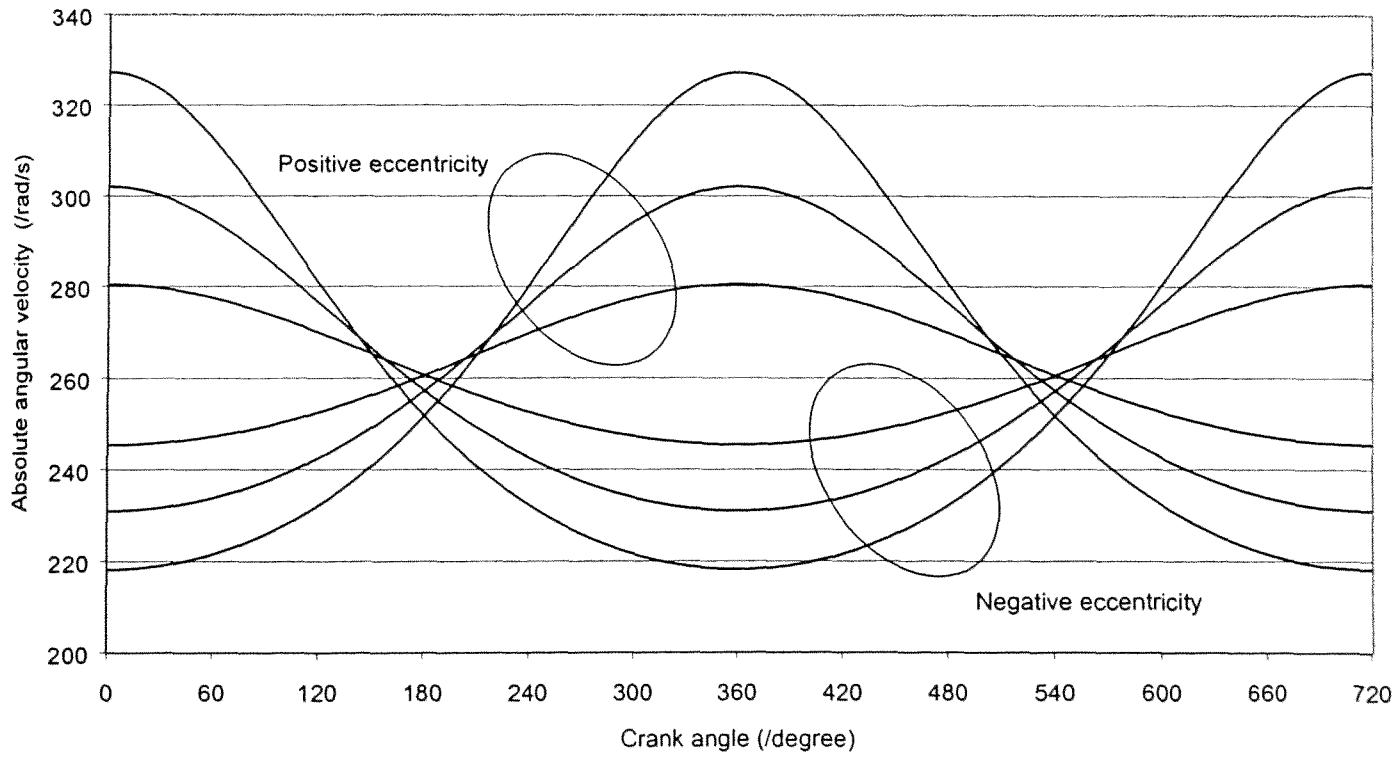


Figure 3.3.2.1.2 Absolute angular velocity of the cam shell for ±1mm, ±2mm and ±3mm, drive shaft eccentricities at 5000 rpm engine speed, for the geometry of System 1 in *table 3.3.1.1.*

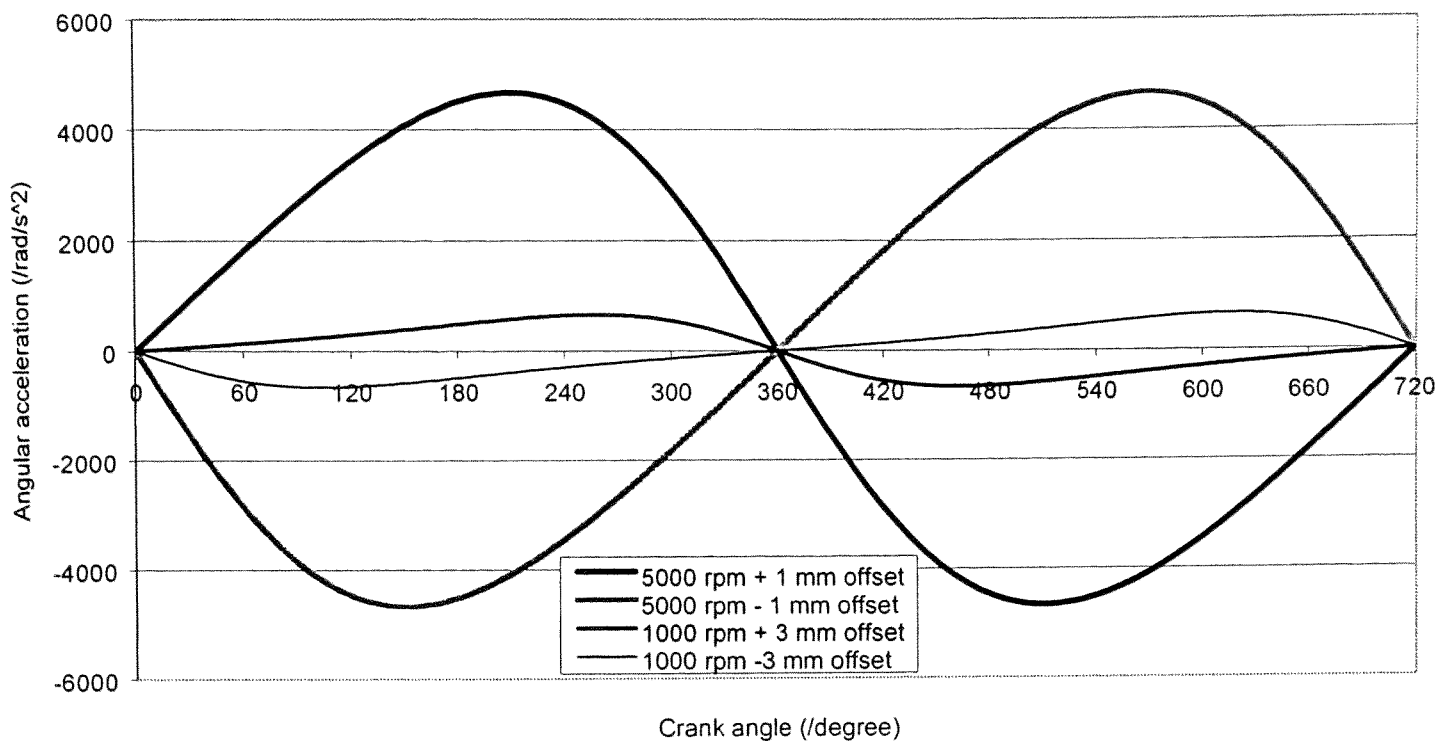


Figure 3.3.2.1.3 Absolute angular acceleration of the cam shell for a variety of drive shaft eccentricities and engine speeds, for the geometry of System 1 in *table 3.3.1.1.*

3.3.2.2 Extension of Raven's method to give valve acceleration

Clearly the geometry of the whole valve train determines the relationship between the cam profile and the valve lift, so for simplicity the discussion from here concentrates on the simplest valve train geometry – "Direct Acting," where cam lift and valve lift are the same. See *figure 3.3.2.2.1.* Other more complex valve trains follow the same rules of analysis, but typically the action of intermediate members such as rollers and rockers are allowed to distort the cam profile in order to get the valve lift characteristics required.

Under steady speed operating conditions, the motion of a direct acting cam follower can be shown to be:

$$\text{Follower velocity}: \frac{d(Lift)}{dC} * \dot{C} \quad \text{----} \quad \text{(a)}$$

$$\text{Follower acceleration}: \frac{d^2(Lift)}{dC^2} * \dot{C}^2 \quad \text{----} \quad \text{(b)}$$

Where: $Lift$ = cam lift and C = cam angle

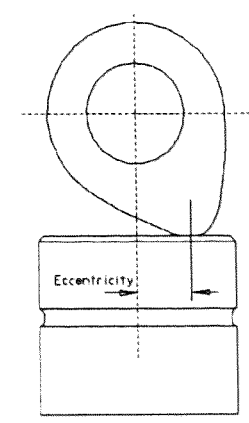


Figure 3.3.2.2.1 Geometry of a direct acting follower and cam.

But with the variable angular velocity of the cam profiles in this mechanism (from Raven's method) the resulting cam follower accelerations are different:

$$\text{Acceleration}: \frac{\mathrm{d}^2(Lift)}{\mathrm{d}C^2} * \dot{C}^2 + \frac{\mathrm{d}(Lift)}{\mathrm{d}C} * \ddot{C} \quad \text{----} \quad \text{(c)}$$

The combination of the results of the Raven's method analysis and the above derivation of valve acceleration allow the forces in all of the components of the VET system to be calculated (with suitable assumptions about friction.)

The differences between conventional valve motion and that with this type of VVA arise from the fact that the angular velocity of the cam shell ($\dot{C}$) is not constant and there is an extra term involving cam shell angular acceleration ($\ddot{C}$ - non-zero) in the equation for cam follower acceleration that results in different absolute cam follower accelerations for a given engine speed and non-zero drive shaft eccentricity. The phasing of the positive and negative cam shell accelerations can lead to either higher cam follower accelerations (reduced period) or lowered cam follower accelerations (extended period) when compared with the nominal cam profile at the same engine speed. Charts showing the effects on valve velocity and acceleration are shown in the next section.

This feature allows the cam profile and valve springs, particularly, to be optimised in a different way, as the base profile used can be different from that used for a fixed cam characteristic, and therefore the use of this type of VVA mechanism has a number of implications to the design of the valve train:

3.4 VALVE TRAIN IMPLICATIONS

A detailed treatment of the design and analysis of a modern valve train system is outside the current scope, as it is a vast subject in its own right - the fact that there are considered to be five fundamental types of valve train layout also complicates the discussion. See *figure 3.4.1* which shows these five layouts.

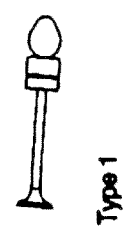
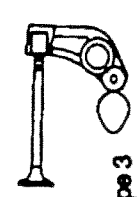
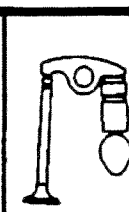
Mechanism / Feature	 Type 1	 Type 2	 Type 3	 Type 4	 Type 5
Natural Frequency (Hz)	2000 -3000	1200 -1500	900 -1400	900 - 1400	400 - 700
Effective Mass @ Valve (gr)	140 - 160	80 - 120	120 - 160	130 - 170	240 -290
Maximum RPM	6500 ++	6500 +	6000 +	6000 +	4000 - 6000
Friction (A-E)	E	A	B	C -D	C - D
Overall Engine Packaging (A-E)	D - E	D - E	B	C	A

Figure 3.4.1. The five fundamental valve train layouts (Jacques, 1997). Letters A to E are rankings, with A the best and E the worst. It should be noted these are from a North American perspective.

However, despite the multiplicity of system layouts it can be seen that there are certain common moving components, with the most significant of these being the cam lobe, cam follower, hydraulic lash adjuster and valve spring. The smaller components, spring retainer, cotters, valve stem seal and spring seat, whilst still being important and requiring careful detailed design are less problematic than the significant items mentioned above and do not have significant impact on engine design or layout, nor do they affect the operation of the engine unless they fail.

As already mentioned, for simplicity this discussion is confined to the valve train with a direct acting tappet, "type 1" in *figure 3.4.1*, but there are direct analogues of the all features discussed for those systems involving roller followers, with similar implications to the cost, durability and particularly overall function.

As the major thrust of this paper is the investigation of how engine performance is affected by the use of VVA, it is most appropriate to discuss those aspects of valve train design that affect diesel engine operation and how they are influenced by their use with VVA. The features of a valve

train that influence engine operation are: cam lobe, cam follower, hydraulic lash adjuster and valve spring. These items also influence the size and layout of the engine.

In this context the item least affected by its use with VVA is the hydraulic lash adjuster, which is sensitive to cam follower loads at all speeds, and has the tendency to "squash" or leak down slightly during each valve lift cycle and then fully or partially, as time allows "pump up" again to take up any lash whilst the follower runs around the base circle of the cam. The understanding of these apparently simple devices is difficult and the reader requiring a more complete understanding of them is referred to: (Dammers, 1997), (Mews, 1994), (Watson and Chow, 1991) and (Phlips and Schamel, 1991.) These devices affect engine operation by altering the integral under the valve lift curve as they leak down and therefore affect the gas flows in the engine. There is apparently no widely used correlation to predict this characteristic as a function of speed.

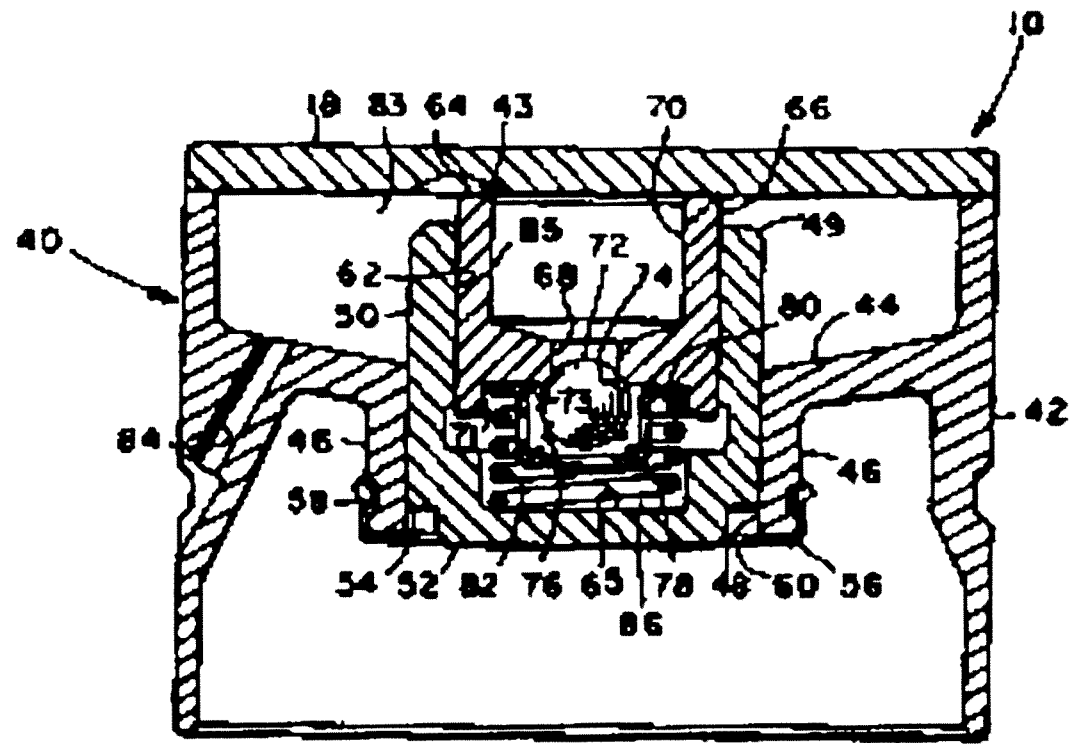


Figure 3.4.2 Typical, modern direct acting tappet with hydraulic lash adjuster (Dammers, 1997).

From *figure 3.4.2* it can be seen that the hydraulic lash adjuster, as installed in a valve train with direct acting tappet, increases the overall height of the engine and increases the reciprocating mass of the system. The height increase is typically of the order of 12 to 15 mm, and the increase in mass 20 g, which in turn increases the demands on the valve spring. However, the benefits of service-free and quiet operation are viewed as sufficient to accept the height penalty in most cases.

3.4.1 Cam follower, cam curvature and spring design for fixed valve train

The components that have the potential for significant re-optimisation when used with variable period VVA are the cam lobe, cam follower and valve spring:

The normal design procedure would be to define the cam period and lift and from these the detailed cam profile, follower diameter and spring design would follow:

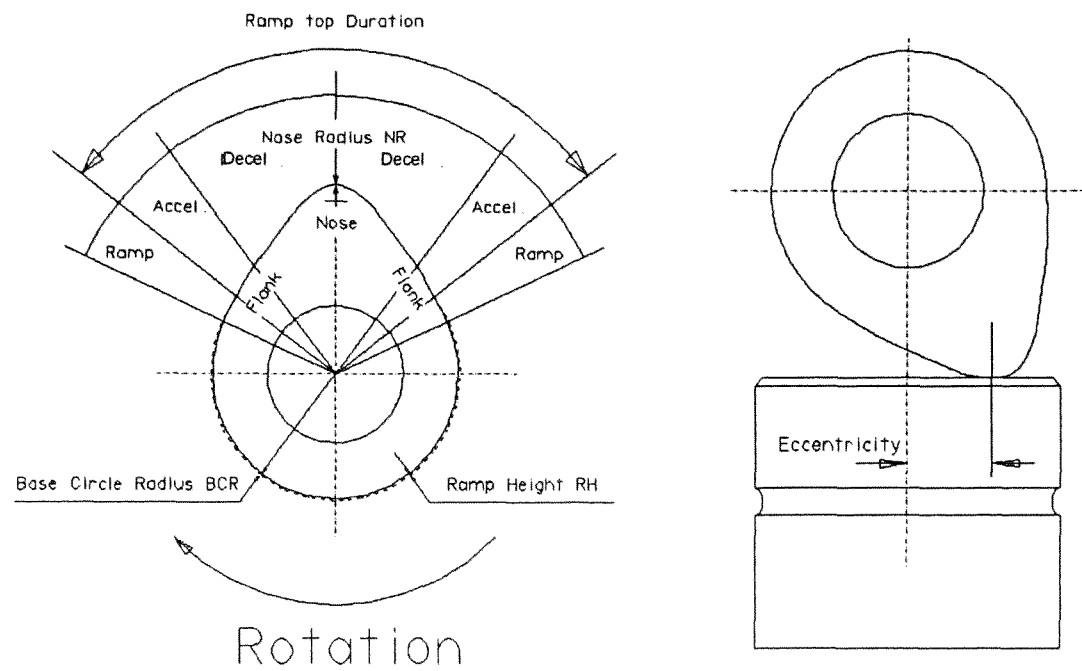


Figure 3.4.1.1. The key features of a cam profile and geometry for a valve train with direct acting tappet.

The cam profile would be designed to have appropriate flank and nose radii (see *figure 3.4.1.1*) for durability. From the detailed cam profile the maximum eccentricity of the cam profile would dictate the diameter of the cam follower such that the line of contact between the cam and follower does not run off the edge of the tappet. (With this type of follower its stiffness reduces significantly with a large diameter, which is not helpful with a high speed valve train.) As would be expected there is a strong link between maximum eccentricity and cam period and lift. Eccentricity is the feature that corresponds to valve velocity, so the greater the lift, the higher the velocity needed to achieve the lift in the angle available and the greater the eccentricity. Similarly the shorter the period of the cam, the less angle is available for the lift to be achieved, again leading to higher velocities and, therefore, greater eccentricity. See *figure 3.4.1.2.*

There is also a link between cam eccentricity and follower length: The greater the eccentricity the longer the follower needs to be to maintain an acceptable length to diameter ratio, typically around unity, in order that the follower does not tip too much in its bore. Excessive tipping can lead to durability, noise and friction problems.

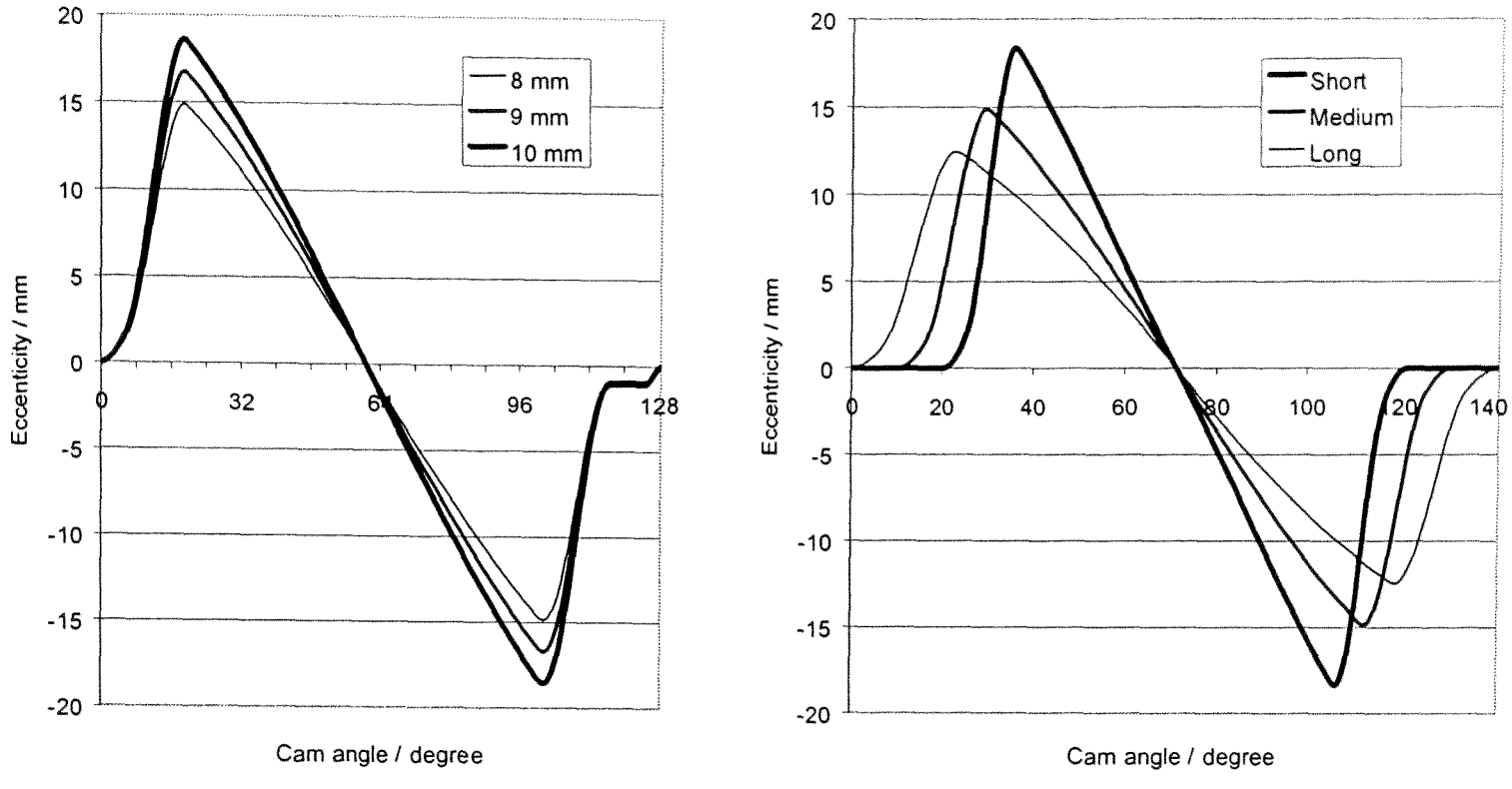


Figure 3.4.1.2. The effects of cam lift and period on eccentricity.

Within cost and durability constraints the valve train designer will try to minimise the masses of the reciprocating parts of the valve train system, namely: the valve, the cam follower (including hydraulic lash adjuster "HLA" if not stationary), the spring retainer, the cotters and a portion of the spring mass. This is the case because the lighter this assembly the softer the spring can be for a given cam profile and the lower the spring forces the lower the friction and contact stresses in the system. Also the lower spring force allows a spring with smaller working stress range which improves durability. Given that these masses are sensibly minimised the cam profile determines the spring design. Since conventional valve springs have finite rates and working stress ranges, the spring will be designed to provide the force necessary to maintain contact between the cam lobe and cam follower up to some defined speed - normally 500-1000 rpm above maximum rated speed. The spring itself will also be designed to be unaffected by the harmonic content of the cam profile to avoid resonance in its coils.

The installed spring specification is dictated by the reciprocating mass and its maximum acceleration when controlled by the spring. This in turn is dictated by the detail of the valve deceleration. As with the eccentricity, the accelerations are strongly influenced by cam period and lift; again short period and high lift both increase acceleration levels. *Figure 3.4.1.3.* left, (over the page), shows the effect of lift, maintaining the same 10% spring margin with the same spring fitted length increases the spring working stress range by approximately 25%. The right hand

chart shows the effect of cam duration. In this case the valve lift has been kept at 9mm and the positive acceleration period at 20° cam, but the negative acceleration period has been extended by 5° cam. This reduces maximum valve velocity and acceleration and reduces the spring requirement, to below that of the 8mm lift 260° duration camshaft.

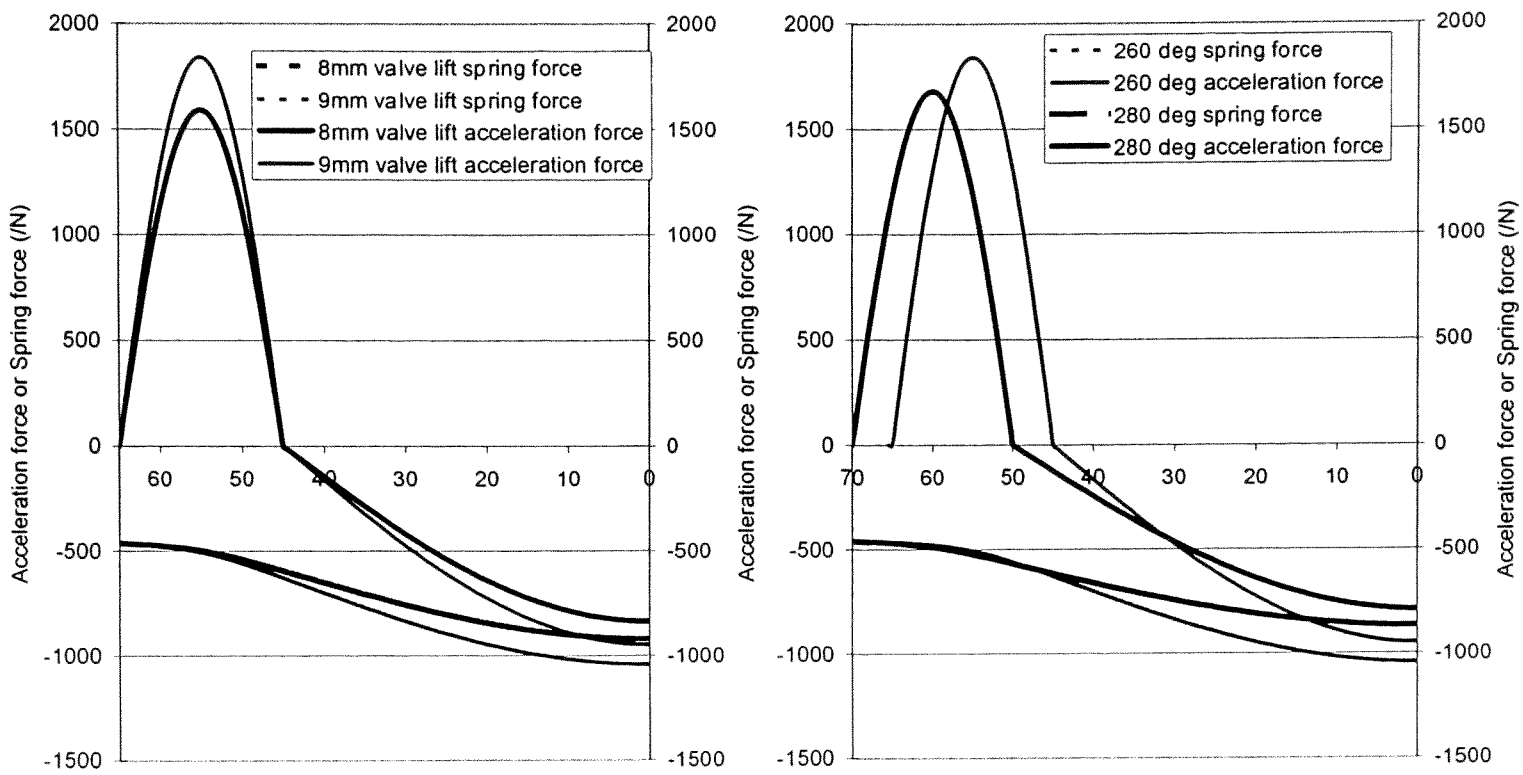


Figure 3.4.1.3. The effect of lift (left) and cam period (right) on spring requirements.

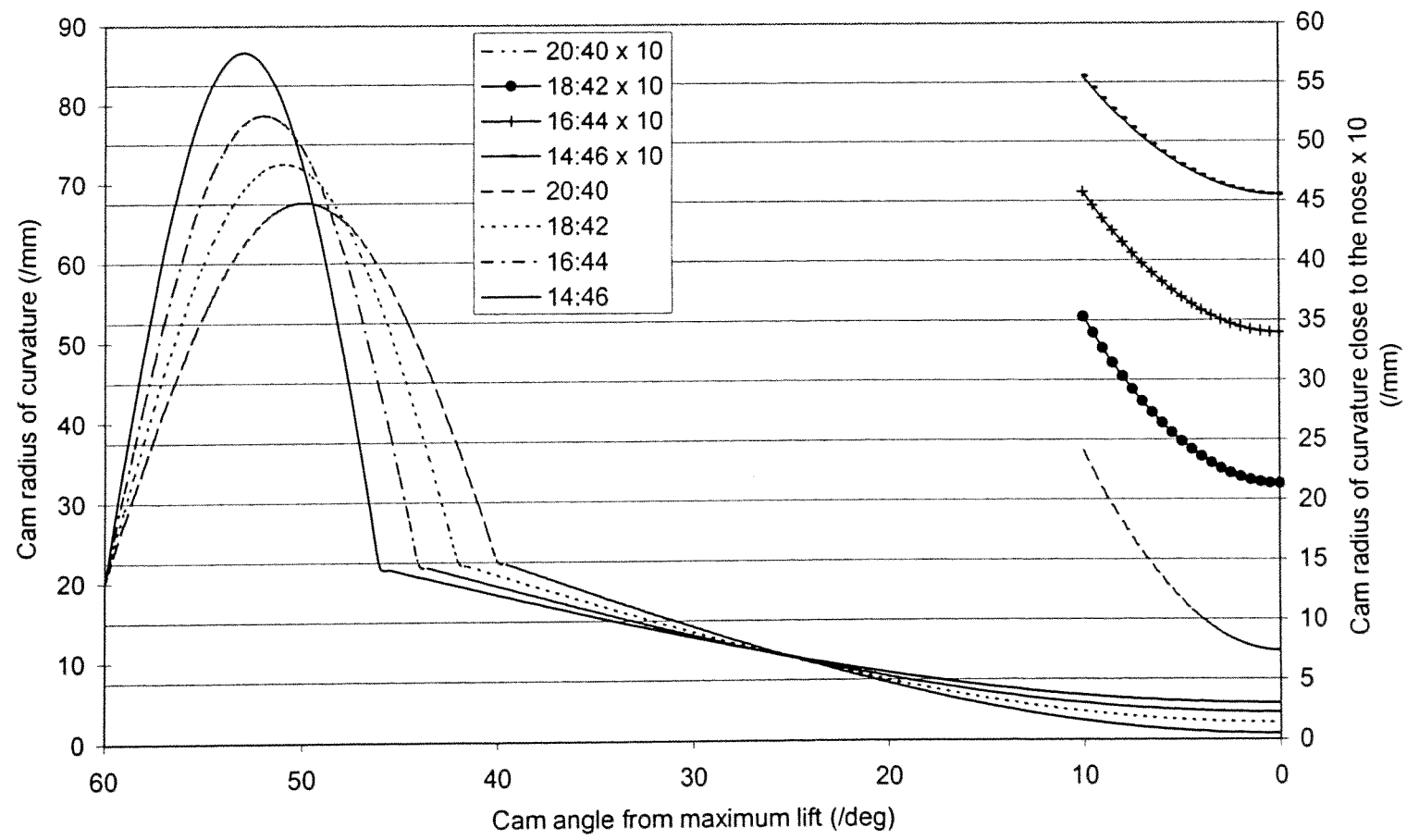


Figure 3.4.1.4. The effect of acceleration ratio (positive period to negative period) on instantaneous radius of curvature.

Another feature of the valve train with a direct acting tappet is that in road going engines it is normally the nose of the cam that is most susceptible to wear, particularly during cranking when sliding velocities are low and lubrication poor. So maximisation of the nose radius of curvature is important. Whilst this can simply be increased by increasing the base circle radius, this approach can lead to unacceptably large cams that in many cases increase the overall height of the engine. The alternative is to control the ratio of positive to negative valve acceleration periods, allowing a longer period for the valve to be decelerated. *Figure 3.4.1.4* shows the effect of altering the acceleration period ratio on nose radius. The legend shows the ratio representing the *period of the positive acceleration: period of the negative acceleration* for each of the curves and the overall curvature profile and the nose radius x 10. The nose radius at 20:40, at 0.76mm would not be durable, but all of the others would be acceptable. Clearly, nose radius can also be increased by lengthening the cam period and using the extra period for the negative acceleration period.

It can also be seen from *figure 3.4.1.4* that as the positive acceleration period is reduced, so the flank radius of curvature increases (in-line with increased acceleration) and from the earlier discussion it will be noted that eccentricity will also be increased.

In a conventional valve train design exercise the cam profile would need to be optimised to provide adequate operation throughout its operating envelope, which would typically result in a cam with a period in the range 236° to 244°. These cams usually have a small nose radius (approximately 1.6mm to 2.0mm) and stiff springs to control the valve motion.

From the foregoing it should be apparent that being able to increase the period of a cam profile would yield benefits in the reduced size of the tappet and reduced valve accelerations, at a given speed, leading to a reduced spring requirement. If we consider combining this with the variable period VVA mechanism such that the effective cam period could be reduced to somewhat less than the normal requirement indicated above and extended to a period considerably longer than could normally be used, it can be seen that several of the problems associated with valve train design can be overcome and a range of cam periods that match the operating characteristics of an engine can be obtained.

It will be noted that in the following figures the distortion of the curves caused by the use of the variable period VVA is asymmetric, because in the case of the light duty diesel engine there is no opportunity to alter the lift significantly at overlap TDC, which means that only exhaust opening

and intake closing can be altered. The following curves are all for the intake case and intake closing only is affected.

3.4.2 Cam follower, cam curvature and spring design with non-constant velocity VVA systems

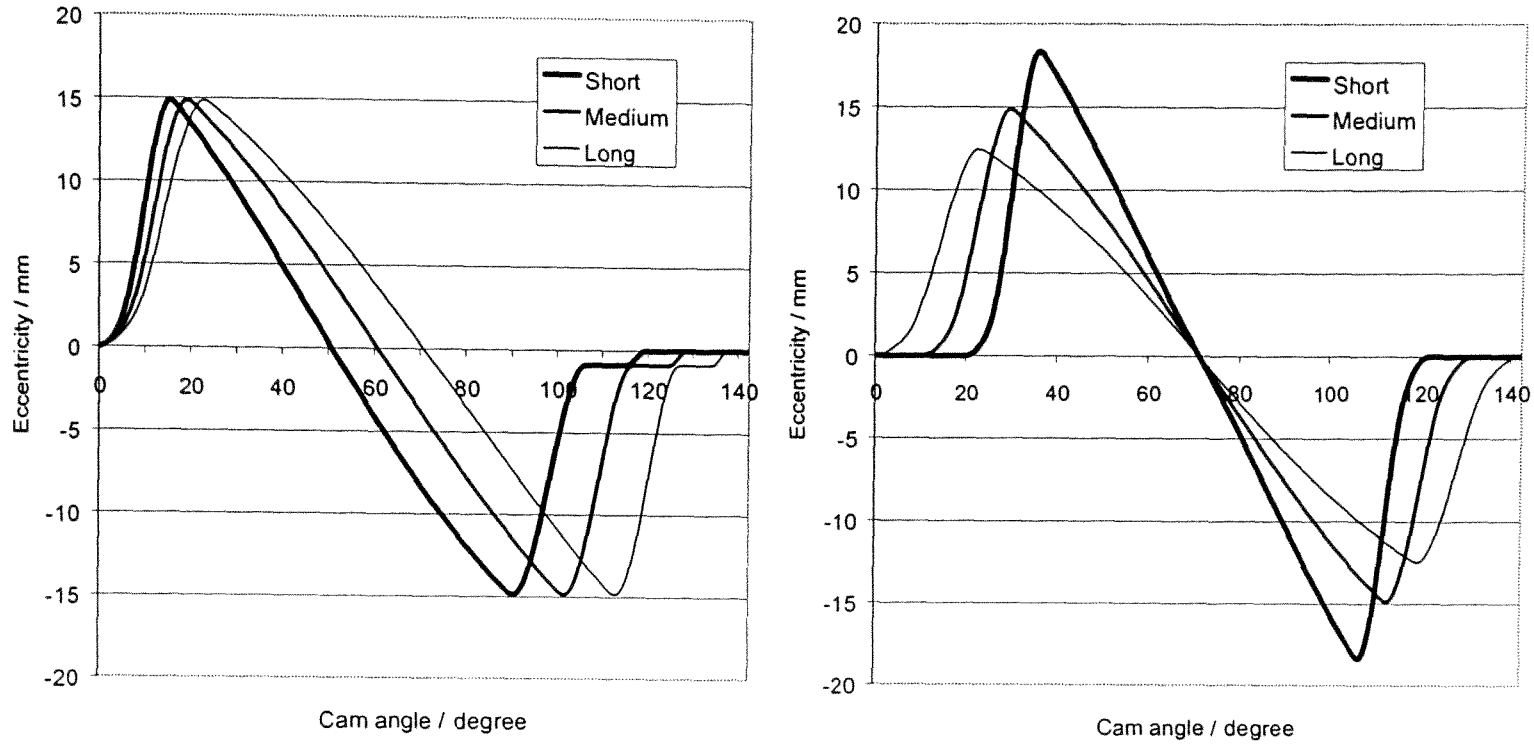


Figure 3.4.2.1. The eccentricity characteristics for a family of cam periods, with variable duration VVA (left) and fixed cams (right).

It can be seem from *figure 3.4.2.1* that the use of variable duration VVA with a longer period cam profile can produce lower eccentricities even at shorter net profiles than the typical standard fixed profile. This results from the fact that the cam shells do not rotate at constant speed providing the higher valve velocities necessary for the shorter period whilst the maximum eccentricity is a fixed feature of the actual cam profile.

Figures 3.4.2.2 and *3.4.2.3* respectively show families of acceleration curves resulting from fixed cam designs, with the positive acceleration period held constant, and with the same durations generated using the variable duration VVA system. (In both cases the standard duration curve is the same and is the basis for the curves generated by the variable duration VVA system.)

It can be seen from *figure3.4.2.2* that when the variable duration VVA mechanism is used to reduce the effective cam period to less than that of the standard fixed profile, higher values of positive and negative accelerations result and that the acceleration curves are skewed, producing unequal distortions of the accelerations on opening and closing flanks of the cam. This is because of the asymmetric timing of the mechanism relative to the valve lift curve.

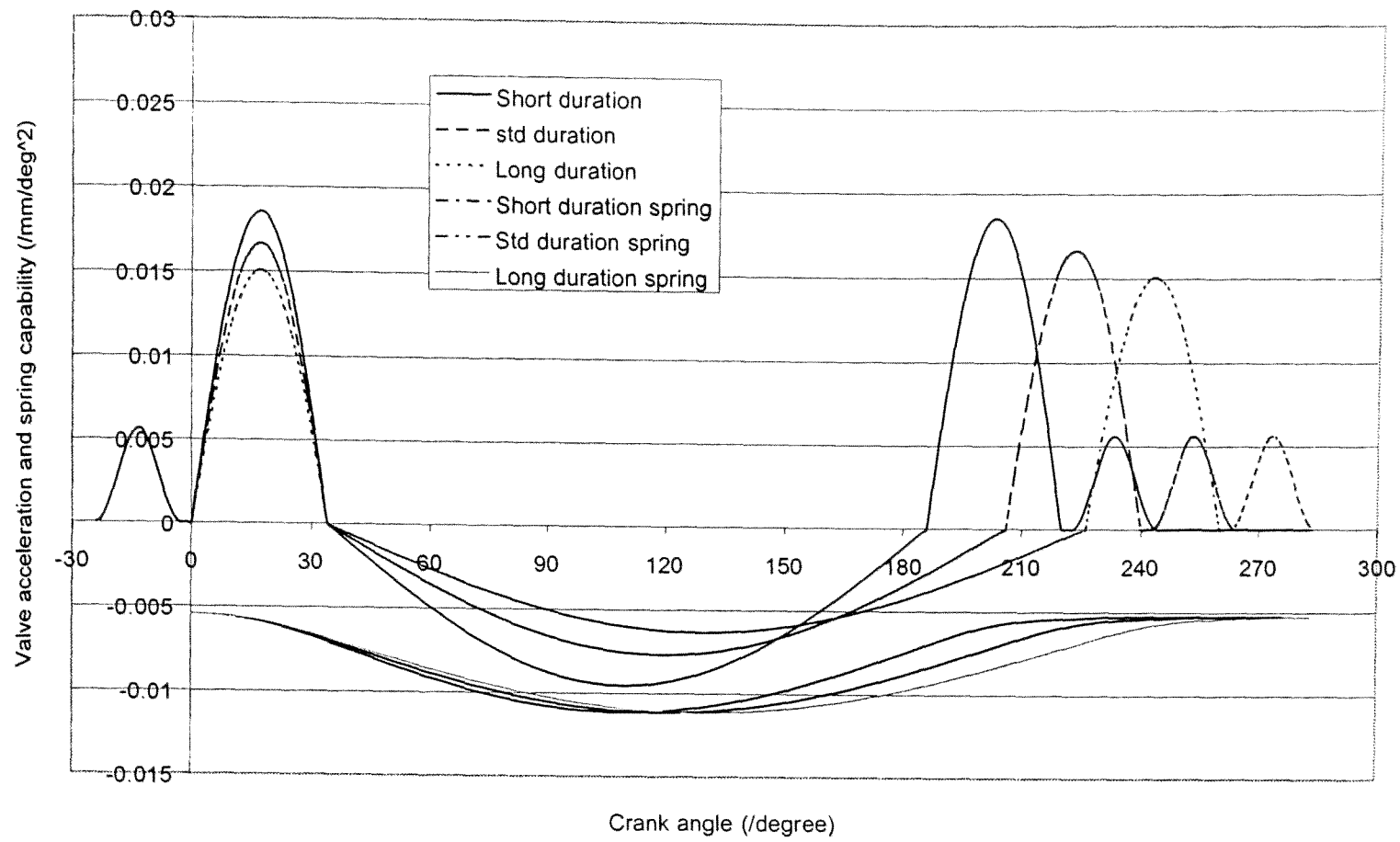


Figure3.4.2.2. The acceleration characteristics for a family of fixed geometry cams with the same periods as in *figure 3.4.2.3.*

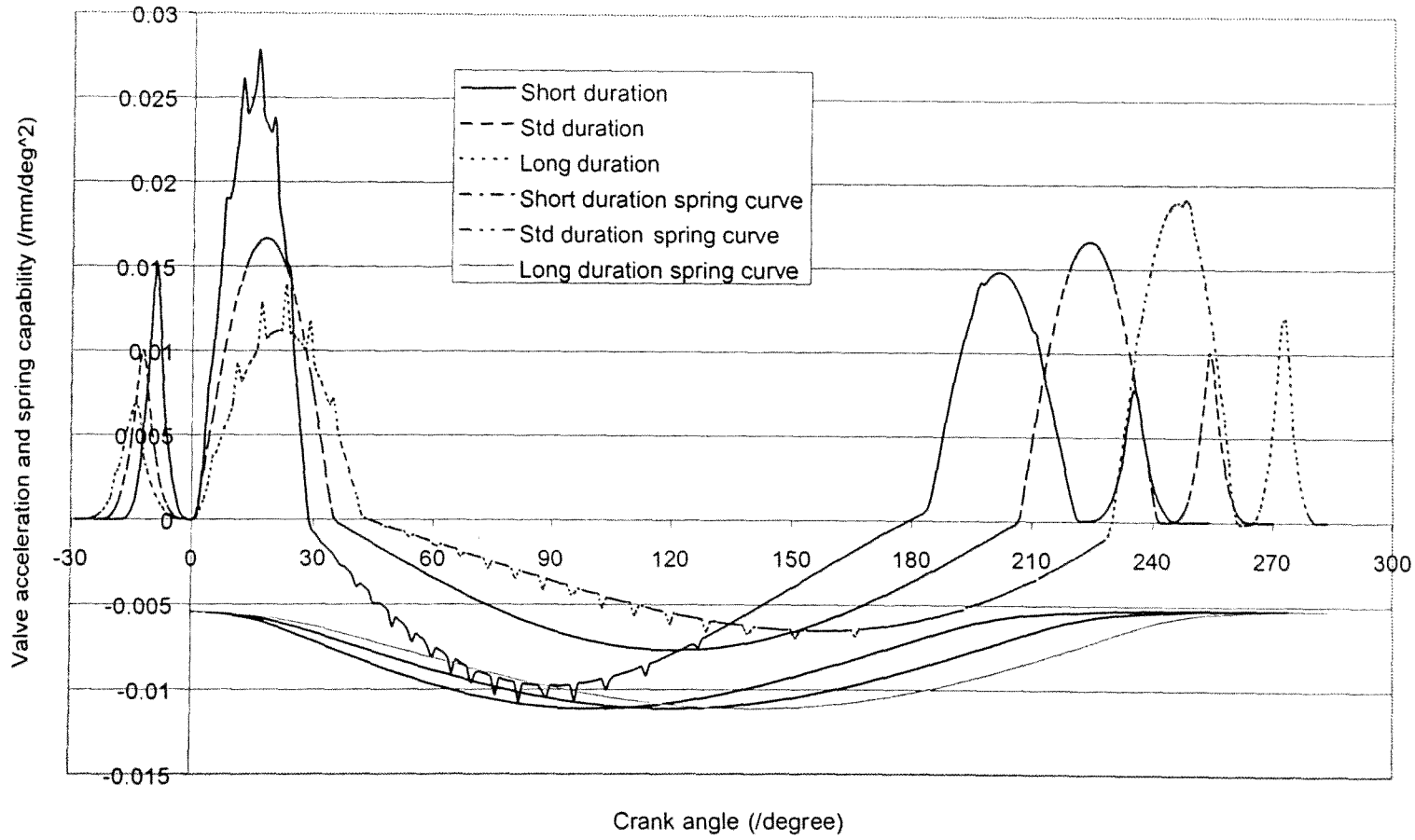


Figure3.4.2.3. The acceleration characteristics for a family of cam periods generated with variable duration VVA with the same periods as in *figure 3.4.2.2.*

Figures 3.4.2.2 and *3.4.2.3* also show the families of spring lines associated with the cam profiles. These are calculated and reduced to "effective valve accelerations" at 5500 engine rpm and use the mass, spring seated load and spring rate of a current production valve train. This is

the characteristic of the valve spring used with the standard duration cam profile . (5500 rpm represents 1000 rpm over the typical maximum speed of a current high speed light duty diesel engine.)

When considering the ability of the valve spring to control the motion of the reciprocating parts of the valve train it is important to allow an amount of spring force in excess of that required to control the motion. This is often referred to as spring "margin" and visually is the vertical distance between the negative acceleration curve and the spring line, but can be quantified as the ratio of spring capability to valve train acceleration.

It can be seen from *figures 3.4.2.2* and *3.4.2.3* that as the duration of the cam profiles is reduced so the spring margin is also reduced. This is the case with both fixed and VVA valve train operation. But it should be remembered that to fit with the natural requirements of the engine the shorter periods will only be used at low engine speeds and that spring margin is a function of the square of engine speed. *Figure 3.4.2.4*. Conversely at higher speeds the natural requirement of the engine is longer valve open periods and the variable duration mechanism produces absolute accelerations which are lower than those of the typical standard fixed profile. This allows the use of a softer spring.

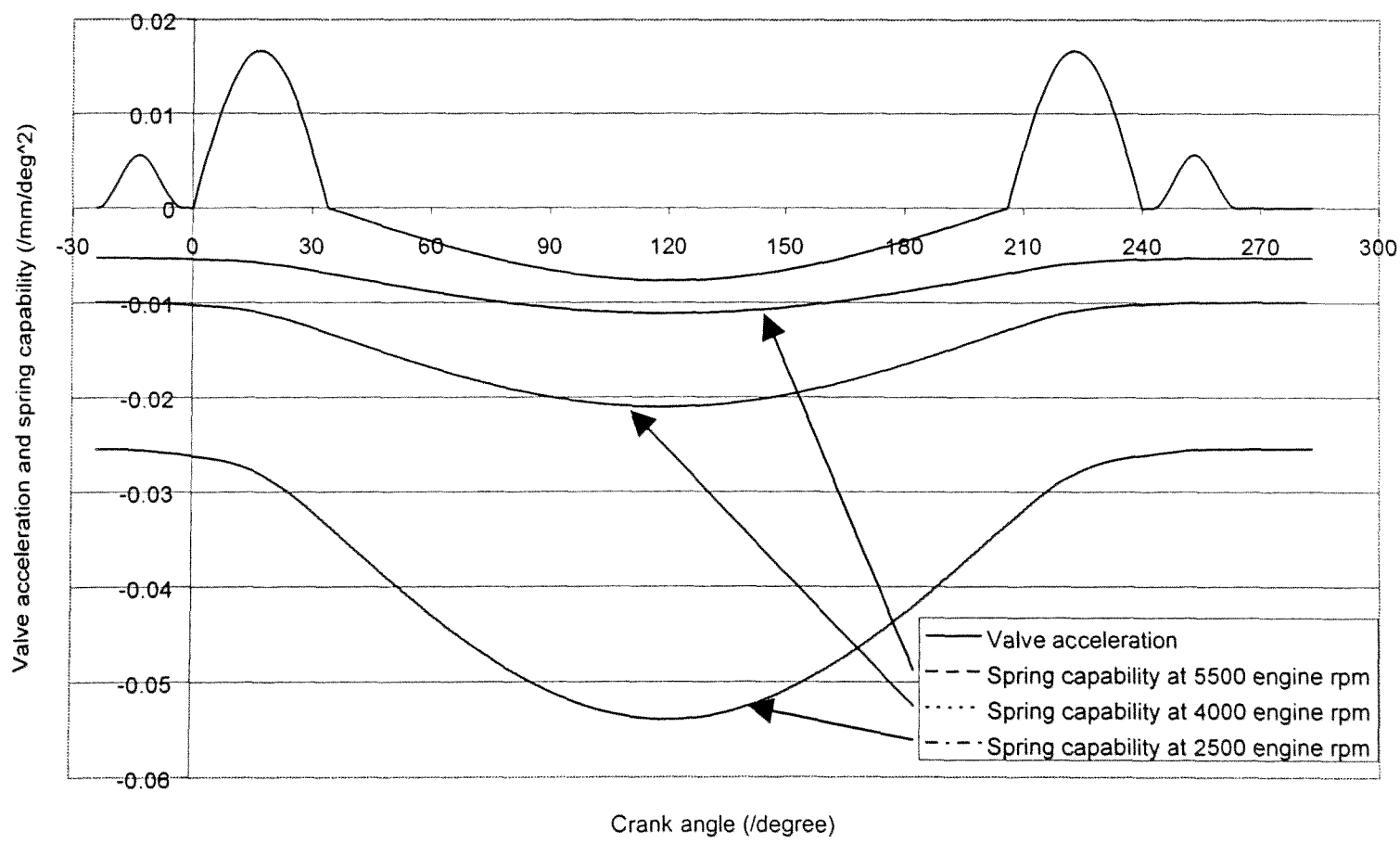


Figure 3.4.2.4. The acceleration characteristic for the standard period cam, as shown in *figure 3.4.2.2*, and spring capability lines at varying engine speeds

3.4.3 Cam profile design for operation with variable duration VVA

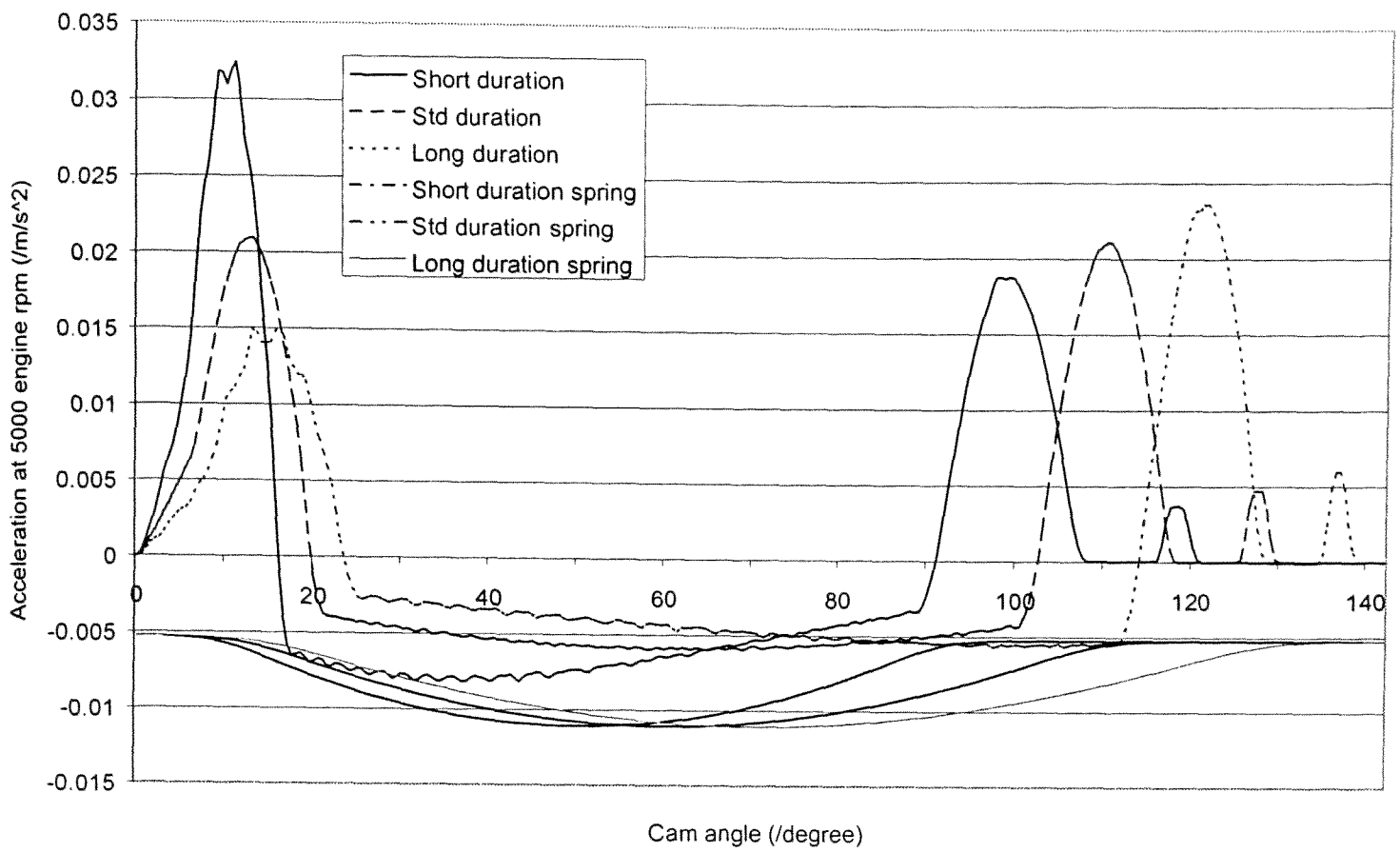


Figure 3.4.3.1. The acceleration and spring capability characteristics for a family of cam periods generated with variable duration VVA with the same periods as in *figure 3.4.2.2*, but with a different cam design process.

Figure 3.4.3.1 shows a similar family of cam acceleration and spring capability curves to those shown in *figure 3.4.2.2*, but with a base cam profile designed with a different method. The standard duration profile in *figure 3.4.2.2* was designed using a "multi-sine" technique, whilst that in *figure 3.4.3.1* was designed using a polynomial approach. It will be apparent that with the multi-sine approach the minimum spring margin is at full lift, whilst with the polynomial design it is at the "knee," close to the beginning of the deceleration curve. It can be seen from contrasting these two figures that the spring margin requirements of the variable duration VVA system are better protected with a cam profile designed by the multi-sine method.

3.5 CONCLUSIONS

From a review of potentially suitable VVA systems the *constrained non-constant velocity* type has been selected for its suitability for application to modern light-duty diesel engines because it can control valve opening duration and allows EVO and IVC to be moved without any significant changes to IVO and EVC . The kinematics of the mechanism have been analysed and it has been shown how the mechanism's behaviour distorts the valve open period through its non-constant angular velocity and how the modifications to the basic cam profile that the use of this type of VVA system allows can ease the mechanical design constraints on valve trains for diesel engines.

The major effects which the implementation of a variable duration VVA system, such as that proposed by Mitchell (1980), can have on valve train design are:

- Tappet diameter can be reduced because cam eccentricity can be restricted.
- Tappet length can be reduced in proportion to tappet diameter
- The implications of this are that valves can be placed closer together, as required by the very small bores currently being used for light duty diesels and valve angles can be narrowed whilst still allowing space for the injector.
- For a given base circle size the cam nose radius of curvature can be increased. The consequence of this is that contact stresses between the cam and follower can be reduced.
- Spring rates can be reduced as absolute valve accelerations can be controlled, leading to reduced cam to follower stresses and friction.

4 ENGINE PERFORMANCE PREDICTION

Increasingly, engine performance prediction, through computer simulation, is being used as a tool in the "Rapid Prototyping" toolbox of the engine developer. This trend has followed the realisation that as hardware development on an iterative, test, modify, retest, basis has become increasingly expensive, so computing power, that makes accurate computer simulation realistic on acceptable time scales, has become cheaper.

The increasing availability of cost effective computing power has allowed the development of simulation models that include more and more sophisticated physics, to represent the processes taking place inside the engine and its associated systems, and effective numerical methods for producing solutions to normally intractable equations. This has led to modern engine simulation models now being widely used. The data produced by these models is regularly used to predict operating trends, and is now starting to be accepted as producing good quantitative results without significant "tuning" of the models. This is particularly so in terms of full load operation, but increasingly accurate predictions of pumping work, heat transfer and cylinder residuals can also be produced leading to indications of part load fuel economy trends.

However, it is widely accepted that these models are not yet mature in their treatment of combustion and are particularly lacking in the prediction of the formation of unwanted gaseous emissions and particulate matter during and after combustion and it is in these areas that the majority of current effort is focussed.

4.1 THE DEVELOPMENT OF ENGINE SIMULATION

4.1.1 Introduction

Engineers have long wished to be able to understand the implications of the design changes they routinely make to engine design. In the early period of development of the internal combustion engine the design "improvements" were made either on a trial and error basis or on the basis of experience from earlier trial and error. This experience based process arose because of the difficulties faced by the IC engine engineers: the processes in a conventional internal combustion engine with reciprocating pistons are discontinuous:

> During the "open part" of the cycle, when either the intake valves, or exhaust valves, or both are open, the cylinder is connected to the external pipe systems that form the intake and / or the exhaust systems, and the piston motion and cylinder contents cause motion in the gases in the pipe systems.
>
> During the closed part of the cycle when both valves are closed what happens in the cylinder has no direct impact on the motion of the gases in the pipe systems although there may still be residual wave action.

These discontinuous processes are difficult to describe and analyse, and the internal combustion engine had been in existence for many years before the methods for describing and analysing these processes began to be developed in a useful form.

In addition to the problems associated with the discontinuous nature of the flows within the pipe systems of the engine, the very complex flows, combustion processes and heat transfer taking place in the cylinder during the closed part of the cycle are very difficult to describe and analyse. In turbo-charged engines the behaviour of the turbocharger when subject to rapidly varying inlet conditions also adds complexity.

Engine performance prediction through simulation appears to have started shortly after the second World War and development of a number of techniques was quite rapid. The methods ranged from relatively simple **Quasi-steady** methods, through **Filling and emptying** methods to **Wave action** methods (Benson, 1982) and on to **3-Dimensional** methods. The first of these

classifications represents the simplest and least detailed and the others follow in order of increasing complexity of solution and detail of output. A brief explanation of each follows:

4.1.2 Simple models

4.1.2.1 Quasi-steady methods:

This approach considers the engine system as a series of interconnected components, where the performance of each of the components is represented by its steady state characteristics, which are often obtained experimentally. The components are connected by the gas flow through them and by pressure ratios across them. No mass accumulation is allowed between the various components and therefore the manifolds, pipes etc are assumed to have negligible volume.

The relative simplicity and lack of "physics" of these types of model makes them simple to construct and analyse using network theory or analogue or digital computers, but the very lack of fundamental physical modelling makes them of limited use. The further the operating design is from the original calibrated model the more care needs to be taken in the interpretation of the results.

4.1.2.2 Filling and emptying methods:

This method is one step along the path of increasing use of fundamental physical modelling from the quasi-steady method in that the manifolds between the engine and turbocharger are represented by volumes. This means that these volumes are capable of losing or accumulating mass of the gas within them. The consequence of this is that unlike the quasi-steady method the mass flow rates around the system can vary. This results in a set of first order non-linear ordinary differential equations which define the conditions in the volumes of the system, i.e. the cylinders and manifolds, and in transient operation the speeds of the turbocharger and engine. (Watson and Marzouk, 1977)

This type of model is much more realistic than the quasi-steady method, but requires an order of magnitude more computational effort to resolve. However, there is another limitation which is that as this model type represents the conditions in the manifolds by a single pressure and temperature it does not have the ability to resolve manifold tuning; this requires the use of a wave action method. Despite this limitation this method is still applicable to models for use in the

development of engine control systems and has found recent favour for this application (Lancefield *et al* 1996), (Muller, 1998).

4.1.3 Wave action methods.

At present, this simulation method is the most widely used and offers a large amount of very detailed information about what is happening in an engine system. Wave action methods involve the solution of the unsteady, compressible gas flow equations and allow the representation of varying gas pressures and velocities in the intake and exhaust manifolds. This method requires a solution to the sets of non-linear hyperbolic partial differential equations which describe the passage of a pressure wave through a compressible medium.

These methods are usually restricted to one spatial dimension and cannot strictly be used for describing two and three dimensional entities such as pipe junctions. This limitation has led to these methods being described as 1-D. However much recent work has overcome this limitation by extending the physical modelling involved.

Wave propagation has been studied for many years and Rayleigh (1910) investigated "finite" waves (as opposed to small amplitude acoustic waves.) and Earnshaw (1910) proposed a solution for finite waves travelling in one direction. This work was further developed during the first half of the twentieth century, but was ultimately overtaken by the method of characteristics, the solution to which was initially produced by a graphical method. A variety of methods have been proposed and developed for the solution of the equations required to describe finite waves in gases. Probably the most widely known are the **Method of characteristics**, the **Lax Wendroff** method and the **Finite difference** method all of which have the considerable advantage over the earlier methods that they are inherently capable of simulating engines under transient operation. Whilst a detailed discussion of these topics is outside the scope of this piece of work a brief history and bibliography for each of the above will be provided below, but Benson (1982) provides a good overview of the earlier work whilst Peters and Gosman (1993) provide a review of the method of characteristics and a detailed discussion of the finite difference methods.

4.1.3.1 Method of characteristics

Riemann, (1885) made a significant contribution in developing the theory of the method of characteristics, which allows for finite waves travelling in opposite directions along a pipe. An early example of its use in the development of internal combustion engines was when De Haller (1945) applied this technique to the analysis of an exhaust system. Jenny, (1950) extended the method to cover area changes in the pipes, friction, heat transfer and flow through turbochargers. However, both used graphical techniques for solving their equations.

Shapiro, (1954) proposed a numerical method for solving the non-linear hyperbolic partial differential equations of unsteady flow, but Benson *et al*, (1964) appear to have been the first to use a computer to solve these equations. A detailed discussion of the method of characteristics and the use of computers to solve the associated equations can be can be found in Benson (1982).

However, once the computer based solution to the method of characteristics was well established, as is usual some sought to improve the efficacy of the tool by seeking greater speed of solution and greater accuracy. Winterbone *et al* (1991) suggested that a method based on the work of Lax and Wendroff, was more computationally efficient and gave greater resolution at high frequencies.

4.1.3.2 Lax Wendroff method

This, like the method of characteristics provides a numerical solution to the non-linear hyperbolic partial differential equations of unsteady flow, but the method uses a Taylor's series expansion of the base differential equations (Lax and Wendroff, 1964). McLaren *et al* (1975) applied the technique to the analysis of pipe systems on reciprocating compressors and Takeyama *et al*, (1987) applied a derivative method to gas flow optimisation in a 4 valve engine.

Poloni *et al* (1987) investigated and contrasted the accuracy and performance of the Lax Wendroff method with that of a well established method of characteristics code and concluded that although the result for the two sets of calculations were essentially identical the Lax Wendroff technique was twice as fast.

During this period when the debate over the relative merits of the method of characteristics and the Lax Wendroff method was being held, a third method of simulating the unsteady compressible flow in engine ducts was proposed. This was the finite difference method:

4.1.3.3 Finite difference methods

These methods are derivatives of the numerical techniques that have been developed for multi-dimensional Navier-Stokes codes, as discussed by Gosman, (1985), for example, but reduced to a single dimension for use in one dimensional flows (Morel *et al* 1990).

In its application to engine manifolds and pipes the fluid dynamics are approximated by using a large number of small volumes, on each of which equations of conservation of mass, energy and momentum are imposed. These equations are written in a finite difference form and solved on a staggered mesh system whereby the equations of energy and conservation of mass are solved for each volume and that for the conservation of momentum is solved for each interface between two volumes (Walter and Chapman 1979, Morel *et al* 1988 –1 and Peters and Gosman 1993).

This basic method has been extended and developed beyond the true 1-D parallel straight pipe, to include the most significant "real" features of engine pipe systems: heat-transfer to and from the flow, wall friction, curved pipes, gently tapering pipes, junctions of two or more pipes, pipe entrance losses (abrupt reductions of section) and pipe exit losses (sudden expansions) (Morel *et al* 1988 – 1).

This method is the basis of the two most widely used, commercially available, engine simulation codes, Ricardo's "WAVE" and Gamma Technology's "GT Power."

However, even though many of the real physical features of engines that are strictly 3-D can be very accurately approximated by this 1-D method, certain aspects of the flows within engines cannot be adequately represented by this method and 3-D methods are required to provide the extra detail:

4.1.4 3-Dimensional methods:

The main driver behind the use of 3-D codes within full engine simulation is the increasing desire to develop and use fully phenomenological (based on observed or measured facts) combustion models. These require a detailed knowledge of the large scale flow regimes and turbulence levels in the cylinder for all crank angles (Spalding 1976). The importance of these factors to combustion are discussed in more detail in a later section.

At the fluid flow level it is apparent that in most engines the design features that affect the flow regime and turbulence in the cylinder are the port shape, flow between the valve head and valve seat and the interaction between the cylinder walls, combustion chamber and piston and the incoming flows (Gosman 1985, Kent *et al* 1989, Alkidas and In-Soo 1991, Lee *et al* 1993, and Church and Farrell, 1998). To a good approximation, flows out of the cylinder during the exhaust stroke and during overlap have little effect on the bulk flows or turbulence levels, only taking with them both bulk and turbulent kinetic energy at the level existing in the cylinder (Poulos and Heywood 1983).

For many years the definition of port shapes has been a "black art" with expert developers using many hardware iterations to refine a port to provide the correct mixture of flow characteristics. The intake port has the primary function of allowing as much air or air/fuel mixture into the cylinder as possible. However, ports often have to provide other functions as well, such as generation of "swirl" (diesels and lean burn gasoline), or "tumble" (usually used in 4 valve gasoline engines). Both swirl and tumble are bulk rotating flows in the cylinder with the former rotating about the cylinder axis and the latter about an axis perpendicular to the cylinder and aligned with the crankshaft.

The longevity of these bulk flows can be important when they are used to move the air past the fuel sprays, as they commonly are in diesel engines, and thus it is important that they exist well beyond the end of the compression stroke. Whereas in gasoline engines it is the destruction of these large scale flow regimes, by features in the combustion chamber as the piston approaches TDC firing , producing high intensity small scale turbulence that is important for providing rapid and reliable combustion.

As the relationships between bulk flows and turbulence and combustion have become better understood so increasingly 3-D codes have been used to refine the designs of the ports,

combustion chambers, valve positions and angles and piston crown shapes. See for example Gosman *et al* 1991, Johns and Jones 1991 and Watkins *et al* 1991.

The computer software codes that produce the flow information for the complex 3-D flows described above are collectively known as "Computational Fluid Dynamics" codes, or CFD codes. However, they require very significant amounts of computer processing power, run time and "fine tuning" to produce accurate results.

This has resulted in the use of hybrid models using 1-D codes for the majority of the simple flow fields and 3-D codes to provide detailed information about the in-cylinder conditions for heat transfer and combustion prediction during engine simulation. This has led to the provision of interfaces between the 1-D wave analysis codes such as Wave (Vectis) and GT Power (Star CD) and CFD codes (Lowe and Morel 1992). These hybrid modelling regimes provide a good compromise solution with acceptable run times and levels of detail.

However, the majority of routine engine simulation, even in the larger vehicle manufacturers, is still carried out using 1-D codes and only very detailed studies are carried out using CFD. The prevailing circumstances and nature of the work undertaken during this research project were such that 1-D codes were thought adequate, provided that certain features of the engine were modelled sufficiently to allow the model to depart from its calibrated and verified operating conditions and still produce reliable results.

The following section provides an overview of the modelling principles and sample references for the most significant hardware building blocks employed in the engine model for the prediction of the performance of a diesel engine with VVA.

4.2 1-D CODE BUILDING BLOCKS

The aim of this work was to investigate the effects of VVA on light-duty, turbo-charged and inter-cooled, direct injection diesel engines and, therefore, the modelling system needed to include sufficient physics to deal with many different engine systems. The system used was GT-Power, from Gamma Technologies of Westmont, Illinois, USA. This is a well developed code and was expected to be able to predict engine performance characteristics within a few percent without the need to fine tune the models and thus it placed great emphasis on the physical modelling of engine systems. (Gamma Technologies 2001)

GT-Power includes a very large number of building blocks, but for the purposes of this discussion the model building blocks described will be limited to those involved with:

Fluid flow.[1]

In-cylinder models.

Turbines and compressors.[2, 3]

This section provides an overview of the operation of the model building blocks associated with the above groups and references for the interested reader, whilst sections 4.3.2 and 5.1.1detail the work carried out to generate and implant the data required to establish and correlate a baseline model without VVA, and the modifications required to the model for operation with VVA, respectively. *Figure 4.2.1* shows the major system components of the model that was developed.

[1] The GT-Power code models the complete system of flows on an instantaneous non-steady flow basis using a finite volume type analysis.

[2] The flows through the compressor and turbine are assumed to be quasi-steady, using steady flow characteristics obtained by the manufacturer from bench tests. Not only are the non-steady operating points often well outside the measured data, but there is evidence in the literature of significant differences between steady and non-steady performance.

[3] The turbo-charger model allows for instantaneous torque balance between the turbine and compressor which, therefore, requires the supply of the rotor moment of inertia to calculate angular accelerations.

4.2.1 Fluid flow

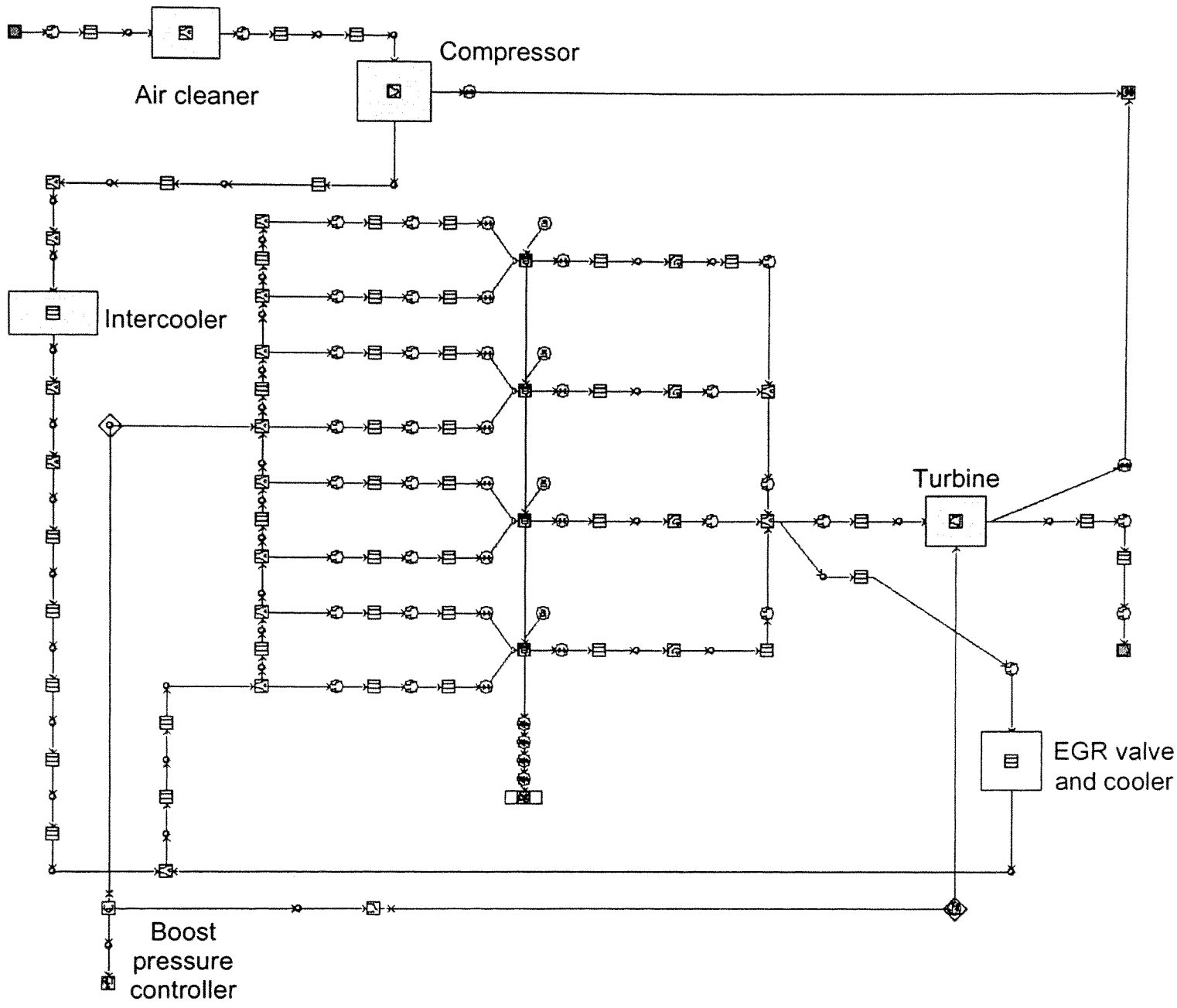


Figure 4.2.1.1 Overview of the major sub-systems employed in the simulation model for the prediction of the effects of VVA on light-duty diesel operation.

These building blocks describe those parts of the engine system that convey and modulate the gas flows into and out of the cylinders, from the air pickup through to the intake valve, (excluding the compressor) and then from the exhaust valve outwards through the exhaust system, (excluding the turbine.)

4.2.1.1 Pipe friction or pressure losses

The pipes represented can be round, rectangular or irregular in cross section, straight or curved and parallel or tapered. The user can specify friction multipliers to manually control the pressure loss, but there are default settings for the surface roughnesses of standard materials such as steel tubing, cast iron and cast aluminium as well as many others, which are used together with the geometry of the pipe to automatically calculate the pressure losses (Fox and McDonald, 1992 and Miller 1990).

4.2.1.2 Heat transfer

Heat transfer effects in the pipe systems are calculated through the use of the Colburn analogy (Colburn, 1933 and Kreith and Bohn, 1993). The user only has to enter a wall temperature for the pipe and the code will calculate heat transfer to/from the fluid for steady state operation. The system is also able to deal with transient operation when the surface temperatures of the surfaces and fluid are both calculated. In this case the user entered wall temperature serves only as an initial condition.

4.2.1.3 Junctions

This is probably the most difficult of the pipe system components for the user to define as care is needed in specifying the lengths in the junction model and angular relationships between the pipes meeting at the junction. However, three general types of junction are specified in order to guide the user: 1. right angle junctions, such as would typically be found in intake manifolds at the junction between the plenum and intake runners, 2. a generalised junction for a number of pipes joining into a broadly spherical surface, this is particularly suitable for modelling junctions where opposing flows meet and 3.second type of generalised juntion that deals with multiple pipes, all with predominantly the same flow sense joining to a (larger) pipe, as might typically be found in the collector joining a group of exhaust primary pipes to a secondary pipe (Blair 1996 and Winterbone and Pearson, 2000).

These models are specifically designed to deal with the conservation of momentum in 3-dimensions and hence the spatial detail required is substantial. In addition they deal with heat transfer and pressure loss or recovery at their entries or exits.

Of particular interest in this area is the modelling of pulse converter exhaust manifolds, as the junctions between the exhaust primaries and the manifold can influence the operation of the turbo-charger significantly (Bassett *et al* 1999 and Winterbone and Pearson 2000).

4.2.1.4 Orifices and valves

Of particular interest in this project is the treatment of orifices and valves. Both rely on measured data to calculate the discharge coefficients, which are typically different in the two flow directions. The discharge coefficients are calculated from the isentropic velocity equation for flow through an orifice and are defined as the ratio of the *effective area* to the *reference flow area*. This model would typically be used to treat throttles or poppet valves, but can deal with most measurable variable (or fixed) flow restrictions, with normal and choked flow (Stone, 1992).

When used for poppet valves controlling the flow into and out of engine cylinders these measurements and calculations result in tables of *forward* and *reverse* discharge coefficients, indexed by the ratio of valve lift to a reference diameter, D_{ref} where D_{ref} is the diameter used to calculate the reference flow area and is typically the valve head diameter.

The use of measured flow data allows the effects of the combustion chamber and ports on the flows to be reflected in the calculation of the discharge coefficients. These measurements are usually taken on steady flow rigs, with relatively low depressions, typically less than 1 metre of water (Ford use 10" and 20" of water). Annand and Roe (1974) discuss the varying flow regimes through intake and exhaust valves and the experimental methods for obtaining the data for use in the simulation models.

4.2.2 In-cylinder models

During the closed part of the cycle the gas dynamics of the pipe systems have no direct influence on the motion of the cylinder contents. The in-cylinder mixture motion results from the flow field generated during the induction stroke, in the case of port injected engines, or from its combination and interaction with the fuel injection process in the cases of diesel and direct injection gasoline engines. In addition to influencing the combustion, as mentioned above, these fluid motions strongly influence the heat transfer between the cylinder contents and the piston crown, cylinder head, valves and cylinder walls.

It is also important to recognise that the products of combustion, such as exhaust residuals and mixtures of fuel vapours and air do not behave as perfect gases and have specific heat capacities that vary significantly with temperature (and to some extent with pressure) and their correct prediction is essential to accurate simulation of the processes taking place in the cylinder. However, the correlations used to calculate these gas properties are well known (for instance Krieger and Borman, 1966 and Olikara and Borman, 1975 and their work in implementing computer programs to use the JANAF tables, 1971). These correlations are widely used and the simulation codes typically do not allow access to these core parts of their operation and no user control is available, so no further discussion will be given of this topic.

In addition to the above three areas of combustion, heat transfer and gas properties, modern simulation codes are beginning to incorporate models to predict emissions, but this area of work is not yet regarded as mature, and despite in some cases predicting trends it cannot be relied upon to the same extent as performance prediction.

4.2.2.1 Combustion

As mentioned above a detailed knowledge of the in-cylinder mixture motion is essential in fully 3-D simulation of the combustion process and a number of well developed techniques exist: (Bazari, 1992), (Yoshizaki et al, 1993) and (Morel and Wahiduzzaman, 1996) However, these methods are very demanding of computer resource and rely on data that is often difficult to obtain. As a consequence, at present, the majority of engine simulation is carried out using lower order methods because they are much faster to implement and use. The discussion here concentrates on the lower order methods, used to calculate the ignition delay (from start of injection to start of combustion) and the fuel burning rate, in this investigation of the effects of VVA on diesel engine performance.

4.2.2.1.1 Ignition delay

The ignition delay is a very important parameter of combustion, as it affects engine performance, fuel economy, combustion noise and engine out emissions, and as a consequence there has been considerable work in this area: Wolfer, (1938) proposed a correlation that was responsive to cylinder temperature and pressure, whilst others (Hardenberg, 1979 and Olree, 1984, for example), added terms that included the effect of diesel fuel cetane number. More advanced correlations have been introduced more recently (Han *et al* 2000 and Kim *et al* 2000), but these later forms again suffer from the difficulty of obtaining the correct data for their use.

For this piece of work the Wolfer correlation was selected. There is further discussion of this in section 4.3.2.2.

4.2.2.1.2 Fuel burning rate

The simplest method of providing a "combustion characteristic" is to force a cylinder pressure-volume characteristic onto the engine model. Pressure-volume traces have been measured for many years and provide a reliable source of data that can characterise the combustion process in order to investigate engine behaviour, but under operating conditions that are the same as (or only slightly removed from) the operating condition at which the pressure volume diagram was measured. This method was extended to produce "apparent heat release" curves, which predict the rate at which the cylinder contents need to change in temperature to produce the (measured) changes of pressure. This approach provides a basic "shape" to the combustion characteristic that

can be scaled to allow for changes in the amount of fuel present and within limits for changes in the trapped mass of air. However, these forms of non-physical approach do not lend themselves to the investigation of transient or widely varying operating conditions as large amounts of measured data are needed.

Wiebe (1956) developed a method of describing the characteristic shape of the mass fraction of fuel burned, as a function of crank angle, using an exponential equation of the form:

$$x(\theta) = 1 - \exp(-a[(\theta - \theta_0)/\Delta\theta_b]^{m+1})$$

where $x(\theta)$ is the mass fraction burnt at crank angle θ
θ_0 is the crank angle at the start of combustion
and $\Delta\theta_b$ is the duration of the complete combustion process

a and m are constants that can be adjusted to produce heat release characteristics that match measured data from a given engine at a specific operating point (Stone 1992-1).

Watson *et al*, (1980) proposed the summing of two Wiebe curves with significantly different constants to allow a more accurate representation of combustion. They also investigated the effects of varying cylinder temperature and pressure and produced correlations to link the values of the coefficients a and m to the cylinder conditions. These relationships were derived from measured data at a number of operating conditions and their paper demonstrated that they had successfully produced relationships between these coefficients and the cylinder conditions that held over the majority of the engine speed and load range. However, whilst this approach allowed parametric investigation of changes to the shape of the heat release curve, it was still limited by its inability to respond to variations in residuals.

Modern diesel fuel injection systems are capable of profiled or multiple shot injection (*Figure 4.2.2.1.1*) These produce very different combustion characteristics from the traditional single shot injection that was common a few years ago. The almost total absence of the premixed spike (to help with refinement) and the continued burn until late in the expansion stroke has required the use of 3-term Wiebe functions with the three constituent parts being called premix, main and tail functions.

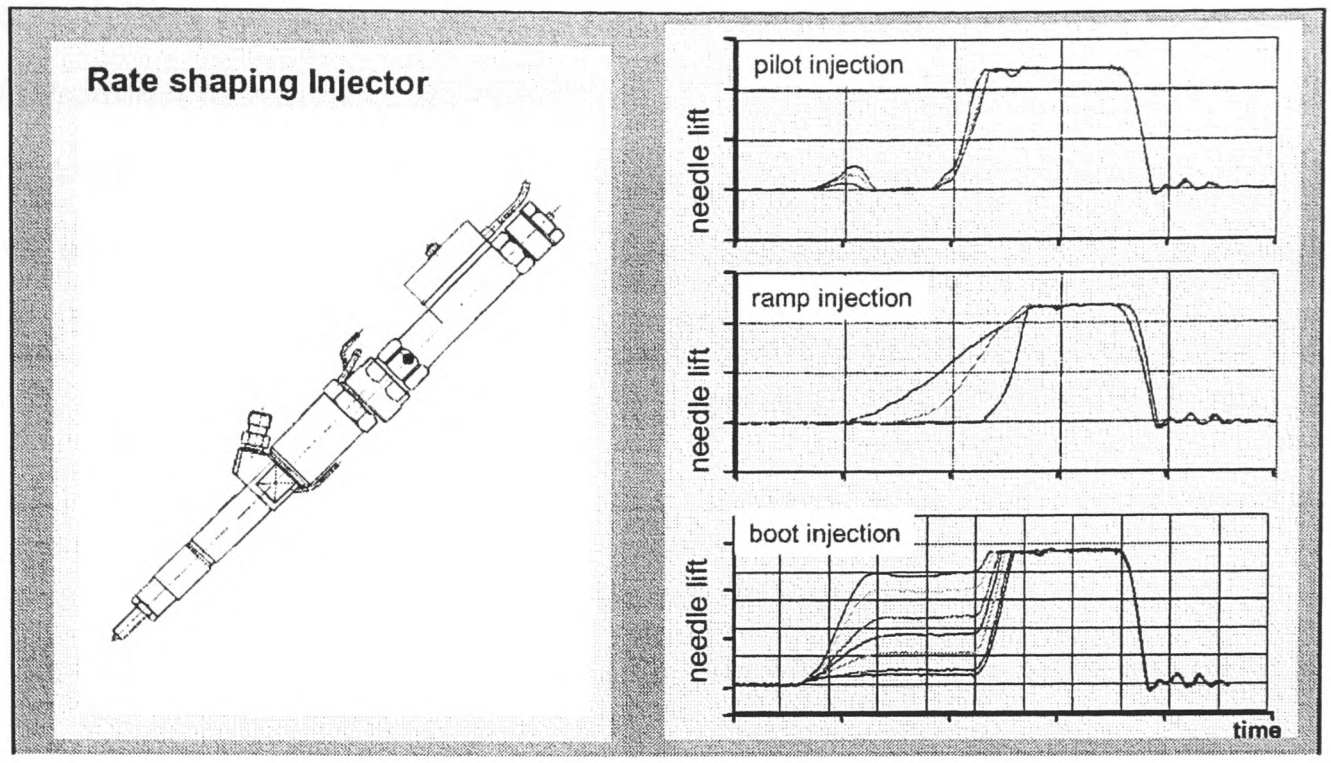


Figure 4.2.2.1.1 Common-Rail injector with profiled and multi-shot characteristics (Hummel *et al* 2000).

The 3-term Wiebe function is widely used for investigations of transient operation, particularly where the engine simulation model is embedded in a control model for control system, calibration and drivability development as it provides a good level of detail for transient engine operation whilst minimising computer run times (Osborne and Morris, 2002). This was a major consideration in the selection of this technique for the VVA investigation, of which there is further detailed discussion in section 4.3.2.2, where the 3-term Wiebe model implemented is described.

4.2.2.2 Heat transfer

With the simplest combustion model, which imposes a pressure crank angle relationship on the engine model, heat transfer in the cylinder is implicitly included in the results as the pressure characteristic is based on the net heat released.

With the Wiebe type combustion models generating fuel burning rate data, heat transfer to the engine structure needs to be modelled. As with the combustion models, as computer power and understanding of the underlying physics improved, so heat transfer models became increasingly sophisticated and accurate. Similarly, they also range from zero-dimensional correlations through to full 3-dimensional, multi-zone solvers, of which (Morel and Keribar, 1985), (Morel *et al* 1988 – 2) and (Bohac *et al* 1996) provide some discussion. However it is important to differentiate between the differing types of heat transfer models and their specific purposes.

For engine modelling two primary types of heat transfer models are useful: 1) Those that calculate *instantaneous spatially averaged* heat flux to the chamber walls and 2) those that calculate *instantaneous local* heat fluxes. The first of these types is most widely used for engine performance simulation and uses zero-dimensional correlations, whilst the second is primarily used for detailed study of components such as the piston, cylinder bore, combustion chamber and are necessarily 3-dimensional in their approach (Heywood, 1988-3.) Only the former type was of interest in this work.

A variety of zero-dimensional heat transfer models have been proposed to calculate *instantaneous spatially averaged* heat flux to the chamber walls: Eichelberg (1939), Annand (1963), Benson (1982), Woschni (1967) and Annand and Ma (1971). These correlations all use characteristic features of the cylinder, such as the bore, mean piston speed and mean gas properties (Stone 1992-2).

Heywood (1988-3) discusses the work of Lefeuvre *et al* (1969) and Dent and Sulaiman (1977), who proposed an analogy with the correlation for forced convection heat transfer over a flat plate Heywood also compares this approach with Annand, Woschni and measured data.

Of these, the correlation developed by Woschni has found continued widespread use and development. Woschni's base equations can be reduced to the following (Stone, 1992-2):

The spacial average coefficient of instantaneous heat flux, h is given by :

$$h = 129.8 p^{0.8} u^{0.8} B^{-0.2} T^{-0.55} \quad (\mathrm{Wm^{-2}K^{-1}})$$

where :

p = instantaneous cylinder pressure (bar)

B = bore diameter (m)

T = instantaneous mean gas temperature (K)

and :

$$u = C_1 \bar{v} p + C_2 (\frac{V_S T_r}{p_r V_r})(p - p_m)$$

where :

p_m = equivalent cylinder pressure under motoring conditions

V_S = Swept volume (m^3)

V_r, T_r and p_r are evaluated at some reference condition in the cylinder such as inlet valve closing and C_1 and C_2 are coefficients

From consideration of the differing conditions pertaining during the different parts of an engine cycle it should be clear that the coefficients need to have different values during gas exchange, compression, combustion and expansion. Sihling and Woschni (1979) proposed alternative values of these coefficients for high speed direct injection diesels with high levels of swirl, while Watson and Janota (1982) proposed that the compression and expansion be modelled as polytropic processes to provide an alternative estimate of p_m.

From the above it can be seen that there are differences between the methods of calculation of the *instantaneous spatially averaged* heat fluxes and that they are reliant upon coefficients that need to be refined to reflect engine operating conditions and type. Therefore, as shown by Heywood, it is not surprising that the different correlations predict widely differing heat transfer coefficients. Fortunately predictions of engine output are not very sensitive to errors in heat transfer calculation and typically a 10% error in in-cylinder heat transfer will only produce a 1% error in predicted engine performance.

GT Power uses the Woschni correlation with modifications to the coefficients during the periods when the valves are open, and increases the heat transfer whenever the flow velocities into the cylinder are large, either during intake or back flow from the exhaust. This form of Woschni is used for the performance predictions carried out for this research.

4.2.2.3 Emissions

As mentioned earlier the prediction of emissions is still in its infancy, currently being able only to provide information about trends, but of limited use in quantitative analysis. In the case of diesel engines the emission of NO_x and particulate matter are of concern.

Clearly the emissions produced by an engine are by-products of combustion and to predict emissions requires detailed data about the temperature distribution and chemical composition in the cylinder. From this it can be seen that 3-dimensional modelling of the diesel fuel injection spray patterns and fluid motions in the cylinder are essential for satisfactory predictions (Bazari, 1992).

Whilst GT Power has models based on the work of Hiroyasu and Kadota (1976 and 1983) and Nagle and Strickland-Constable (1962) to predict soot formation and its subsequent burn up, and NO_x formation, since the detailed combustion models were not being used no emissions data was generated.

4.2.3 Mechanical systems

4.2.3.1 Friction

Various detailed models for predicting the friction from engine sub-systems have been proposed, but it is normal to use a simplified correlation or measured data. The GT Power code uses a model proposed by Chen and Flynn, (1965.)

$$FMEP = \mathrm{C} + (\mathrm{P_f} * P_{max}) + (\mathrm{MPSF} * V_{mp}) + (\mathrm{MPSSF} * V_{mp}^2)$$

where:

C = The constant part of the *FMEP*

P_f = The peak cylinder pressure factor

P_f = Maximum cylinder pressure

MPSF = Mean piston speed factor

MPSSF = Mean piston speed squared factor

V_{mp} = Mean piston speed

The coefficients can either be regressed from measured data, or based on values that have been found typical for similar engines. However, caution must be exercised in the use of measured friction data as there is always a difference between motored and fired friction. This will be apparent from the consideration of piston ring and piston to bore friction, which can be expected to be dependent upon cylinder pressure, which clearly differs between fired and motored conditions. However, despite this difficulty this correlation has been widely and successfully used and was used in the simulation to investigate VVA in diesel engines.

4.2.3.2 Turbines and compressors

As the power output and efficiency of modern diesel engines is highly dependent on the use of turbochargers to increase the mass flow through the engine, the use of turbochargers is now nearly universal for light duty automotive diesel engines. They are also becoming increasingly sophisticated with variable geometry turbines already finding widespread use and variable geometry compressors under development.

In concept turbochargers are simple devices, comprising an exhaust gas driven inward-flow-radial turbine and centrifugal compressor on a common shaft. Originally both parts of the turbocharger were considered as continuous flow devices, but clearly in this application the turbine is subject to fluctuating inlet conditions and the compressor experiences pressure waves in the intake manifold pipes.

Of these fluctuating conditions it is the "pulse" effects of the exhaust blow down flows from the cylinders and how they are treated that are most important and must be correctly modelled if correct engine performance predictions are to be achieved.

4.2.3.2.1 Turbines

Two approaches are commonly taken to the treatment of the exhaust flows into the turbine: *Constant pressure turbocharging* and *pulse turbocharging*. The first of these utilises a system to smooth the pressure at the inlet to the turbine by connecting all of the exhaust pipes to a large chamber (many times engine displacement) and feeding the turbine from this large volume. The large ratio of chamber volume to engine cylinder volume leads to the almost complete dissipation of the kinetic energy of the exhaust gases leaving the cylinders and to minimal pressure fluctuation in the chamber, and consequently almost constant pressure at the inlet to the turbine. The second approach attempts to utilise the significant kinetic energy available to increase the energy supplied to the turbine. (Watson and Janota, 1982)

The difficulty of rigorously designing a turbine to operate efficiently under highly fluctuating inlet conditions at a variety of operating speeds and loads means *pulse turbocharging* rarely provides higher shaft output to the compressor than constant pressure turbocharging. There is also another significant operational problem associated with pulse turbocharging:

In engines with more than 3 cylinders it is the case that the high pressure pulses resulting from the exhaust valve of one cylinder opening will influence the low pressure part of the exhaust process in another cylinder, unless suitably selected cylinders are grouped together and used with multiple entry turbines. (Yeo and Baines, 1990)

Despite these difficulties, small displacement, light duty diesel engines always use *pulse turbocharging* systems, as constant pressure systems are necessarily large, (space is always at a premium) and have poor transient response because of the time taken to change the pressure in the chamber (good transient drivability is vital to customer acceptance). Most 4 cylinder engines of this type use single entry turbines, although twin entry devices are being adopted by some manufacturers, and those with six and more cylinders typically use two turbochargers because of packaging and thermal stress problems in twin entry devices.

From the above it should be apparent that the correct modelling of strongly pulsating flows in the exhaust manifolds and the turbine are important and as a consequence much work has been done in these areas.

Birman, (1946), Meier, (1971), Benson, (1982), and more recently Bassett *et al*, (2000), all discuss the design of exhaust manifolds with pulse converting junctions. *Figure 4.2.3.2.1.1* shows a typical pulse converting exhaust system junction schematic. The key characteristics of a pulse converter manifold are small total volume (to create significant pressure pulses) and nozzle-like junctions between the exhaust runners and the main tube which is connected to the turbine (to convert pressure to kinetic energy.)

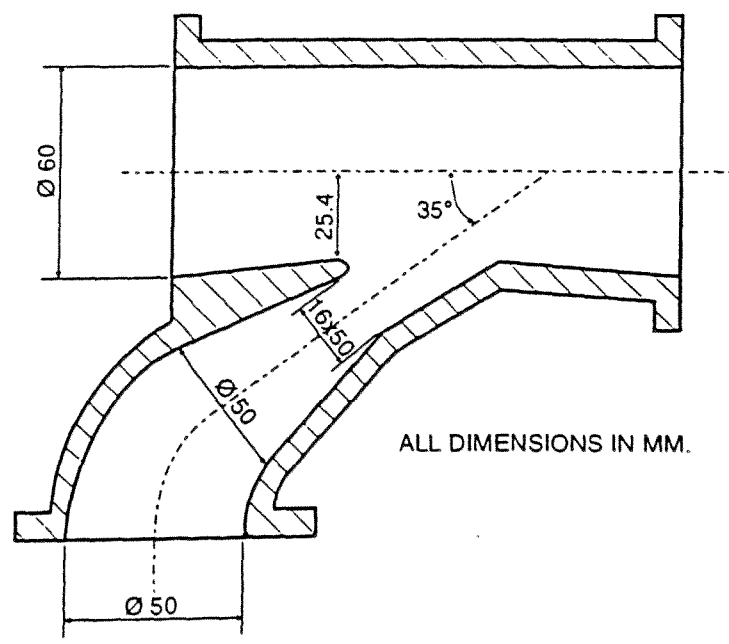


Figure 4.2.3.2.1.1. Schematic of a pulse converting exhaust system junction. (Bassett *et al*, 1999)

GT Power typically simulates the junctions by treating the entry pipe as a tapered, bent pipe joining with a pair of larger diameter pipes. This is necessary to correctly calculate the flow coefficients as the main pipe, although nominally straight needs to be treated as a pair of pipes meeting the entry pipe (Bassett *et al*, 1999).

Wallace and Adgey (1967-8), Yeo and Baines (1990) and Winterbone *et al* (1990) all explored the extent to which the operation of the turbine was affected by unsteady flow conditions. The unsteady inlet conditions manifest themselves as rapidly fluctuating pressure ratios across the turbine. In general as the pressure ratio rises the mass flow through the turbine increases and the turbine accelerates. The reverse is also true, but the efficiency of the device also varies with pressure ratio and mass flow rates. As might be suspected it is extremely difficult to test turbines with unsteady flows and the majority of test data is based in steady state "gas stand" tests. Unfortunately the pressure fluctuations can cause the turbines to operate well away from the areas where steady state data can be obtained, and extrapolation of data is therefore necessary if modelling, based on the measured performance data, is to be accurate (Watson and Janota 1982).

For modelling purposes, to characterise a turbine it is necessary to know its efficiency and mass flow rate as functions of pressure ratio and inlet temperature. This data is usually determined by the turbine manufacturer and provided either as graphs or tables. In the case of the VGT these are typically measured at four nozzle settings from closed up to fully open. There is further discussion of how the VGT of the target engine was modelled in section 4.3.2.3.

4.2.3.2.2 Compressors

The typical compressor for a light duty diesel is a single stage outward flow radial device of fixed geometry, capable of producing pressure ratios of up to approximately 3:1. The advent of VGTs has generally increased the mass flow capacity of the compressor in comparison with engine capacity and led to increased engine output. But it has also meant that more turbine power can be extracted at lower mass flows, with the consequence that at low engine speeds the compressor can more readily be forced to operate in the region close to the stall line than would have been the case with a wastegate controlled turbine. In addition the use of VGTs also allows the compressor to be driven to higher speeds and pressure ratios than would have been common with a wastegate controlled turbine.

As with turbines the compressor performance data is measured on a steady flow test stand (a much better approximation for the compressor than it is for a turbine) but again the area of operation covered by the data is generally smaller than that over which it can be exercised by the combination of the engine and turbine. Again, the consequence is that extrapolation of the measured data is necessary to encompass the complete operating region of the device.

The extension of the compressor map was an area of significant work in the establishment of the baseline simulation model and is covered in detail in section 4.3.2.4.

Having described and discussed what are considered to be the most important model building blocks in their generalities, the next section describes the work carried out to establish the detail of the model, concentrating on the in-cylinder models, the turbo-charger and the addition of the VVA model, and the correlation of its predictions with the data provided by the engine manufacturer.

4.3 CALIBRATION OF THE BASELINE MODEL

In order to demonstrate that the model had the correct characteristics to predict engine behaviour in response to varying valve timings it was necessary to correlate it to known engine operation and performance with standard valve timings.

The correlation data made available by the engine manufacturer was a mixture of engine test data (obtained on a dynamometer rather than from a rolling road) and extensive simulation results from a model that had been well correlated to test data. The value of the simulation results was particularly in the level of detail available, as the modelling code predicted and recorded many internal conditions that would not normally be measured on a test bed, but were of great value in understanding and correlating models.

The output of the model was compared against the baseline data for a large number of operating characteristics at steady state converged operating points. The operating points considered were all full load and covered the speed range from 1000 rpm to 4500 rpm.

In order to get a good match between the calibration data and the GT-Power simulation, it was necessary to implement the following enhancements to the model:

1. Modelling of the VVA cam profiles (4.3.2.1)
2. A more sophisticated combustion model to describe the fuel burning rate with modern fuel injection (4.3.2.2)
3. Extend the turbine and compressor maps (4.3.2.3) and (4.3.2.4)

The extension of the turbine and compressor maps required an empirical approach, but the comparisons made with the baseline data (4.3.3) show this to have been effective.

4.3.1 Description of the engine

The engine to be simulated was a state of the art 4 cylinder diesel engine of 1998 cc (86mm bore, by 86mm stroke) with two intake and two exhaust valves per cylinder, common-rail fuel injection, electronically controlled EGR valve, EGR cooler, air to air intercooler and a variable nozzle inward flow radial turbine, (under boost pressure demand control,) driving a radial compressor. See *figure 4.3.1.1.*

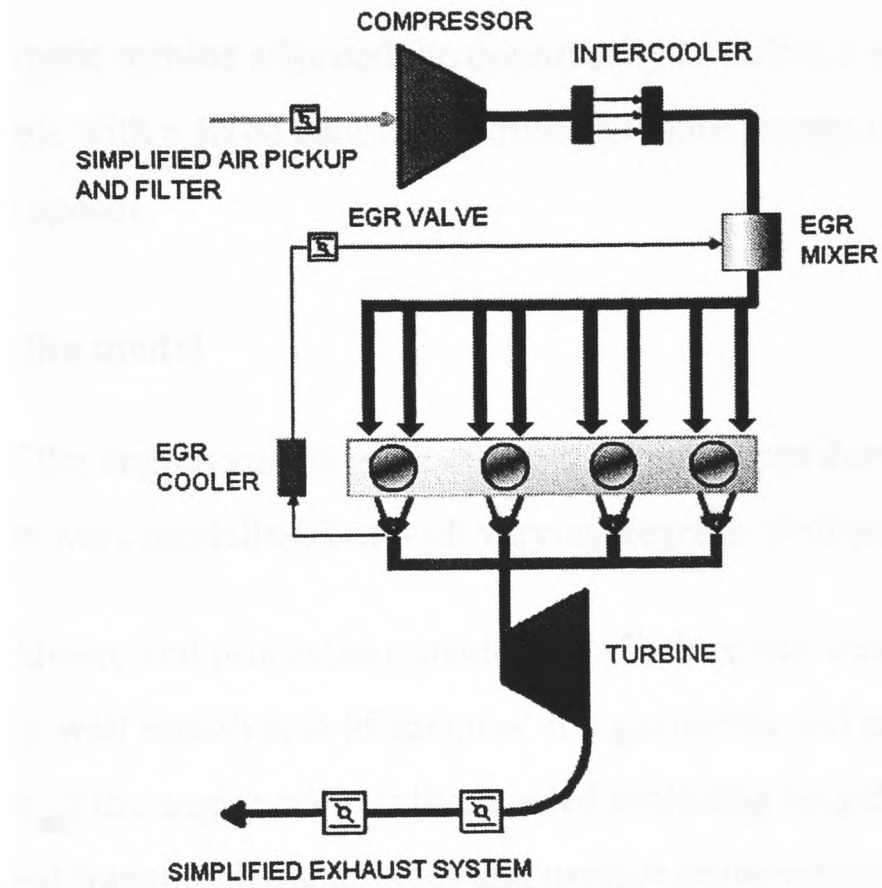


Figure 4.3.1.1. Engine systems overview

The two intake valves were controlling the air flows through separate helical ports comprising a short "high flow" port and a long "swirl" port, with different flow coefficients, but identical valve opening and closing timings. The two exhaust valves, again with identical timings controlled the flow into a single exhaust port.

The fuel injection system was utilising "pilot" and "main" injection only, with the fuel mass to be injected per-cylinder, per-cycle being calculated as a demanded value on a cycle by cycle basis.

The EGR valve was located downstream of the EGR cooler to minimise the temperature to which the valve was exposed. The EGR cooler used engine coolant to absorb the unwanted heat. This system was only active at part load, but the additional volume of the system, attached to the exhaust manifold, had an effect on the engine's operation under all conditions.

The exhaust gas driven turbine was integrated to the exhaust manifold opposite the exhaust runner from cylinder three. The turbine was of the variable nozzle type with the inlet guide vane angles set by an electrical actuator in response to a demanded "boost pressure." The boost pressure was sensed in the inlet manifold, opposite cylinder two.

The compressed air was cooled by an air to air intercooler, in the in-vehicle installation, but with a water cooled version for test bed running.

The use of a variable nozzle turbine afforded the opportunity to utilise a larger compressor than would have been possible with a fixed geometry turbine as more energy could be fed to the turbine at lower engine speeds.

4.3.2 Description of the model

All physical features of the engine and its geometry and all processes during both open and closed parts of the cycle were modelled, but with varying degrees of physics involved.

The majority of the hardware and processes outside the cylinders was modelled with a substantial amount of physics using well established techniques: the geometric and physical properties of the pipe systems either side of the engine were fully detailed including lengths, bends, materials, surface roughnesses, heat transfer characteristics and outside temperatures (representing their locations in an under-bonnet installation,) with the exception of the system down stream of the turbine, which was represented by two pipes and two orifices rather than a detailed model of the full exhaust system. (This approach has been demonstrated to provide a very good approximation to exhaust system behaviour without the need for a detailed, and necessarily slower, model representing the muffler systems, Smith, (1999)). The intercooler and the EGR cooler behaviour was readily constructed using the same level of detail as the pipes of the majority of the system.

Using slightly less physics and relying more on measurement, the EGR valve flows were modelled using flow coefficients calculated from measured data combined with standard modelling blocks. But, whilst the intake and exhaust poppet valve flows were again modelled using discharge coefficients derived from measured data and standard model blocks, the model dealing with the valve opening characteristics needed to be extended to deal correctly with the behaviour of the variable duration VVA system.

As might be expected the standard models in GT-Power allow the widely used cam phasing VVA systems to be modelled directly, but the variable duration VVA system alters the effective shape of the cam profile. It therefore required some additional code to be written to represent the mechanism and generate the effective cam profiles that an engine would experience. This piece of code had no effect on the physics being modelled and since the valve flow data was measured for valve lifts that exceed the physical valve lift used by the engine only interpolation of data was required to generate the flow coefficients.

The in-cylinder processes, such as combustion and heat transfer and those associated with the turbo-machinery, were less well defined in their operation and physics and relied more on measured data.

It was this latter group of sub-model that represented the majority of the work required to establish a well correlated model from which to explore the engine behaviour outside the standard configuration. The following sections describe the work undertaken in the specific areas of VVA cam profile generation, combustion and cylinder heat transfer and turbine and compressor mapping.[1]

4.3.2.1 VVA modelling

It should be remembered that the VVA system selected is a variable angular velocity system, where the individual valve lift profiles experienced by the engine differ from the nominal cam profile as a function of crank angle and operating set point. Sections 3.2 and 3.3 provide a detailed discussion of this, including the full dynamics (rigid body) of the cams and valves. But as with most simulation codes of this type, GT-Power did not need anything more than valve lift on a crank angle basis. To provide this information a piece of dedicated software was written.

This was integrated into a piece of Fortran from GT-Power which provided "stubs" for code implementing "user sub-routines." When compiled this produced a dynamic link library executable program (.dll) that operated with the main software suite at run time.

([1] It should be noted that the process of fine-tuning a model of this nature should not involve arbitrary tuning of coefficients, which in most cases, where full physics is used, can be left as defaults, but is more involved with the adjustment of the sub-models that do not contain substantial physics.)

The bespoke piece of software used fundamentally the same functions to deal with both intake and exhaust valve timings. It operated by loading the nominal valve lift data into arrays and used VVA eccentricity set point data and crank angle passed from the main GT-Power program to calculate the difference between drive shaft angle and cam angle to "look up" the actual cam angle and thence find the valve lifts either side of the actual cam angle, and by linear interpolation determined the actual valve lift(s) to be passed back to the simulation code. Typical valve lift curves generated by the software for diesel engine use can be seen in *figure 3.2.1.3.*

4.3.2.2 Combustion

As has already been discussed in section 4.2.2.2 insufficient data was available to operate the advanced spray combustion model available in GT-Power so lower order correlations were used for heat transfer, ignition delay and fuel burning rate calculations.

For cylinder heat transfer, the built in Woschni correlation was used (Woschni, (1967), but the in-built Wiebe based combustion routine was found to be inadequate for the prediction of ignition delay and fuel burning rates for the type of engine being investigated:

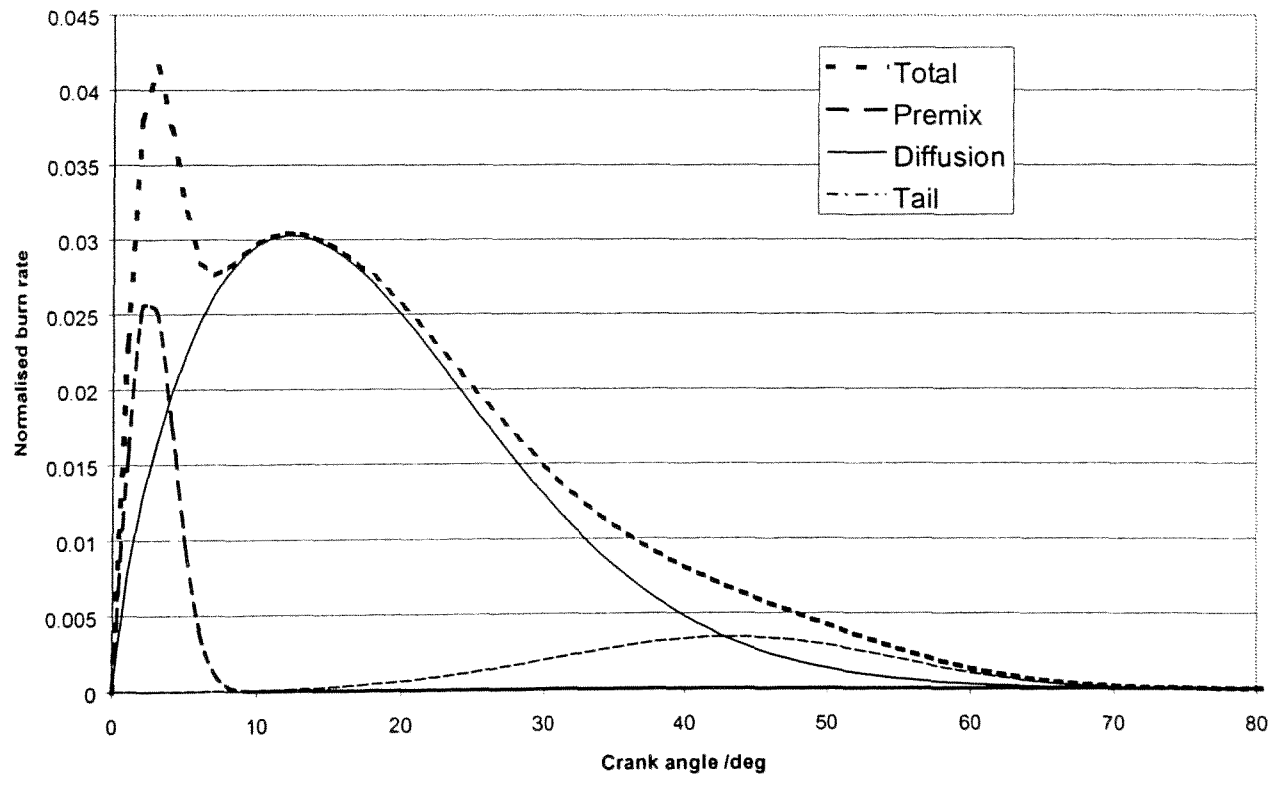


Figure 4.3.2.2.1 The output of the built in GT-Power Wiebe based combustion model when set to use all default settings.

GT-Power has a built in 3 term Wiebe function which, although having predictive capability, was found not to produce results that were appropriate to European, light-duty diesel engines as it produced a large "premixed" spike, which is more typical of the larger cylinder sizes of North

American truck engines. See *figure4.3.2.2.1*. Therefore it was necessary to implement a semi-predictive burn rate combustion model that was appropriate for this investigation. This was implemented as an additional Fortran sub-routine and compiled and linked with theVVA cam profile generation subroutine to produce a .dll file that linked to the main software suite.

The ignition delay implemented was based on the Wolfer correlation (Wolfer 1938) as modified by Watson *et al* (1980). This is shown below and it should be noted that δ is in seconds.

$\delta = 0.00345 \exp (2100/T_{cyl})/(P_{cyl})^{1.02}$ Where T_{cyl} is in Kelvin and P_{cyl} is in bar.

The combustion correlation used was also based on the work of Watson and co-workers. In their work they extended the work of Wiebe, to incorporate an additional, second, exponential term in an attempt to more closely match the measured combustion characteristics of the then current engines. This provided separate burn rate models for the so called "Premixed" and "Diffusion" burning phases. Their individual and accumulated effects can be seen in *figure 4.3.2.2.2.*

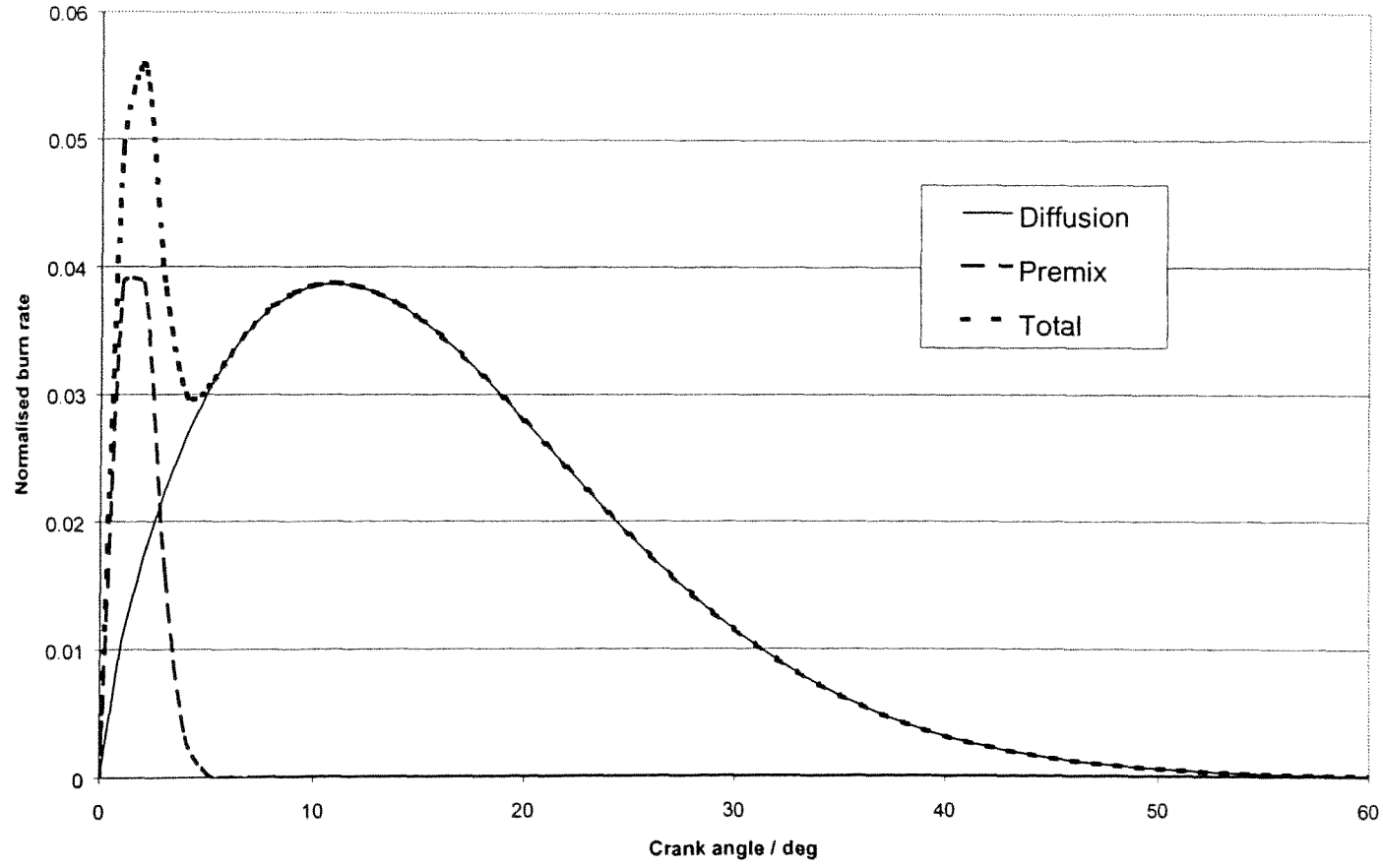


Figure 4.3.2.2.2 The output of the 2-term Wiebe based combustion model proposed by Watson *et al* (1980).

The two stages of combustion had different exponential forms, the premixed generating a very sharply rising and falling curve of substantially shorter duration than that of the overall combustion, while the diffusion stage was of longer duration and less dramatic in form.

$$\dot{M}_p(\tau) = C_{p1} \cdot C_{p2} \cdot \tau^{C_{p1}-1} \cdot \left(1-\tau^{C_{p1}}\right)^{C_{p2}-1} \quad \text{Premixed burn rate}$$

$$\dot{M}_d(\tau) = C_{d1} \cdot C_{d2} \cdot \tau^{C_{d2}-1} \cdot \exp\left(-C_{d1} \cdot \tau^{C_{d2}}\right) \quad \text{Diffusion burn rate}$$

(The coefficients C_{p1}, C_{p2}, C_{d1} and C_{d2} are the so called "shape factors" that determine the shape of the output of the functions. The reader is referred to Watson *et al*, (1980), for a detailed explanation of their effects and the basis for their evaluation.)

This "2-term" description of the process was considered adequate for the engines being modelled at that time, when the premixed "spike" was a recognised feature of diesel combustion, contributing to its typical "diesel knocking" sound that led to diesels being considered unsuitable for most passenger cars.

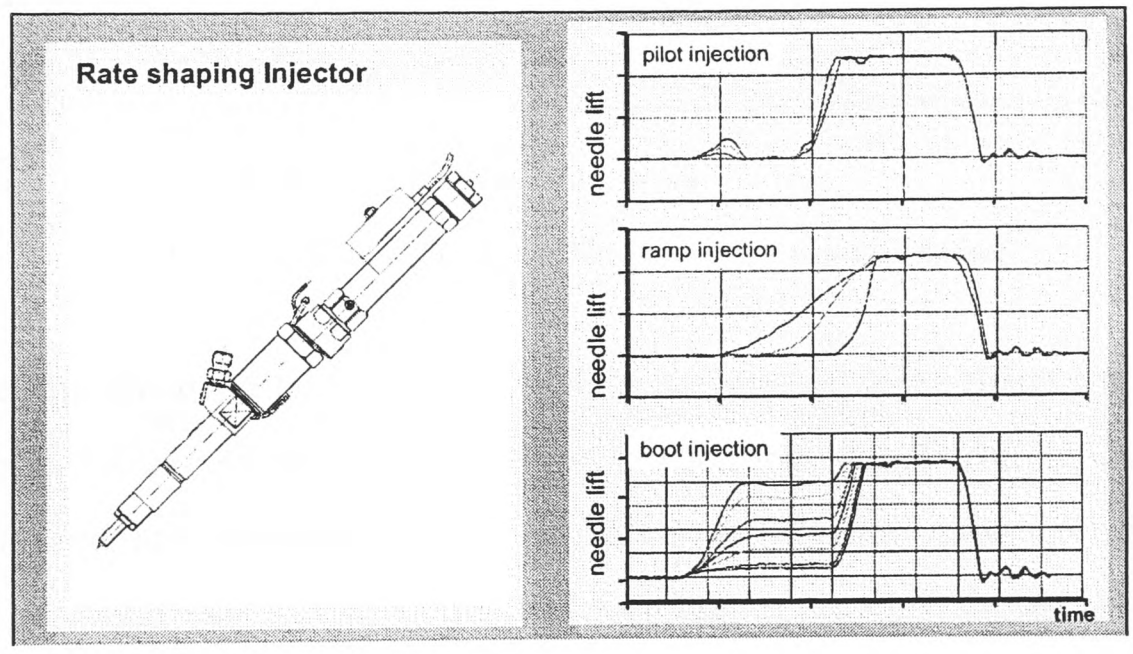


Figure 4.3.2.2.3 Pilot and rate shaped injection characteristics (Hummel *et al* 2000)

More recently, advances in fuel injection systems, with injection rate shaping and multiple injections per firing stroke have allowed considerable control over the rate of pressure rise that causes diesel combustion harshness (Hummel, *et al* 2000). These features in combination with increased injection pressures have allowed substantial fractions of the fuel to be injected after TDC and combustion to continue until late into the expansion stroke.

A consequence of these advances in fuel injection and combustion technology is that the two term curve, proposed by Watson *et al*, (1980) is no longer adequate and a third Wiebe term is needed to more fully characterise the later burn, a so called "tail" burn Wiebe curve. The combination of three Wiebe curves is a useful tool for representing diesel combustion in modern

diesel engines. This is particularly so where pilot injection is used, as this allows the almost total removal of the premixed spike and retarding of the main combustion process. *Figure 4.3.2.2.4* shows typical curves for the representation of the three parts of the combustion process and the form of the overall combustion shape.

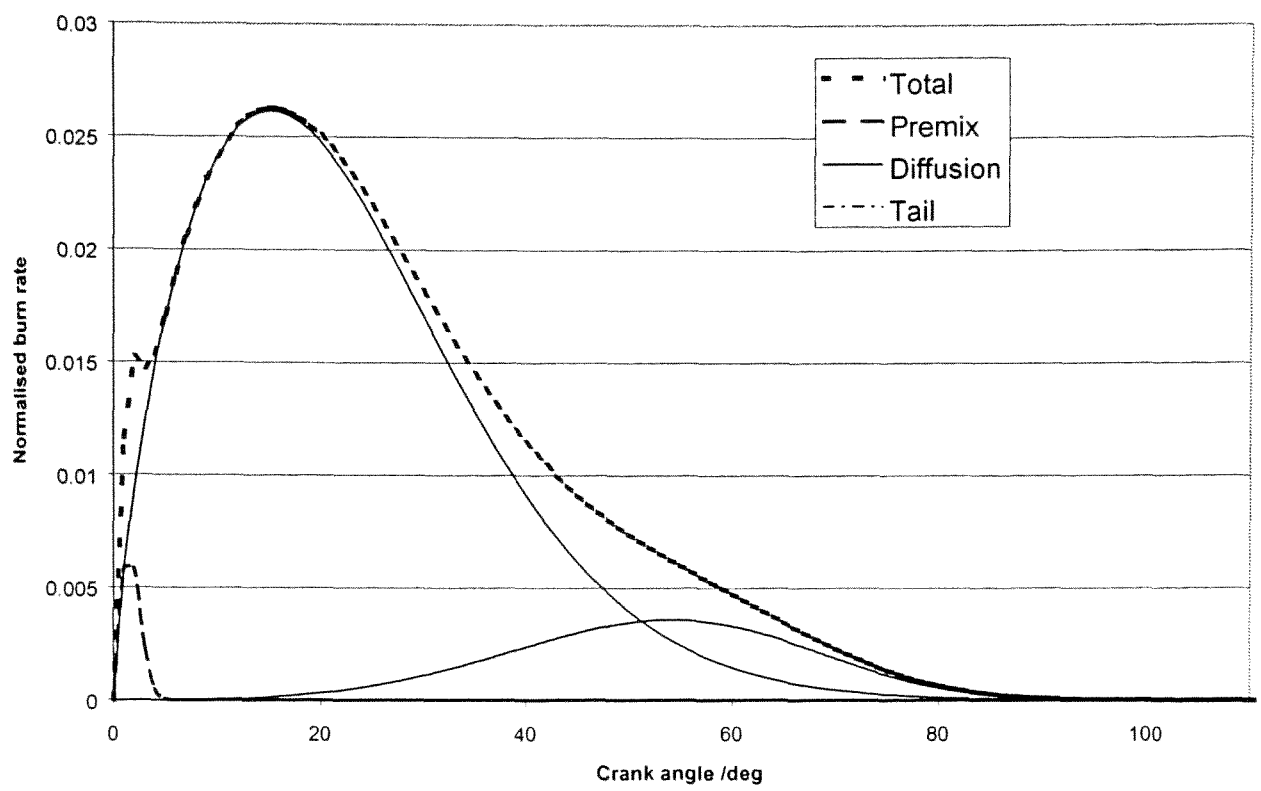


Figure 4.3.2.2.4 The 3-term Wiebe combustion correlation

This subroutine implemented the Wolfer calculation for ignition delay (from start of injection to apparent start of combustion) and generated three Wiebe functions of arbitrary starting timing, duration and fuel fraction –totalling to unity. (It did not use the more spikey form proposed by Watson for the premixed curve, with all three terms being of the form shown above for the diffusion burn.)

The starting timing, the "shape factors" which determined the shape of the individual curves, the duration and the fuel fraction were all passed to the subroutine from the main model. These factors were determined to match the normalised burn curves of the baseline data. *Figure 4.3.2.2.5* shows the effects of the shape factors on the shape of a typical single Wiebe function. *Figure 4.3.2.2.6* shows two sample burn rate curves generated by the developed code compared to the base data it was set to reproduce. These were optimised to match the baseline data as nearly as possible. As is conventional the fuel burning rates represented by the Wiebe curves were in a normalised form with the area under the total curve equal to unity. GT-Power then scaled this curve by the amount of fuel available, to generate the heat released during combustion.

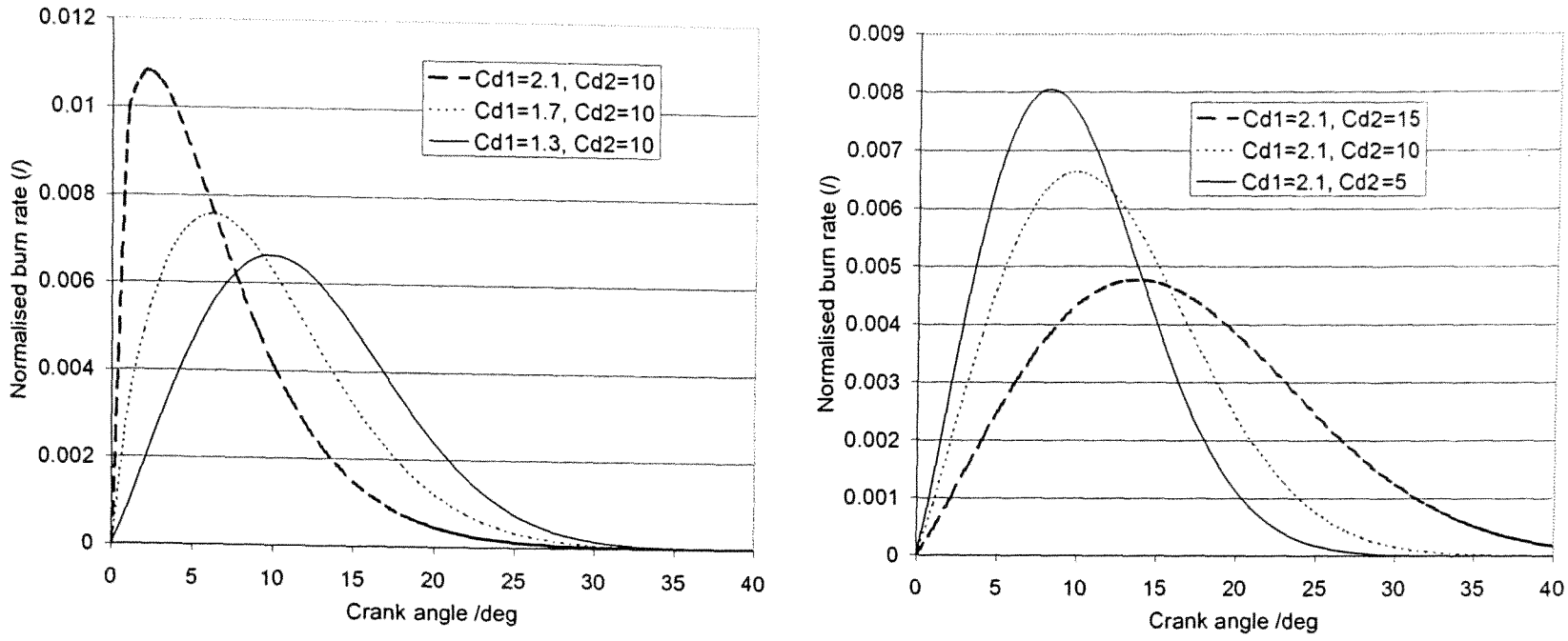


Figure 4.3.2.2.5. The effects of the shape factors on Wiebe curve shape.

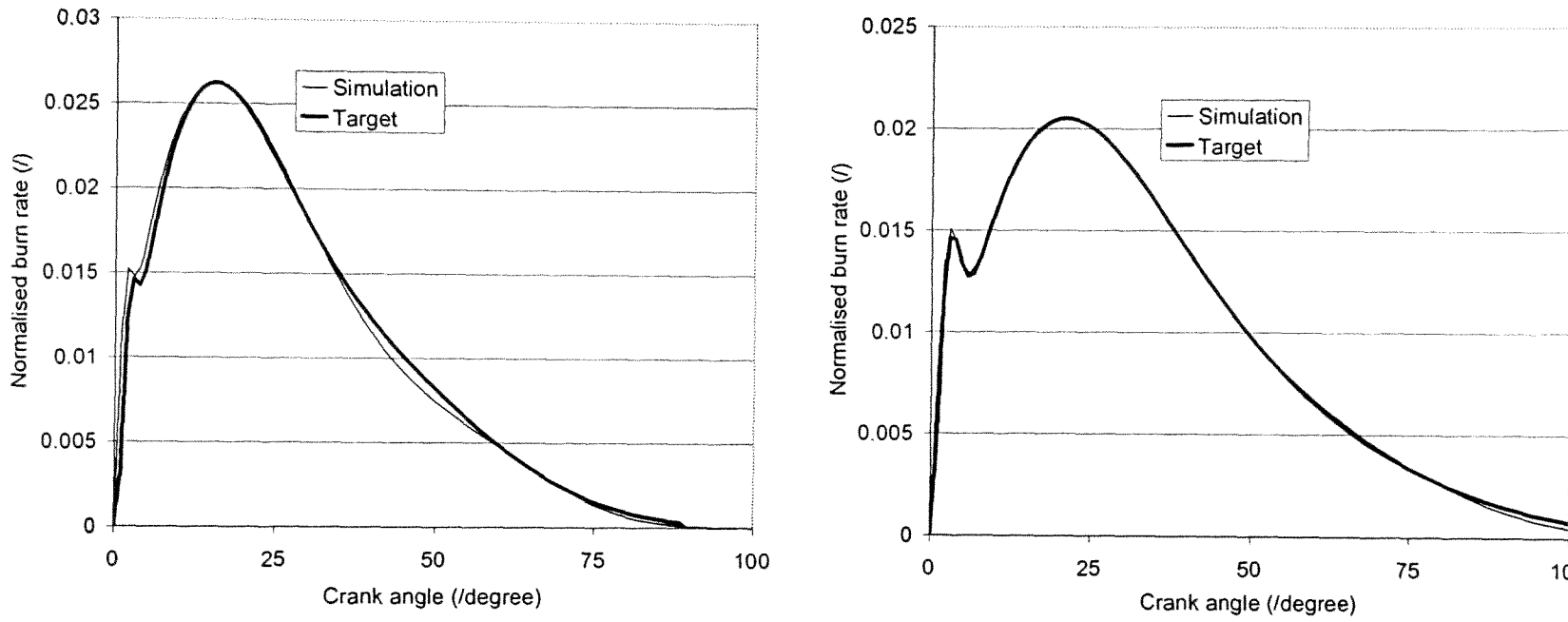


Figure 4.3.2.2.6. Comparison of baseline and burn rate curves generated by the developed code at 1000 (left) and 4500 rpm (right).

All of the above burn rate curves are shown starting at zero degrees crank angle for convenience, but as mentioned above the software calculated the ignition delay as well as the shape of the burn rate curve. *Figure 4.3.2.2.6*, above shows small discrepancies between the software output and the baseline data, in a number of areas, particularly early in the process. The development of cylinder pressure and maximum cylinder pressure are particularly sensitive to the timing of start of combustion and the rate of burning in the first few degrees. A small advance in the timing of start of combustion and small increases in the early rate of fuel burning can cause significant increases in maximum cylinder pressure, so particular attention was paid to these aspects of the burn curves used.

4.3.2.3 Turbine maps

There are two basic types of mechanism used to modulate the turbine entry passages in "variable geometry turbines," those that alter the width of the entry ring and those that alter the angle of the inlet guide vanes and the nozzle aperture. Two names are commonly in use for these types of device: Variable Nozzle Turbines (VNT) and Variable Geometry Turbines (VGT.) In the following the abbreviation "VGT" will be used to refer to the turbine used in the engine under investigation, as it is the most generic.

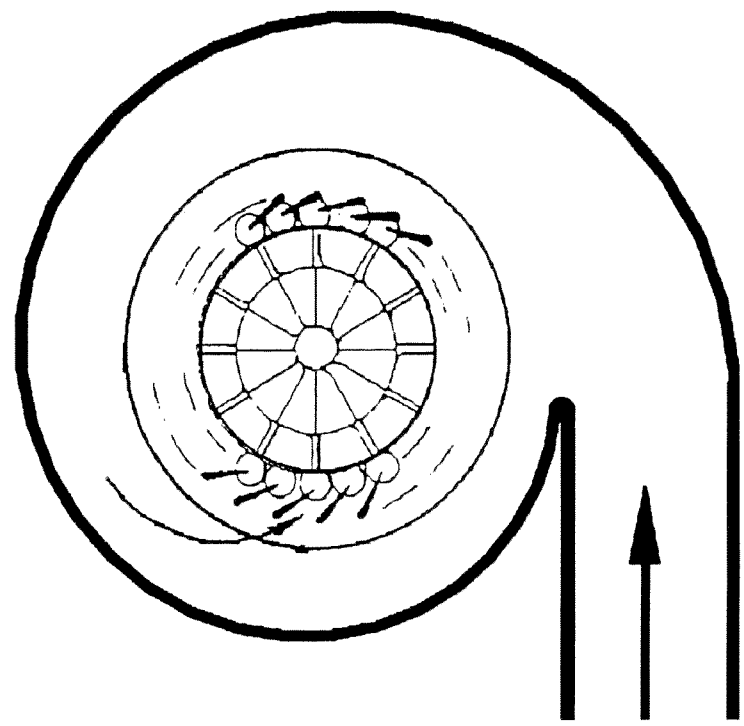


Figure 4.3.2.3.1, Variable geometry turbine schematic with inlet guide vanes closed (top) and open (bottom)

The turbine used in the target turbo-charger was of the variable inlet guide vane type. See *figure 4.3.2.3.1,* which shows the vanes closed (top) and open (bottom). The performance data provided by the manufacturer, covered four "rack" settings for the inlet guide vanes: closed, 1/3rd, 2/3rd and fully open. For these settings, efficiency and mass flow data were provided against pressure ratio for a varying number of constant operating speeds. For the closed rack setting only one speed line was available, for the 1/3rd open rack three speed lines, for the 2/3rd open and fully open rack settings six speed lines were available. These groups of speed lines represent only part of the operating characteristic of the turbine at a given setting. Operation outside of this data, at higher and lower pressure ratios and higher and lower speeds than covered by the manufacturer's data is likely to occur in normal operation. (The difficulty in measuring this type of data, particularly at the lower mass flows and speeds results in the paucity of information (Winterbone and Pearson, 2000). The situation is worsened by the fact that the data is conventionally measured on a steady flow rig whilst the flows in normal operation are highly pulsating.)

Producing maps that cover the operating conditions experienced by the turbine under normal engine operation therefore required extrapolation of the data. *Figure 4.3.2.3.2* shows the data points provided to the pre-processor (highlighted as lines with solid symbols) and the extent of the extrapolated data produced automatically by the GT-Power pre-processor for the four nozzle settings. The closed nozzle graph differentiates between the manufacturer's data (with solid data points) and two additional "synthesised" lines provided with the baseline correlation data (shown with open data points.)

In standard operation the turbine setting (control input to the VGT) was controlled by a proportional-integral-differential (PID) controller, responding to a boost pressure measurement in the intake of the engine and a target boost pressure. This controller responded by closing the nozzles to increase boost pressure and vice versa. Controller gains were optimised broadly following the recommendations of Ziegler and Nichols (1942) although a reduction in gains was needed to provide good convergence at the higher engine speeds. (The author has been informed that the engine management system uses scheduled gains to improve still further on this.)

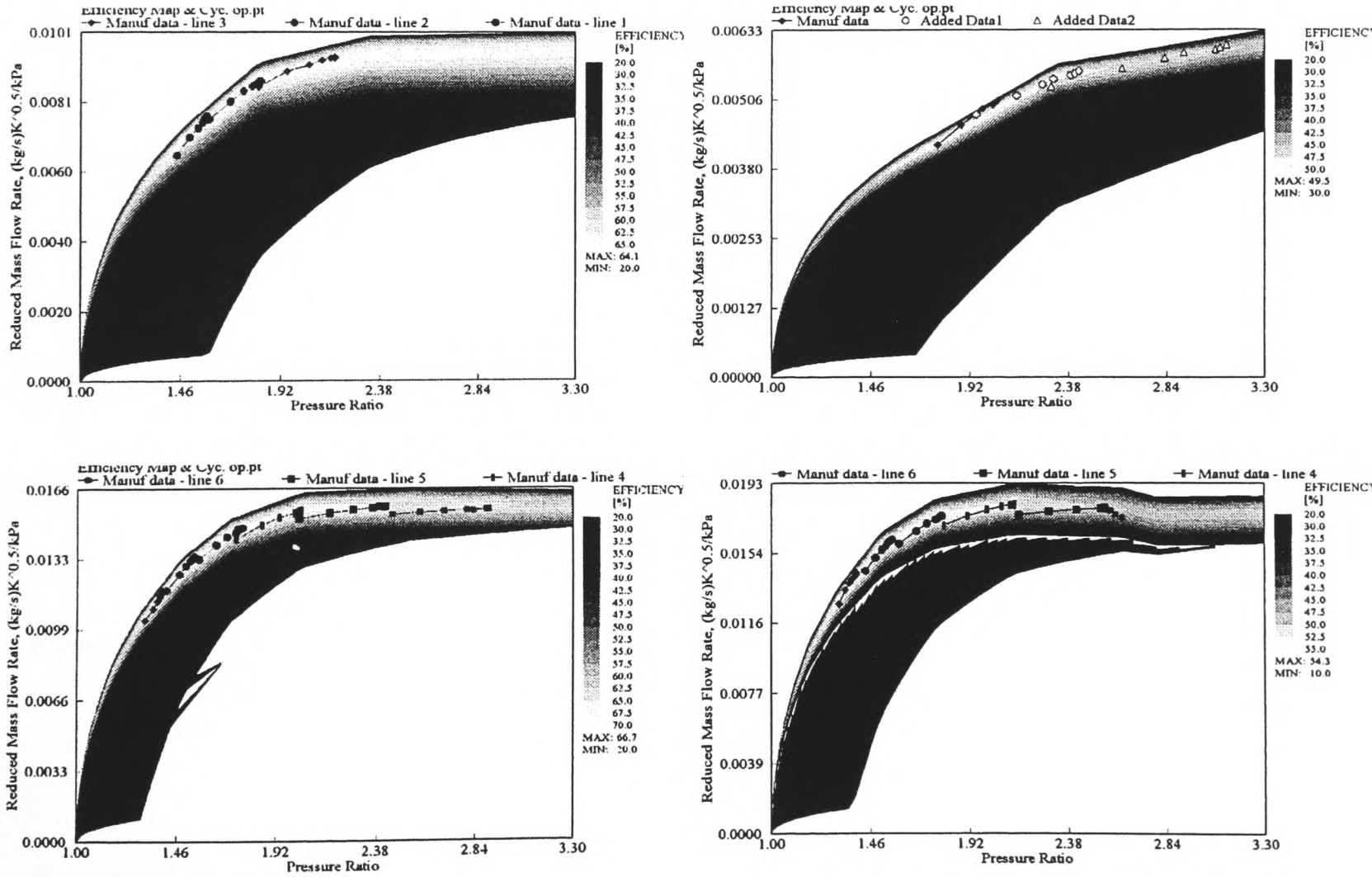


Figure 4.3.2.3.2. Efficiency versus pressure ratio and mass flow rate charts for the turbine at four nozzle settings (Increasing rack moving anti-clockwise from closed nozzles top right.) Raw and extrapolated data. (Basic data shown as solid data points, estimated data shown as open data points and extrapolated data in contours)

As might be expected the operation of the controller typically produced turbine settings that did not correspond to the turbine maps. Thus a built in function of GT-Power was called upon to interpolate between the maps either side of the VGT setting. Thus, the resultant efficiency and mass flow data output was often the result of interpolation between two extrapolated values. This highlights the importance of the means by which the maps are extrapolated.

To highlight the importance of the accuracy of the extrapolation *figure 4.3.2.3.3* shows the turbine operating locus on the efficiency and mass flow maps for the closed nozzles case at 1000 rpm full load. It also shows the raw data from which the map was produced. This figure shows that the operating point of the turbine was running along the edge of the map, away from any measured data. It should be noted that the minimum efficiency on these maps was a user input and was set at 20%.

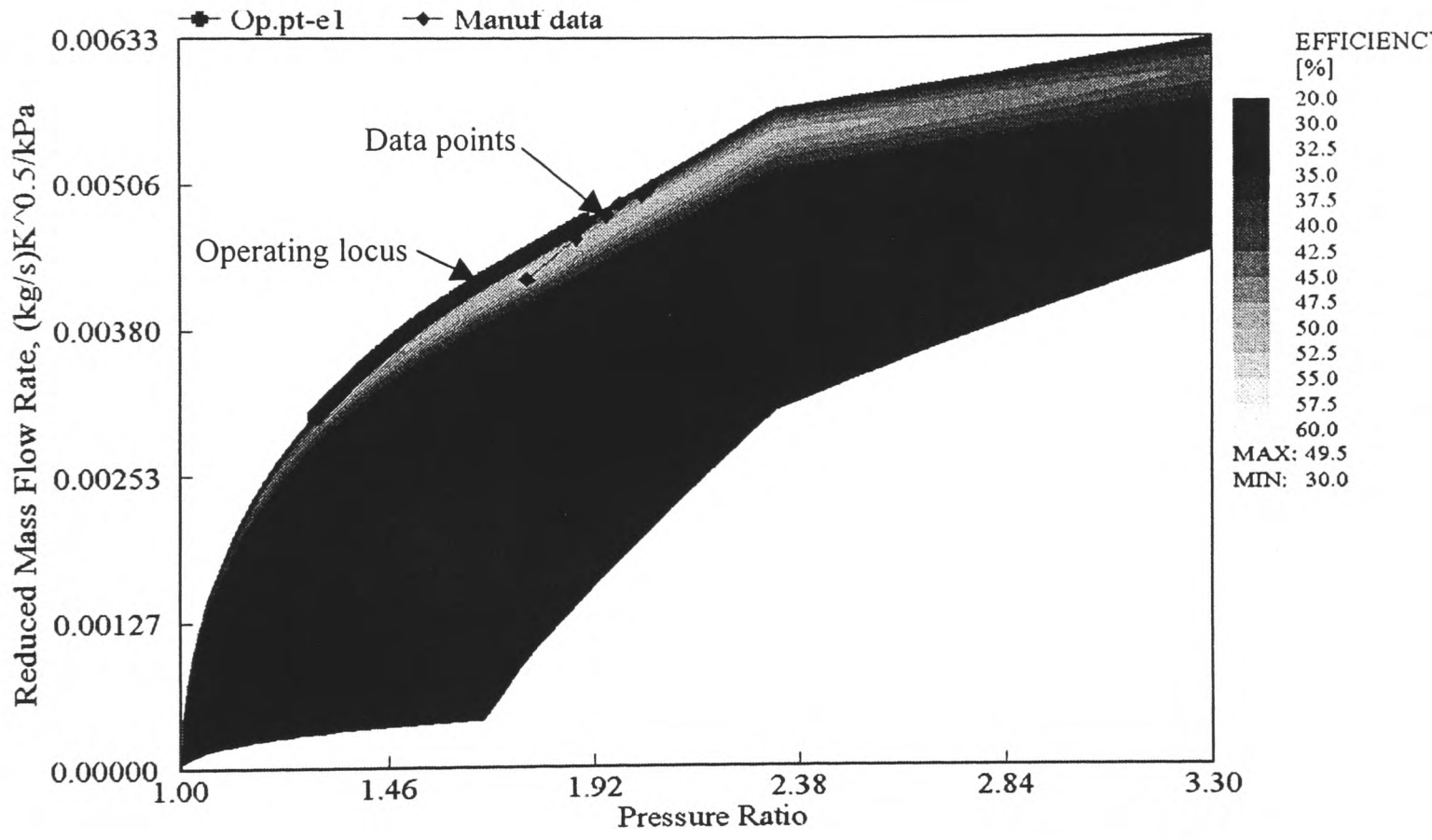


Figure 4.3.2.3.3. 1000 rpm full load, closed nozzle turbine operating locus and raw and extrapolated efficiency contours on pressure ratio and reduced mass flow ordinates.

4.3.2.4 Compressor maps

The process of producing the mass flow and efficiency maps for the compressor might appear less complex than that for the turbine because it is of fixed geometry. But, the fact that it was in use with a VGT meant that it had a larger mass flow capability than would have been possible if the system were of the waste-gate controlled fixed geometry type. The consequence of this was that the compressor could be expected to spend more time operating in the region of the stall line and it was known that correctly predicting operation in this region was difficult.

As with the turbine, discussed in the previous section, the manufacturer's measured performance data for the compressor did not cover the operating area that the engine and turbine were expected to be able to drive the compressor. *Figure4.3.2.4.1* shows the raw speed line data points and the stall line as provided by the manufacturer plotted on the maps showing the resulting efficiency contours on mass flow rate and pressure ratio axes, as produced by the GT-Power pre-processor. This figure also shows the other boundaries of the manufacturer's data.

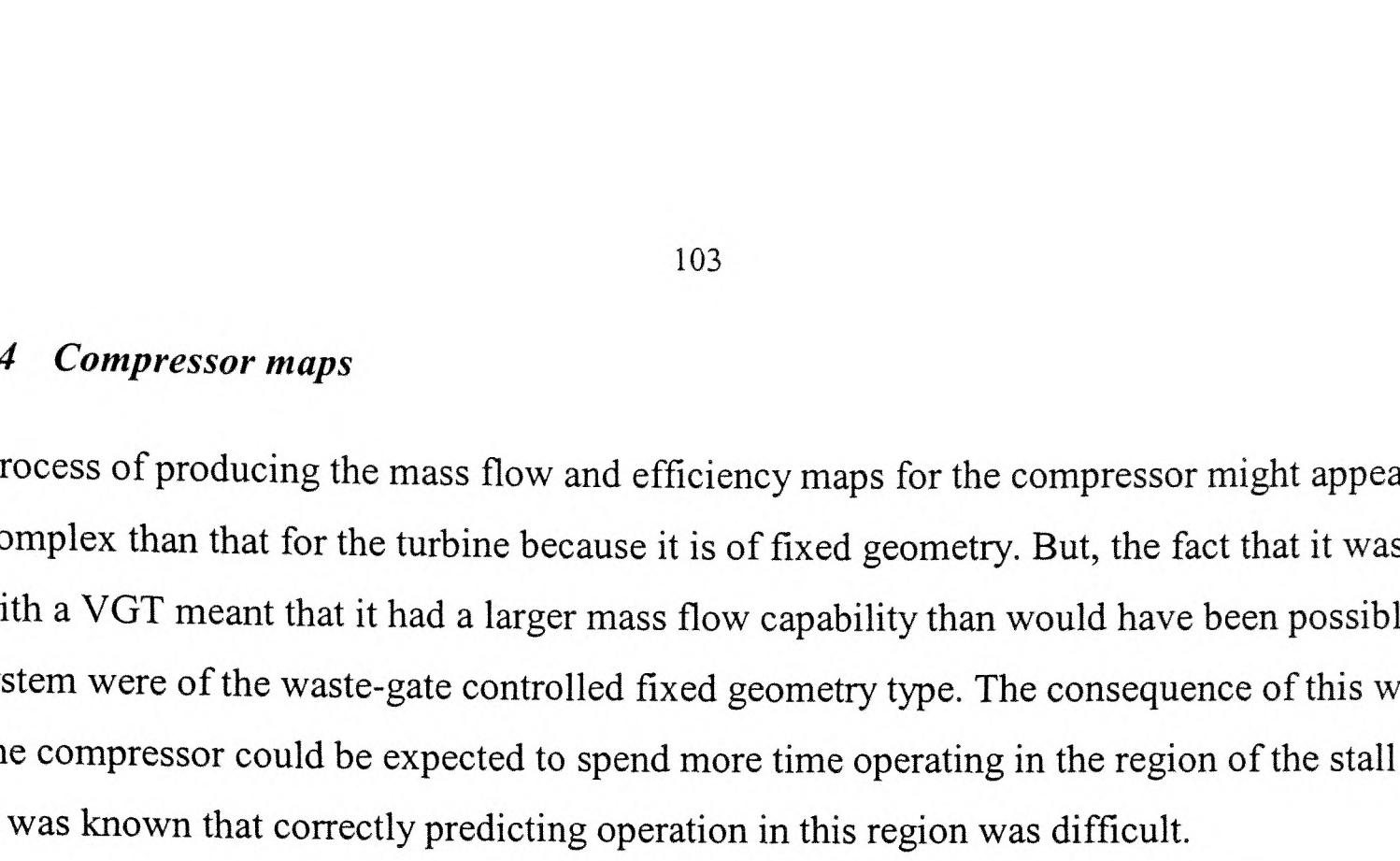


Figure 4.3.2.4.1. Raw compressor data from the manufacturer showing the boundary of the data and their stall line.

A compressor map pre-processor is provided to help with interpolation as this is error prone and time consuming to carry out manually. Its purpose is to provide additional efficiency contours within the scope of the manufacturer's data. However, as the anticipated operating envelope for the compressor was expected to be larger than that covered by the manufacturer's data there was

a requirement for manual provision of data. Typically this manual provision of data entails the extension of the map into three regions: a) higher speeds, pressure ratios and mass flow rates, b) lower speeds, pressure ratios and mass flow rates, and c) further into the region of stall. (It is worth noting that the pre-processor is only able to deal with negative gradients on the speed lines, whereas the manufacturer's data has zero and positive gradients at the lower mass flow ends of the higher speed lines. This can be seen by the separation of the edge of the efficiency contour region generated by the pre-processor and the manufacturer's stall line. See *figure 4.3.2.4.1*

The provision of higher speed and pressure ratio characteristics can be carried out by manual extrapolation of the map as the efficiency contours and speed lines are well behaved in this region. *Figure 4.3.2.4.2* shows the area of the manufacturer's data, bounded by the solid line, and the extension of the base map to higher speeds, pressure ratios and mass flows.

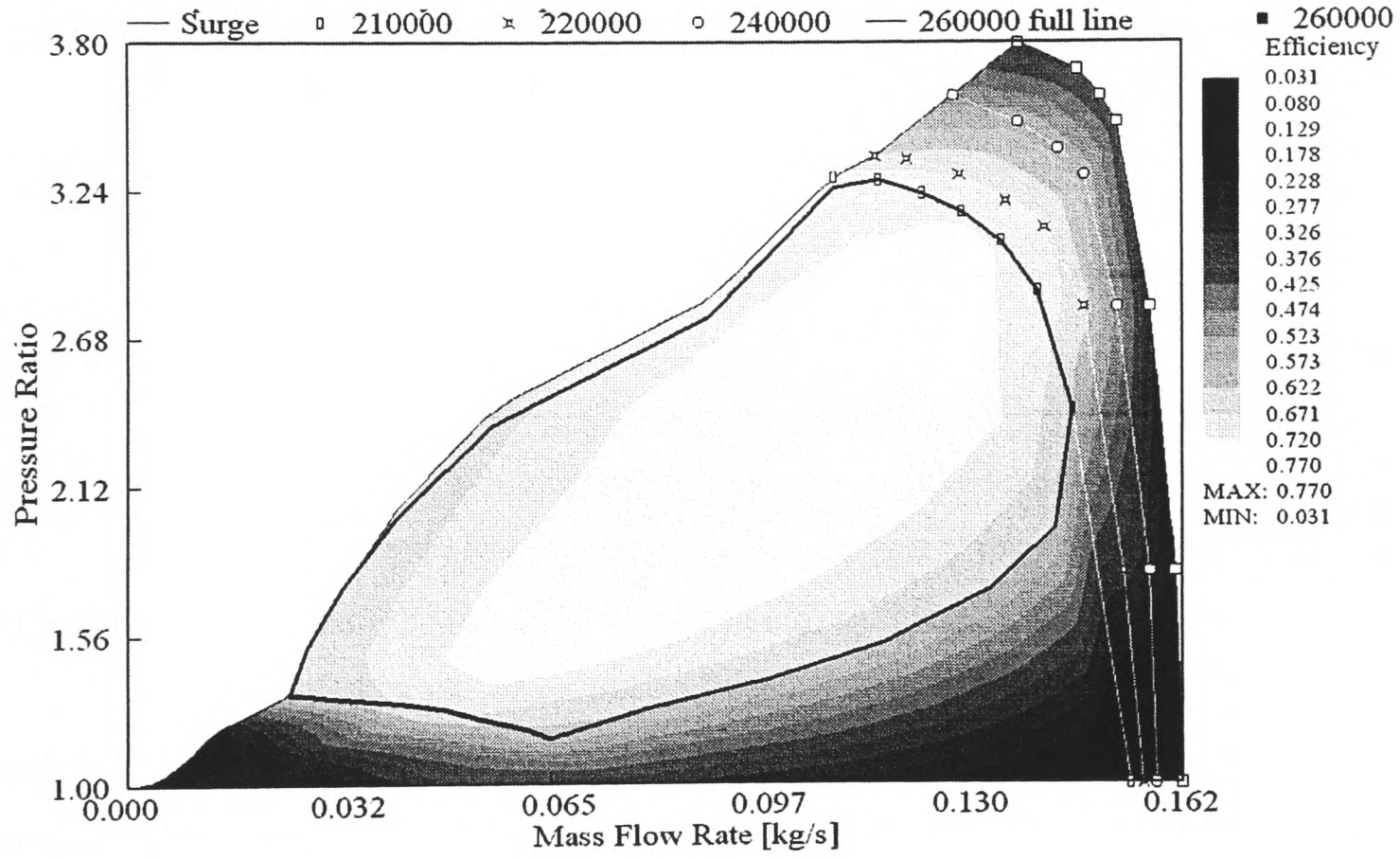


Figure 4.3.2.4.2 Extension of the compressor maps to higher speeds, pressure ratios and mass flows

The region of the map at low speeds and pressure ratios is more difficult to assess and extrapolate as there is little data to base the shape of the curves upon. However, a judgment can be made about the shape of the speed lines, when sketched on the pressure ratio – mass flow map, in relation to those available from the manufacturer and the shape of the efficiency contours can sensibly be judged from the original data. But is must be emphasised that this process is rather unscientific as no rules exist for this procedure and no accurate data is available to characterise

the operation of compressors in this region. *Figure 4.3.2.4.3* shows the maps with the extra low speed lines added to the lower left corner.

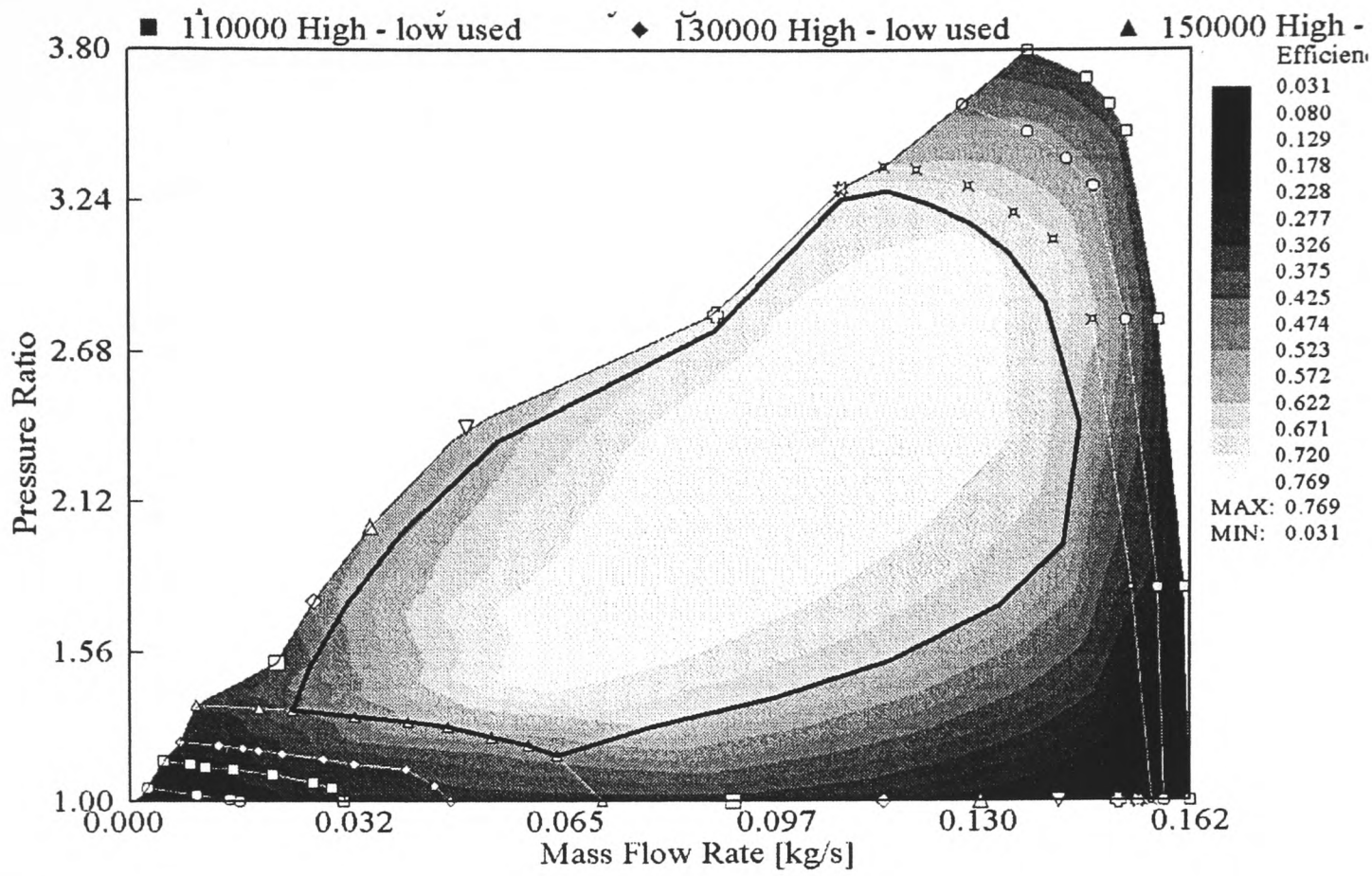


Figure 4.3.2.4.3 Additional high and low speed lines and data points extending the manufacturer's data lines added to the compressor map.

The final area, requiring extension of the maps, is to the left of the stall line. It is known that consistent operation in heavy stall can destroy the compressor. (The secondary flows set up between the blade tips cause vibrations which can lead to fatigue failure of the blades.) Care is taken in the calibration of the engine management system, so that this destructive form of stalling does not occur. However, it is known from test bed measurements on this engine at low engine speeds and high load that the compressor is operating in the stalled region for part of each engine cycle. This has been concluded for two reasons: it is audible, and the loss of efficiency associated with operation in stall leads to increases in the compressor outlet temperature above those that would normally be seen.

For simulation purposes it is important to be able to predict the compressor efficiency correctly in this region as it has a major influence on engine output. This is particularly so with this piece of work as the use of VVA allows the turbine energy supply to be increased forcing the compressor to operate at higher pressure ratios with similar mass flow rates, causing it to move further into the stall region. Benson (1982) carried out work to characterise the compressor beyond stall and into reverse flow, but the characteristics in the region between the stall line and well established

reverse flow are not defined, as even with nominally steady conditions the oscillations caused by surge make it difficult to obtain data.

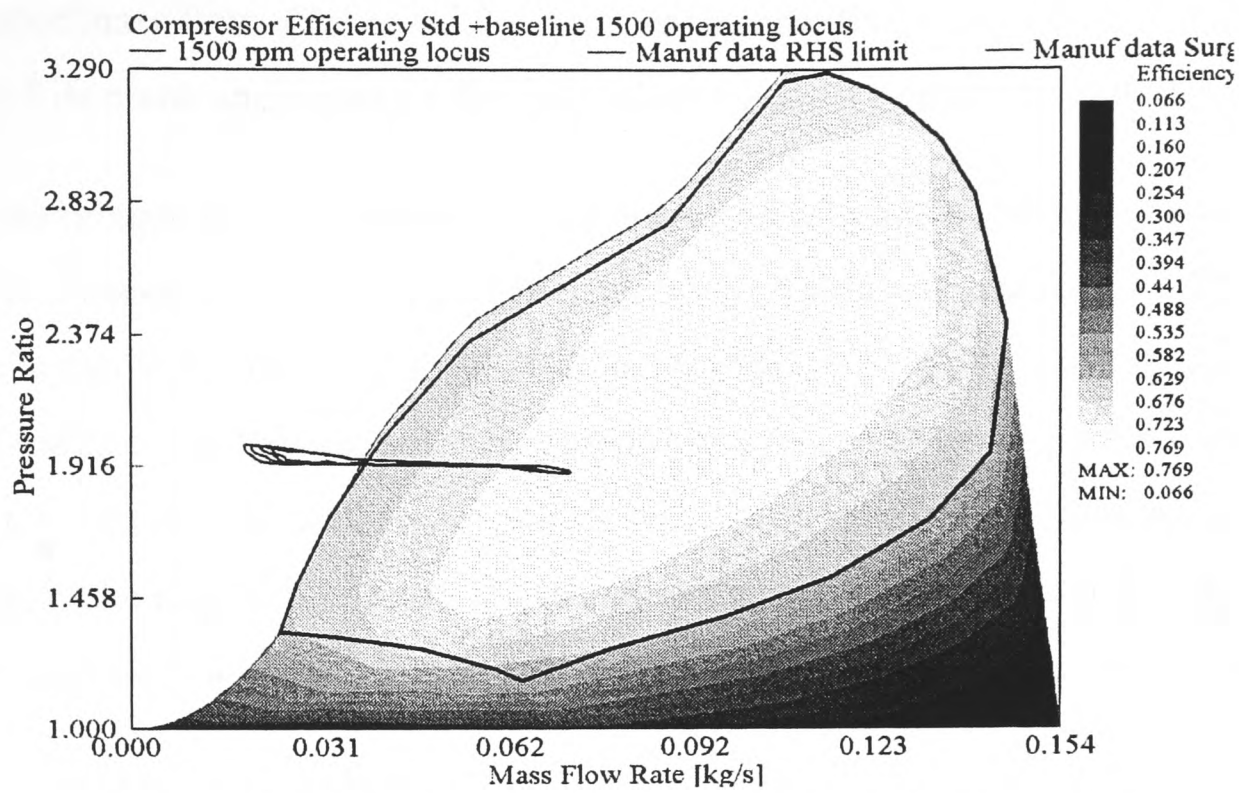


Figure 4.3.2.4.4. Operating locus of the compressor crossing the stall line

The GT-Power compressor model takes no account of stall. The stall line is arbitrarily the edge of the map produced from the data supplied to the pre-processor (not necessarily the data from the manufacturer), and if the operating point of the compressor moves off the left edge of the map the efficiency is held constant at the last value found whilst on the map, rather than continuing to fall, as might be expected following the work of Benson.

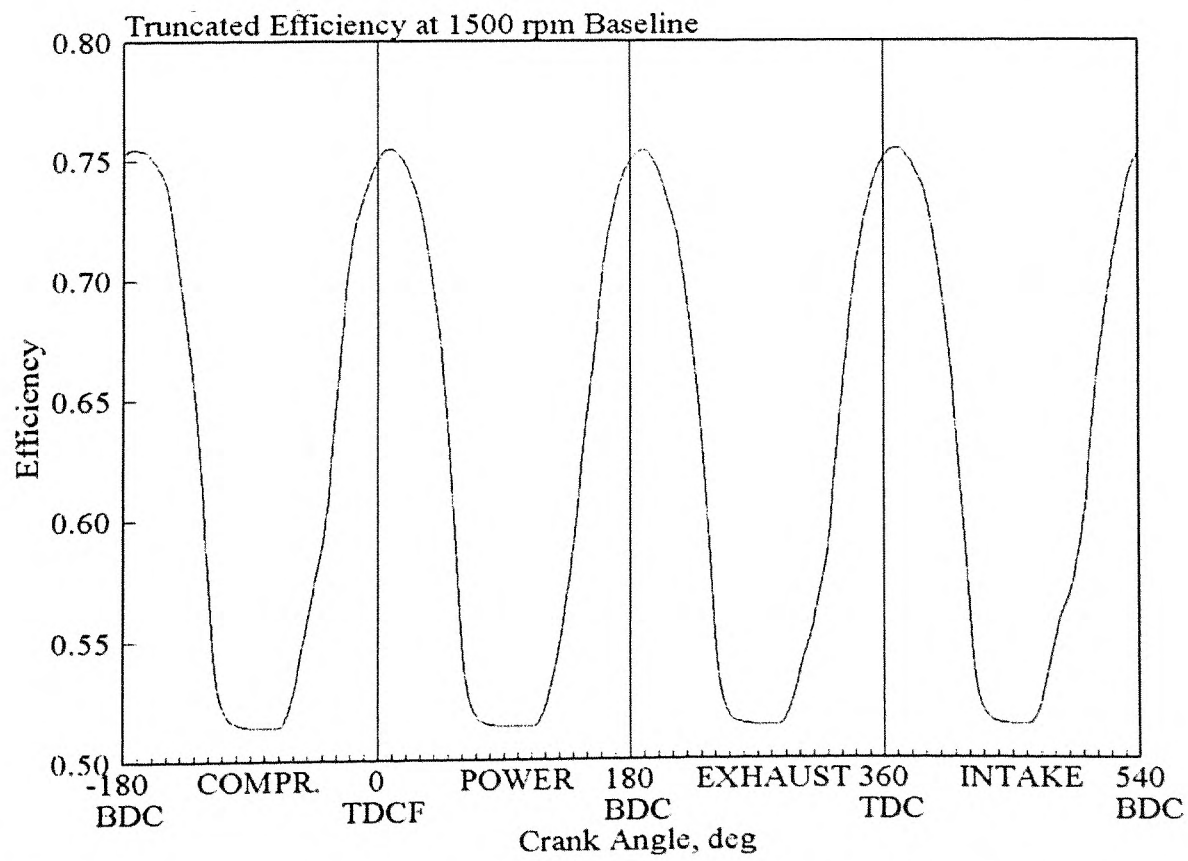


Figure 4.3.2.4.5. Truncation of the compressor efficiency characteristic caused by crossing the stall line

This truncation of the efficiency characteristic leads to a potential for over-prediction of efficiency, with consequent under-prediction of the compressor torque and over-prediction of the speed and thence mass flow. *Figure 4.3.2.4.4* shows the operating locus of the compressor and *figure 4.3.2.4.5* its crank angle based efficiency when the locus crosses the stall line.

From this it can be seen that to correctly predict engine performance with these "oversized" compressors it is necessary to extend the efficiency map into the soft stall region. This is carried out by the same method as outlined above, maintaining the geometry of, and extending the speed lines, and extending the efficiency contours, into the stall region. *Figure 4.3.2.4.6* shows the extension of the map into the stall region, which amounted to adding one more point to each of the speed lines in the region of interest. It also shows the curve fit lines as well as the actual data where the pre-processor adjusts the lines to avoid positive gradients on the higher speed lines.

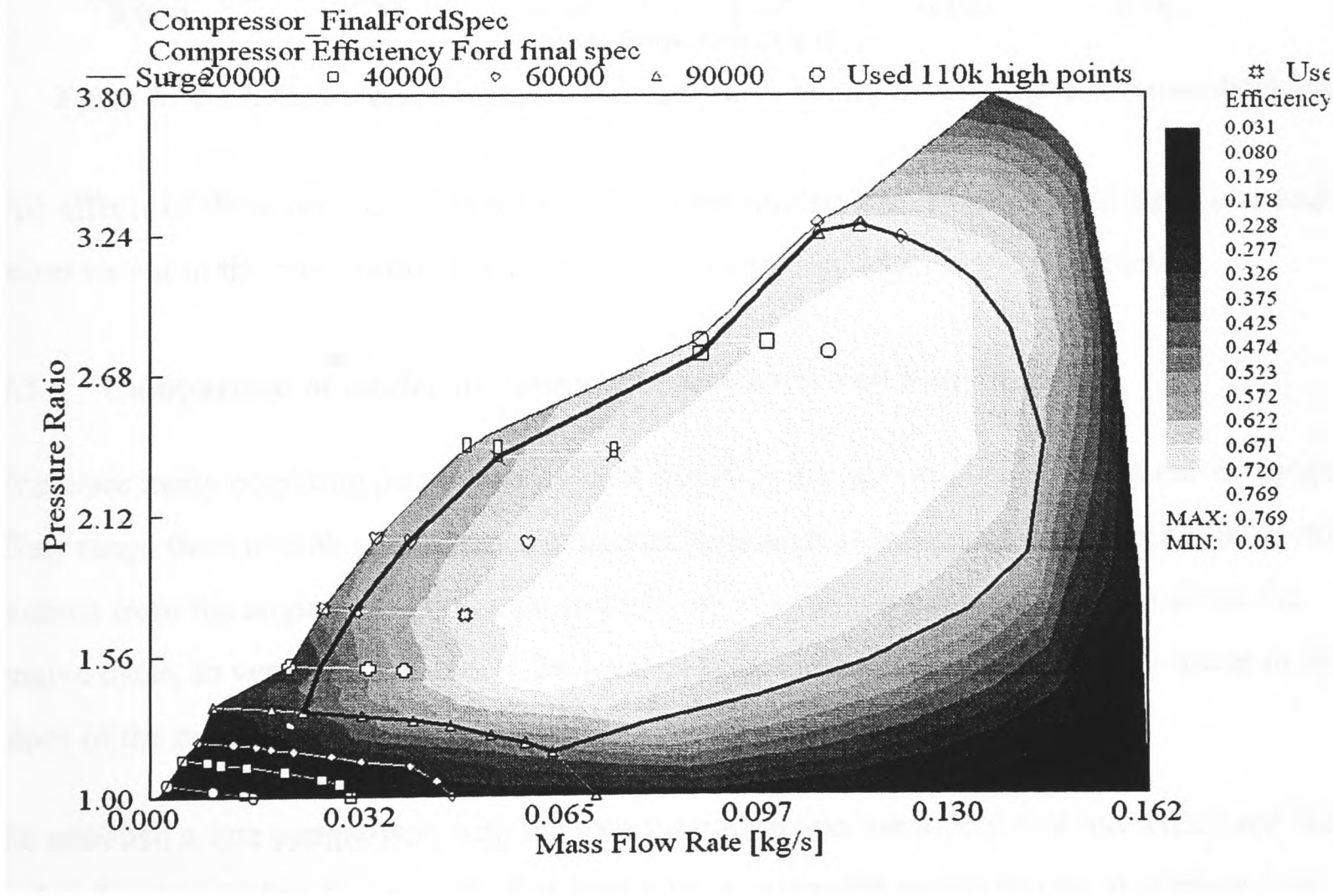


Figure 4.3.2.4.6. Compressor map extensions to lower speeds and into stall.

The resultant maps, with the three extensions discussed above can be seen in *figure 4.3.2.4.7.* This map was used throughout the subsequent evaluation of the effects of VVA on the engine's behaviour.

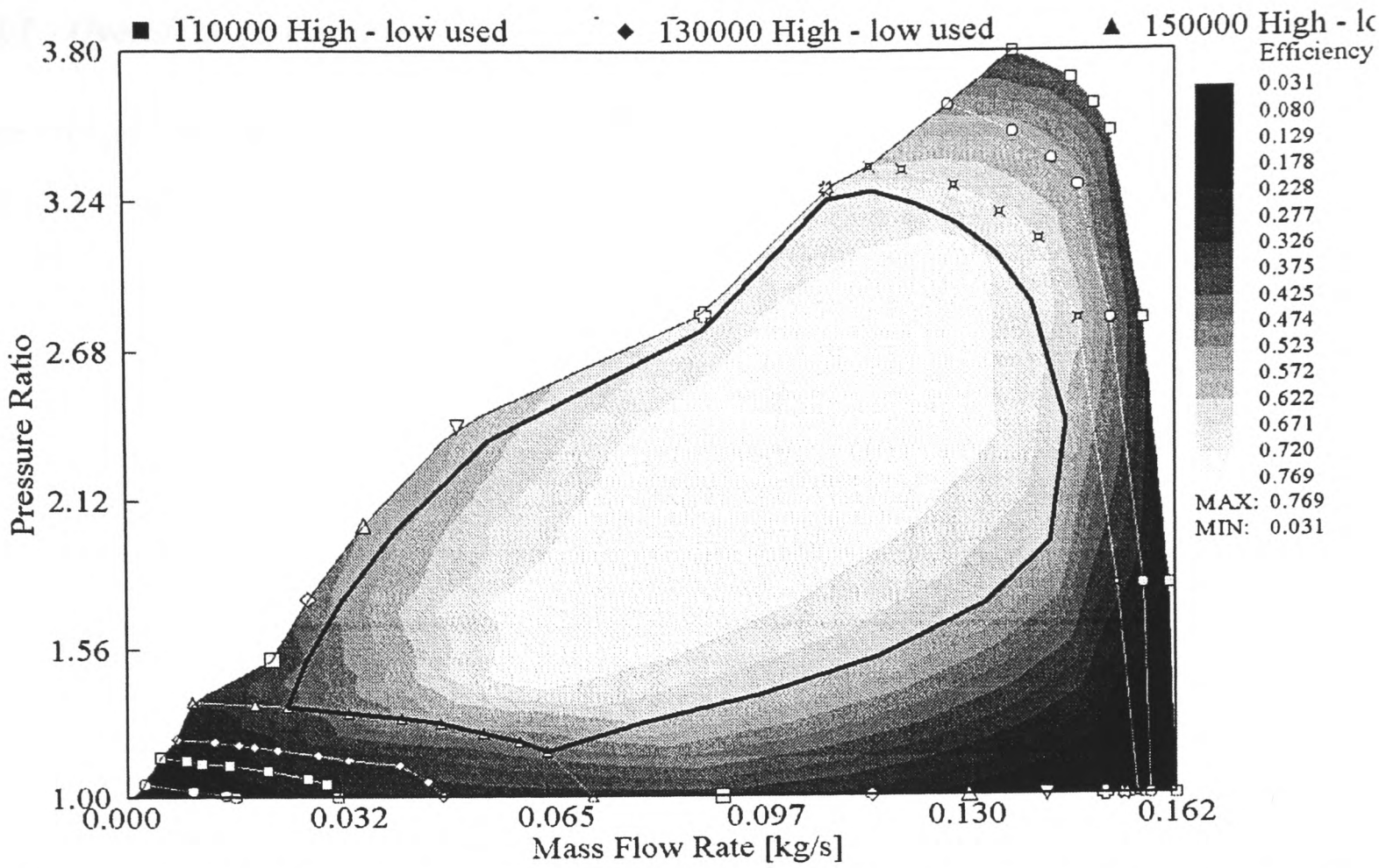


Figure 4.3.2.4.7. The completed compressor efficiency map showing the three regions of extrapolated data

The effects of these limitations in the models of the turbine and compressor in particular and to a lesser extent in the combustion correlation are discussed in detail in the next section.

4.3.3 Comparison of model operating characteristics and baseline data

There are many operating parameters against which an engine simulation model can be judged. They range from overall performance characteristics such as bmep and bsfc which are the true outputs from the engine, through imep and isfc, which provide more information about the engine cycle, to very detailed data at the level of individual pressure and velocity traces in the pipes of the manifolds.

To establish a true comparison with the data for correlation the model was run with fixed fuelling and defined boost levels across the full-load torque curve (the model sought to achieve these defined boost levels using a PID controller on the VGT nozzle actuator). The combustion characteristics were adjusted to produce, as near as possible, identical normalised burn rate curves to those of the baseline data, for each of the engine speeds.

The results of these simulation runs will now be discussed in terms of overall engine performance, combustion and heat transfer and turbine and compressor operation.

4.3.3.1 Overall engine performance

At the highest level engine performance can be assessed through imep and bmep, isfc and bsfc, pmep and fmep and air flow through the engine.

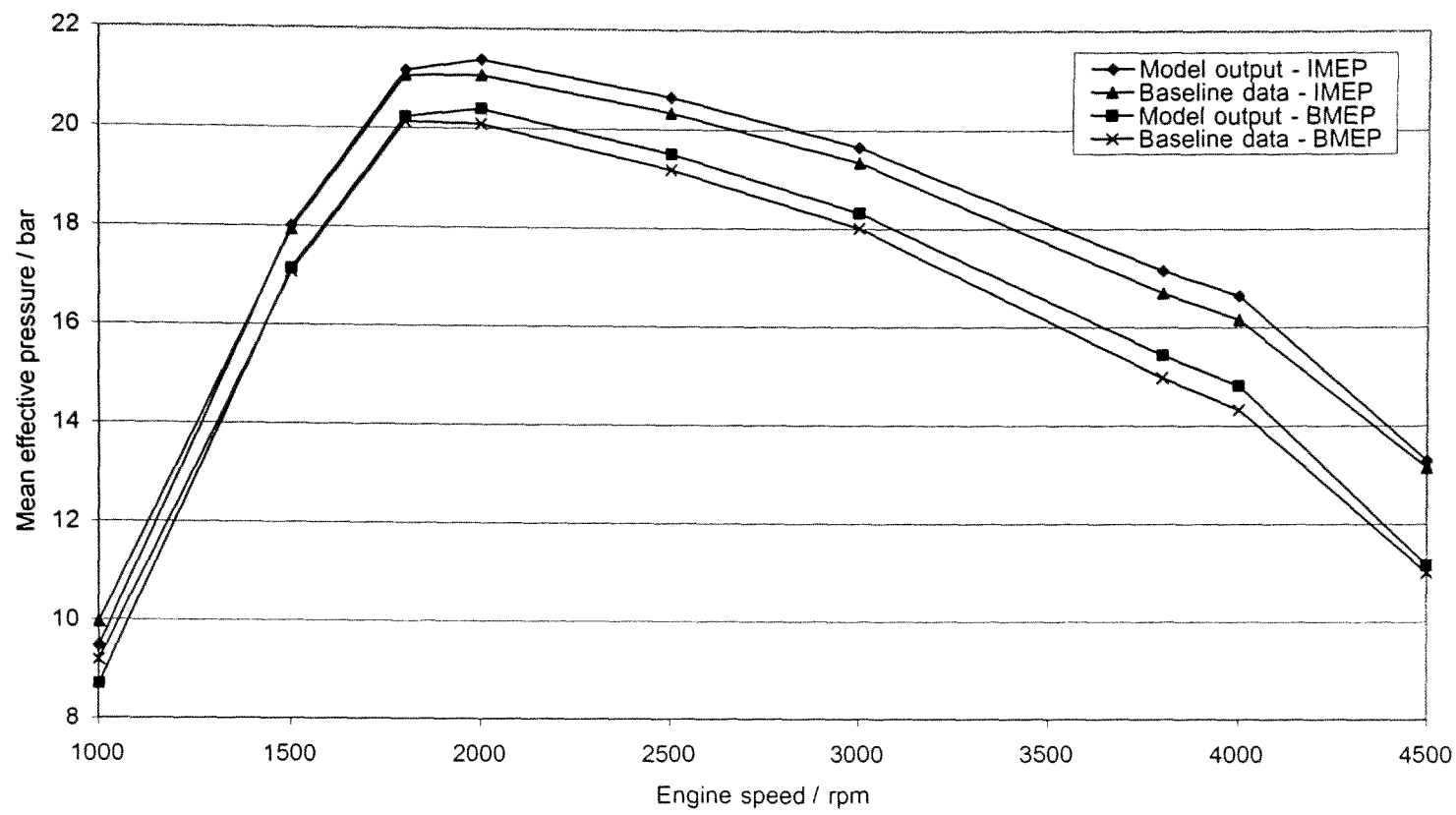


Figure 4.3.3.1.1. Comparison of the model imep and bmep results with the baseline data.

Figure 4.3.3.1.1 shows imep and bmep plots for the full load line of the model and baseline data. It can be seen that the correspondence is good, with the maximum error in imep amounting to 4.8% at 1000 rpm, but with the average error magnitude being 1.9% over the speed range.

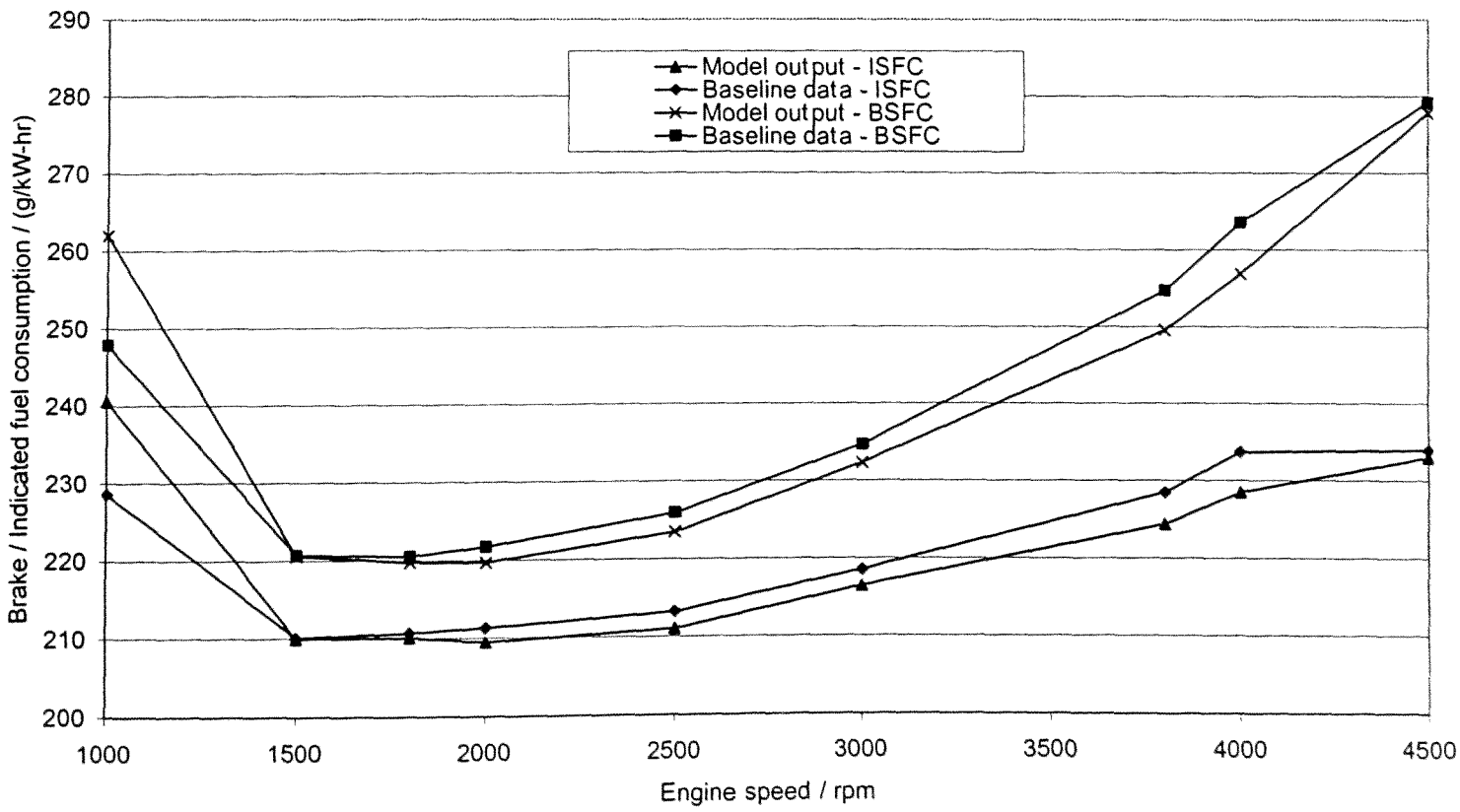


Figure 4.3.3.1.2. Comparison of the isfc and bsfc characteristics of the model and baseline data.

Figure 4.3.3.1.2 shows the isfc and bsfc plots for the full load line of the model and the baseline data. Again the correspondence is good, with the maximum error in isfc amounting to 4.5% at 1000 rpm, but with the average error being -0.76% over the speed range.

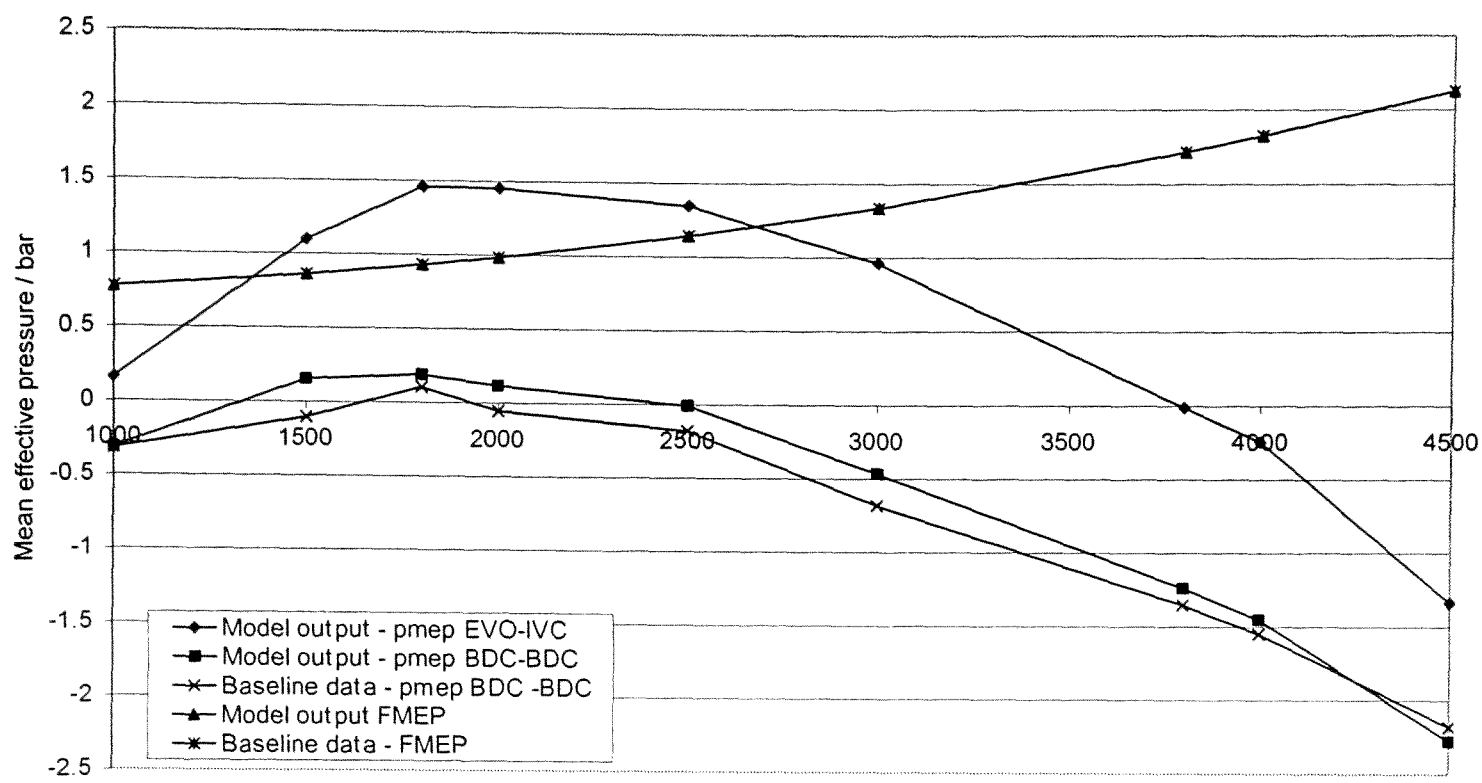


Figure4.3.3.1.3.Comparison of pmep and fmep characteristics of the model and the baseline data. Please note the two fmep curves are coincident as the same model was used in both cases.

When comparing pmep figures little is gained from a direct calculation of error as the percentage differences can be large when only small variation in the numbers exist, and typically with this type of engine the pumping losses are small. The definition of pmep also needs to be considered: for convenience many simulation codes calculate pmep from bdc-exhaust to bdc-intake, rather than from EVO to IVC. This distorts the information, particularly as positive work is done on the piston, above bdc, even after the exhaust valve is open, and significant negative pumping work is typically done between bdc-intake and IVC. In this section the definition of pmep from bdc-exhaust to bdc-intake is used as this is the only form in which the baseline data is available. *Figure 4.3.3.1.3* shows the pmep and fmep characteristics of the model and the baseline data and again it demonstrates that the magnitude and form of the characteristics are in good agreement. To highlight the differences between the bdc to bdc and EVO to IVC pumping work, the EVO to IVC values from the model are also plotted in *figure 4.3.3.1.3*.

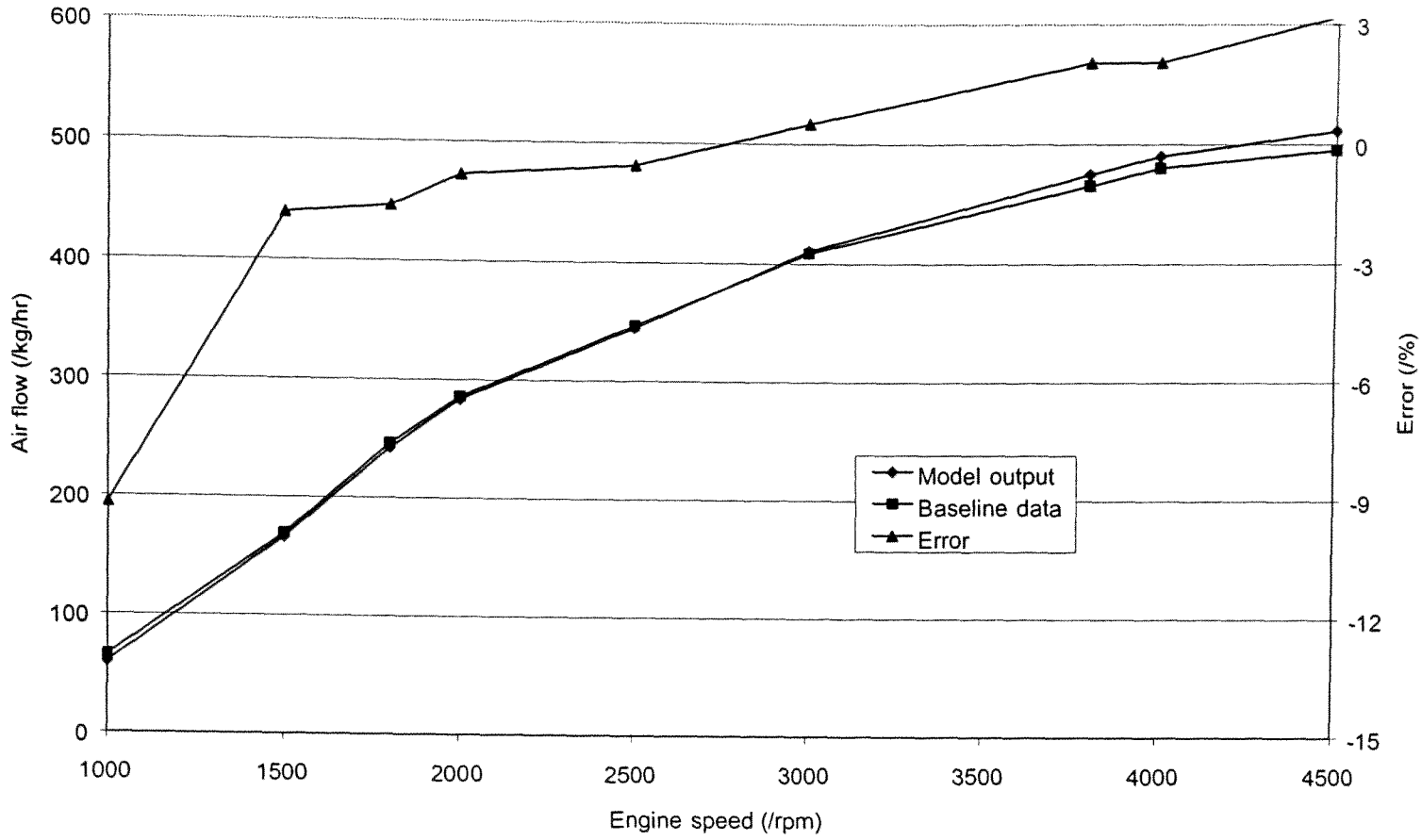


Figure 4.3.3.1.4 Comparison of the air mass flow rates for the model and the baseline.

As was mentioned earlier the model correlation to baseline data was carried out with fixed fuelling for each operating speed. Thus differences in air flow also resulted in changes of air fuel ratio, with corresponding changes in gas temperatures in the cylinders and in the exhaust system particularly. They may also have resulted in smaller discrepancies in temperature in the intercooler and other intake piping. *Figure 4.3.3.1.4* compares the air mass flow rates for the model and the baseline. It can be seen that in general the correspondence between the model and baseline was good, with the error typically less than 3%, except at 1000 rpm where it was 9%. For the operating points from 1000 rpm to 2500 rpm the air flow was under-predicted, but, from 3000 rpm to 4500 rpm the air flow was over predicted. *Figure 4.3.3.1.5* shows the effect these differences had on air-fuel-ratio.

Since the comparison with the baseline was carried out with fixed fuelling and prescribed boost levels at all speeds, if the boost target was achieved, then discrepancies in air flow were caused by differences in volumetric efficiency. *Figure 4.3.3.1.6* compares the volumetric efficiencies of the model and baseline. It can be seen that the model under-predicted the volumetric efficiency referred to manifold conditions up to and including 3000 rpm and over-predicted it above 3000 rpm. It was not possible to find a clear explanation of these differences, as not all data was available for comparison. However, it is thought that the most likely causes of these discrepancies were differences in heat transfer in the intake pipes and intercooler, and slight

differences in cylinder pressure at the beginning of the intake stroke causing greater residual fraction.

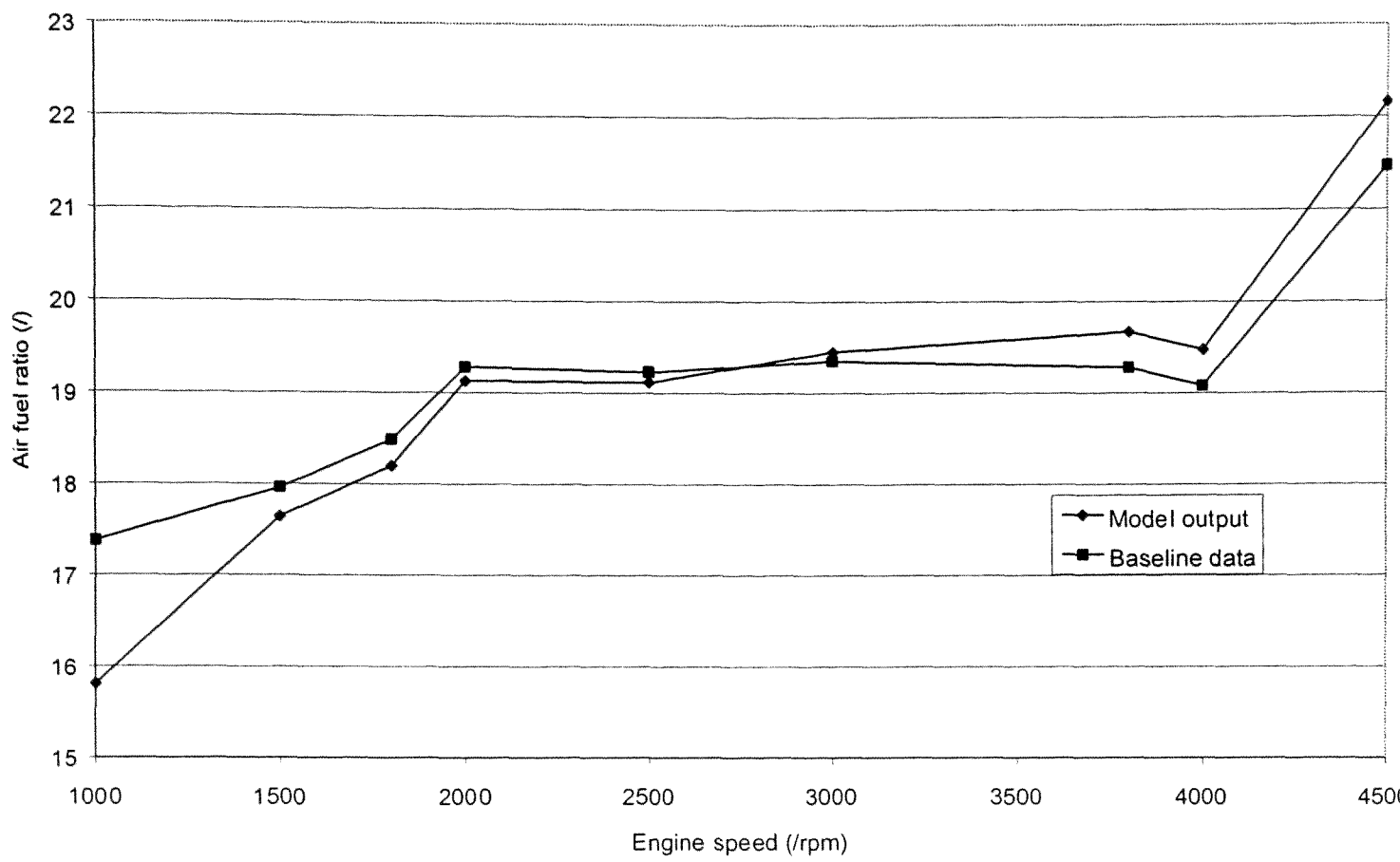


Figure 4.3.3.1.5 The effect of air flow differences on air-fuel-ratio. (Fixed fuelling.)

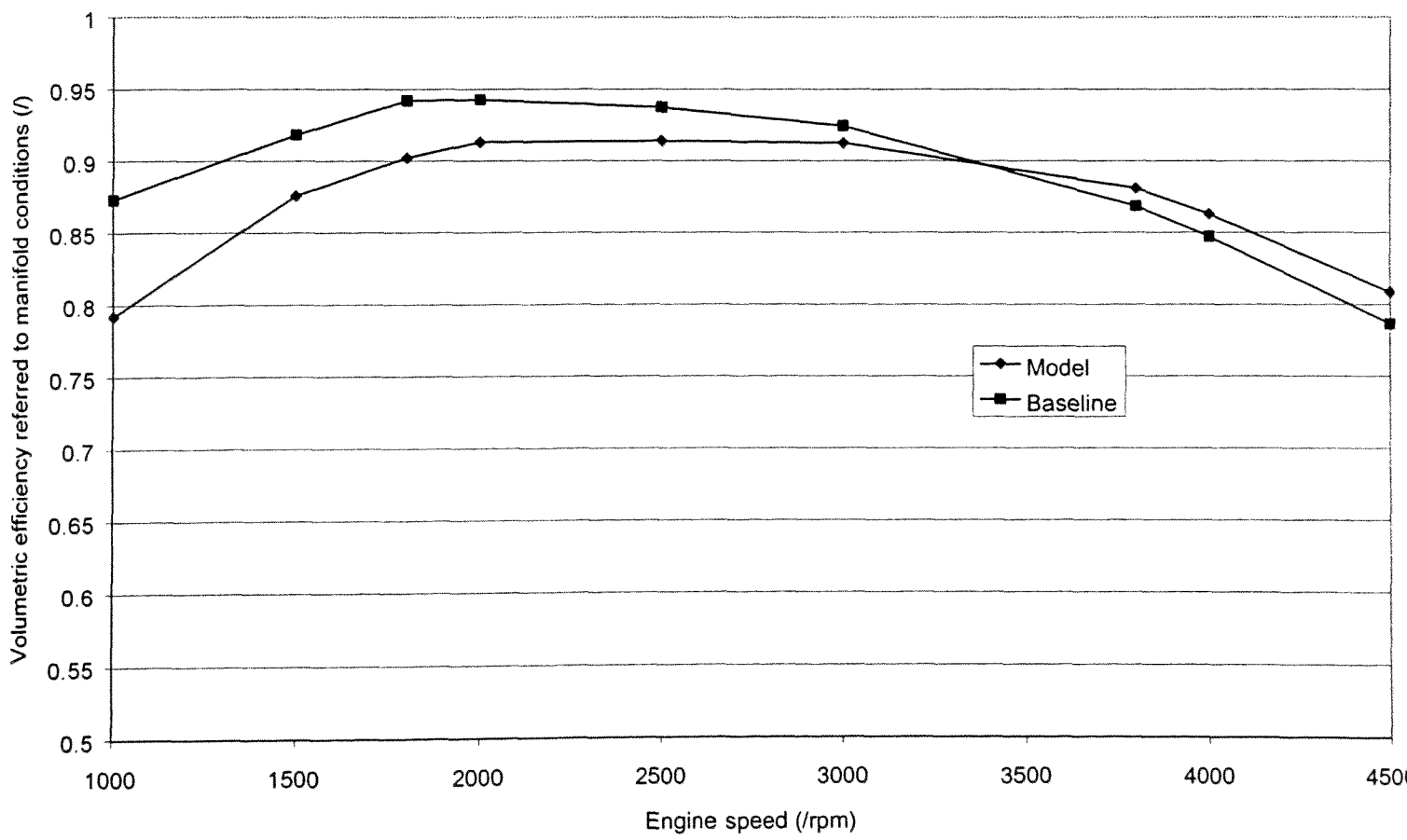


Figure 4.3.3.1.6 Volumetric efficiency referred to manifold conditions

4.3.3.2 Combustion and cylinder heat transfer

4.3.3.2.1 Combustion

As already mentioned the combustion correlation used consisted of an ignition delay based on the work of Wolfer (1938) and a three part Wiebe function extended from the work of Watson *et al* (1980) to generate the normalised burn rate curve. The individual burn rate curves were matched to the baseline data as closely as possible for each operating speed. *Figure 4.3.3.2.1.1* shows the quality of curve fit achieved at four speeds.

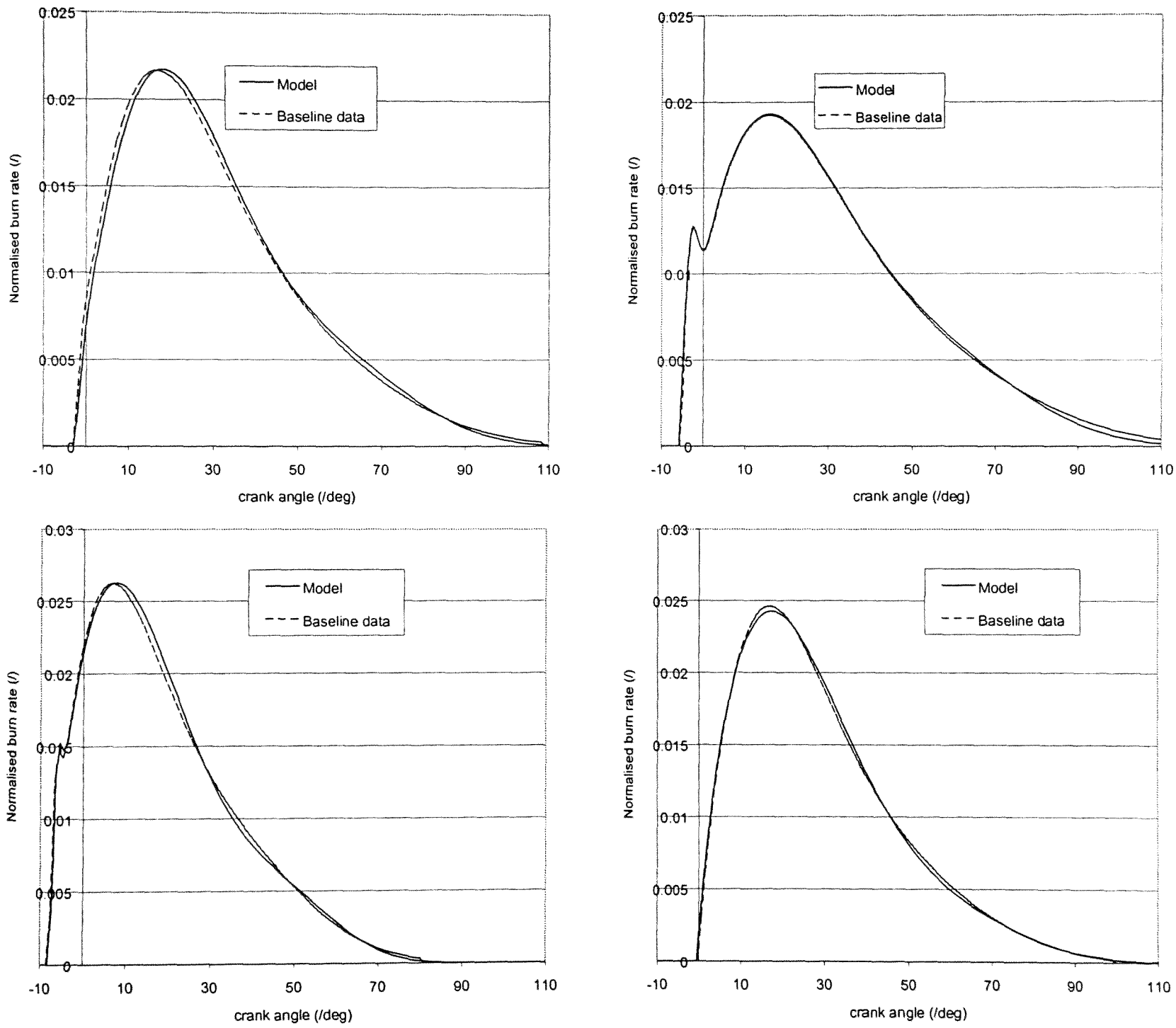


Figure 4.3.3.2.1.1. Correlation of normalised burn rate curves at 1000 (top left), 2000 rpm (top right), 3000 rpm (bottom left) and 4000 rpm (bottom right).

The importance of the correct shape and timing of the combustion curves goes beyond simply predicting correct imep. For most modern light duty diesel engines the maximum cylinder

pressure, P_{max}, that can be permitted is determined by the structural strength of the cylinder head and its fixings. Thus the timing of the start of combustion and the rate of change of burn rate in the early stages of combustion become important if the structural limits of the engine are not to be exceeded. The engine being simulated in this exercise had a nominal P_{max} limit of 150 bar. To allow for production variation in compression ratio between the cylinders, P_{max} was limited in practice to approximately 144 bar. (0.1mm variation in piston bump height changes the compression ratio by $\approx$ 2% for this engine)

Thus two other important features for the assessment of the quality of a combustion model are P_{max} and the timing of P_{max}. *Figure 4.3.3.2.1.2* shows the comparison between the model and baseline data for these variables. The agreement between the model and baseline for P_{max} is good, with the maximum errors occurring at the extremes of the speed range. The timing of P_{max} has a maximum error of one crank degree, which is of the order of the crank angle steps used by the simulation code. As a consequence there is a potential error in start of combustion of up to a simulation crank angle step. The crank angle step over the speed range investigated was between 0.7 and 1.2 crank degrees.

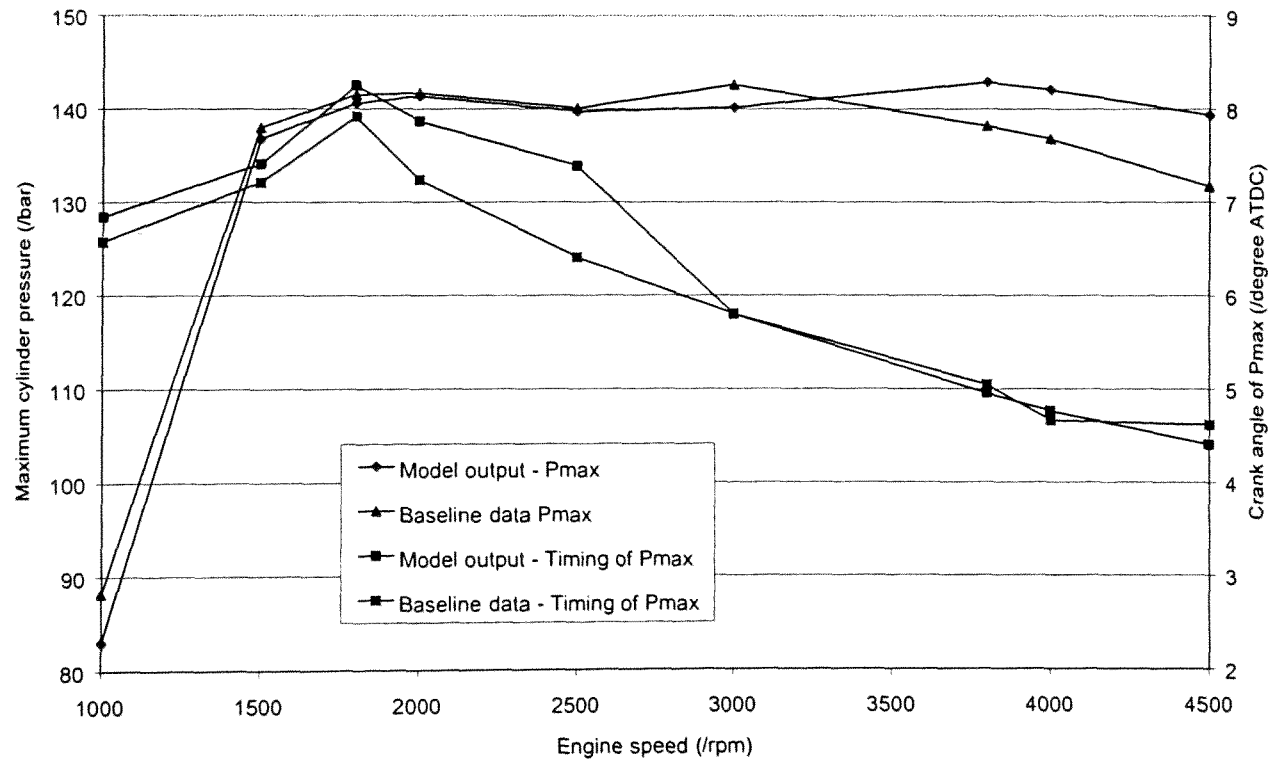


Figure 4.3.3.2.1.2. Maximum cylinder pressure and its timing.

In order to assess the impact of the effects of discrete crank steps and accuracy of ignition delay calculation, a limited sensitivity analysis was carried out to investigate the effect of the start of combustion on P_{max} and its timing.

Figure 4.3.3.2.1.3 shows the effect of artificially varying the start of combustion on P_{max} and its timing for the 2000 rpm operating point (Fuel burning rate as per *Figure 4.3.3.2.1.1*). As might be expected P_{max} increased with earlier start of combustion, and the timing of P_{max} advanced in line with the earlier combustion. The magnitude of these variations showed that the potential timing errors associated with the implementation of the ignition delay or its calculation did not cause any unacceptable variation in either P_{max} or its timing, with P_{max} remaining below the structural limitation of 150 bar, even when the burn curve was advanced by 1.5 crank degrees. Thus it can be seen that the model was predicting the correct trends for P_{max} and its timing and the results were also acceptable quantitatively.

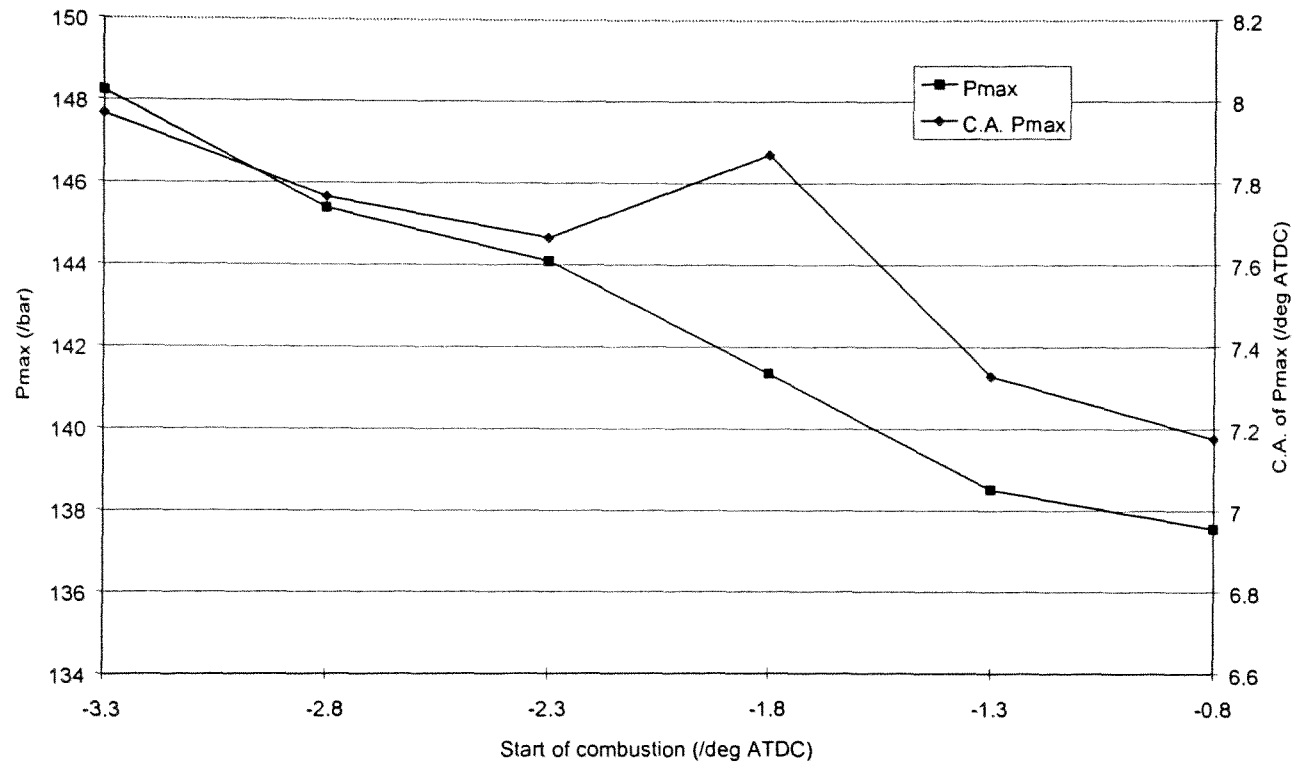


Figure 4.3.3.2.1.3. Variation of pmax and its timing as a function of start of combustion.

4.3.3.2.2 Cylinder heat transfer

The correlation used for this calculation was one based on Woschni, but GT-Power implements a modification to the coefficients during the valve open periods, particularly when there are large flows *into* the cylinder through either intake or exhaust valve. *Figure 4.3.3.2.2.1*, below, shows the total heat transfer to the cylinders, as a percentage of available fuel energy, over the speed range investigated.

The maximum differences occur at 1000 rpm and 1800 rpm, where the discrepancies are close to 8% of the total heat lost. These amount to approximately 2.46% and 1.3% respectively of the total fuel energy available at these speeds.

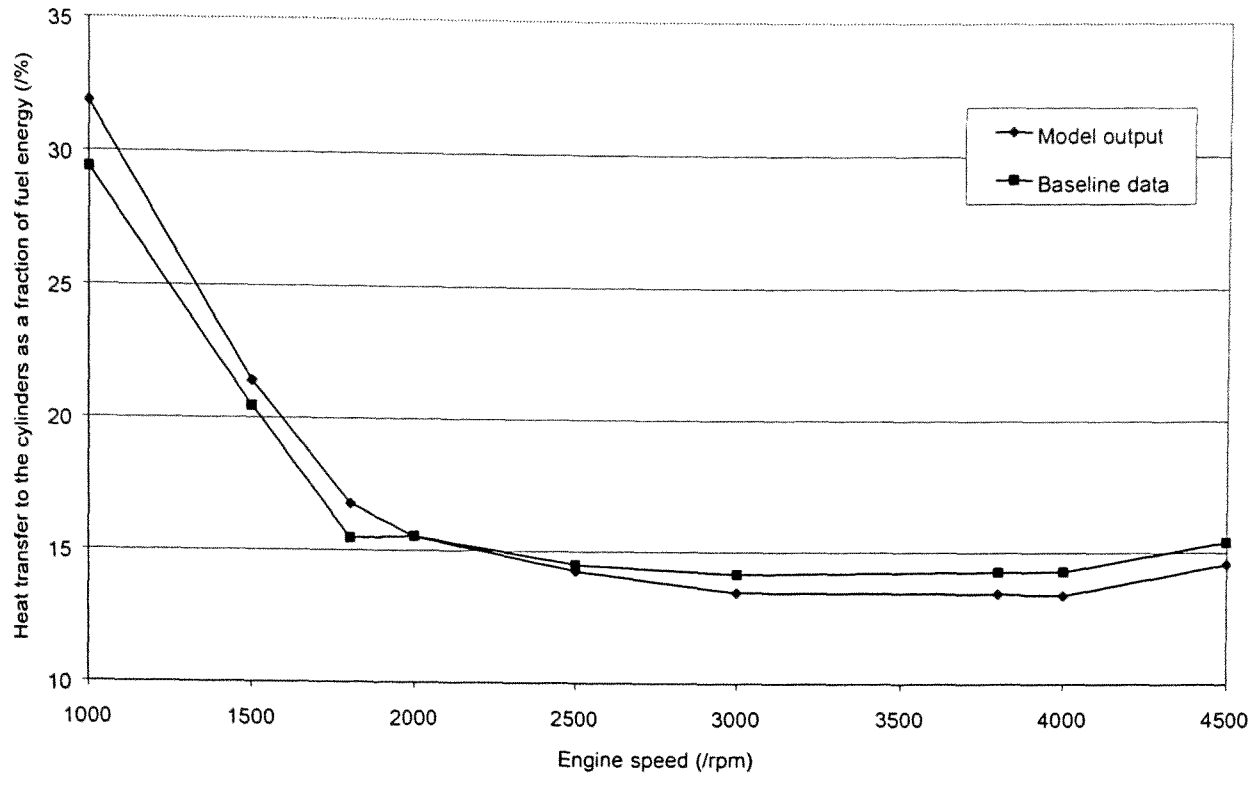


Figure 4.3.3.2.2.1. Cylinder heat transfer as a percentage of fuel energy at full load.

Thus, it can be seen from these data that the cylinder heat transfer trend is correctly predicted and whilst there are errors of up to 8% in the comparable values their effect on predicted engine output is small.

4.3.3.3 The turbo-charger

It has been demonstrated that the overall performance of the model matched the baseline well. Further, it has been demonstrated that the combustion and cylinder heat transfer results from the model correlate well with the baseline data. Despite this, the operation of the turbo-charger should also be closely inspected, especially since the modelling of the turbine and compressor performance are somewhat empirical and potentially difficult, as mentioned in sections 4.3.2.3 and 4.3.2.4. In the following it should be remembered that the turbine setting was controlled by a PID controller with a prescribed boost level target for each engine speed.

4.3.3.3.1 Turbine operation

It has already been shown that the model under-predicted air mass flow at the operating points up to and including 2500 rpm and over-predicted it at those above that. But since the boost pressure was prescribed a lower mass flow could be expected to require less turbine power and potentially a more open nozzle rack setting. *Figure 4.3.3.3.1.1* Shows that at all speeds apart from 1000 rpm the target boost level was achieved. *Figure 4.3.3.3.1.2* shows a comparison between the turbine power outputs of the model and baseline and confirms that lower turbine power is required for

lower mass flow. It also shows that when the mass flow is over-predicted greater turbine power is needed. *Figure 4.3.3.3.1.3* shows the turbine speed and turbine settings for the model and the baseline. It shows that the turbine speed correlation is good and that as expected when lower mass flows are predicted (at and below 2500 rpm) the turbine settings are more open in the model. But it can also be seen that this is also the case when the predicted mass flow is higher despite *figure 4.3.3.3.1.4* showing that the turbine efficiency predicted by the model is lower than the baseline for all speeds.

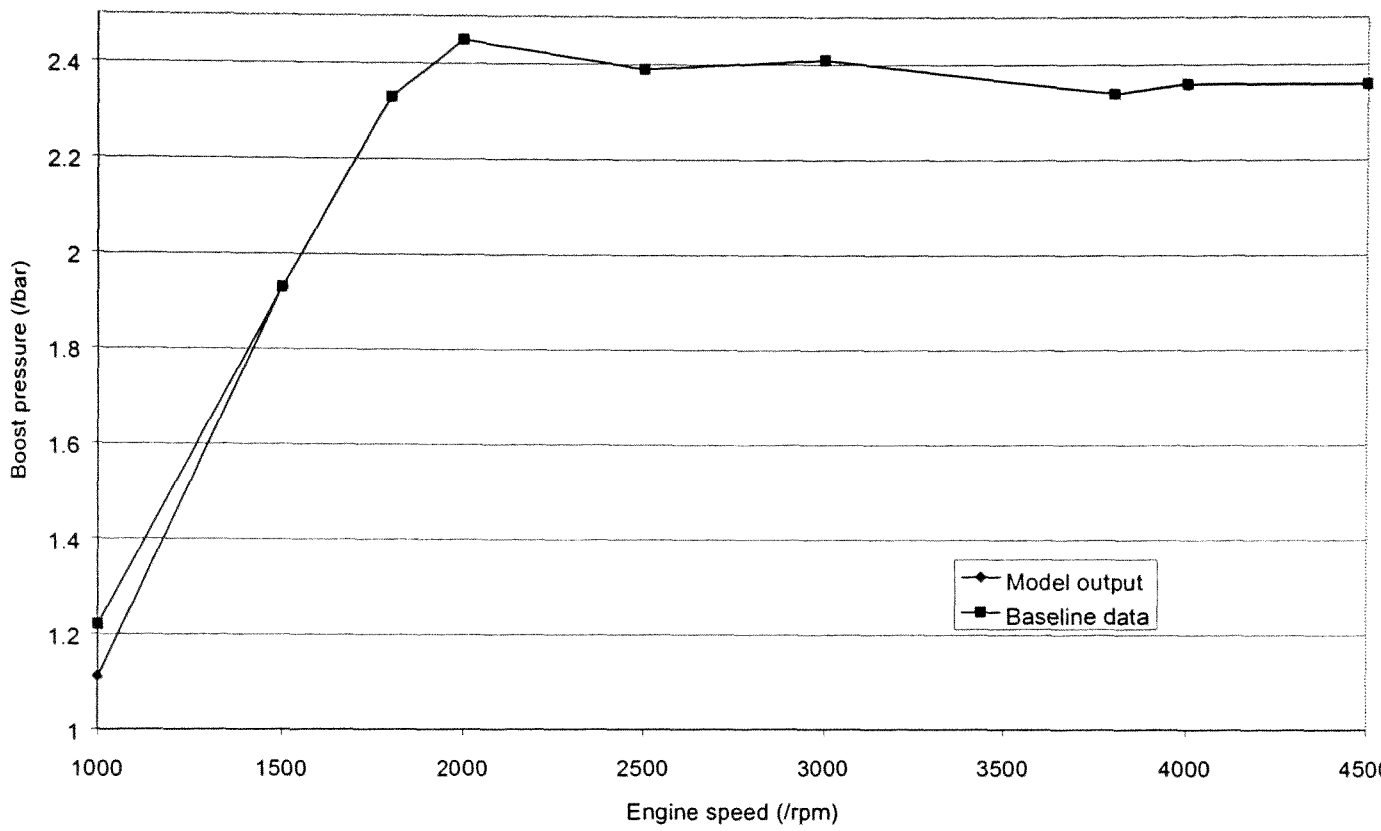


Figure 4.3.3.3.1.1 Target boost level and those achieved by the model.

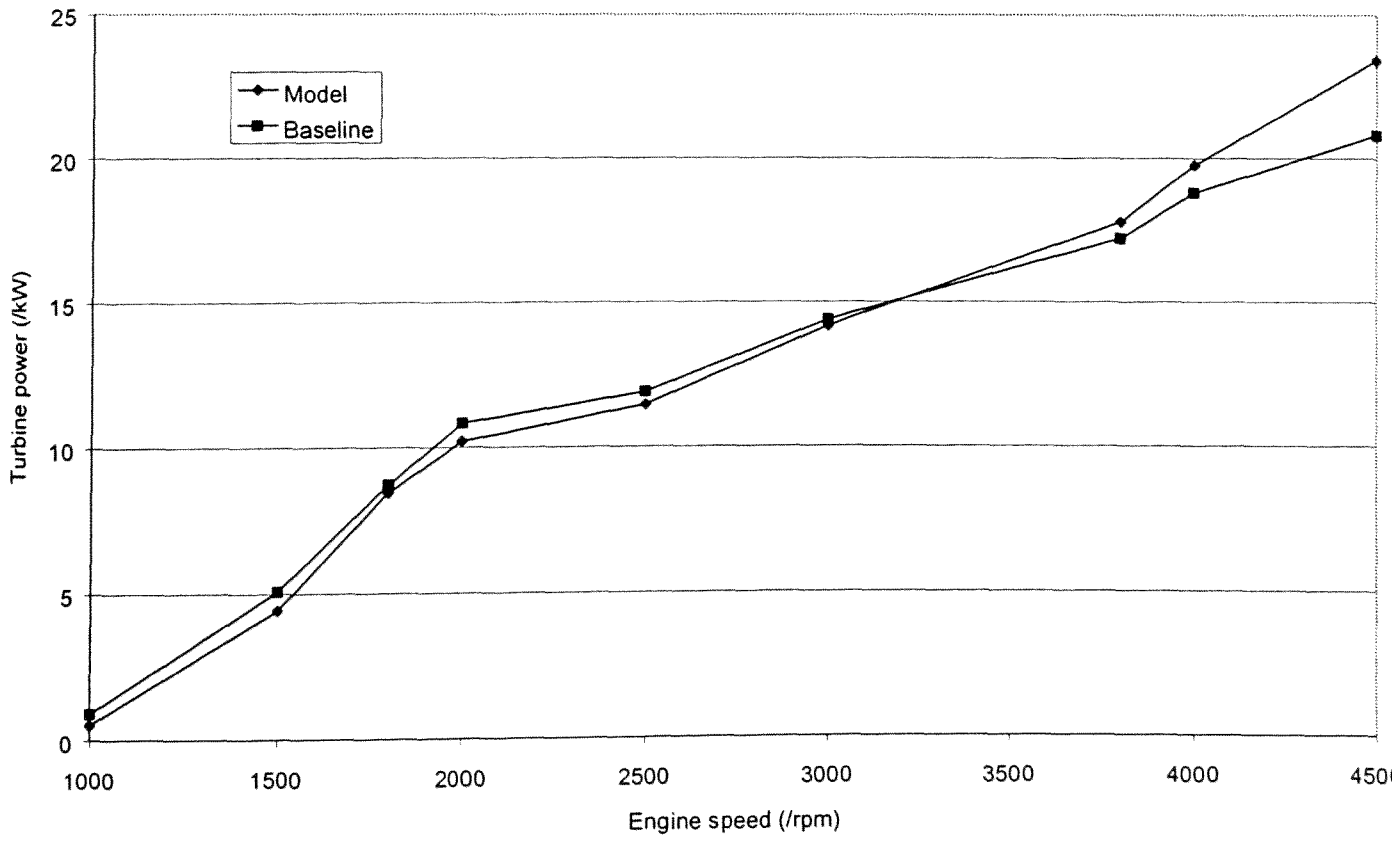


Figure 4.3.3.3.1.2 Turbine power.

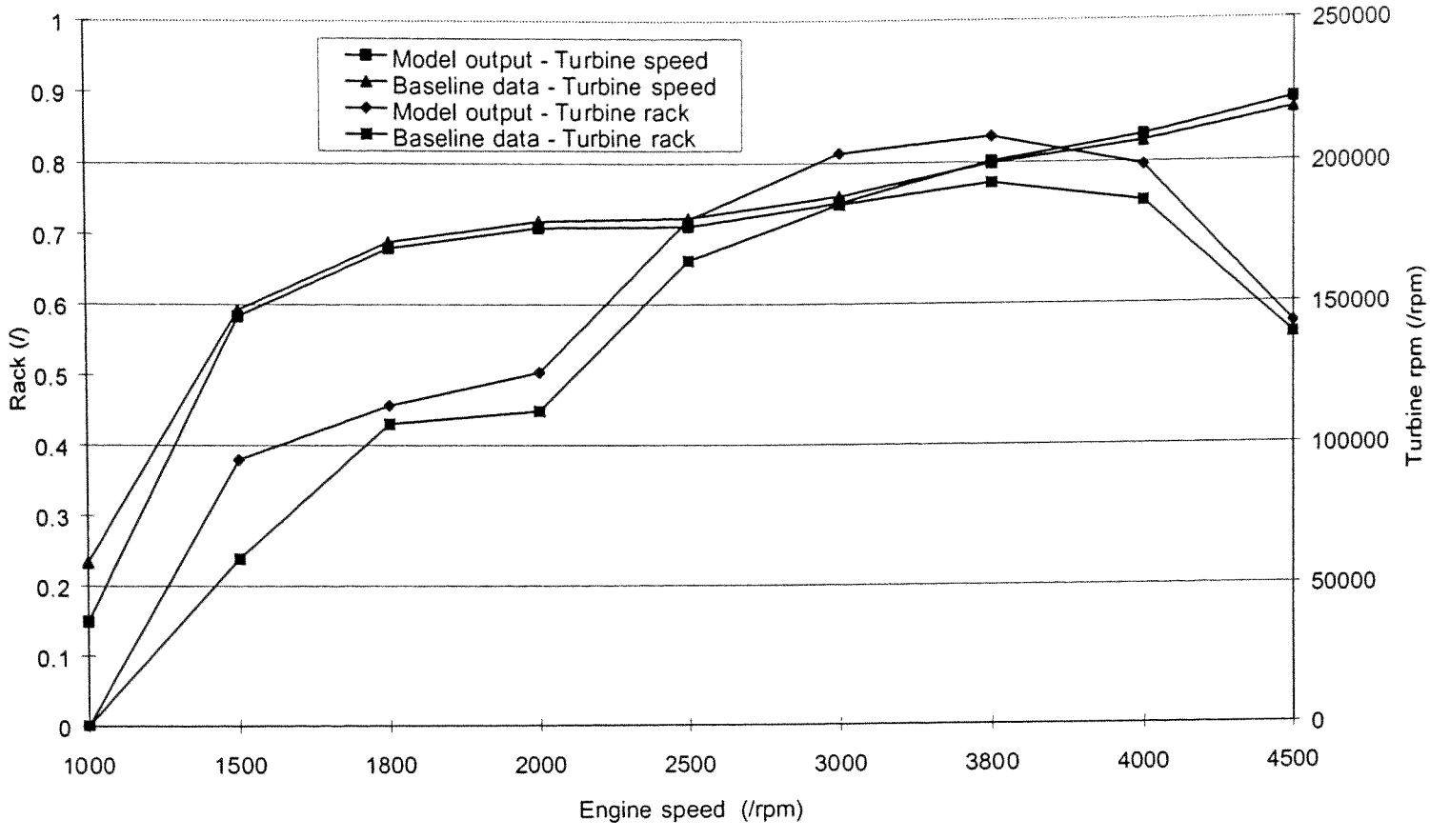


Figure 4.3.3.3.1.3 Comparison of model and baseline turbine speeds and turbine nozzle positions

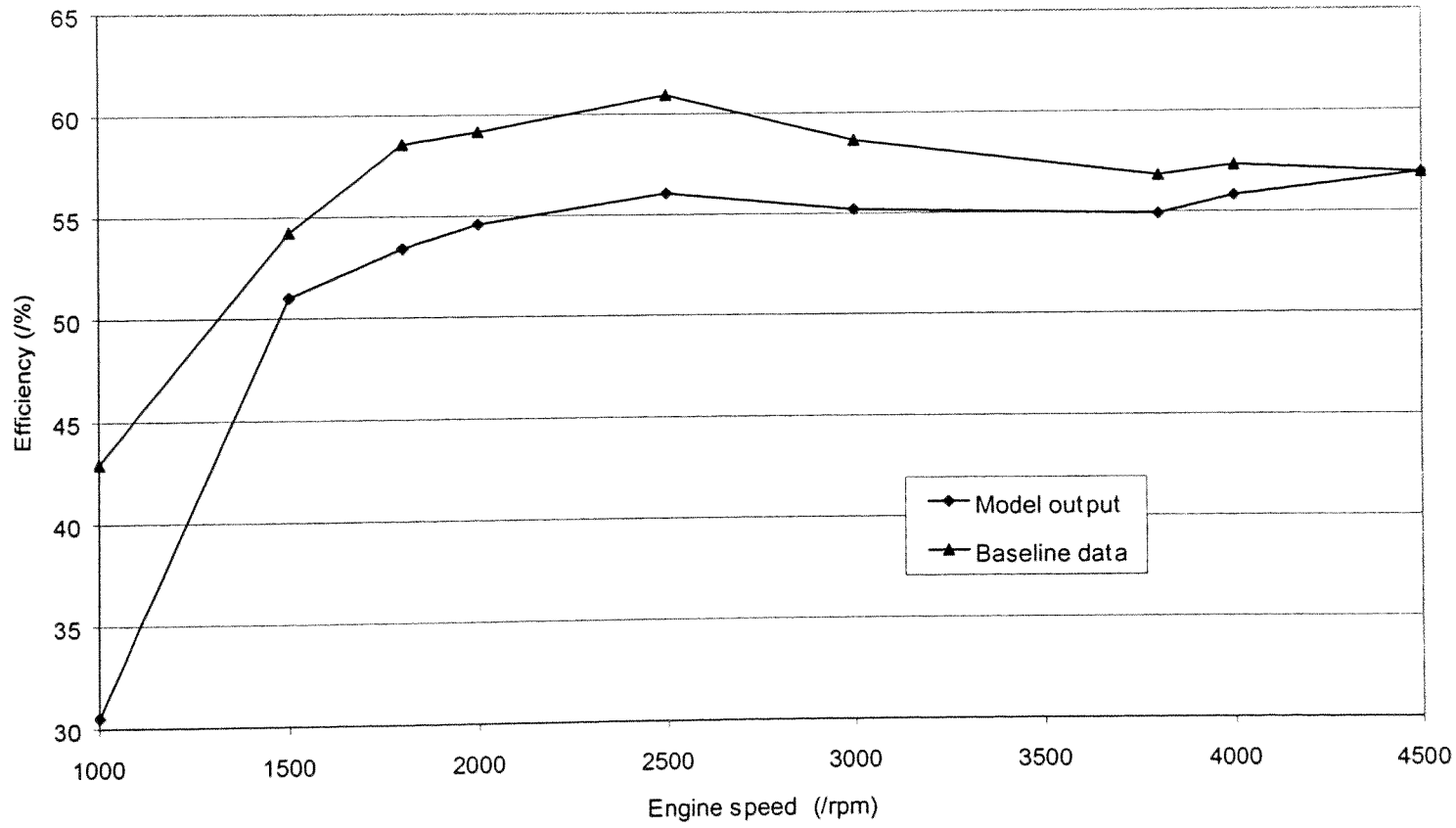


Figure 4.3.3.3.1.4 Turbine efficiency

In the foregoing it can be seen that the 1000 rpm operating point is the least well correlated. The turbo-charger was not able to produce the required boost pressure because its operating efficiency and speed were lower than those for the baseline. *Figure 4.3.3.3.1.5* shows that, at 1000 rpm, the turbine was operating at the edge of the closed rack map in a region that was extrapolated from the raw data. The significant difference between the model and baseline at this speed highlights

the difficulties of extrapolation of manufacturer's test data as in this case the baseline is also the result of simulation, with another commercially available code, and both models have been operating well away from manufacturer's data.

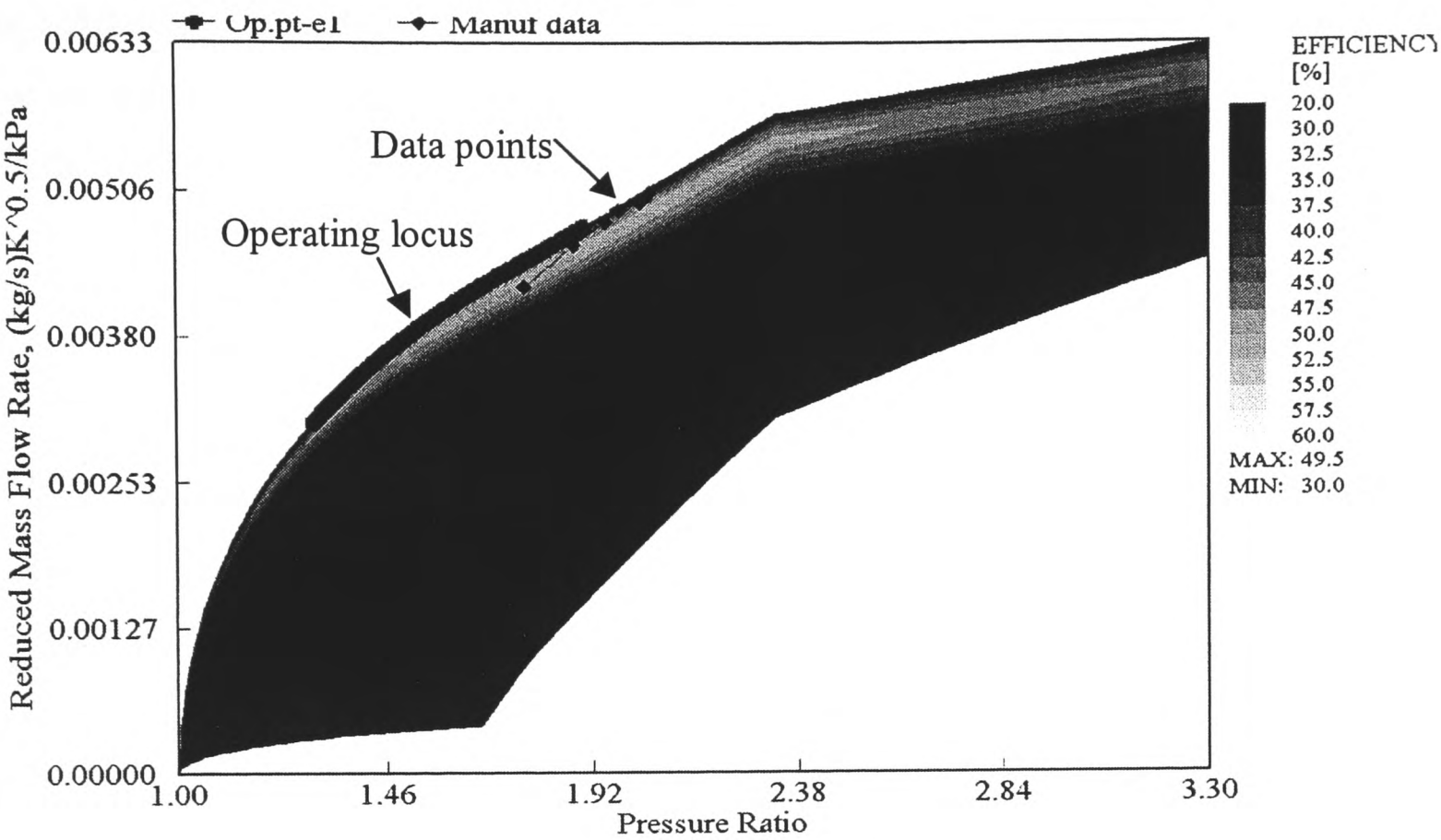


Figure 4.3.3.3.1.5 Turbine operating locus for 1000 rpm full-load on the closed nozzle rack efficiency map. Also shown is the original data from the manufacturer used to generate the map

Another consequence of operating with fuelling that was only a function of speed is that with reduced air mass flows, as were predicted from 1000 rpm to 2500 rpm, increased temperature at the turbine resulted. Similarly with higher mass flows the turbine inlet temperature could be expected to be lower. This was shown to be the case and the data are shown in *figure 4.3.3.3.1.6*. This figure also shows that for all operating speeds, other than 1000 rpm, the temperature differential across the turbine was greater in the model than in the baseline data. This difference in temperature differential ranged from approximately 1% to 8% of the baseline differential (excluding 1000 rpm and 4500 rpm where the differences were larger) and may be a partial explanation for the similar turbine outputs despite lower efficiencies.

Thus it can be seen that there were a number of discrepancies between the predictions of turbine performance and the baseline data. These included the inability to achieve the desired boost pressure at 1000 rpm , small errors in turbine speed across the full load line, differences in nozzle settings required to achieve the boost targets, and differences in efficiency and temperature differentials. There are a number of potential reasons for these differences: direct comparison was

difficult because the differences in mass flow through the engine moved the turbine to slightly different operating points from those of the baseline. Also, since all of the baseline data used for comparison was the result of simulation carried out using another commercial simulation code, using a different turbine data pre-processor it is likely that differences in the resultant maps exist. However, despite all of these concerns it was felt that overall the predictions were acceptable for use in the later study.

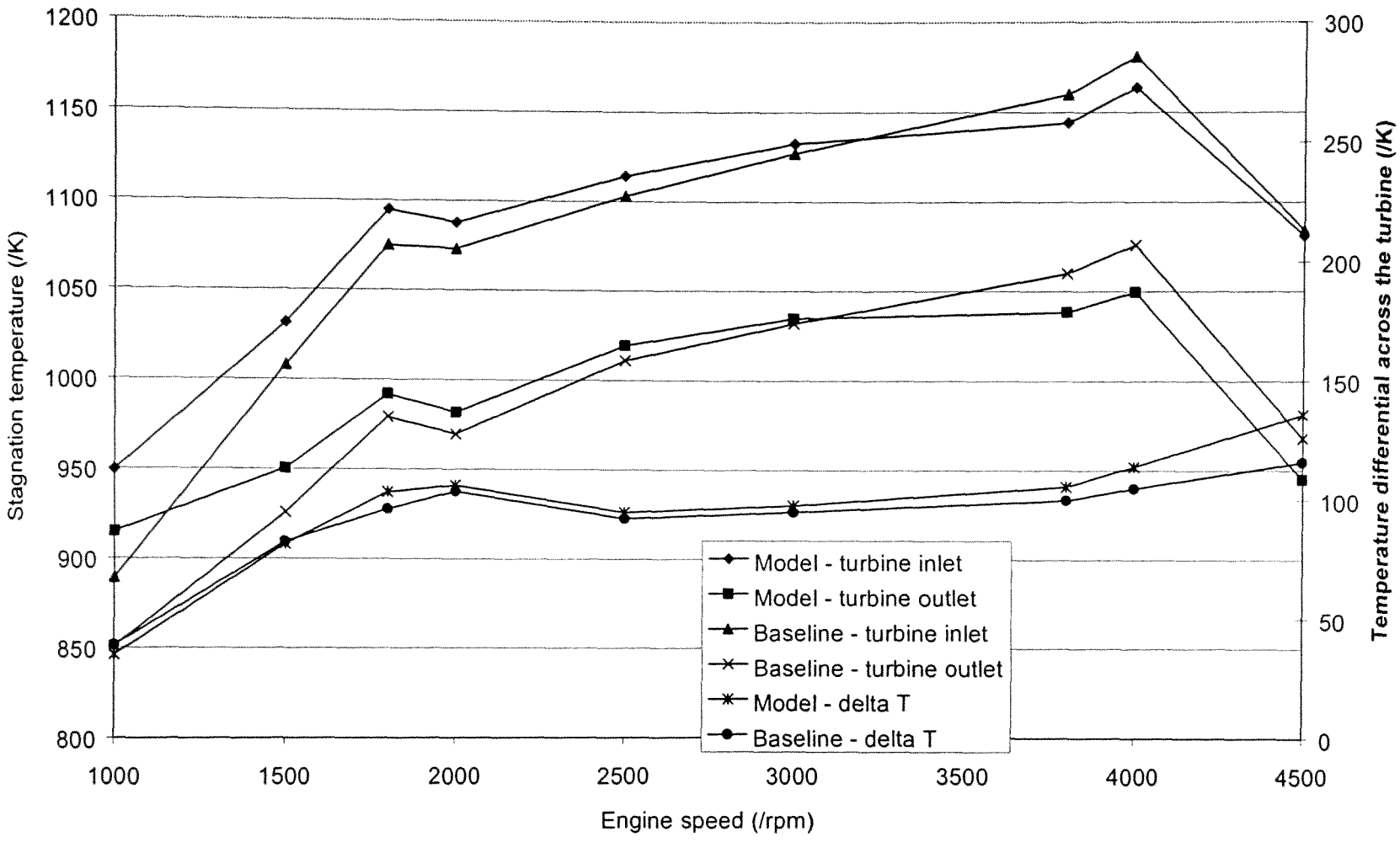


Figure 4.3.3.3.1.6 Turbine inlet and outlet temperatures and temperature differentials

4.3.3.3.2 Compressor operation

Unlike the turbine, which through its variable geometry can be modulated to provide a good match over a large part of the engine's operating regime, the compressor was a fixed geometry device. But, like the turbine, the generation of the maps to be used by the simulation model used partly empirical extrapolation as described in section 4.3.2.4. As a consequence there was some uncertainty about the results and, since the baseline compressor data was also generated by simulation using a different code and pre-processor there was no guarantee that the detail of the baseline data was accurate, other than the fact that overall the predicted engine behaviour correlated well with measured data.

Of primary concern was the correct prediction of compressor efficiency, as in general reduced efficiency requires more power to achieve a given boost pressure at a given mass flow, and a more closed turbine setting results, leading to higher pumping work and increased fuel consumption.

Figure 4.3.3.3.2.1 shows the compressor efficiency across the full load operating line. It can be seen that in general the correspondence is good, particularly at engine speeds of 1800 rpm to 4000 rpm. Outside of these the predicted values are less well correlated. Examination of *figures 4.3.3.3.2.2 – 4* offer some explanation of this.

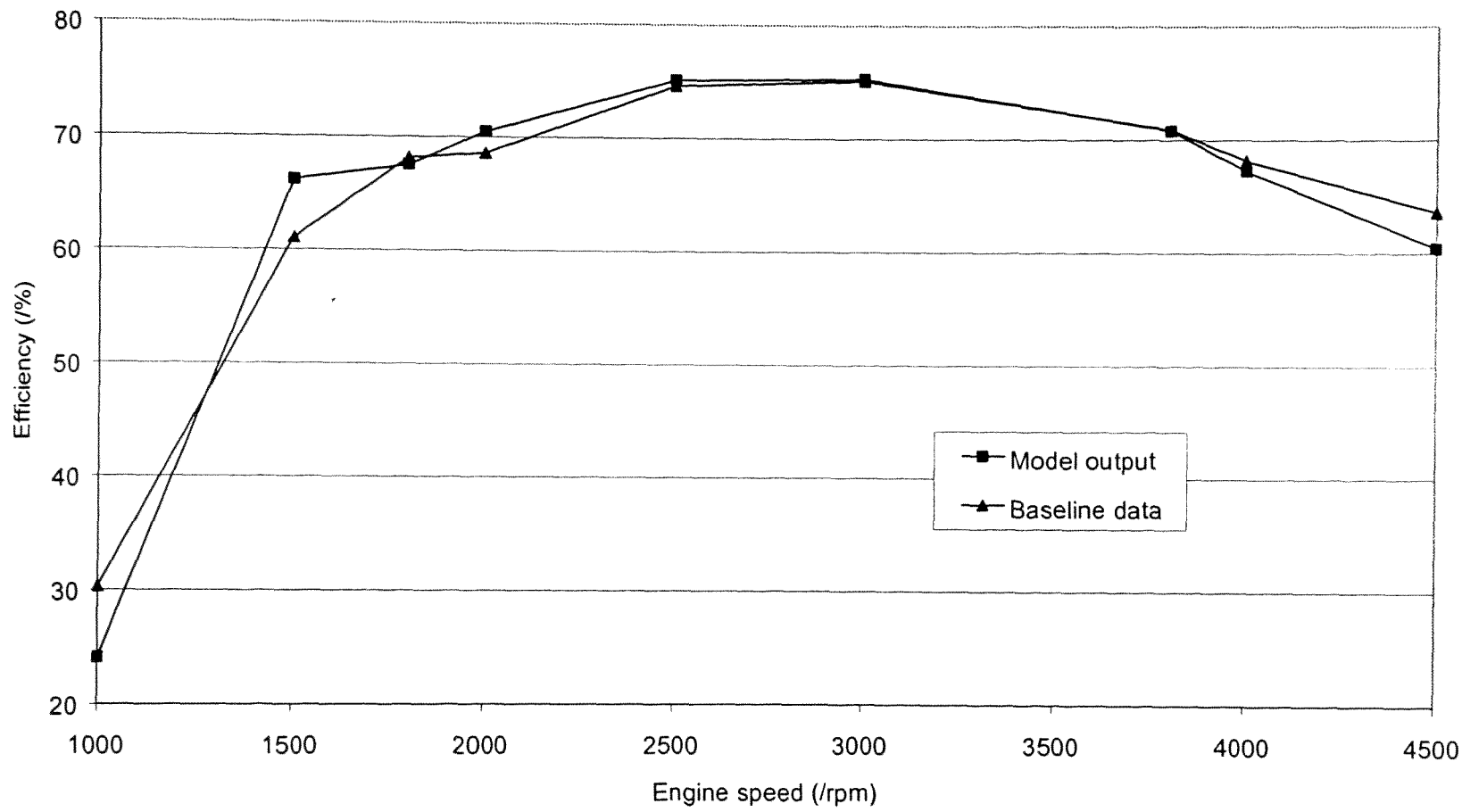


Figure 4.3.3.3.2.1. Compressor efficiency.

Figures 4.3.3.3.2.2 shows the compressor operating locus at 1000 rpm. It also shows the area of the map that is based on measured data (inside the solid line) and highlights the extent to which this operating point is reliant upon extrapolated data. This will also be the case with the baseline data and the differences are likely to be caused by the detail of the extrapolation method.

At speeds of 1500 rpm, 1800 rpm and 2000 rpm a different phenomenon occurred: whilst the average compressor efficiency was within the area of the map populated by manufacturer's data, as shown by *figure 4.3.3.3.2.3*, inspection of *figure 4.3.3.3.2.4* shows that for these engine speeds the compressor operating loci moved outside the region of manufacturer's data and even across the revised surge line of the extrapolated map. As has been shown, GT-Power continues to use

he last efficiency value found on the map when the operating locus leaves the mapped area. It is ıot known how the code used to generate the baseline data dealt with this problem.

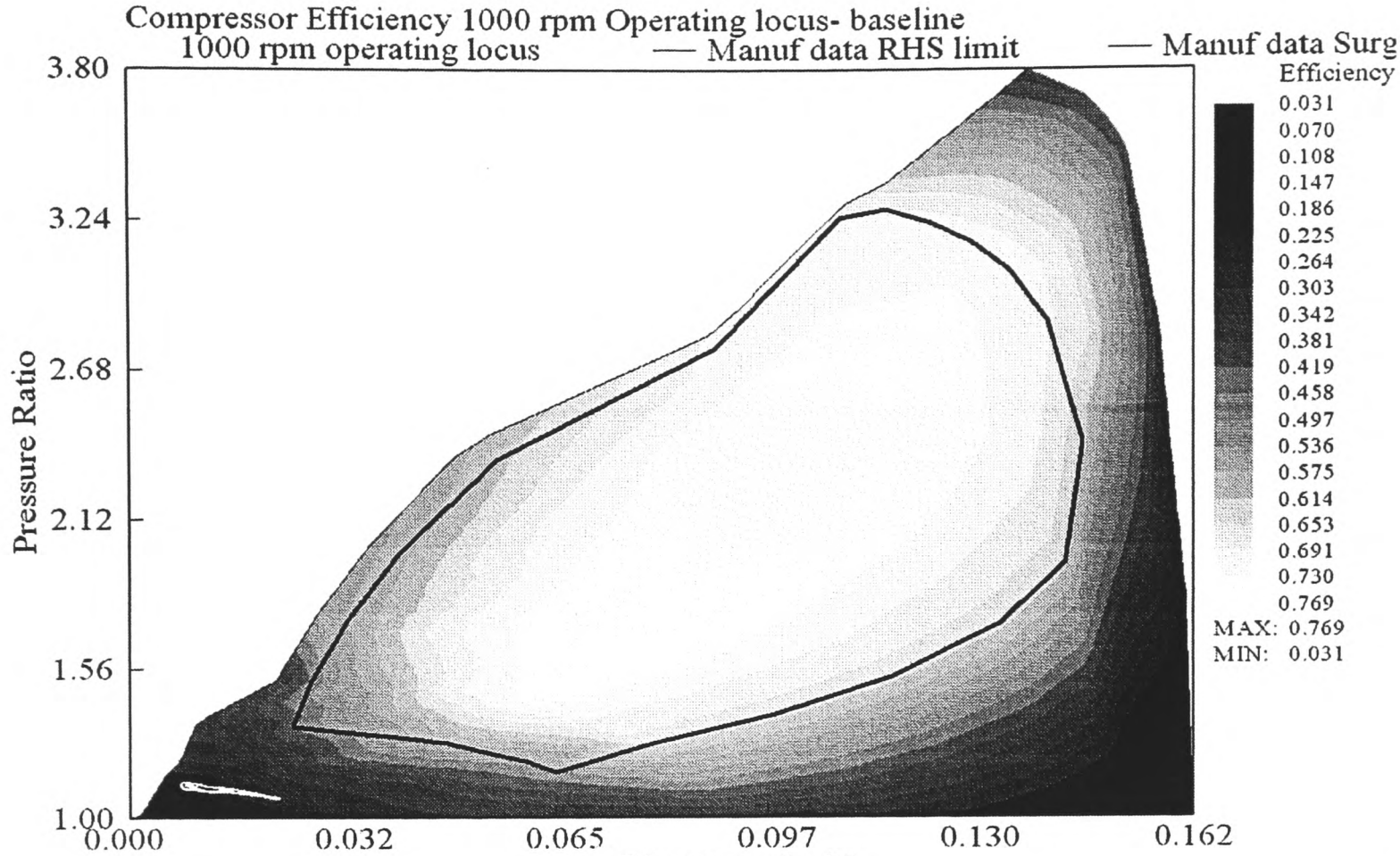


Figure 4.3.3.3.2.2 Operating locus of the compressor at 1000 rpm and the area where measured data is used (Inside solid line)

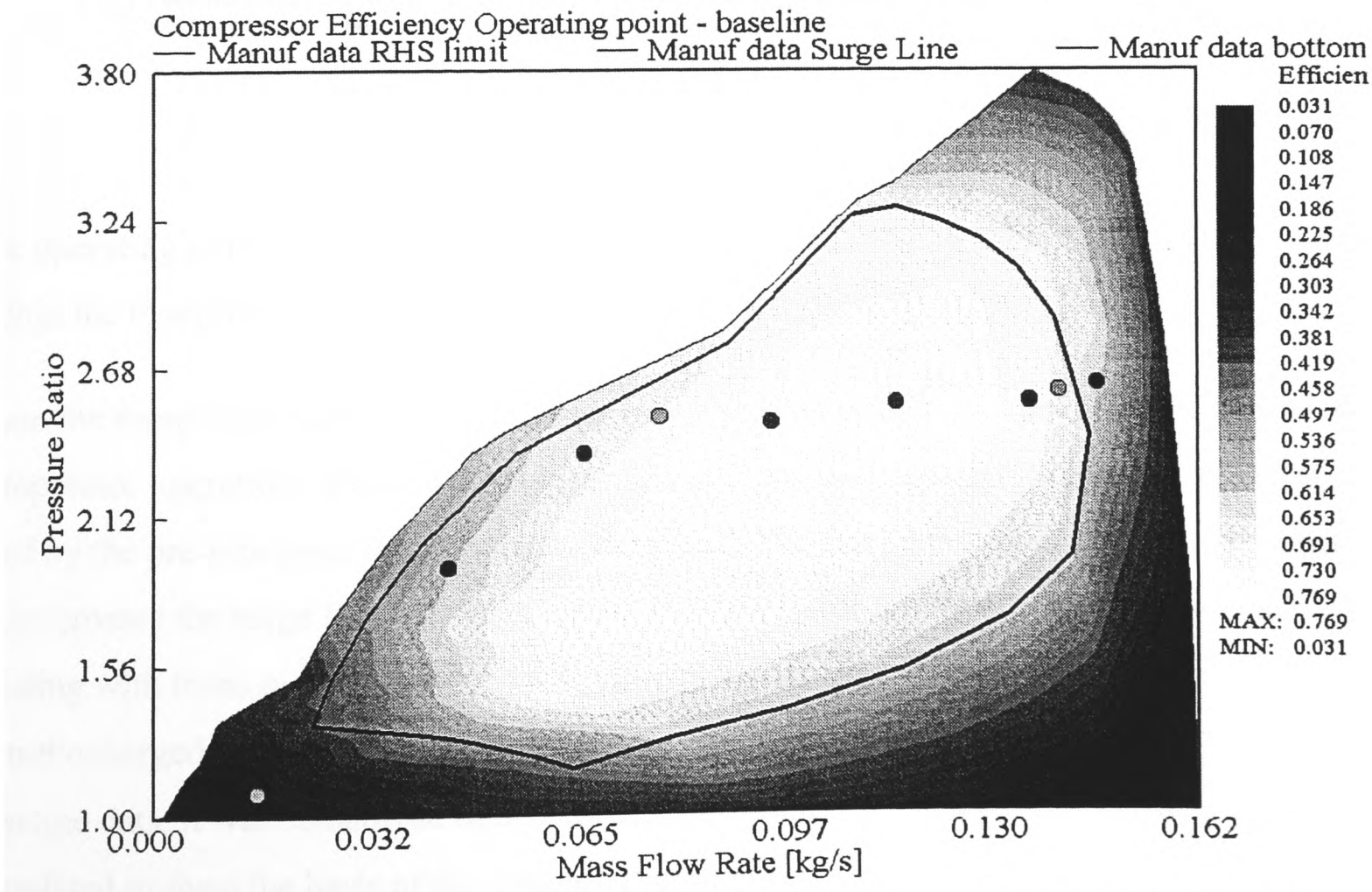


Figure 4.3.3.3.2.3 Average compressor operating points - increasing speed upward and to the right

Figure 4.3.3.3.2.4 also shows that the operating point at 4000 rpm is marginally inside the area of manufacturer's data and that at 4500 rpm it is outside. It is considered that because these operating points are both affected by the extrapolation of the map to higher speeds, mass flows and pressure ratios the differences are probably caused by differences in the manually extrapolated data and pre-processor assumptions.

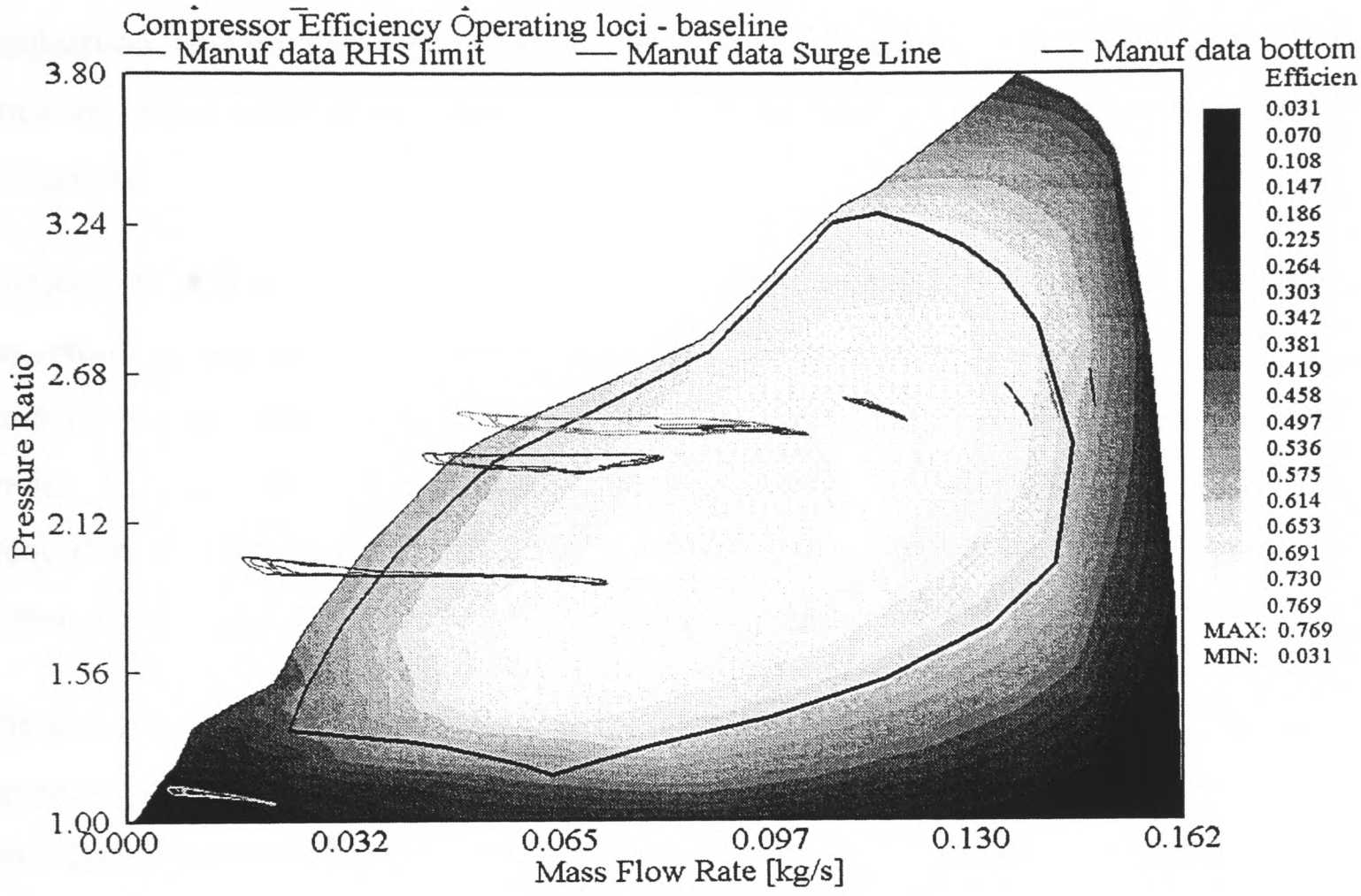


Figure 4.3.3.3.2.4 Compressor operating loci - increasing speed upward and to the right

The operating points at 2500 rpm , 3000 rpm and 3800 rpm match very closely as they are well within the manufacturer's data.

From the foregoing it can be seen that there are a number of matters that affect the predicted compressor operation: accuracy of manual data extrapolation, assumptions made and methods used by the pre-processor to generate the maps and the extent to which the compressor operating locus crosses the surge line and what approach is used to deal with efficiency when it does. Dealing with these matters is part of the process of producing well correlated simulation models of turbocharged engines. Whilst there were detailed differences in the behaviour of the model and baseline data, it was considered that the predicted compressor results were sufficiently well correlated to form the basis of the ongoing investigation.

4.3.3.4 Discussion of the overall model predictions

As already mentioned, when discussing the quality of the results from the simulation of engine performance, there are a number of levels at which they can be assessed: global lumped outputs such as bmep and bsfc, imep and isfc which contain more detailed information about the internal processes (but do not display it explicitly), through the detailed operation of the sub-systems such as combustion, heat transfer, turbo-charger operation, and finally into the most detailed information, wave action in the pipes. But which are important depends on the purpose of the investigation.

The objectives of this piece of work were to investigate the effects of VVA on those aspects of the operation of light duty diesel engines that are of interest to the engine and vehicle manufacturers, such as full load torque, part load fuel economy and increasing load transient operation. In each of these the quality of the simulation of the turbo-charger is very important. So the requirement is for a good correlation of the overall engine behaviour and, within the limitations of the models used, a reasonable representation of the turbo-charger.

Of the global outputs the correlation of bmep, imep, fmep and pmep are good and since the comparative simulations were carried out using the same fixed fuelling the quality of bsfc and isfc correlation carries over.

The burn rate curves were adjusted to be, as near as possible, the same as the baseline, so good correlation of this aspect was to be expected, but in conjunction with the predictive ignition delay good agreement was found with both maximum cylinder pressure and its timing. (It may be worthwhile pointing out that the burn rate curve was the only sub-model that was "adjusted" for correlation.) There were however minor differences in cylinder heat transfer, but it was known that GT Power used a modified Woschni, whereas the baseline results were produced using standard Woschni. The differences between the model and the baseline were in the behaviour during overlap and so had little effect on engine output or fuel consumption as would have been the case if the differences occurred during the closed part of the cycle.

The sub-systems that were least well correlated were the turbine and compressor, particularly at low speeds: The overall air flow through the engine, correlated well, except at 1000 rpm, but it should be remembered that for this comparison the boost pressure was controlled, so the only discrepancy was at 1000 rpm where the turbo-charger could not achieve the required boost.

More detailed inspection of the results revealed that turbine efficiency was being under predicted and compressor efficiency was being slightly over-predicted and these effects were to some extent cancelling each other out. Also the turbine settings were more open for the majority of engine speeds despite the under-prediction of turbine efficiency. This may have been because of the greater predicted temperature differential across the turbine.

The 1000 rpm and 1500 rpm operating points highlighted contrasting problems for the compressor: at 1000 rpm, although the operating locus of the device was entirely contained within the efficiency map, it was in a region of extrapolated data which had only a small gradient perpendicular to the efficiency contours and was almost flat parallel to the mass flow axis. The low speed and mass flow precluded large changes in pressure ratio that would have been required to climb the efficiency "hill." As a consequence the locus simply ran parallel to the mass flow axis, at more or less constant (low) efficiency. The efficiency values in this region were entirely extrapolated and the higher efficiencies of the baseline device were probably caused by differences in the extrapolation techniques and pre-processor operation.

At 1500 rpm, the operating locus ran off the edge of the compressor efficiency map, leading to the model truncating the efficiency at the value found at the edge of the map. It is known that compressor efficiency falls rapidly after crossing the surge line, but it is not known by how much. As a consequence this truncation of the efficiency may have led to an over-prediction of the average compressor efficiency.

These two conditions are symptomatic of the problems associated with the extrapolation of the compressor map. A different set of efficiency values for the very low speed and mass flow regions and extension further into the soft surge region would probably overcome these deficiencies, but there is no rigorous basis for this. Similar differences in the data extrapolation for the turbine maps is likely to have occurred and led to differences in its predicted operation.

However, overall the behaviour of the model predicted trends and values well over the full load operating speed range and was considered adequate for use for the investigation of the effects of VVA. But it became clear that it was essential to bear in mind the possible problems, particularly with the turbo-charger, in the interpretation of the results from this investigation.

4.4 CONCLUSIONS

A simulation model was constructed using a commercially available code, GT-Power and with the exception of the turbo-charger and combustion the model used a high level of theory and physics and did not need any adjustment to achieve good correlation with baseline data. However, production of the turbine and compressor maps relied on extrapolation of manufacturer's data to cover the necessary operating regions. This was an approximate process, reliant upon estimation of trends in the measured data and was the only area of model development where matters of judgement had the potential to significantly influence the results of simulation.

The combustion modelling, implemented through the use of normalised fuel burning rate curves was adjusted (for each known steady state operating point) to be as near as possible, the same as the baseline, so good correlation was to be expected at the correlated operating points, but since the fuel burning rate characteristics were not responsive to trapped conditions there was the possibility that where predicted operating points (with VVA) were far from the correlated points, errors due to incorrect combustion characteristics could have occurred.

The full-load correlations between the model and the baseline for bmep, imep, fmep and pmep values and trends were good (maximum errors of 5% but typically less than 3%) and since the comparative simulations were carried out using the same fixed fuelling the quality of bsfc and isfc correlation carried over. There were, however, more significant differences in cylinder heat transfer, but it was known that GT Power used a modified Woschni, whereas the baseline results were produced using standard Woschni, but, this only had a minimal effect on output.

The sub-systems that were least well correlated were the turbine and compressor, particularly at low speeds: The overall air flow through the engine, correlated well, (maximum error of 12% at 1000 rpm, less than 3.5% from 1500 rpm to 4000 rpm, and 4.4% at 4500 rpm). It should be remembered that for this comparison the boost pressure was controlled, so the only discrepancy was at 1000 rpm where the turbo-charger could not achieve the required boost.

More detailed inspection of the results revealed that turbine efficiency was being under predicted and compressor efficiency slightly over-predicted and these effects were to some extent cancelling each other out.

It was significant that at 1000 rpm engine speed, both the turbine and compressor were operating in areas of their maps that were the result of extrapolation of manufacturer's measured data whilst at 4500 rpm the turbine was right at the edge of the measured data and the compressor in an extrapolated region. This highlighted the importance of the techniques used to extrapolate these operating maps as errors in this process can significantly affect the predicted engine performance.

Another potential problem with predicting compressor operation occurred when its operating locus ran off the edge of the compressor efficiency map, as happened at the lower engine speeds at full load. GT-Power truncated the efficiency at the value found at the edge of the map, but it is known that compressor efficiency falls rapidly after its operating point crosses the surge line. However it is not known by how much. It is possible that this truncation of the efficiency may have led to an over-prediction of the average compressor efficiency.

These potential problems at high and low speed are symptomatic of the problems associated with the extrapolation of the compressor maps. A different set of efficiency values for the very low speed and mass flow regions and extension of the maps further into the soft surge region would probably overcome these deficiencies, but there is no rigorous basis for this. Similar differences in the data extrapolation for the turbine maps is likely to have occurred and may have led to differences in its predicted operation.

Despite these concerns, overall the model predicted trends and values well over the full load operating speed range and was considered adequate for use for the investigation of the effects of VVA.

5 SIMULATION OF THE EFFECTS OF VVA APPLIED TO A DIESEL ENGINE

Having established that the results generated by the model were acceptable, it was necessary to make changes to the model (notably the implementation of AFR based fuelling control for full load operation, section 5.1.1, provision of controlled EGR flow for part load and transient operation, section 5.2.1, and VVA controllers for transient operation, section 5.3.1) to allow it to produce results for the various operating regimes to be investigated. Once these changes had been implemented investigations were carried out to quantify the benefits in steady state, full load performance, discussed in section 5.1, part load fuel economy, discussed in section 5.2, and transient torque rise, which is discussed in section 5.3.

In all further discussions of valve timings only the VVA setting numbers will be used, to avoid confusion about the standards used to define valve timings, which vary widely. *Table 5.1* shows the ramp bottom and notional ramp top timings associated with the VVA setting numbers used. In all cases it is simplest to remember that the lower numbers relate to the shorter effective valve open periods, setting number 4 is the standard timing and the larger numbers relate to the longer than standard valve open periods. Since there is little or no change in overlap timings we are primarily concerned with intake valve closing and exhaust valve opening timings. (Ramp top timings are calculated at 0.1mm lift for opening and 0.2mm lift for closing timings.) It should be noted that the standard engine has hydraulic lash adjusters to control valve clearances. These have a speed dependent leak down characteristic, which means that actual valve timings are speed dependent. Whilst GT power and the code used to generate some of the baseline data both had the capability to model this behaviour it was not used in either case, for lack of information.

VVA setting	x /mm	Intake valve				Exhaust valve			
		Opening		Closing		Opening		Closing	
		RB	RT	RB	RT	RB	RT	RB	RT
1	3	338.1	352.7	577.3	545.6	154.2	170.3	390.9	364.4
2	2	336.2	351.3	586.7	556.6	143	159.5	392.5	365
3	1	334.4	350.5	597.2	567.2	131.6	149	394.3	365.7
4	0	333.6	349.8	608.8	578	120.3	137	395.2	366
5	-1	332	349	619.5	588.9	110.2	127.5	399.1	366.2
6	-2	329.7	348.3	630.6	599.5	99	116.3	400.9	366.5
7	-3	329	347.8	640.9	610.6	88.7	105.3	402.7	366.7

Table 5.1 Correspondence between VVA setting number and ramp bottom and ramp top valve timings, °after TDC(f) (Ramp heights 0.1mm opening and 0.2mm closing). x is drive shaft eccentricity and R = 15mm as in *figure 3.3.2.1*

5.1 STEADY STATE FULL LOAD OPERATION

Once the non-VVA baseline model had been correlated, the model was altered to allow full load operation with the VVA active. Having extended the model, it was noted that there were some differences in the way the model converged when using AFR fuelling control, so a standard method of starting and allowing the model to converge was established. This method was then used for all full load steady state simulations.

The method employed to optimise full load valve timing was to investigate the effects of intake valve timing, with exhaust valve timing held constant at its standard value. From the resulting data an optimum intake valve timing was selected for each engine speed. The intake valve timings were then held constant at these settings whilst the exhaust valve timings were varied. A discussion of simulation convergence and of the results from intake VVA and intake and exhaust VVA are presented in the following sections.

5.1.1 Additions and changes to the model

During the baseline correlation simulations the valve timings were held constant, at the standard values, although the VVA software was installed. For the investigations to follow, the VVA settings became the independent variables, and were used as inputs across their full ranges, for both intake and exhaust valves.

As mentioned earlier, the baseline performance data was specified using a target boost pressure for each operating condition. Therefore, for baseline correlation, the model was also fitted with a PID controller to adjust the VGT setting in order to achieve the target boost pressure.

It was anticipated that increases in air flow and output would be achieved with altered valve timing, one consequence of which would be an increase in boost pressure. Thus boost pressure control was not required for this investigation, as it would negate any potential for increased boost, and the PID controller was removed.

A limited investigation into full load operation, with standard valve timings, showed that the VGT settings and resulting boost levels (the target boost values) were close to optimum for minimum fuel consumption. Therefore it was decided to fix the VGT settings at the values at which they had stabilised with the target boost values in the non-VVA model.

Again, as mentioned earlier, the baseline correlation was carried out with fixed fuelling, but for similar reasoning, as air flow was expected to increase with the VVA active, it was decided that the operating air-fuel-ratio, AFR, would be held constant at the baseline value. This was carried out using a feature of the fuel injector model. This model had the capability to control to a lower AFR limit, intended for smoke limit control. But if excess fuel were always available it would always provide the amount of fuel to run at this lower AFR limit. As this was achieved through the injector model it operated on a cycle by cycle and cylinder by cylinder basis as the trapped mass in each cylinder was known on this basis, so there were no control system delays or offsets.

5.1.2 Model convergence with fixed fuelling and AFR controlled fuelling

When using GT – Power, simulating a normally aspirated 4 cylinder gasoline engine to convergence at a stable operating condition would normally be expected to take ten to twenty complete engine cycles. After this period the cyclic behaviour of all gas flows around the engine will have stabilised. However, with a turbo-charged engine this is not the case, as the turbo-charger has inertia and therefore, the model takes longer to converge. Reduction in the turbocharger inertia is commonly used to reduce convergence times.

Advice from other users of engine simulation software suggested that in excess of one hundred cycles might be required for convergence of turbocharged diesel engine models. To help with reducing the time to convergence GT-Power includes a number of aids: allowing the specification of initial conditions in pipes, initial turbo-charger speed and time varying turbocharger inertia. There is also a facility to start a new simulation "case" with the converged operating conditions of the previous operating point, "Old," or to ignore this and use the specified initial conditions, "New."

Consideration of the operation of a turbo-charged engine highlights the fact that engines with exhaust driven supercharging systems have "history." That is their operating conditions are not just a function of the fuelling and speed, but are also affected by their past operating history. This is even the case when starting a new simulation that is apparently steady state. The operation of the turbo-charger remains transient for a considerable period.

To identify the significance of these matters a limited investigation was carried out into the effect of: AFR and fixed fuelling control, model initial conditions, and turbine inertia. This was carried out at 1500 rpm full load.

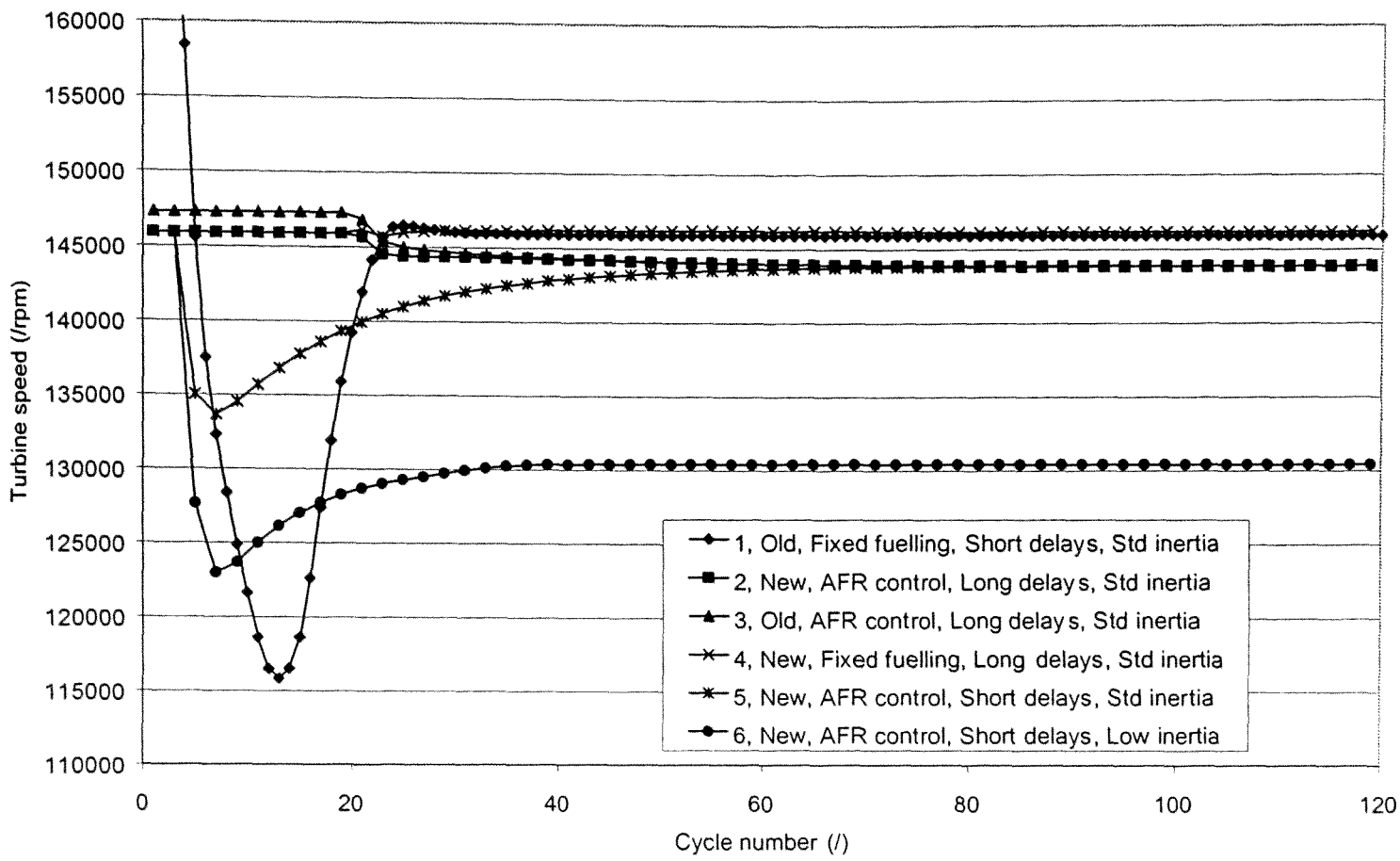


Figure 5.1.2.1 Turbine speed versus simulation cycle number.

Figure 5.1.2.1 shows the differing configurations tested and their effects on the turbine speed. Contrasting lines 1 and 4, which have differing initial speeds, as might result from using "Old," and periods over which the turbo-charger inertia was modulated[1], it can be seen that despite the fuelling being fixed at the same level, they converged to slightly differing final speeds, air mass flow rates, *figure 5.1.2.2* and consequently to differing AFR values, *figure 5.1.2.3.* Inspection of lines 2 and 3, which have differing initial conditions, shows that with AFR control they converged to the same turbine speed and mass flow rate. Inspecting line 5, which again uses AFR control, but had the shorter delays, shows the model suffered a significant dip in turbine speed, but still recovered to the same final speed and air mass flow rate. Contrasting lines 5 and 6, which only differ in turbo-charger inertia, shows that with the lower inertia, the dip in speed experienced was greater and the system converged to substantially different final turbine speed and air mass flow rate.

(***[1] GT-Power allows the user to select a number of cycles during which the turbo-charger inertia is effectively infinite followed by a number of cycles over which it reduces to the nominal value. The number of cycles set for this investigation were 3 and 5, referred to as "Short delays" and 20 and 50, referred to as "Long delays"***)

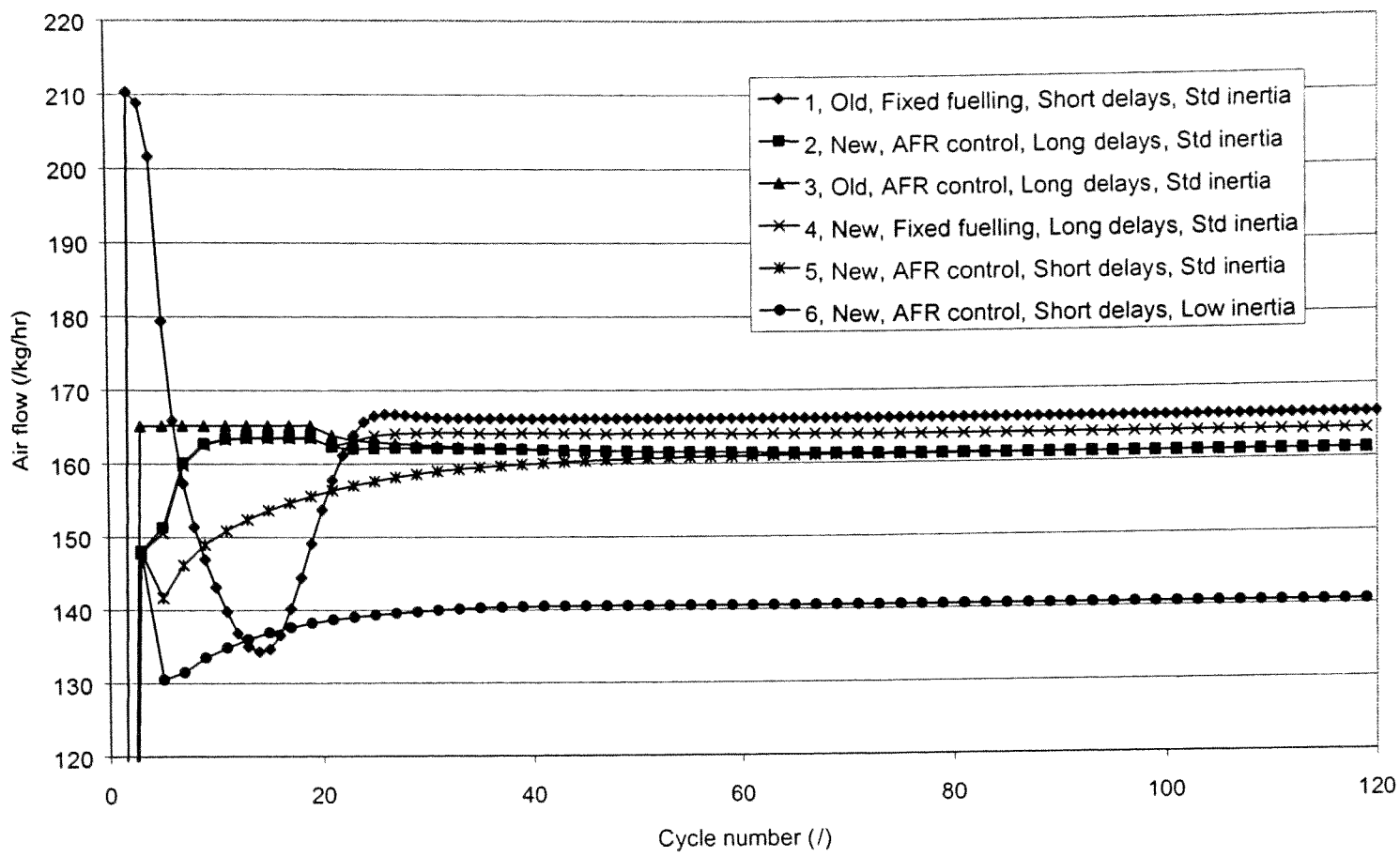


Figure 5.1.2.2 Air mass flow rate versus cycle number for various initial conditions

With the exception of case 6, the differences between the fixed fuel and AFR controlled values can be explained by the differences in predicted air flow between the baseline data, (which had been used for the calculation of the AFR values applied,) and those of the VVA model with fixed fuelling as described in section 4.3.3.1 However, the low inertia case 6 is significantly different from any of the other results, indicating that care needs to be taken with the reduction of inertia for speeding convergence.

The foregoing shows that the converged operating point of the model is dependent upon the nature of the fuelling control, the initial system conditions and the turbo-charger inertia, as these all affect the course the engine and turbo-charger take through their operating spaces. As a consequence, in using a model, it is important to use a standardised starting configuration for initial conditions, fuelling regime, and turbo-charger inertia characteristics for all comparable simulation runs, in order to minimise the deviations from the nominal trajectory of operation. (Despite this it should be recognised that changing the valve timing promotes the use of a different trajectory.) The standard starting configuration used was "New" initial conditions, AFR control, the 20 and 50 cycle inertia delays and standard turbo-charger inertia run over 120 engine cycles.

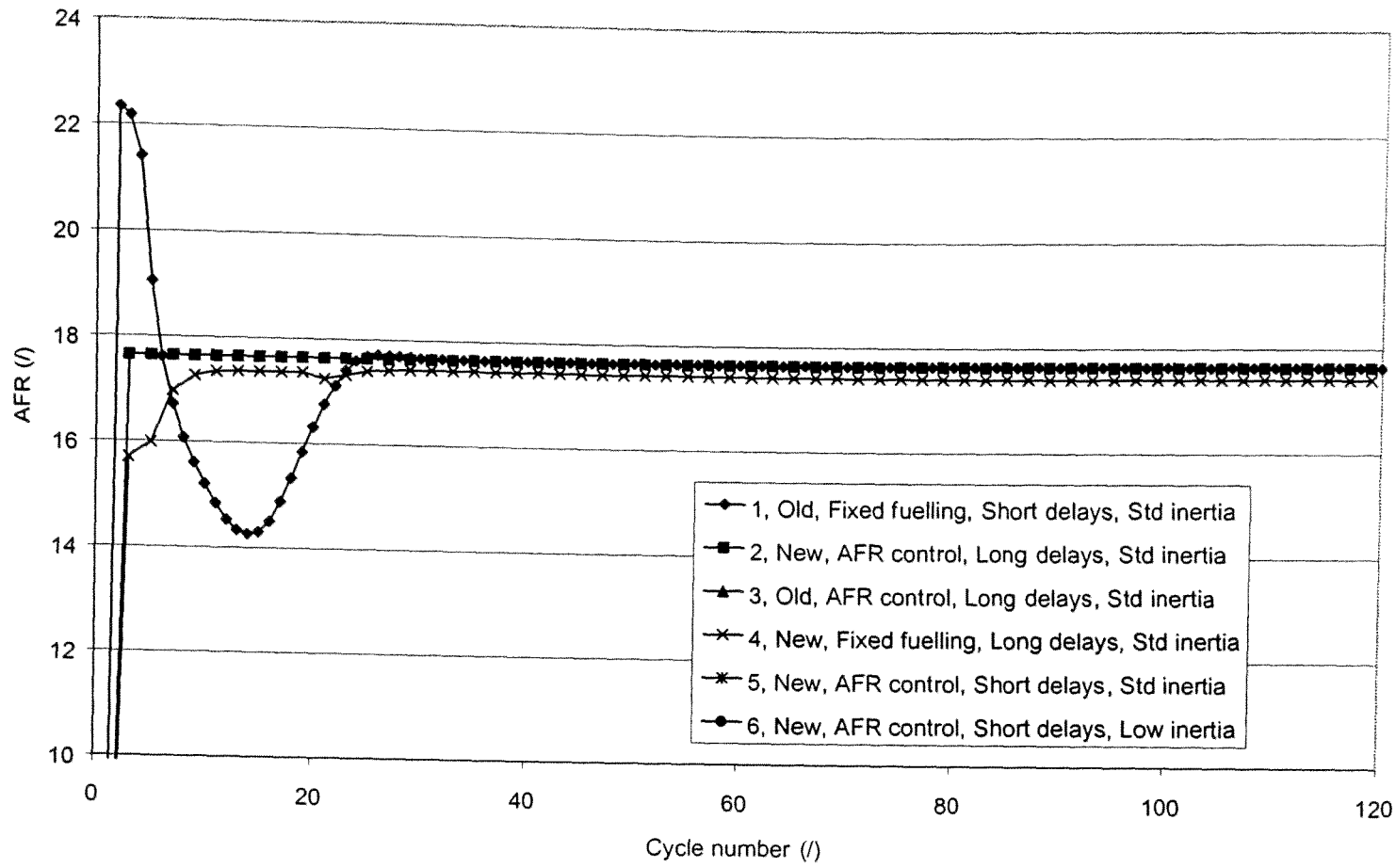


Figure 5.1.2.3 AFR characteristic for various initial conditions.

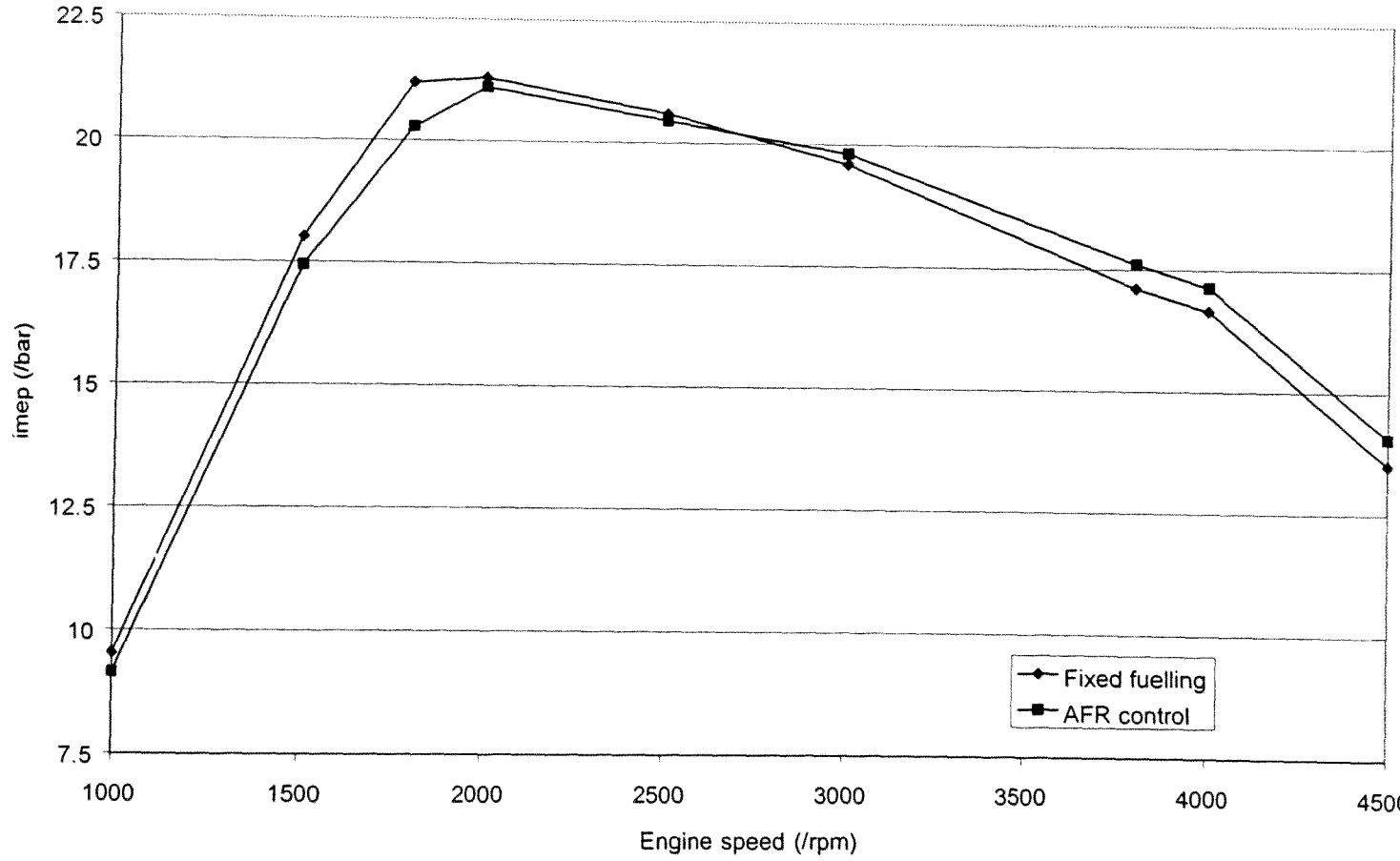


Figure 5.1.2.4 imep characteristic for AFR controlled and fixed fuelling.

Since all of the AFR values used were taken from the baseline data (as they were acceptable for normal engine operation and avoided smoke problems in the actual engine) the discrepancies in air flow between the model and the baseline discussed in section 4.3.3.1 produced differences in engine output between fixed fuelling and AFR control across the whole speed range as shown in *figure 5.1.2.4*. As a consequence a new set of characteristics needed to be used as the basis for

comparison when evaluating the effects of VVA. From here forward, unless otherwise stated, the nominal characteristics for comparison are those generated by the model using the standard starting configuration and standard valve timing. *Figure 5.1.2.4* contrasts the imep for this new AFR controlled characteristic and the corresponding values for the model with fixed fuelling.

5.1.3 Intake VVA

For this investigation the AFR, VGT setting and exhaust valve timings were all held at prescribed values for each speed and the intake valve timings were varied over their full available range. The investigation looked at lumped performance parameters, such as imep, (where the expected increases were found at low speeds), at the details of the work distribution in the cycle and at the operational limitations of the turbocharger.

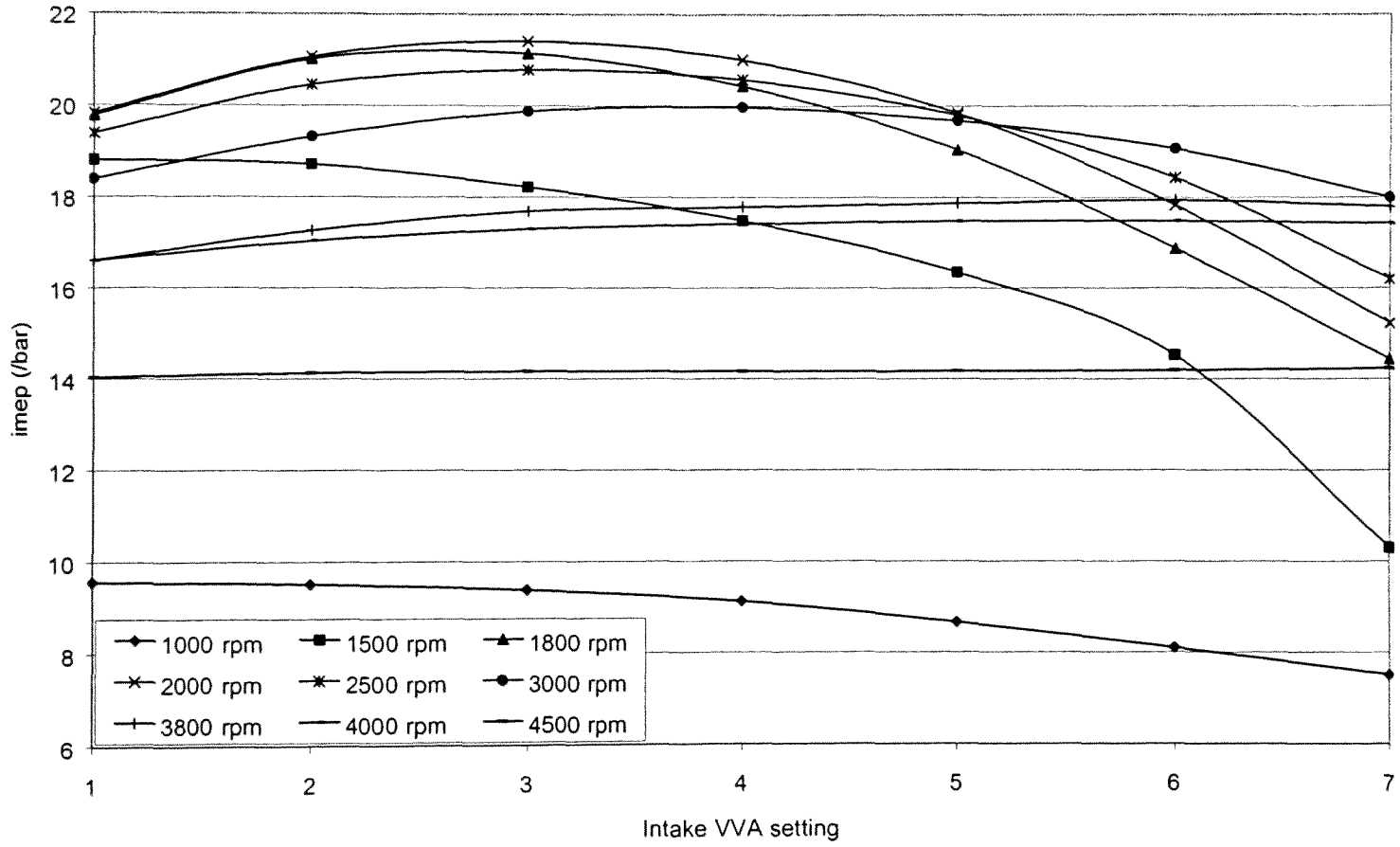


Figure 5.1.3.1 imep as a function of intake valve closing timing over the full speed range.

First, considering the overall impact of the intake valve closing timing on engine output: *figure 5.1.3.1* shows the imep characteristics as a function of intake valve closing setting. *Figure 5.1.3.2* shows these plotted to provide percentage improvements related to the standard valve timing and shows increases of up to 7.6% at 1500 rpm with the earliest IVC and the expected trend of optimum output requiring later IVC as engine speed rises.

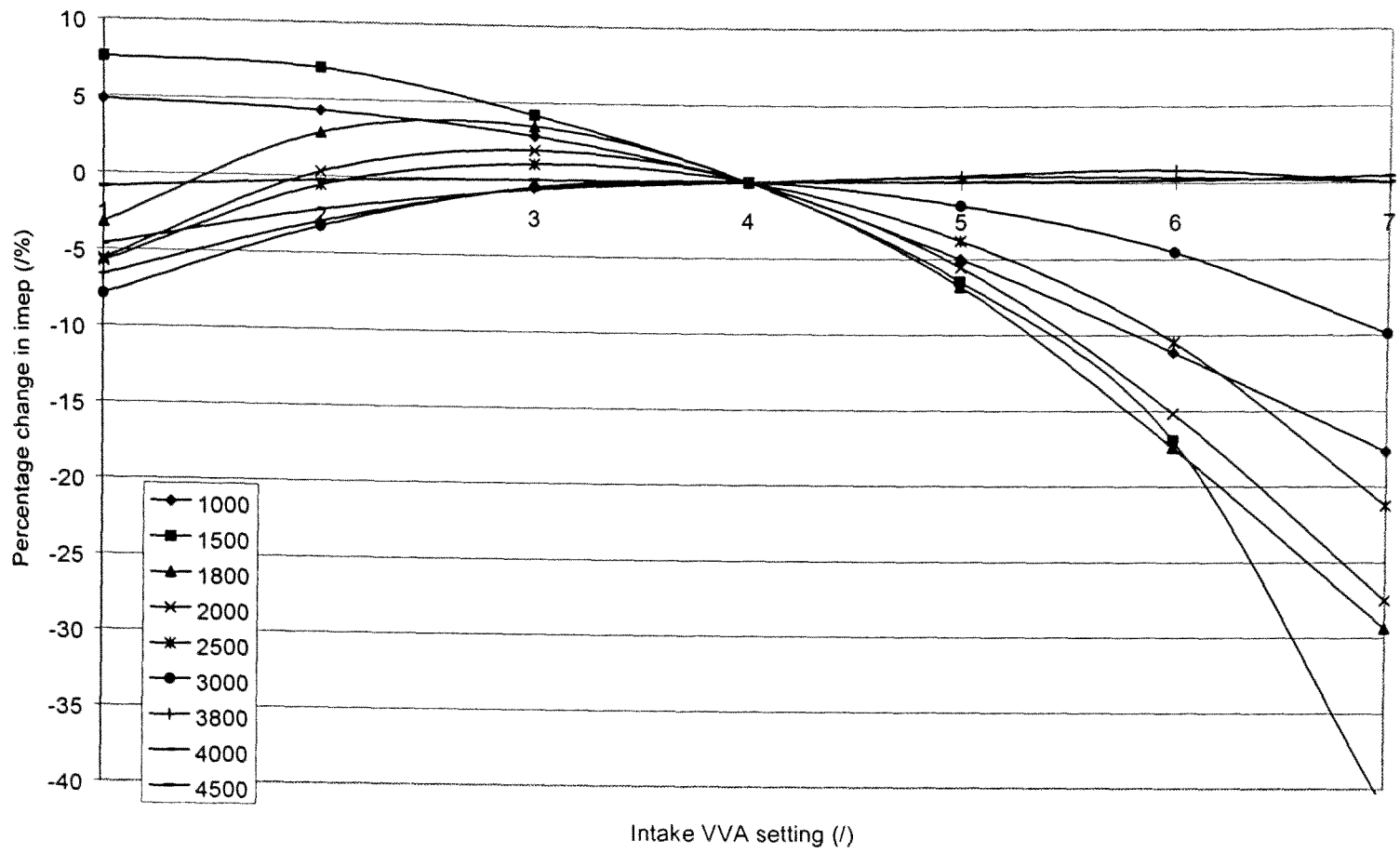


Figure5.1.3.2 Percentage change in imep as a function of intake valve closing timing over the full speed range.

The effect shown by this pair of graphs is the result of control of air flow, through modulation of volumetric efficiency. It is well known that intake valve closing is the dominant factor in determining volumetric efficiency in normally aspirated engines, especially if there is little valve overlap for exhaust system activity to influence the gas exchange process. In light duty diesel engines the high compression ratio typically means there is little overlap, so the induction stroke can be considered more or less in isolation and a strong link between intake valve closing timing and volumetric efficiency is expected. However, the presence of a turbocharger complicates this picture.

Figure 5.1.3.3 shows the percentage change in volumetric efficiency referred to ambient conditions and *figure 5.1.3.4* shows the percentage change in volumetric efficiency referred to manifold conditions. This distinction is important as the operation of the turbo-charger affects the volumetric efficiency when referred to ambient conditions, whereas to a first approximation volumetric efficiency referred to manifold conditions is a function only of speed and IVC. (Small effects caused by cylinder residual contents can alter the valve timing for the optimum volumetric efficiency.)

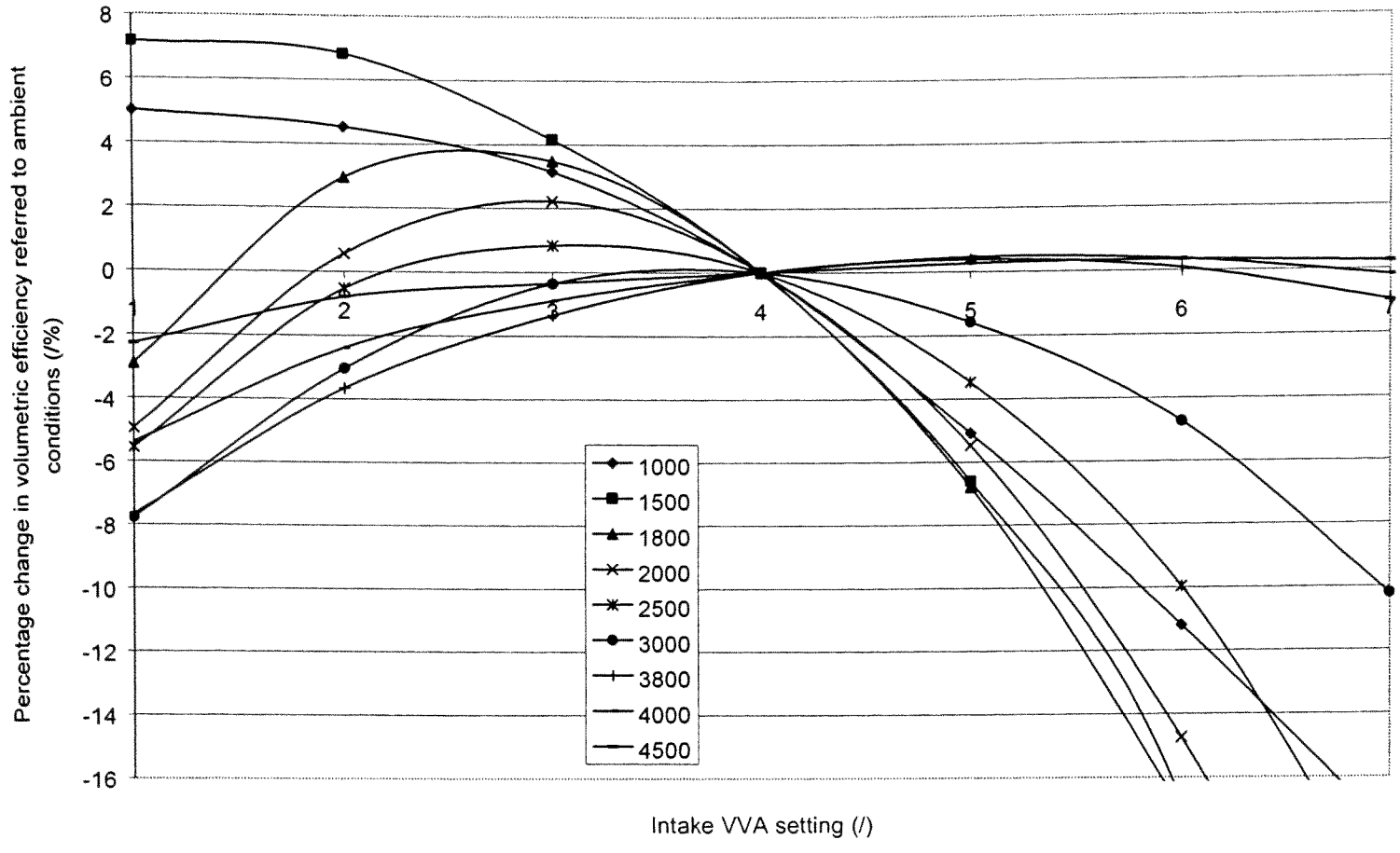


Figure 5.1.3.3 Volumetric efficiency referred to ambient conditions as a function of intake valve closing timing

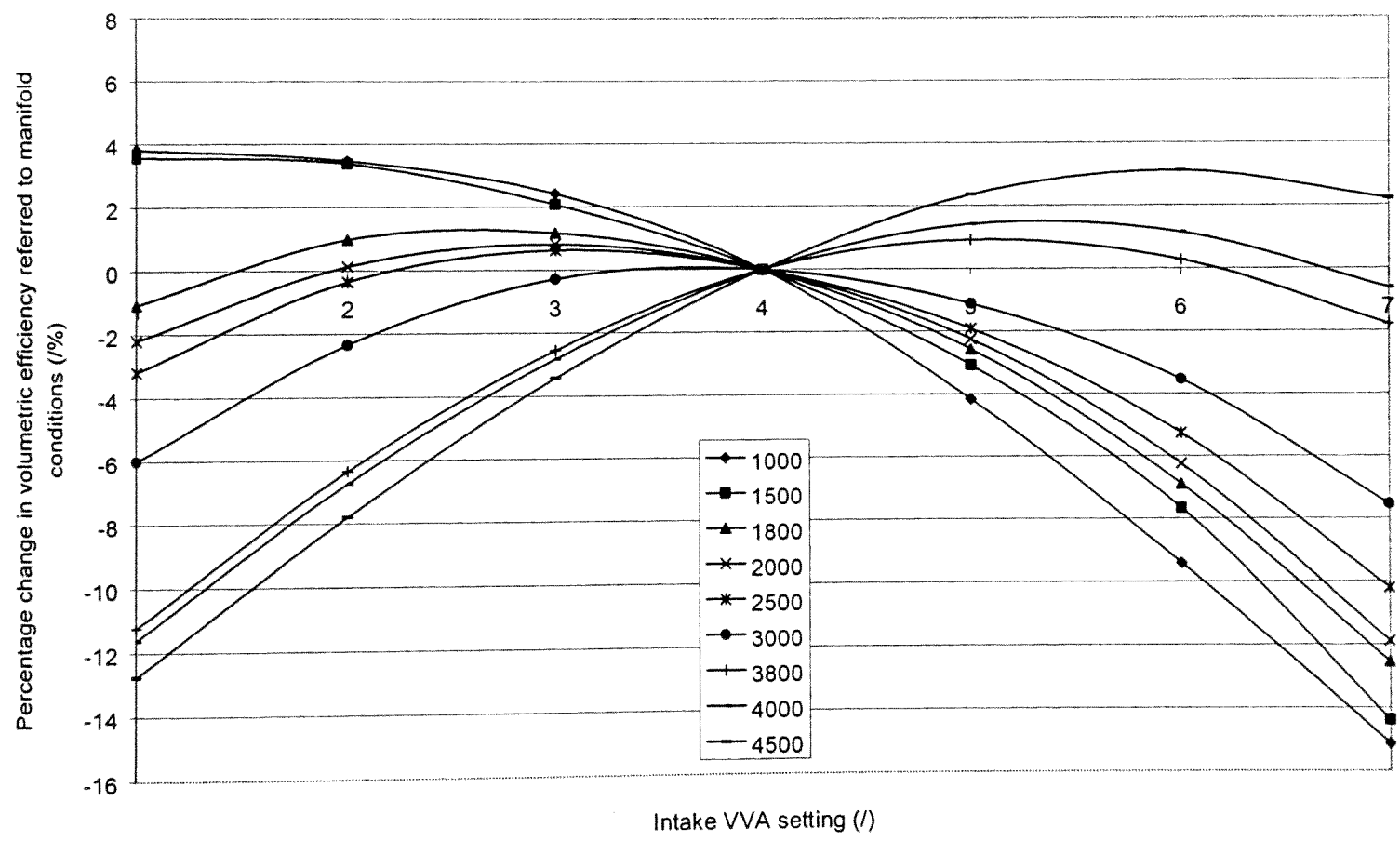


Figure 5.1.3.4 Volumetric efficiency referred to manifold conditions as a function of intake valve closing timing

The extent to which the turbo-charger masks the true effect of intake closing VVA on volumetric efficiency can be seen by contrasting these two graphs. It masks the underlying effects of early IVC and hides the effects of later IVC at the higher speeds, making the determination of the optimum setting from the graphs referred to ambient conditions more difficult. This is

particularly so for the higher speeds (3800 to 4500 rpm) which have no clear maxima in the case of volumetric efficiency referred to ambient conditions.

However, inspection of the graphs of volumetric efficiency referred to manifold conditions does reveal clear maxima. For the work in investigating the effects of exhaust valve timing the values used for the intake valve timing were chosen from these curves.

Comparing *figures 5.1.3.2* and *5.1.3.3* shows that the percentage changes in volumetric efficiency referred to ambient conditions are very similar in magnitude to the percentage changes in imep. This is to be expected as the amount of fuel injected is proportional to the air flow and the combustion characteristics of the model are fixed for each speed.

However, it is interesting to note that for speeds up to and including 2500 rpm the changes in volumetric efficiency related to ambient conditions, produced by earlier than standard IVC, are greater than those referred to manifold conditions. At 3000 rpm the standard IVC is near optimum, whilst at 3800 rpm and above the volumetric efficiencies related to ambient conditions are lower than those referred to manifold conditions. This trend with increasing engine speed highlights the importance of the operational limitations of other systems such as the turbine and particularly the compressor, and of other aspects of operation related to the unwanted pumping work carried out during the cycle, as it is a combination of these that is restricting the output at the higher speeds.

In seeking to identify the factors limiting the influence of IVC on performance further analysis was carried out. Since the setting of the VGT and the exhaust valve timing were held constant for this first stage of the investigation and the only way in which IVC can influence output (if the exhaust is separately optimised) is through volumetric efficiency, it was considered that to a good approximation the influence of the exhaust side could be ignored and the investigation concentrated on the work carried out in the engine in the period from TDC overlap ,TDC(o), to start of injection, SOI. In this period 6 different work quantities were investigated, 3 simply bounded: TDC(o) to BDC, BDC to IVC and IVC to SOI, and 3 compound quantities crossing boundaries: TDC(o) to IVC, BDC to SOI and finally TDC(o) to SOI. In addition air mass flow, absolute manifold pressure and isfc were investigated to see if extra insight was available from these. Of the work quantities, only the total work, from TDC(o) to SOI appears to correlate directly with the engine output. See *figure 5.1.3.5.*

Inspection of *figure 5.1.3.1* showing the imep characteristics, and *figure 5.1.3.5* below, shows that the maxima of the imep curves coincide with the minima in the curves of work from TDC(o) to SOI.

The reason for the high efficiency of the turbo-charged diesel is that, when the turbo-charger is producing boost, positive work is done on the piston from TDC(o) to BDC. See *figure 5.1.3.6.* However, it can be seen from *figure 5.1.3.5* that the negative work carried out during the compression stroke (BDC to TDC) is significantly greater, as these curves include the effects of the work from TDC(o) to BDC. The work from IVC to TDC could be considered as recoverable if EVO and IVC were mirrored and no fuel was added. Therefore, the minima of work from TDC(o) to SOI can be considered as a reflection of maximum trapped mass, as the compression work is directly related to trapped mass. This is borne out by *figure 5.1.3.7*, which shows curves for the air flow rate through the engine and again demonstrates the link between air flow and engine output through the AFR control.

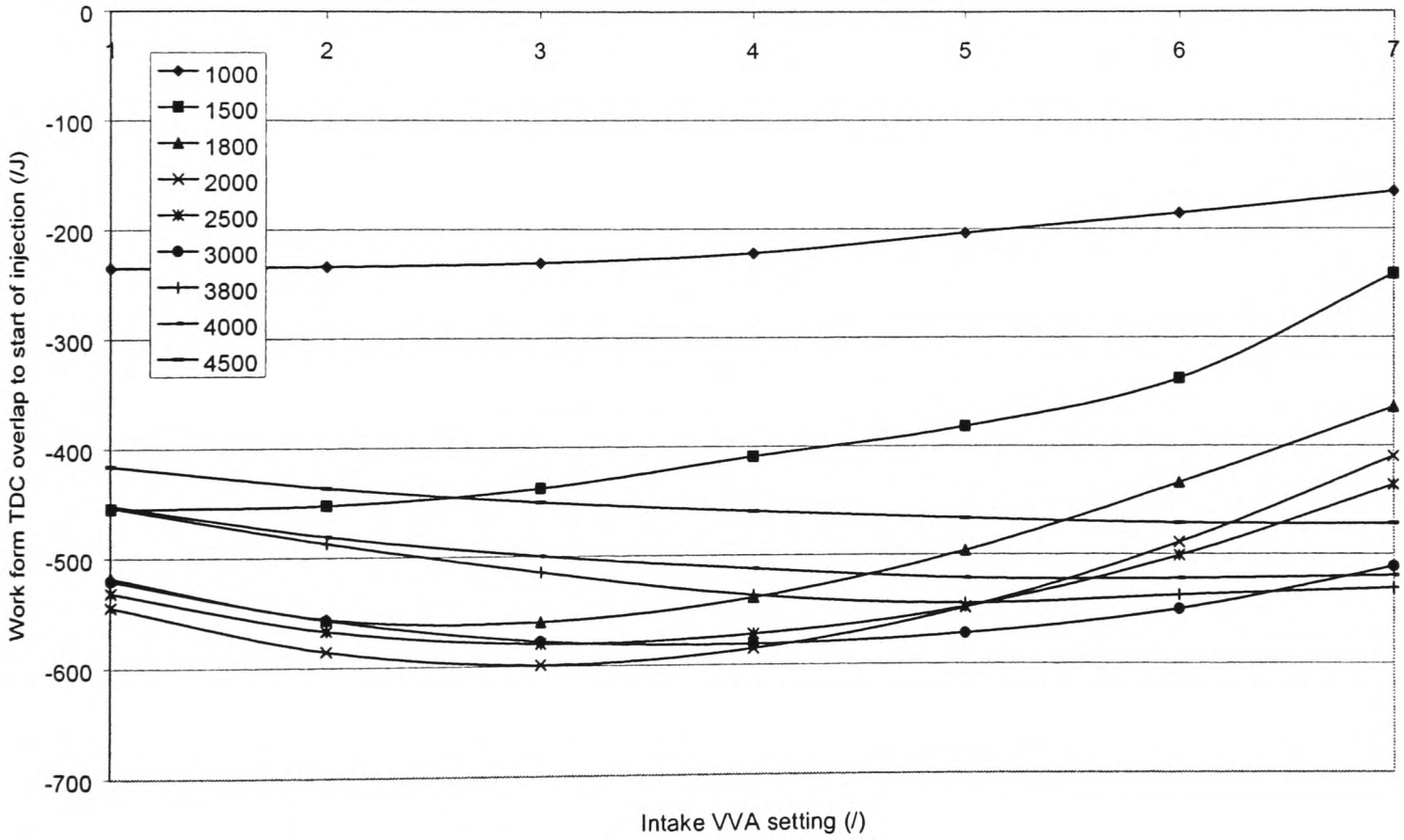


Figure 5.1.3.5 Work from TDC(o) to SOI.

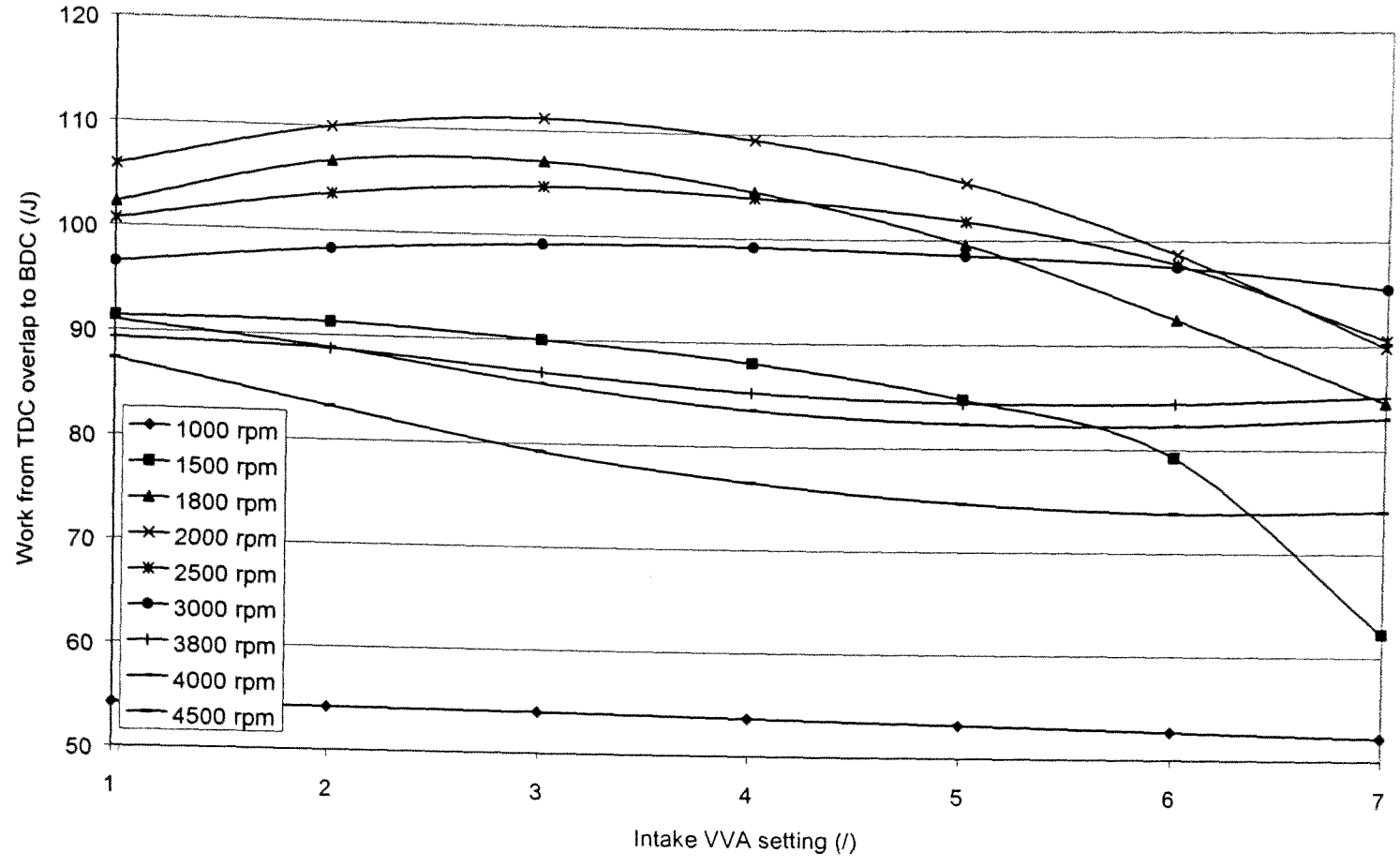


Figure 5.1.3.6 Work from TDC overlap to BDC

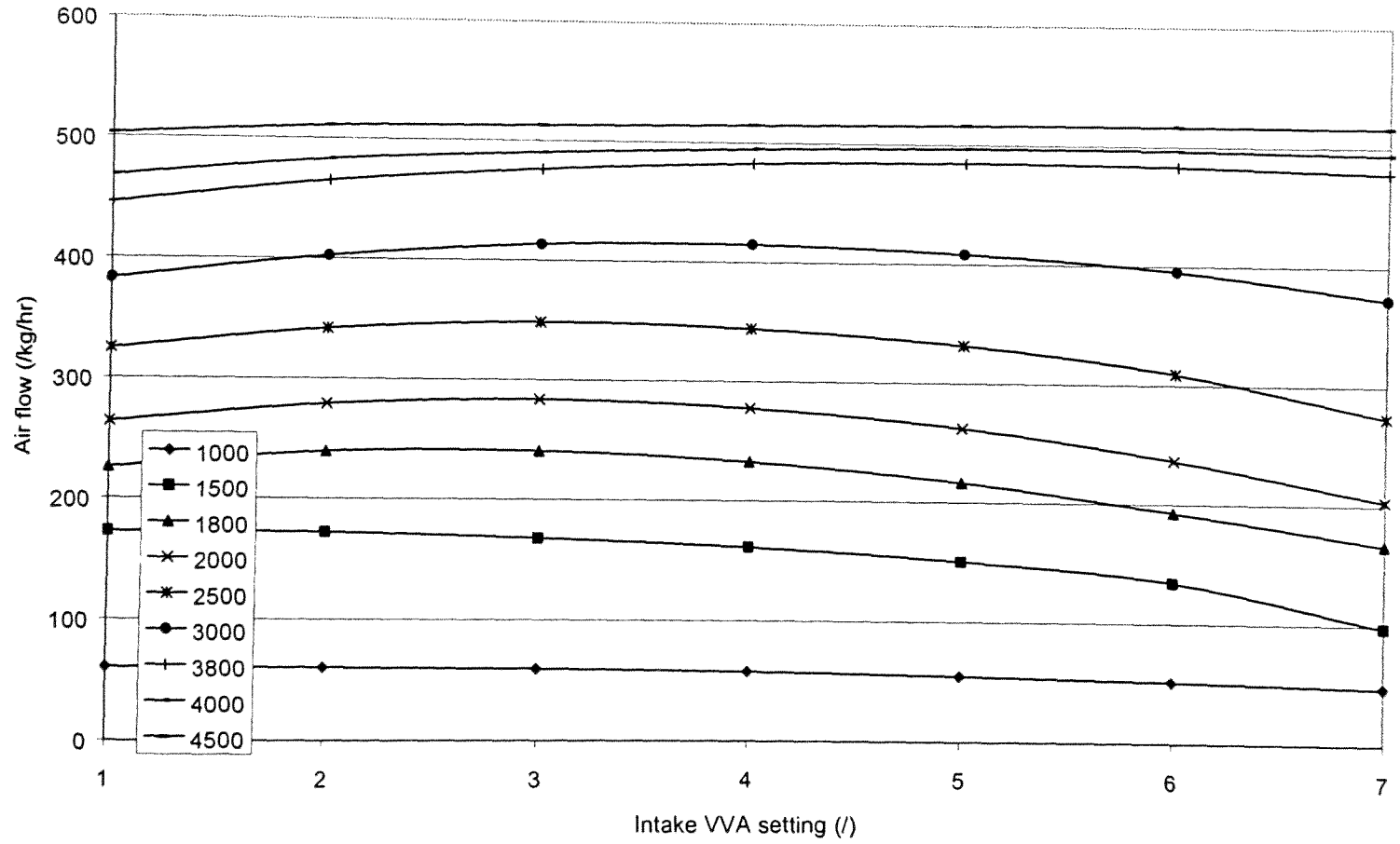


Figure 5.1.3.7 Engine mass air flow rates

It may be thought that maximum air flow would occur at the highest boost pressure, but further investigation showed that this is not always the case. *Figure 5.1.3.8* shows the absolute manifold pressure curves for the various engine speeds. Contrasting these curves with air flow curves of *figure 5.1.3.7* shows that for the speeds up to and including 3000 rpm the peak boost pressure and

peak air flow conditions do correspond, but for the higher speeds the highest mass flows actually correspond to the minimum boost levels.

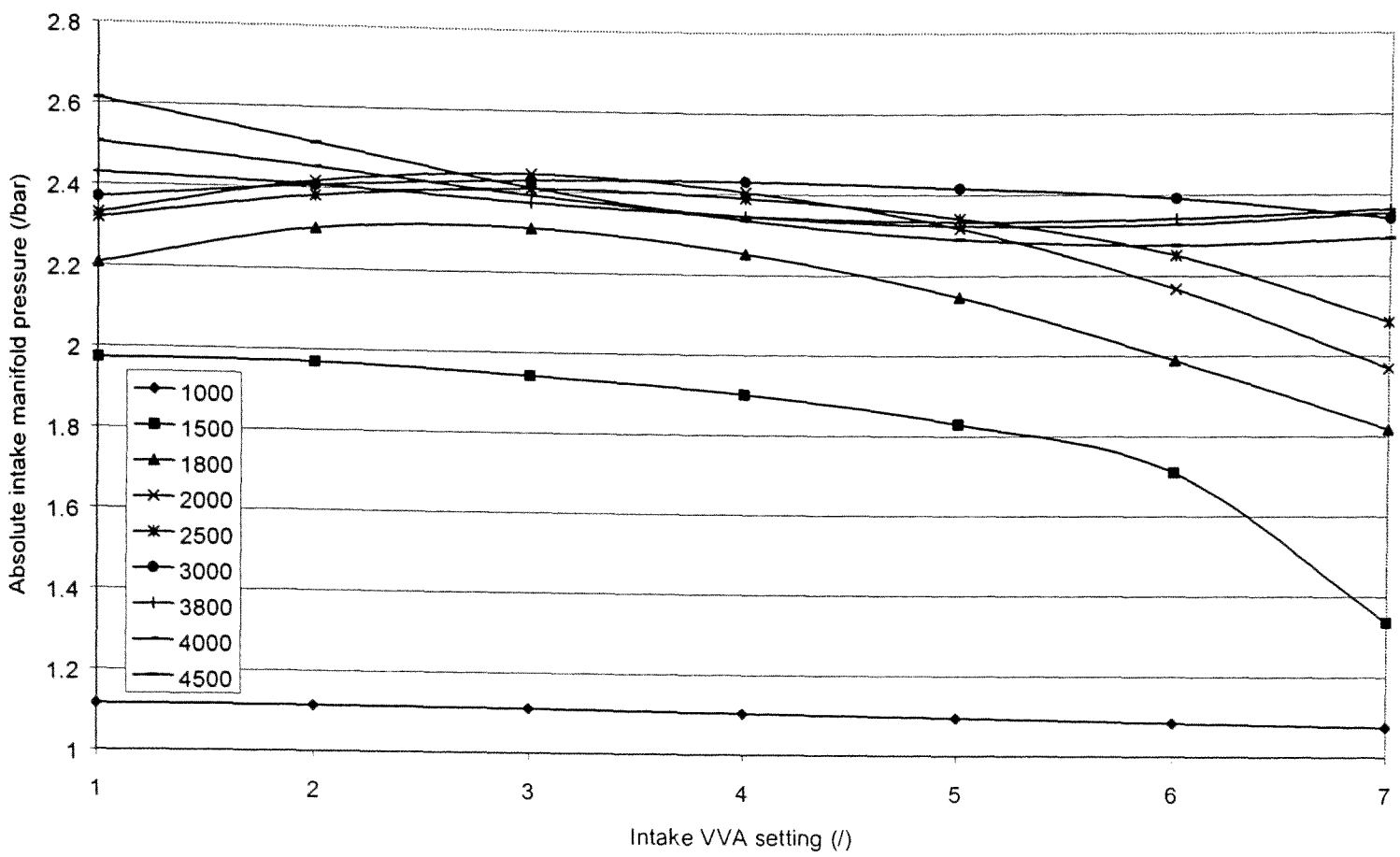


Figure 5.1.3.8 Absolute intake manifold pressure.

An explanation for this can be found by inspecting the operating points of the compressor on its efficiency map. See *figure 5.1.3.9*. The operating points, start with 1000 rpm in the bottom left of the map and generally move up in pressure ratio and mass flow with increasing speeds.

At the speeds from 1000 rpm up to and including 2500 rpm it can be seen that increasing the mass flow has the effect of increasing the compressor efficiency, at 3000 rpm it has little or no impact as it is operating around its maximum efficiency, but for higher speeds it can be seen that increasing the mass flow can only be achieved with a reduction in compressor efficiency. (This leads to an increase in temperature, a reduction in density and an increase in the power required for a given mass flow rate.) It is considered that this is the explanation for the differences in behaviour between the low speeds, where significant increases in output can be achieved, and the very limited response of the engine to IVC at the high speeds. This effect has significance to the evaluation of the exhaust VVA. (See section 5.1.4.)

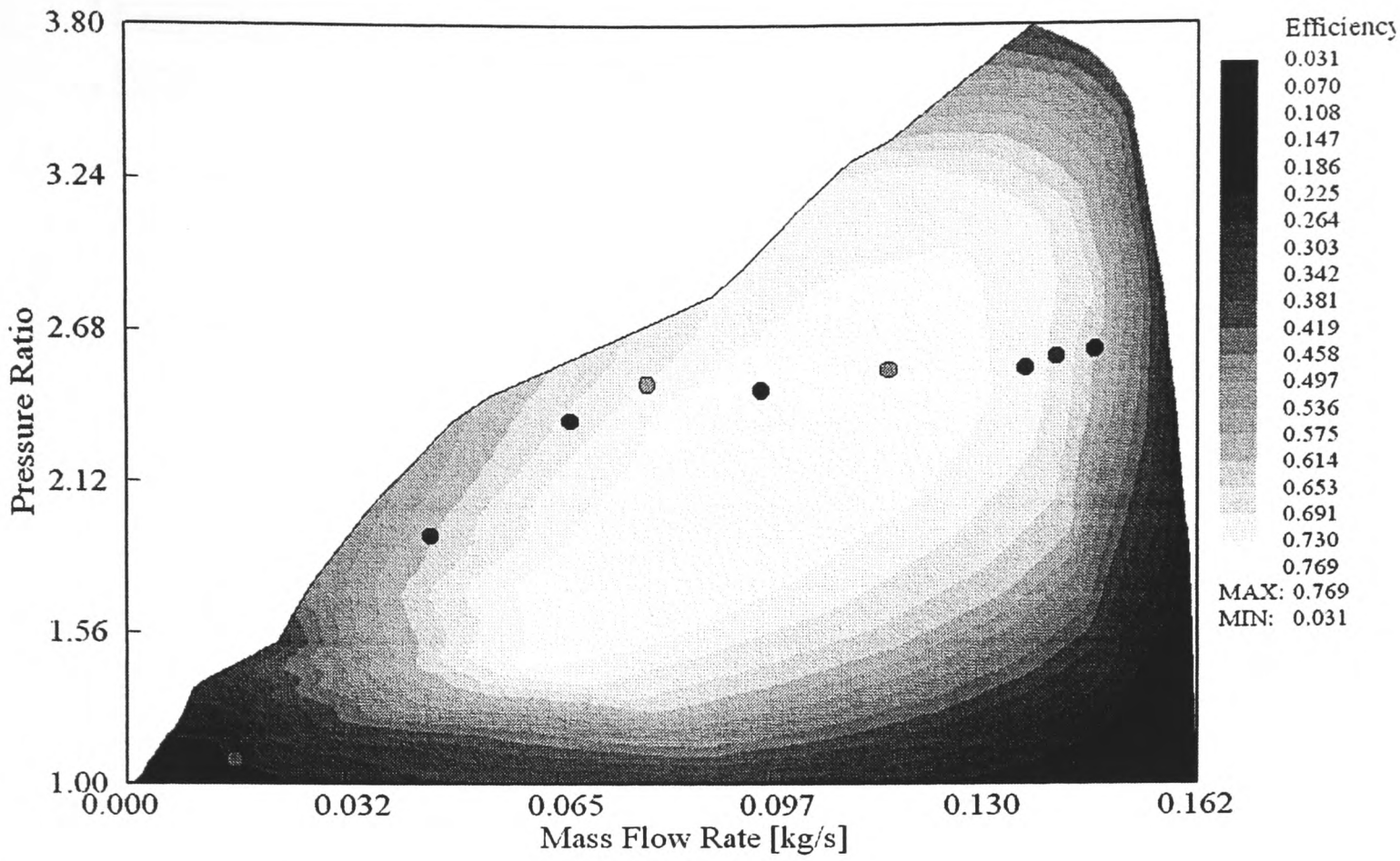


Figure 5.1.3.9 Compressor operating points for the operating speeds (1000 rpm bottom left, trend upwards to the right with increasing speed. Standard valve timings).

Figure 5.1.3.10 shows the effects of intake valve timing on pmep. Here pmep is defined from EVO to IVC, to take into account the positive work done on the piston, above BDC, after the exhaust valve has opened, and the negative pumping work done between BDC-intake and IVC. (It should be noted that a positive value for pumping work in this context means there is positive work output.) *Figure 5.1.3.10* also shows that at all speeds the trend is for pumping work to decrease with retarding IVC, but at the lower speeds the values remain positive over a larger range of IVC timings. However, as the engine speed rises the pmep becomes negative earlier in the IVC range and at 4500 is negative for all IVC timings investigated. In reviewing the proposed intake VVA settings against the pumping curves in *figure 5.1.3.10*, it can be seen that at the lower speeds the optimum intake valve closing timing occurs at the highest pumping work values, (+ve is good), and as the speed increases so the pumping work deteriorates such that at 3800 rpm and above, at the optimum valve timings for maximum volumetric efficiency referred to manifold conditions, the pumping work is negative.

The detailed constituents of the pumping work show that there are two dominant factors in this pmep trend. These are associated with the exhaust valve timing, which was held constant for this first part of the investigation, and the restrictions imposed by the turbine and compressor. These factors are dealt with in more detail in the next section.

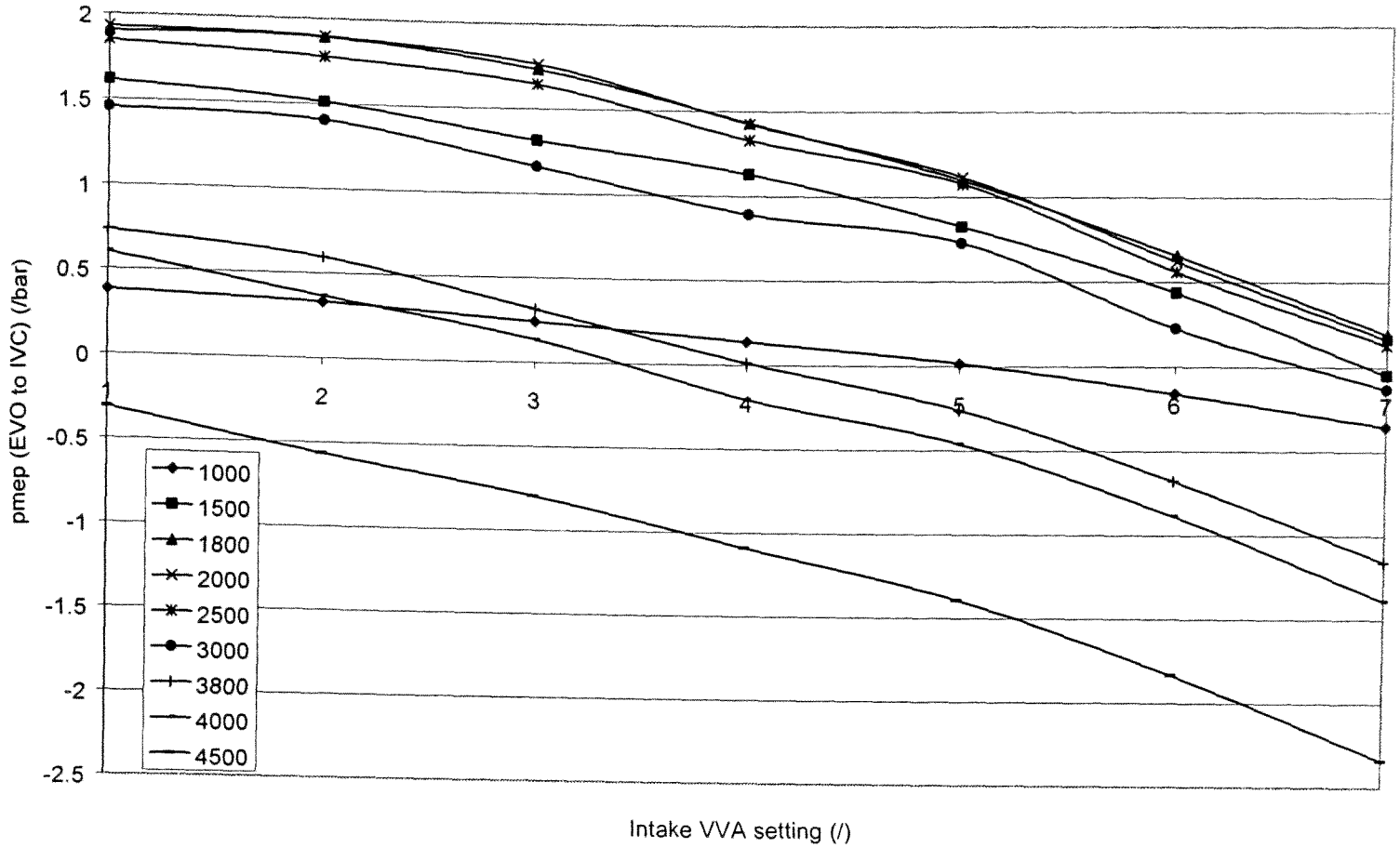


Figure 5.1.3.10 pmep as a function of intake valve timing and engine speed

To summarise: It was found that improvements in engine output could be achieved by optimisation of the intake valve timing, with the benefits largest at the low speeds, where earlier IVC was advantageous. No benefit was available at 3000 rpm as optimum IVC was standard, but at the higher speeds small improvements in output could be achieved by retarding IVC. These primary results are summarised in *table 5.1.3.1.* Trends were also identified that at the higher speeds, and consequent higher mass flow rates, the adverse compressor efficiency and exhaust pumping work characteristics limited the ability of IVC to improve volumetric efficiency.

Turning to the use of these results as adjustments to the model for the investigation of the effects of exhaust VVA on engine output, *table 5.1.3.1* summarises the intake VVA settings for optimum volumetric efficiency relative to manifold conditions and the improvements in imep available with intake VVA alone.

Speed/rpm	1000	1500	1800	2000	2500	3000	3800	4000	4500
Optimum Intake VVA setting (/)	**1**	**1**	**2**	**3**	**3**	**4**	**5**	**5**	**6**
Imep (/bar)	**9.56**	**18.8**	**21.1**	**21.4**	**20.7**	**19.9**	**17.9**	**17.4**	**14.2**
Improvement in imep over std (/%)	**4.8**	**7.6**	**3.5**	**1.9**	**1.0**	**0**	**0.9**	**0.4**	**0.5**

Table 5.1.3.1 Summary of imep values, resultant improvements over standard and the intake VVA settings optimised to achieve them, with standard exhaust valve timings

5.1.4 Intake and exhaust VVA

To recap, for this part of the investigation the intake valve timings were fixed at the nearest integer setting to maximum volumetric efficiency referred to manifold conditions. These were as follows: "1" for 1000 rpm and 1500 rpm, "2" for 1800 rpm, "3" for 2000 rpm and 2500 rpm, "4" for 3000, "5" for 3800 rpm and 4000 rpm, and "6" for 4500 rpm, and AFR and VGT settings were held constant at the baseline values. For this next stage of the investigation the exhaust opening timing was varied over its full range for each of the operating speeds with the intake VVA setting as itemised above. The investigation looked at overall performance parameters, such as imep (where very significant increases were found at low speeds), at the details of the work distribution in the cycle (particularly in the expansion/exhaust half cycle), and at the operational limitations of the turbocharger.

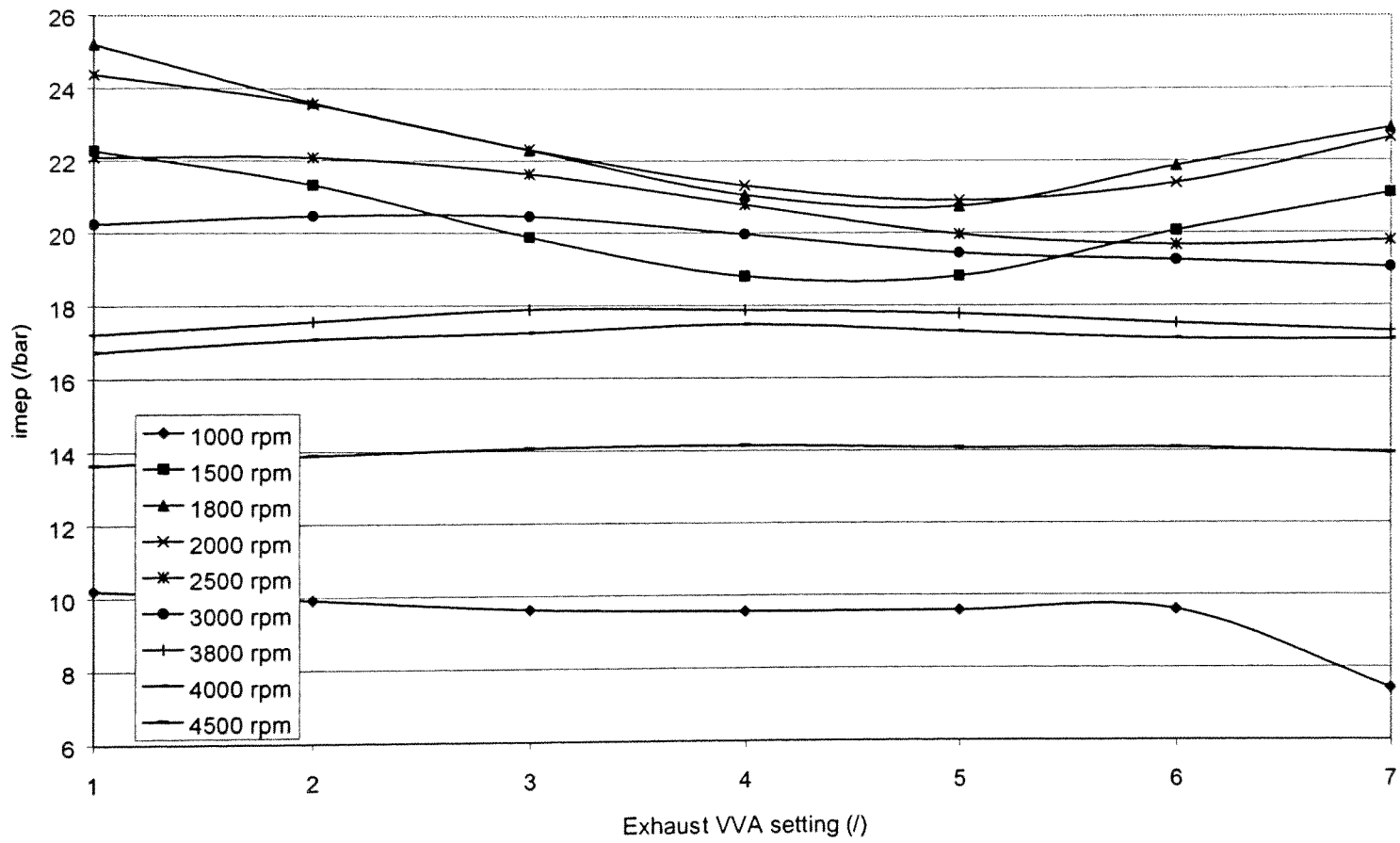


Figure 5.1.4.1 Variation in imep with varying exhaust valve opening timing and optimised intake valve closing.

Figure 5.1.4.1 shows the imep curves resulting from the exhaust VVA simulation sweeps at the optimised intake VVA settings. *Figure 5.1.4.2* shows these changes expressed as percentages of the values obtained with the standard exhaust timing (but with optimised intake timing). It can be seen from *figures 5.1.4.1* and *5.1.4.2* that for the speeds up to and including 2000 rpm the imep could be increased by either retarding or advancing the exhaust valve opening timing from standard, although retarding produced the larger increase. For speeds of 2500 rpm and 3000 rpm, retarding EVO, relative to standard, provided improvements in imep, whilst for the speeds from

3800 upwards the standard EVO appeared to be near optimal. Unlike intake valve closing, which primarily affected volumetric efficiency referred to manifold conditions, EVO affected the expansion work, the interaction between the exhaust gases and the turbine and their associated pumping work, as well as affecting the air mass flow through the engine via its influence on the power available to the compressor.

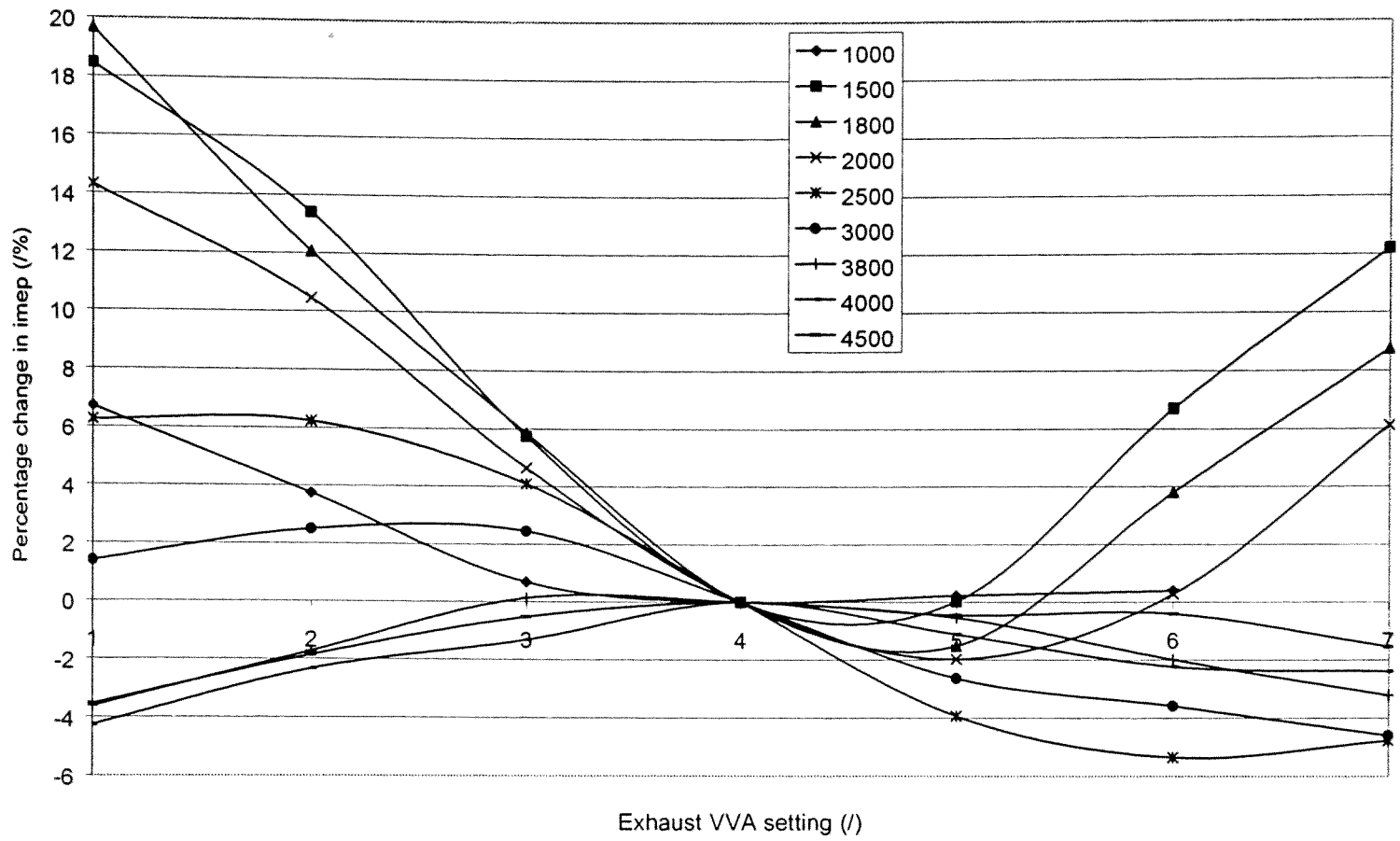


Figure 5.1.4.2 Percentage change in imep (relative to standard exhaust valve timing) with varying exhaust valve opening timing and optimised intake valve closing.

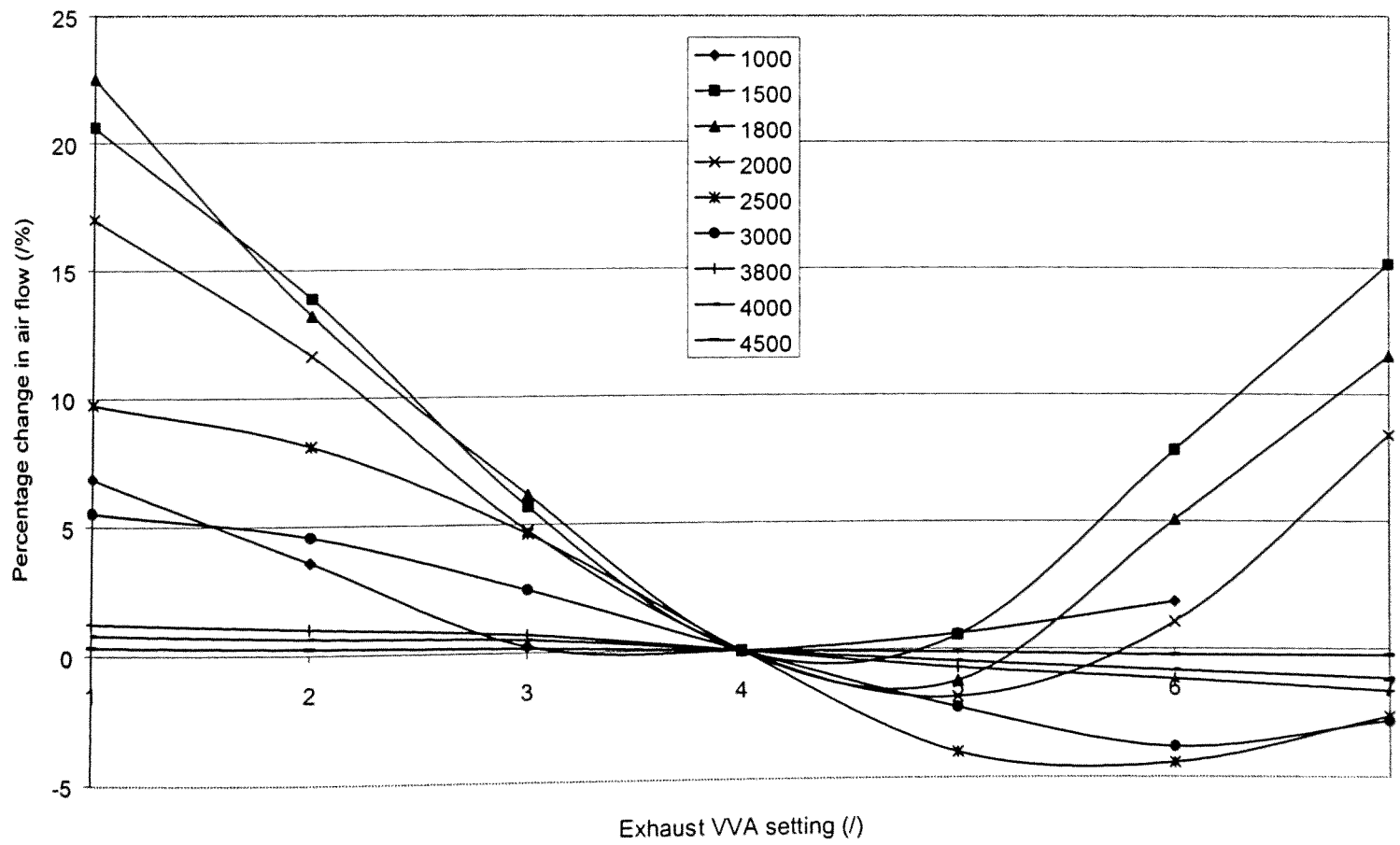


Figure 5.1.4.3 Percentage change in air flow with varying EVO

It can be seen from *figure 5.1.4.2* that the impact of exhaust valve opening timing varies significantly with engine speed: whilst large increases in imep are available at the lower speeds, little improvement is available at 3800 rpm and above. These two speed groups will now be discussed individually.

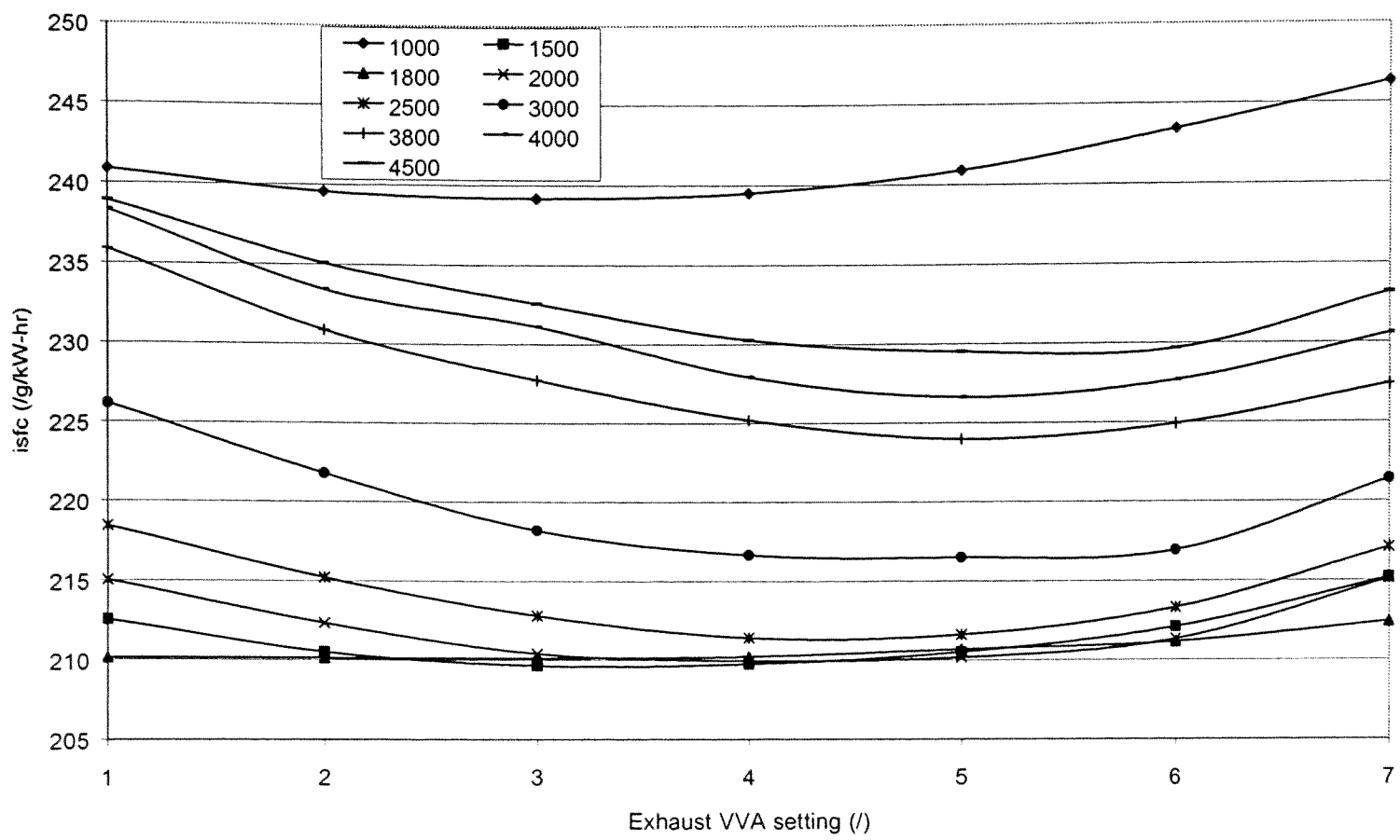


Figure 5.1.4.4 The effect of exhaust VVA on isfc

Speeds below 3000 rpm: It can be seen that, in this lower speed range there are significant increases in imep available, up to 19%, particularly from retarding EVO. However, it is not all beneficial: contrasting *figures 5.1.4.2 and 5.1.4.3*, shows that the imep improvements available are smaller than the changes in air flow through the engine. This indicates that there is an overall drop in efficiency and an increase in specific fuel consumption associated with these increases in output. Comparison of *figure 5.1.4.2* with *figure 5.1.4.4,* demonstrates that increases in output are associated with increased isfc.

Figure 5.1.4.5 shows the large changes in expansion work achieved by varying EVO. At speeds of 1500, 1800 and 2000 rpm increases of output could be achieved by both earlier and later than standard timings, whereas for the middle speeds, 2500 rpm and 3000 rpm, useful improvements were demonstrated only by retarding EVO and they were smaller than at the lower speeds.

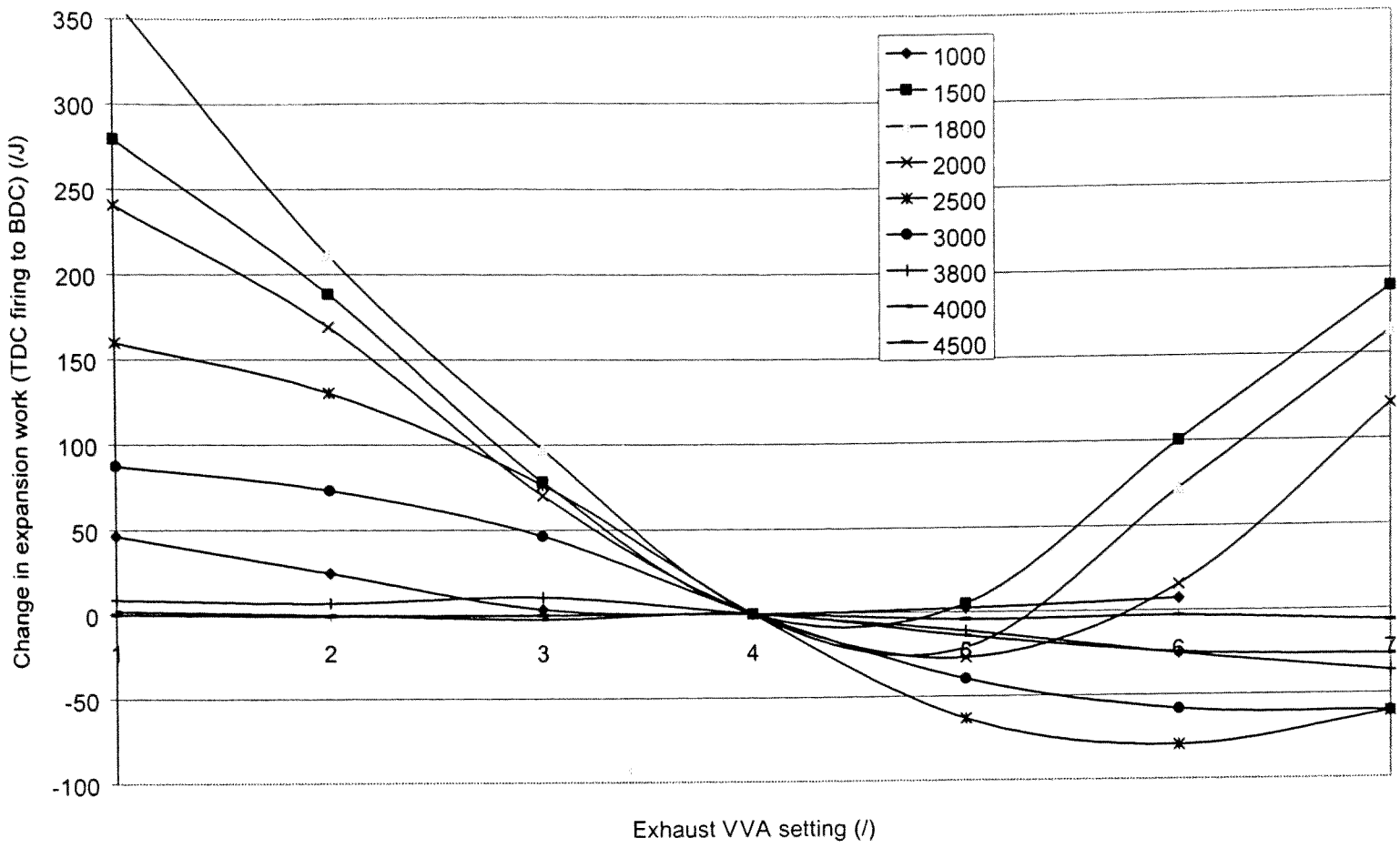


Figure 5.1.4.5 Changes in expansion work with varying EVO

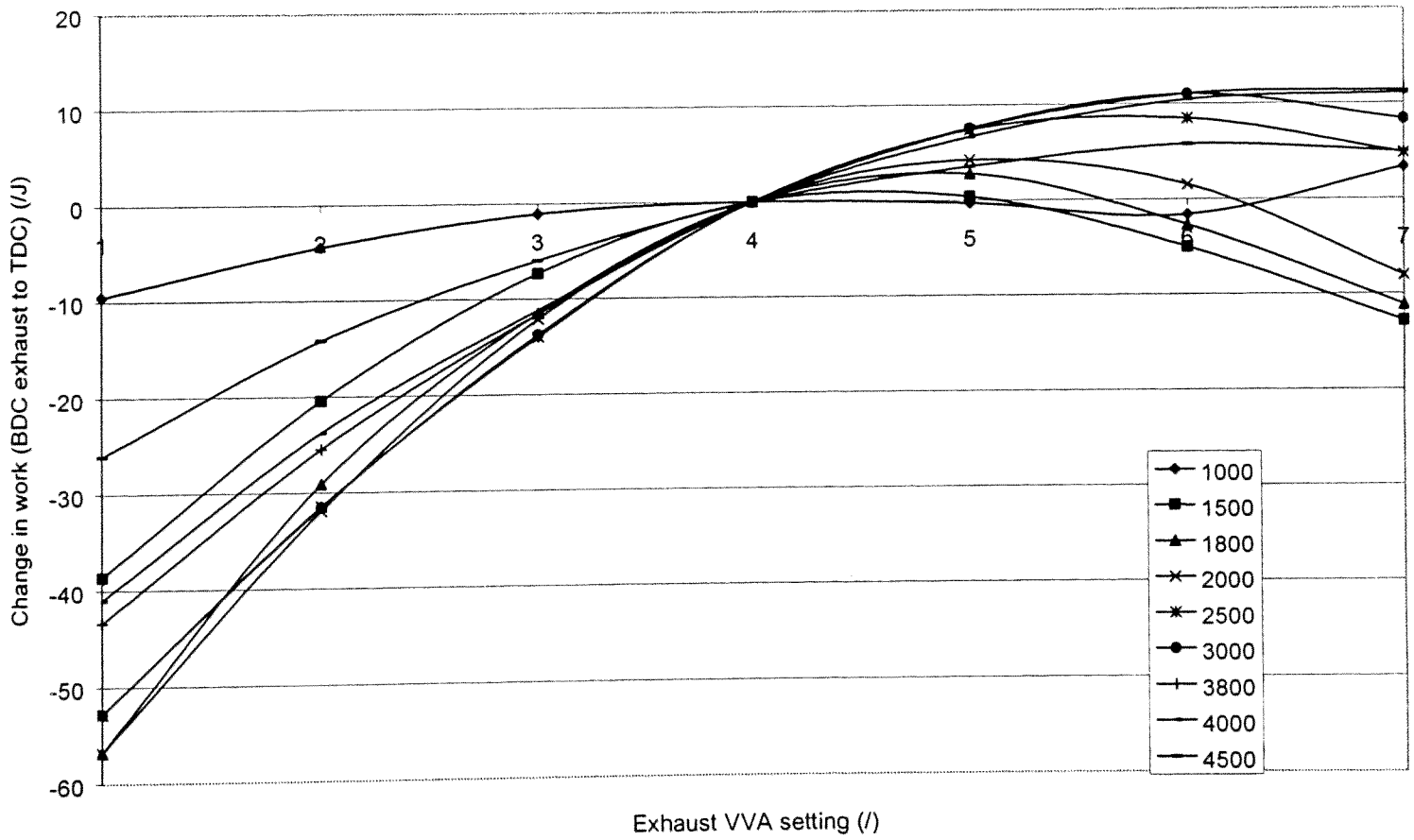


Figure 5.1.4.6 Change in exhaust pumping work with varying EVO

Figure 5.1.4.6, shows the change in exhaust pumping work with varying EVO and as expected, it can be seen that retarding EVO, produced an increase in exhaust pumping work and advancing EVO produced a decrease in exhaust pumping work. However, the key to increasing output by manipulation of the exhaust valve timing is the relationship between the changes in expansion work and exhaust pumping work. *Figure 5.1.4.7* shows the change in total work, from TDC(f) to

TDC(o), as a function of EVO. This, in combination with *figures 5.1.4.5* and *5.1.4.6*, shows why at the lower speeds significant change in output was possible, where the change in expansion work significantly exceeded the increase in pumping work.

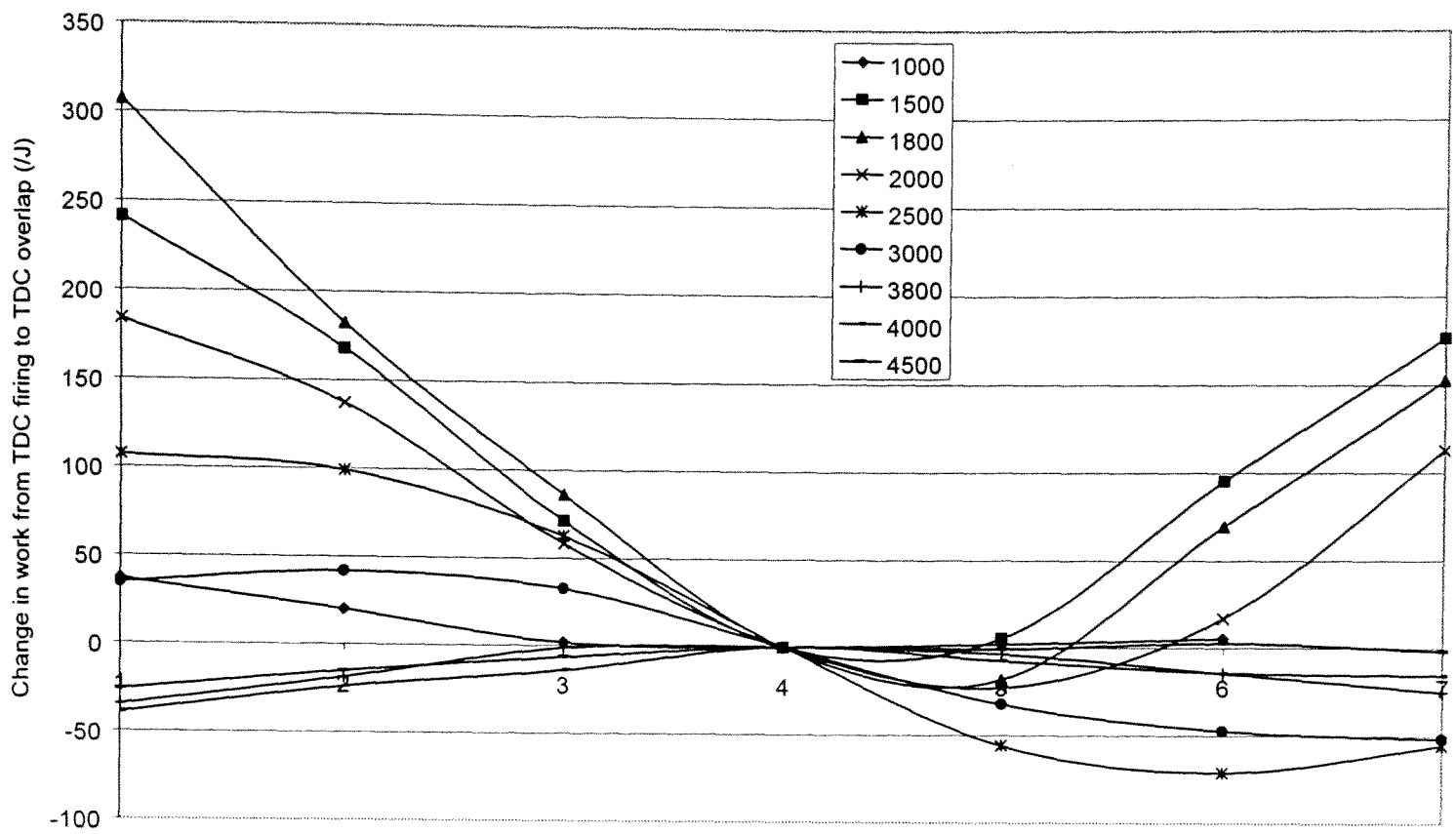


Figure 5.1.4.7 Change in total work from firing TDC to Overlap TDC with changing EVO.

High speeds, 3800 rpm and above: At these speeds, consideration of the change in air flow through the engine, *figure 5.1.4.3* shows a different trend from the imep in *figure 5.1.4.2*, with earlier EVO producing a slight increase in air flow, whilst the imep was lowered. This difference in trend at the higher speeds can, again, be explained by consideration of the work carried out during the half cycle from TDC (f) to TDC(o). *Figure 5.1.4.5* shows the change in work during the expansion stroke and *figure 5.1.4.6* the change in exhaust pumping work, both with respect to changing EVO.

Figure 5.1.4.6, shows the expected changes in exhaust pumping work with retarded EVO producing an increase in exhaust pumping work and advanced EVO producing a decrease. *Figure 5.1.4.7* shows the change in total work, from TDC(f) to TDC(o), as a function of EVO. This, in combination with *figures 5.1.4.5* and *5.1.4.6*, shows why at these higher speeds no significant change in output was possible: for retarded EVO the increase in exhaust pumping work exceeded the increase in expansion work and for advanced EVO the decrease in expansion work exceeded the decrease in exhaust pumping work. Three possible causes for this were identified: 1) the pressure in the cylinder between EVO and BDC was behaving as though the exhaust valves were

shut, i.e. the exhaust system and VGT were acting as restrictions to flow potentially through inappropriate nozzle settings, 2) the compressor was unable to use any extra power available from the turbine and 3) the compressor was acting as a restriction.

Dealing with the first of these, *figure 5.1.4.8* contrasts the maximum, average and minimum pressures in the duct immediately preceding the turbine entry at 1800 and 4500 rpm. It can be seen that at 4500 rpm the minimum pressure was greater than the average pressure at 1800 rpm, indicating the extent to which the exhaust system and turbine were restricting flow. However, from this data it was still not clear if this really was the restriction on high speed performance.

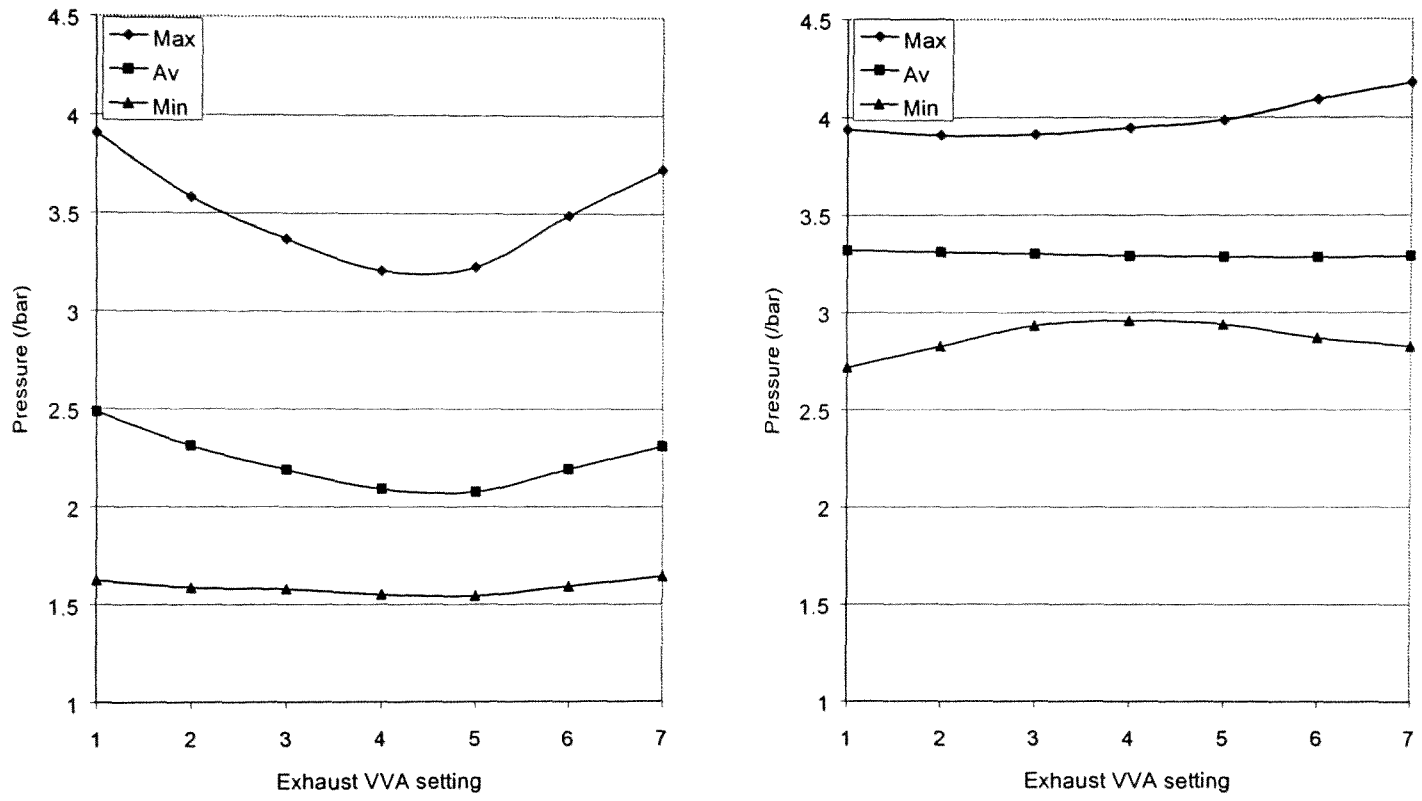


Figure 5.1.4.8 Cyclic maximum, average and minimum pressures in the pipe preceding turbine entry for 1800 rpm (left) and 4500 rpm (right) plotted against exhaust valve opening timing.

As was mentioned earlier the VGT settings used for the VVA studies were taken from the baseline runs, and were those required to produce the target boost levels, with the standard fixed fuelling and valve timings. It might be thought that at the rated engine speed the turbine nozzles would be fully open, but a combination of the overall engine control strategy used and making allowance for the higher turbine speeds required at altitude (to achieve the desired boost levels) actually produce the situation where the VGT nozzles are partially closed even at maximum engine speed. Therefore, it might be thought that to overcome the apparent restriction posed by the turbine opening the VGT nozzle rack might allow the engine to consume more air and produce more torque at the higher speeds.

To investigate this a series of simulations were carried out with the appropriate fixed intake valve timings for the speeds and varying the VGT setting and exhaust VVA settings.

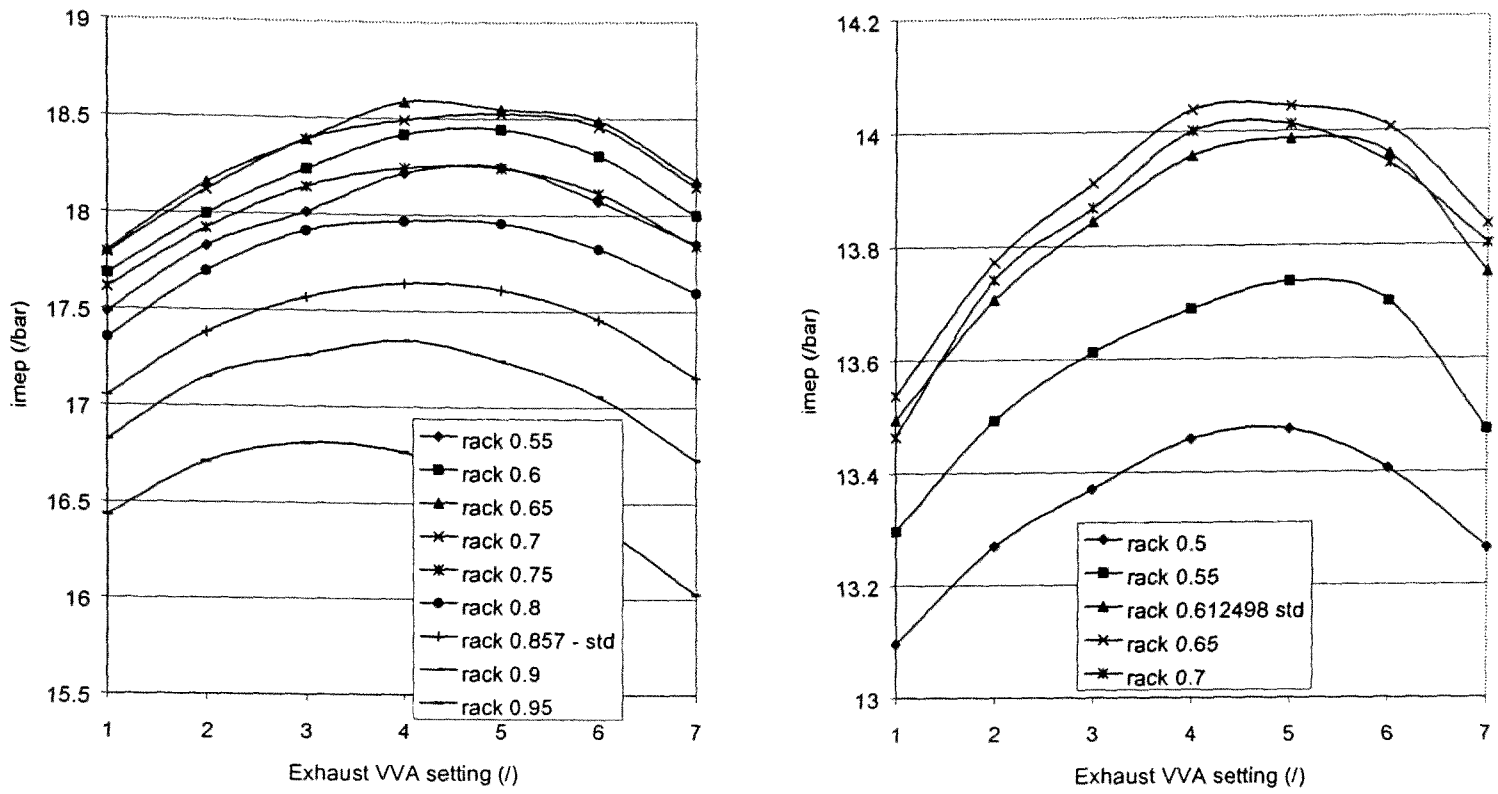


Figure 5.1.4.9 Variation in imep with VGT rack nozzle setting at 3800 rpm (left) and at 4500 rpm (right)

Despite the VGT settings appearing to be restrictive on the basis of the pumping work, at 3800 rpm it was found that more output could be achieved by further closing the VGT setting by up to 20%, *figure 5.1.4.9 (left)*. Beyond this output fell. This further closing of the VGT led to a maximum increase in imep of 5.3% (0.94 bar), with an associated increase of 1.7% in isfc, with optimum EVO for imep close to standard for all VGT settings, except the most open, which was advanced from standard.

As the speed was increased towards the maximum, it was found that the ability to increase output by closing the rack became more limited and ultimately at 4500 rpm the output could only be increased by opening the VGT. Opening the VGT setting by approximately 4% produced an increase of approximately 0.1 bar imep. *Figure 5.1.4.9 (right)* Associated with this was a reduction in isfc of 2.5%. Further opening of the VGT reduced output. Optimum EVO was again approximately standard. It is interesting to note that at 3800 rpm the full range of EVO timing investigated produced a range of approximately 0.7 bar imep and at 4500 rpm only 0.4 bar (contrasted with approximately 4 bar at 1800 rpm). These small increases in output still indicated that there was a restriction in the system and investigation of the airflow through the engine tended to confirm this. It was found that for all VGT settings at all of the higher speeds investigated the air flow fell monotonically with advancing EVO, see *figure 5.1.4.10*, and it is

interesting to note that maximum output did not coincide with either maximum airflow or boost pressure, pointing, again, to the compressor being the restriction.

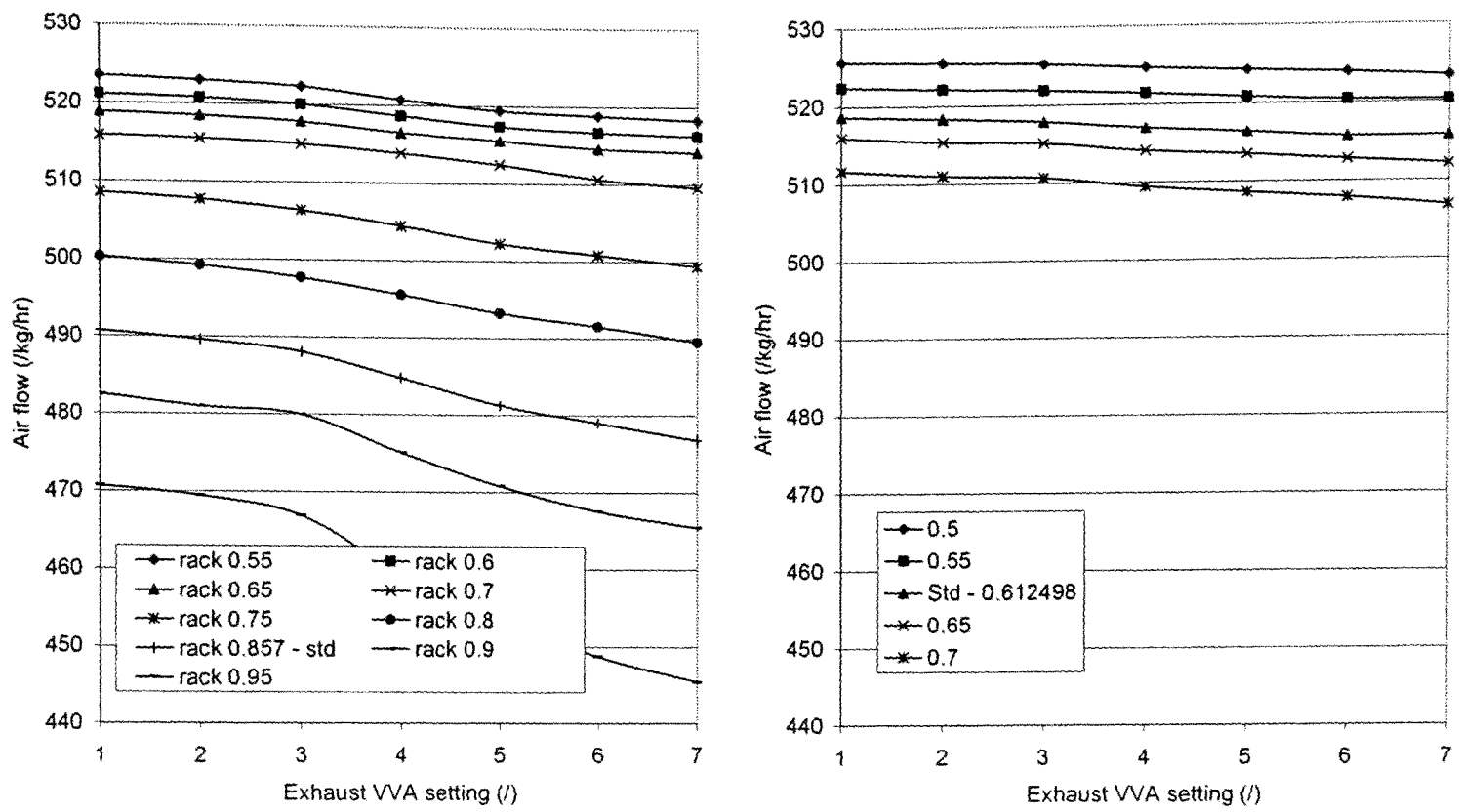


Figure 5.1.4.10 Variation of airflow with changing turbine rack and exhaust VVA at 3800 rpm (left) and 4500 rpm (right)

Investigation of the work distribution in the expansion and exhaust strokes provided some further insight: *figure 5.1.4.11* shows that at 4500 rpm there was almost no change in the work done in the whole expansion stroke, TDC(f) to BDC, irrespective of when EVO occurred, whilst advancing EVO reduced the unwanted pumping work done between EVO and TDC(o), but had little effect on the work done from BDC to TDC(o), so it can be seen that EVO timing had almost no effect on either total expansion work, TDC(f) to EVO plus EVO to BDC or exhaust work, from BDC to TDC(o).

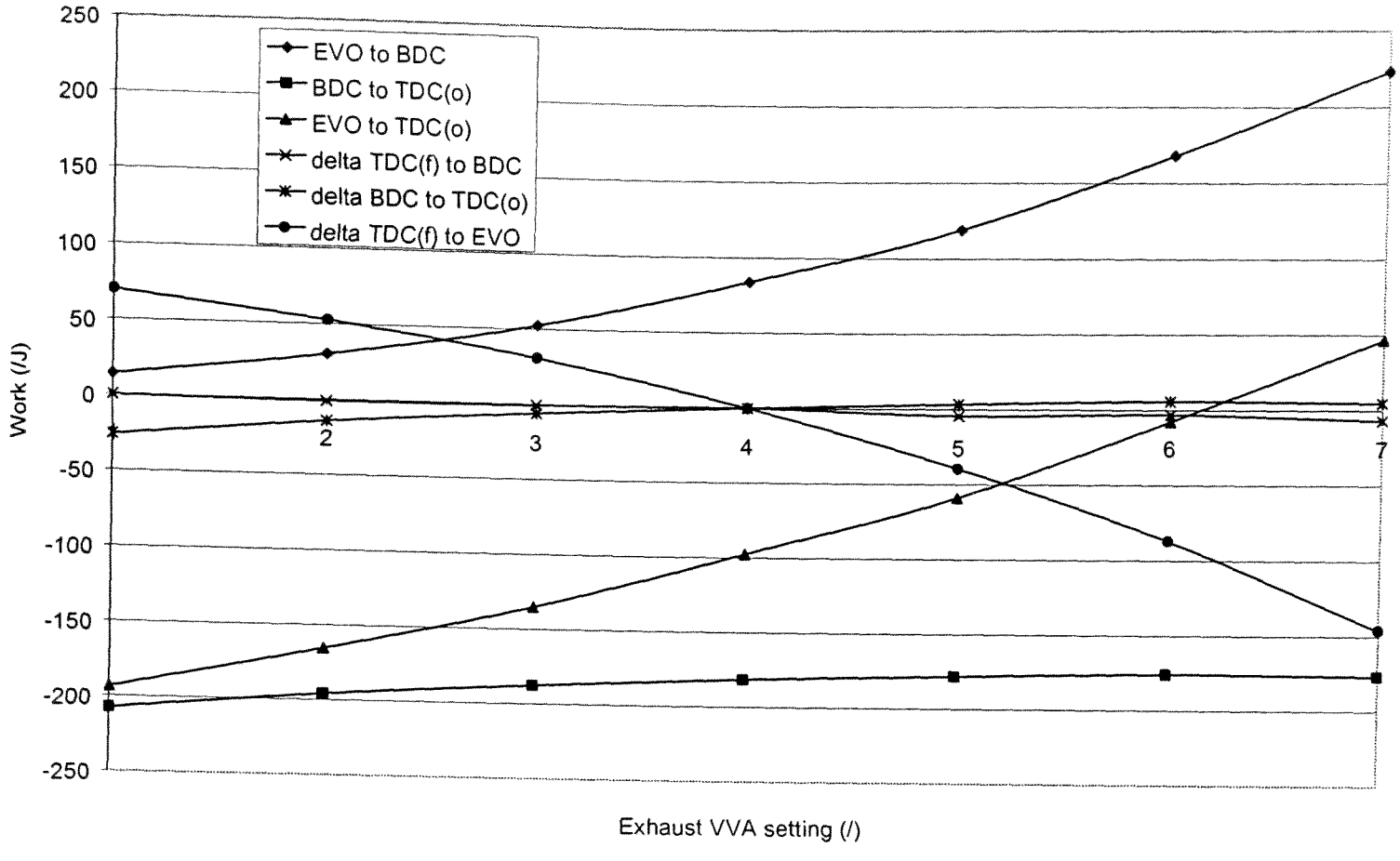


Figure 5.1.4.11 Work distribution in the expansion and exhaust strokes at 4500 rpm

Further, investigation of the cyclic pressures at turbine entry showed that, unlike the lower speeds, at the higher speeds the full range of EVO variation had little effect on these pressures. See *figure 5.1.4.8*. What is particularly noticeable in *figure 5.1.4.8* is the lack of response of the average pre-turbine pressure to variation in EVO. This lack of response to both early and late EVO, at higher speeds, is counter-intuitive as early EVO would normally provide a reduced pressure during the exhaust stroke and retarded EVO would normally produce a higher pressure in the exhaust stroke, (although these trends are visible in the maximum and minimum pressures.) Consideration of *figures 5.1.4.8* and *5.1.4.12* shows how close these pre-turbine pressures are to those in the cylinder.

Contrasting the pumping loop at the most advanced and retarded EVO settings with that for the standard EVO demonstrates another feature of the VVA at 4500 rpm. *Figure 5.1.4.12* shows that with late EVO for the majority of the exhaust stroke the cylinder pressure was higher than that with standard or early EVO. In contrast, with early EVO the cylinder pressure during the majority of the exhaust stroke was lower than with late or standard EVO. However, it also displayed a sharp upturn of pressure in the cylinder towards the end of the exhaust stroke. These features display the trade-offs between the work done in the various parts of the expansion and exhaust strokes as discussed above. However, the upturn in pressure at the end of the exhaust stroke with early EVO is also worthy of discussion:

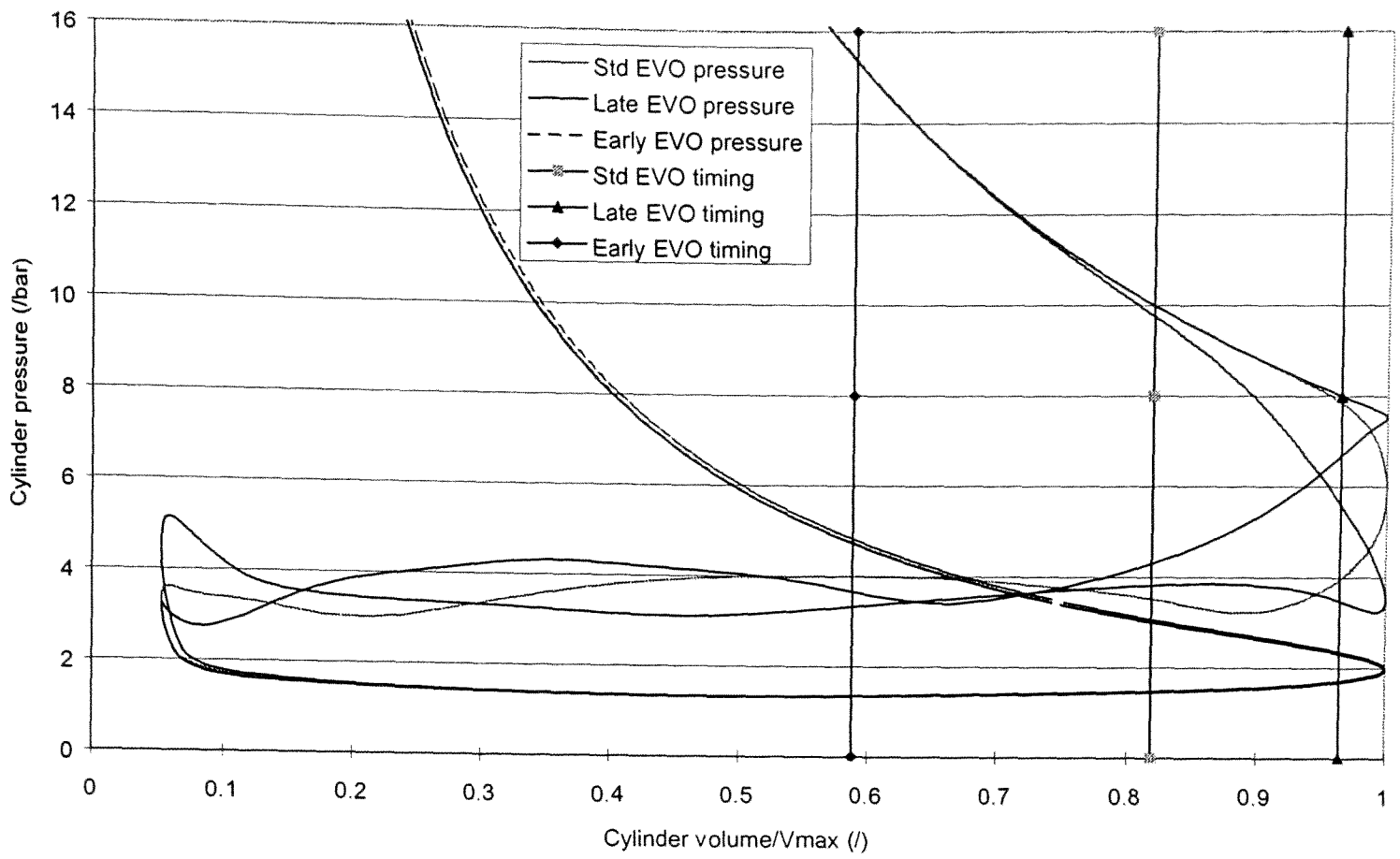


Figure 5.1.4.12. Pumping loops at 4500 rpm with standard, early and late EVO

The cause of this upturn in pressure is seen in *figure 5.1.4.13*, where the valve lift curves for cylinders 1 and 3 are also plotted with the pressure traces. With the earlier EVO, the cylinder 3 exhaust valves open well before those of cylinder 1 have closed, and the blow down pulse from cylinder 3 causes a large rise in the exhaust manifold pressure and a reverse flow into cylinder 1. This is the extreme case, but it happens to some extent with all of the valve timings investigated. However, it would not happen with a twin entry turbine, which might offer some potential to utilise the earlier EVO timings.

However, these effects still do not explain why the engine performance is limited at high speeds. Examination of turbine power, *figure 5.1.4.14*, shows that at 4500 rpm reducing the VGT setting from standard can liberate more power from the exhaust gases. But, as pointed out earlier a slight opening of the rack is required to increase output. Therefore, since the turbine still has some control over the turbo-charger behaviour, the relative insensitivity of the model to intake and exhaust valve timings in the higher speed range points to the air flow capacity of the compressor being the limitation.

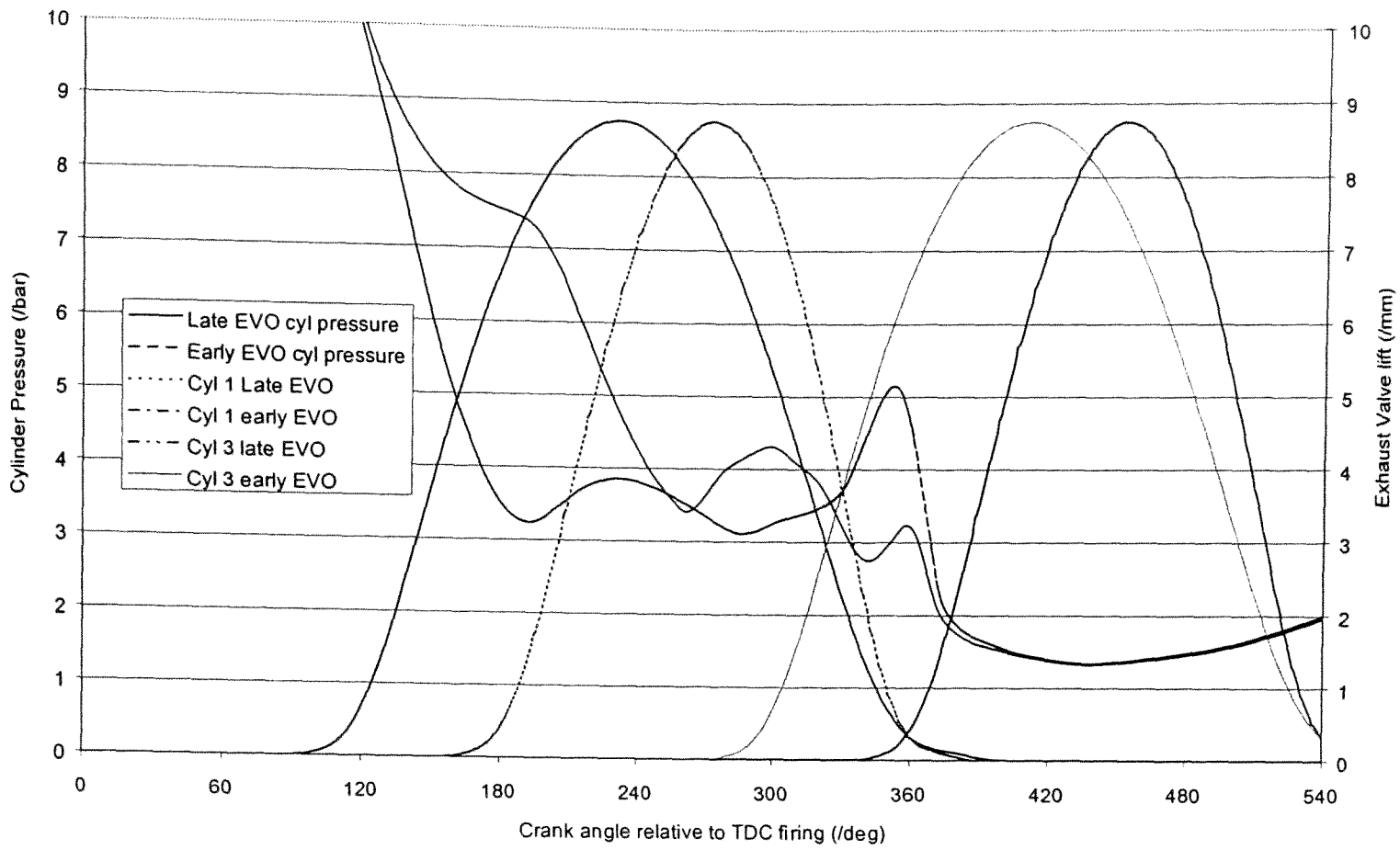


Figure5.1.4.13. Cylinder pressure traces with early and late EVO, at 4500 rpm, showing interference between cylinders 1 and 3

Inspection of the operating points for the compressor at the higher engine speeds highlights a potential problem. *Figure 5.1.4.15* shows the converged, average, operating points for the compressor at all of the full load speeds investigated, with optimised intake and exhaust VVA settings. It can be seen that for the speeds up to 3000 rpm increasing the mass flow tends to increase the efficiency, whereas, at the higher speeds, 3800 rpm to 4500 rpm, increasing the mass flow tends to reduce the operating efficiency of the compressor, requiring more power from the turbine to increase flow. This is demonstrated by *figure 5.1.4.16* which shows the conflicting trends in engine mass flow and compressor efficiencies at 4500 rpm with varying VGT and exhaust VVA settings.

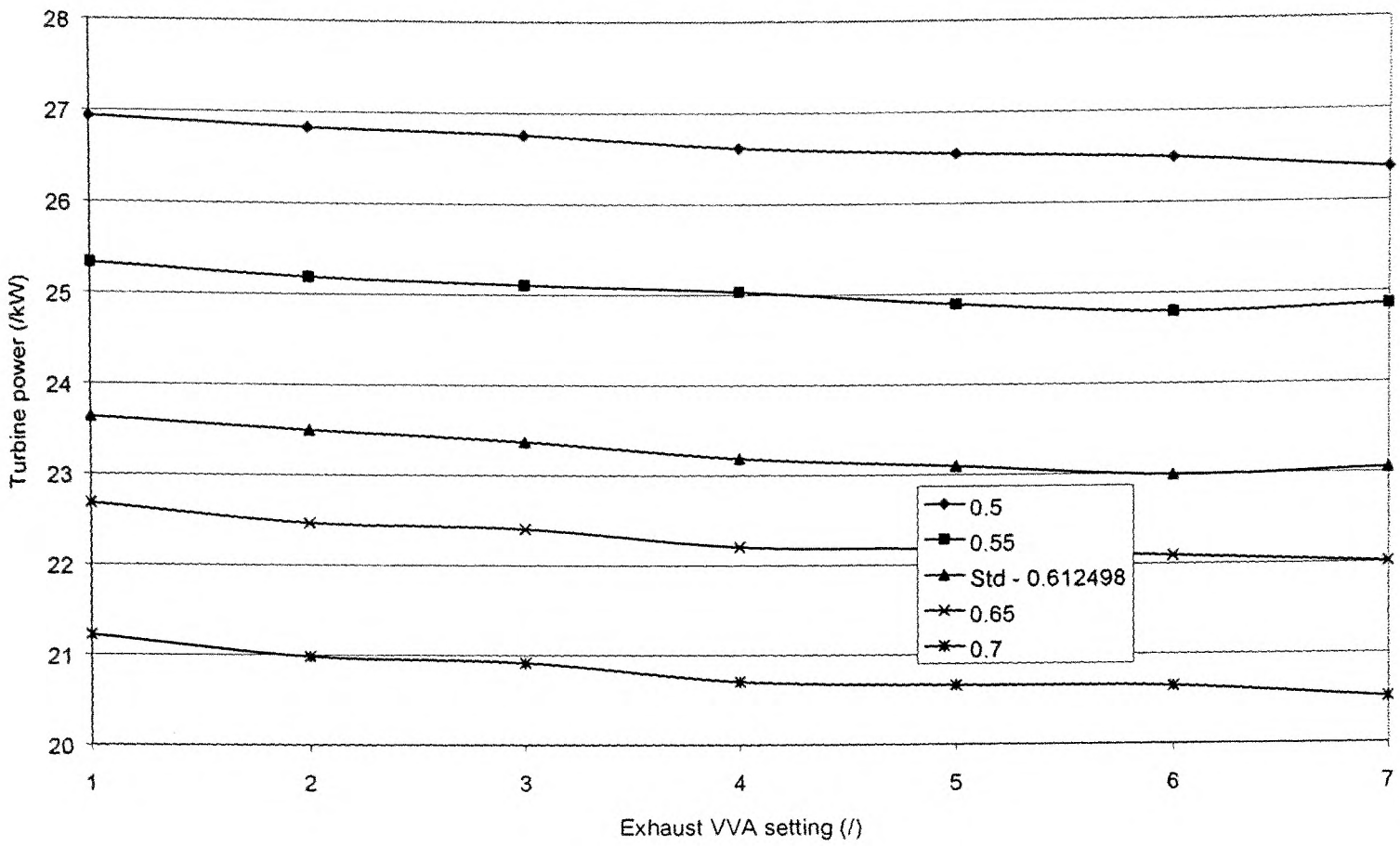


Figure 5.1.4.14. Turbine power at 4500 rpm, with varying rack and exhaust VVA settings

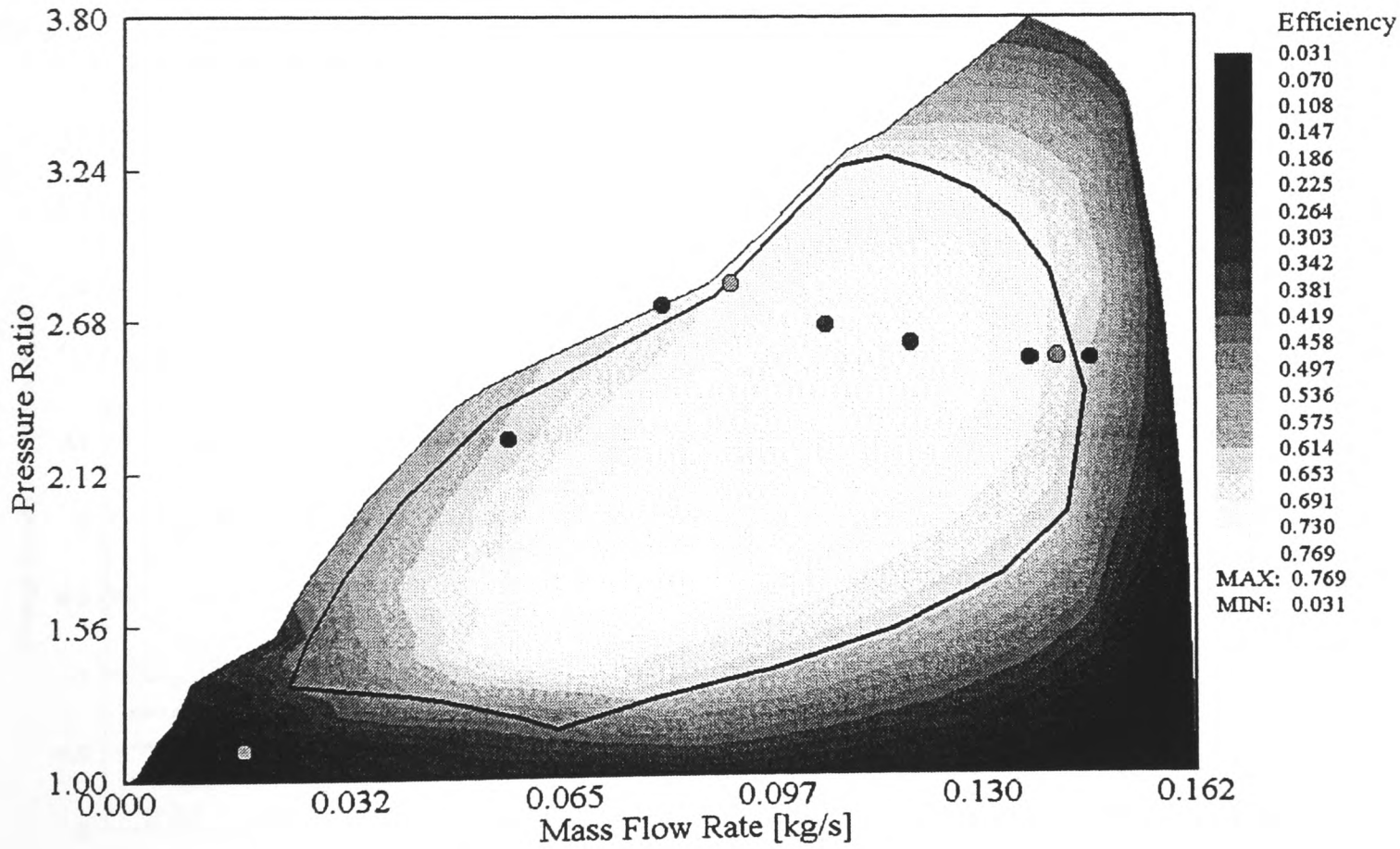


Figure 5.1.4.15. Converged, full load, cycle averaged compressor operating points for optimised intake and exhaust VVA.(1000 rpm lower left, increasing speed moving right)

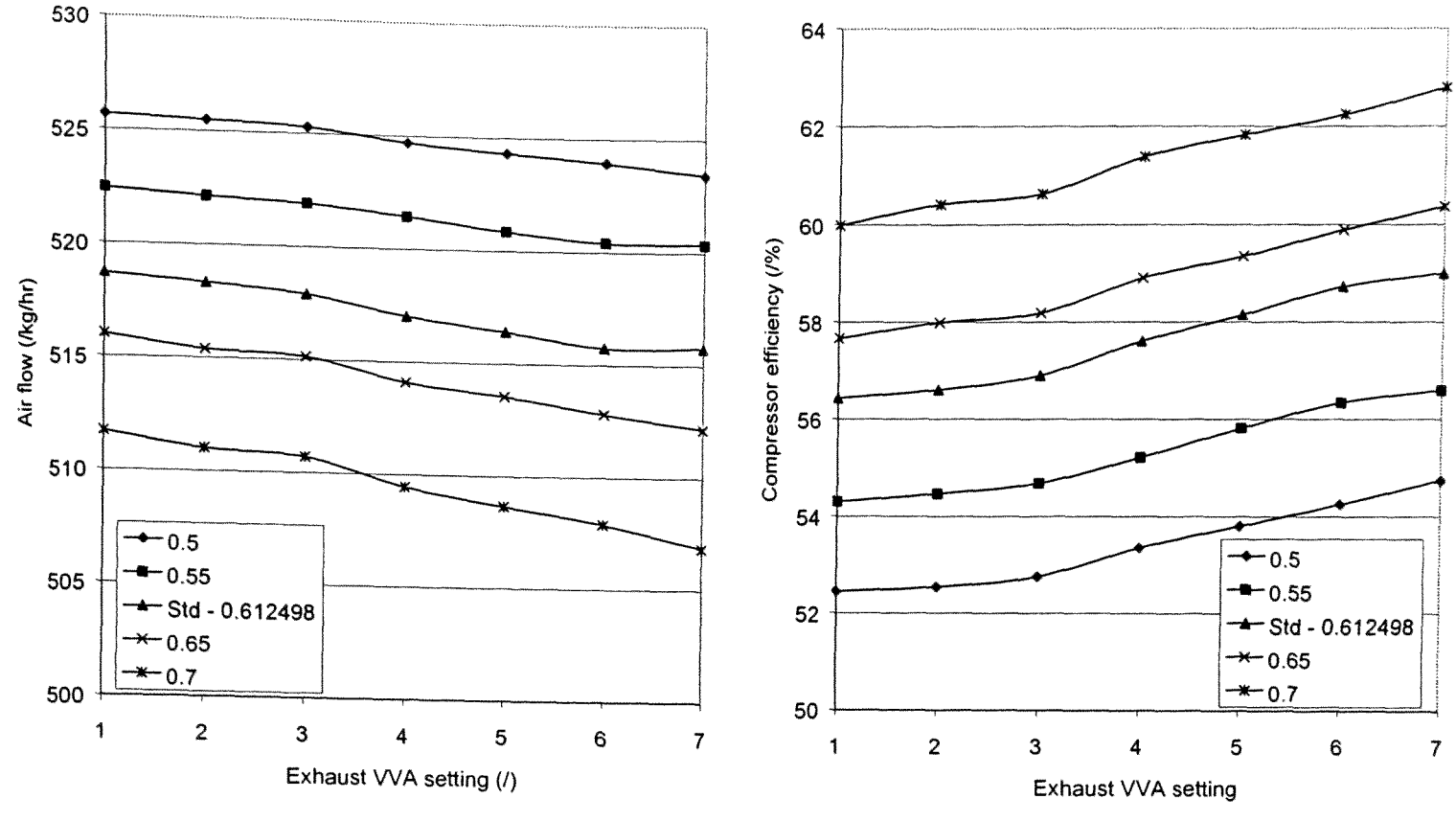


Figure 5.1.4.16 Engine air flow and compressor efficiency at 4500 rpm for varying VGT and exhaust VVA settings

A limited investigation on scaling the turbo-charger demonstrated that increasing the mass flow capacity of the turbine produced small improvements in the engine output, but increasing the mass flow capacity of the compressor produced larger increases of output at the high speeds. See *figure 5.1.4.17.*

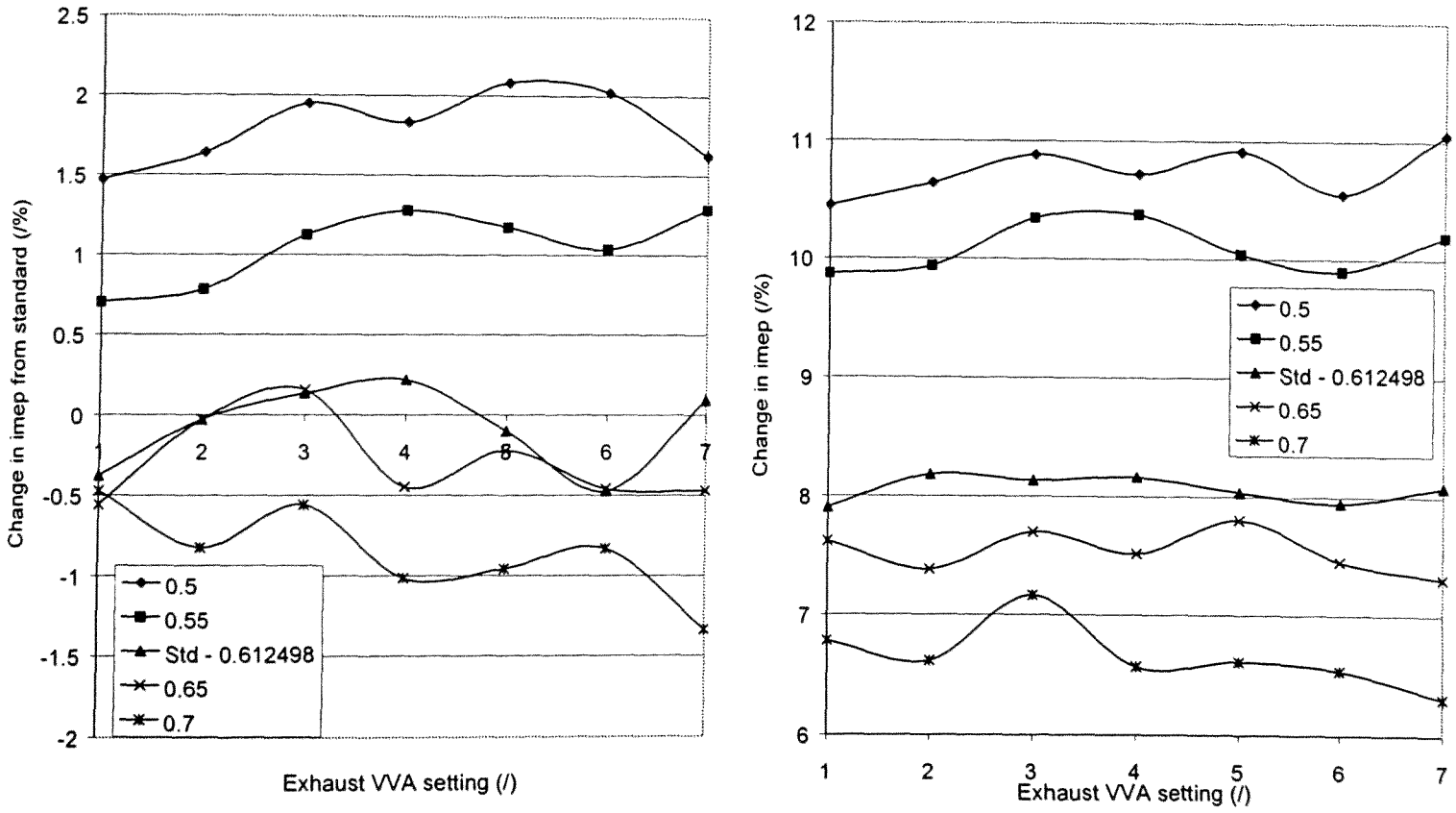


Figure 5.1.4.17. Percentage change in imep with 10% increased turbine mass flow capacity(left) and 10% increase in turbine and compressor mass flow capacities (right) for a range of VGT settings and exhaust VVA settings at 4500 rpm

It should be pointed out that a compressor with an increased mass flow capacity would have even greater difficulty with operation in the region of the stall line at the lower engine speeds. The acceptability of a larger compressor depends on its ability to survive light stall, but is also dictated by its transient behaviour, which is a strong function of its inertia. Dependent upon where in the range of trims the compressor is, it may be possible to increase its mass flow capacity by up to 20%, without physically increasing the frame size. Should this be the case, the only major obstacle is resistance to surge at low engine speeds. If a larger frame size is needed, inertia will increase and extra torque will be needed from the turbine to provide acceptable transient operation. The accelerative behaviour of the turbo-charger in response to VGT setting and VVA inputs are investigated and discussed later, but in order to understand these fully it is necessary to know what operating positions they will be in at the beginning of a rising load transient. This type of transient typically starts from a light-load low-speed operating point where fuel economy is the major consideration, and the next section investigates the effects intake and exhaust VVA can have on part load fuel economy.

Before summarising the results of this section of work, it is important to mention a few factors that need to be remembered in assessing the result:

The VVA settings used were only discrete points and more detailed investigation would probably generate slightly greater improvements. Similarly the VGT settings used to generate the finalised data were those established during the baseline runs – more detailed optimisation would probably generate greater improvements.

In producing these results fixed heat release characteristics were used for any given speed, which did not respond to changes in trapped conditions, either in terms of pressures and temperatures at start of injection or residual content (the ignition delay did respond to temperature and pressure). It can be seen that at the low speed operating points the trapped conditions did vary considerably as trapped mass was significantly increased. Also no account was taken of the maximum cylinder pressure structural limitations of the base engine. At the lower speeds the P_{max} values exceeded the acceptable limit, but this exercise was not constrained in this area as it was known that future engines would be designed either with lower compression ratios and/or higher P_{max} limits. However, it has been shown (Tai *et al* 2002) that minor alterations in injection timing and rate shape can restrict P_{max} without significantly reducing output.

Having mentioned these departures from the actual operation of a real engine it is still considered that the results utilise sufficient physics for them to be representative of what might be achieved in a real engine, but only corroborative testing can confirm this.

Summarising the results and findings: *figure 5.1.4.18* contrasts the standard imep characteristics, with those predicted with optimised intake and exhaust VVA across the full-load speed line. *Table 5.1.4.1* enumerates the imep values and percentage improvements while summarising the VVA settings used to achieve them. These data highlight the potential benefits which are up to 23% at 1500 rpm. In producing these results (with optimised intake settings) it was found that for speeds up to 2000 rpm the imep could be increased by both advancing and retarding EVO, at 2500 and 3000 rpm it could only be increased by retarding EVO and at 3800 rpm and above no significant change in output could be achieved over the whole range of EVO.

At the lower speeds the greatest improvements in imep were achieved with retarded EVO, when it was found that the increase in expansion work was far larger than the consequent increase in exhaust pumping work. It is thought this is because the time available for the exhaust gases to leave the cylinder and pass through the turbine was sufficient for the cylinder pressure to decay between EVO and BDC. But at the high engine speeds it was shown that the pressure in the cylinder and that in the exhaust manifold remained similar for much of the exhaust stroke. Detailed investigation of the work distribution in the expansion and exhaust strokes showed that at 4500 EVO had very little control over either.

Since improvements in high speed performance were minimal, an investigation of potential limiting factors was carried out. It was demonstrated that at 4500 rpm changing the VGT nozzle setting could change the turbine power output, but for any given VGT setting engine output remained largely unaffected by variation in EVO, despite it also being able to increase turbine power. This implied the restriction was probably the compressor. Inspection of the compressor operating points showed that at speeds of 3800 rpm and above any increase in compressor speed and mass flow tended to reduce its efficiency, thus becoming to some extent self regulating and preventing increases in output. A limited investigation of compressor scale showed that scaling the mass flow of the compressor by 10% allowed improvements in output, but as can be seen from *figure 5.1.4.18* at the lower speeds this made the output worse than achieved at the same VVA and VGT settings with the standard compressor.

Thus it can be seen that low speed output can be significantly increased by the use of retarded EVO and advanced IVC, with the standard turbocharger and calibrated VGT settings, but to significantly increase output from 3000 rpm upwards probably requires the use of different compressor hardware and a different calibration. It may also be the case that a twin entry turbine would allow more effective use of advanced EVO by avoiding the cross-talk between cylinders. However, this is a matter for future investigation as insufficient information is available about the packaging of a twin entry turbine on this engine.

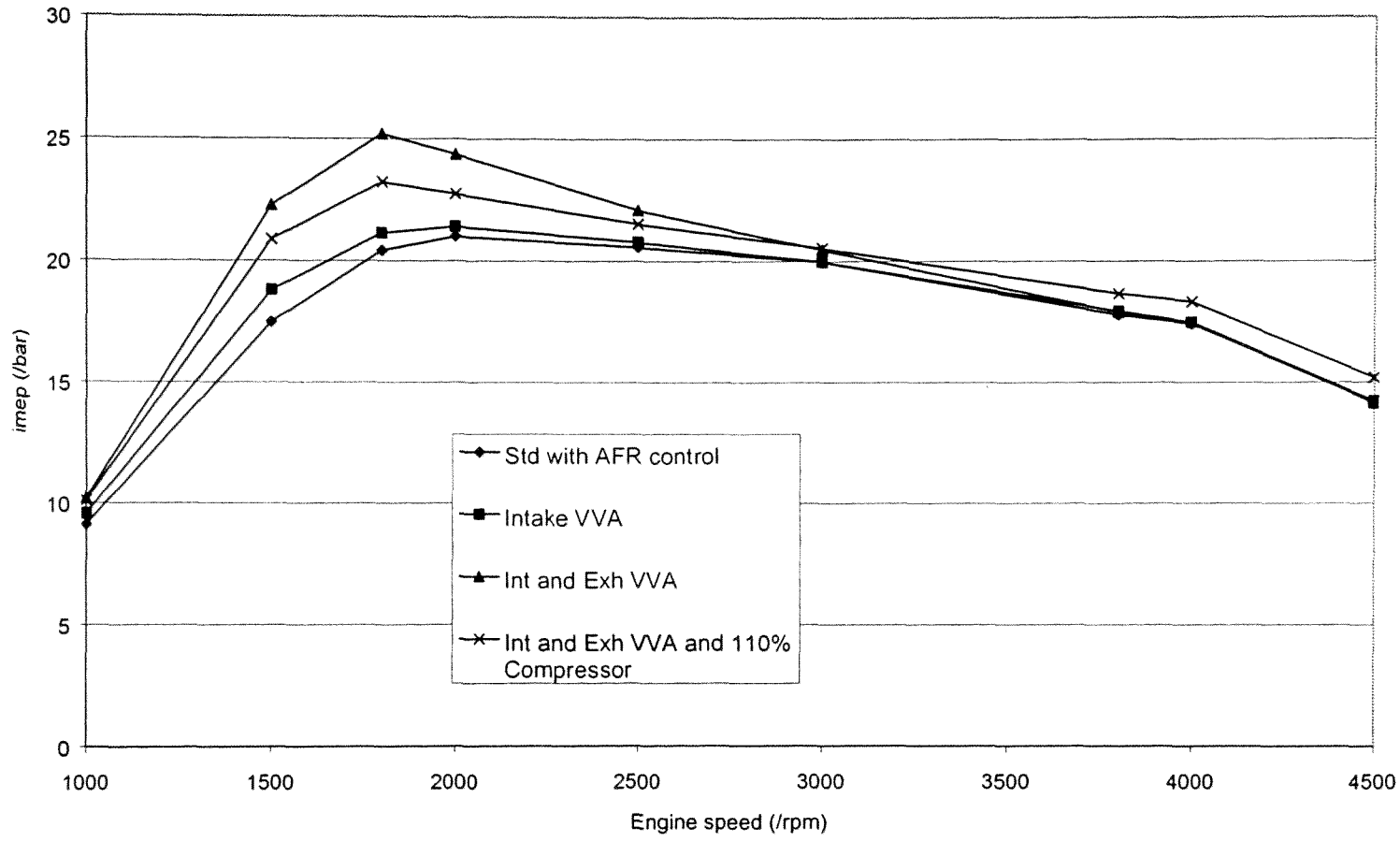


Figure 5.1.4.18 Full-load imep curves with optimised intake VVA, optimised intake and exhaust VVA and optimised intake and exhaust VVA with 110% scaled compressor.

Speed/rpm	1000	1500	1800	2000	2500	3000	3800	4000	4500
Optimum Intake VVA setting (/)	1	1	2	3	3	4	5	5	6
Optimum Exhaust VVA setting (/)	1	1	1	1	1	2	3	4	4
Imep (/bar)	10.2	22.2	25.2	24.3	22.0	20.4	17.8	17.4	14.1
Improvement in imep over std. (/%)	9.03	23.2	19.8	14.1	6.32	2.98	1.15	1.03	0.00

Table 5.1.4.1 Summary of imep values, resultant improvements over standard and the optimised intake and exhaust VVA settings used to achieve them

5.2 PART LOAD OPERATION

The increasing stringency of the emissions regulations applied to diesel engines is currently emphasising the importance of after-treatment. The addition of catalysts and particulate traps is increasing exhaust back pressure, and trap regeneration requires short term enrichment to raise exhaust gas temperatures, both of which are reducing the fuel economy advantage that diesel engines have over conventional gasoline engines. In addition the introduction of direct injection gasoline engines is further eroding the fuel economy advantage the diesel has.

Two practical methods of improving the fuel economy of the diesel engine are available to restore its advantage over gasoline engines:

1. Increasing the specific output of the engine to allow engine capacity to be reduced, leading to reduced weight and friction.

2. Improving the cycle efficiency of the engine through reducing unwanted losses such as friction and pumping.

Section 5.1.3-4 has shown how increases in specific torque can be achieved by the application of VVA; This section investigates the ability of VVA to control pumping work.

5.2.1 Preparation of the model

In part load operation light duty diesel engines use large quantities of EGR to control NO_x. To provide EGR in diesels requires a combination of a conventional, if somewhat larger than normal, EGR valve and, because the engines usually run un-throttled, some means of managing the pressure differential across the engine. Until recently the pressure differential would have been controlled by a throttle, but with the increasing market presence of the VGT, techniques have been developed for using the VGT setting (which controls the inlet guide vane angle and nozzle open areas) to control the pressure differential. Thus it was necessary to modify the model to provide a closed loop controller, for VGT nozzle setting, which was responsive to the required EGR level and a simulation run time input of EGR valve flow area.

The very high levels of EGR used by modern engines make the use of some kind of heat exchanger to lower its temperature very attractive. These are typically either an external "shell

and tube" device, or an in-head passage, both of which reject heat to the engine coolant. This feature was modelled by a separate heat exchanger system with specified outlet temperature.

EGR based control of NOx formation functions by a combination of increasing the overall specific heat capacity of the cylinder contents, which reduces peak cylinder pressure and temperature, and by oxygen depletion or charge dilution, which reduces the rate of combustion and peak combustion temperatures. As with the full load simulation the use of a cylinder-condition-responsive ignition delay and 3-term-Wiebe function to describe the fuel burning rate was tried, but, unfortunately the Wolfer ignition delay correlation was found to significantly under-predict the time from start of injection to start of combustion (by 3° to 5° with 50% EGR) and the shape of the burn curves could not be accurately represented by the 3 term Wiebe equations. These effects are thought to be entirely due to the presence of significant amounts of EGR. Also, because of a lack of detailed data it was not possible to use the sophisticated three dimensional spray burning model present in GT-Power. As a consequence a limited amount of heat release data produced from measured cylinder pressure data was used. The heat release characteristics were held constant for all cases in each simulation run, so no account was taken of variation of ignition delay or heat release rate with changing trapped conditions.

One consequence of altering valve timing is that bsfc and bmep can be altered. Therefore, to investigate part load operation at a fixed bmep requires the adjustment of the fuelling to maintain the required bmep. This requires a controller on the fuelling. But, since the model already had adjustable VGT setting and EGR valve open area, each of which could influence bmep it was considered that there might be multiple solutions for convergence, with bsfc variation among them. As a consequence it was decided that the fuelling amount should be fixed, but with the injection timing and start of combustion aligned with test data. Therefore, in this section of work, the effects of the VVA appear as changes in bmep and bsfc.

5.2.2 Part load operating priorities

Typical, modern, light duty diesel engines do not need to operate at full load in the vehicle certification emissions drive cycles. As a consequence the emphasis in calibration is on part load fuel economy and emissions. Emissions targets must be met, whilst the fuel consumption of diesels is more than acceptable. Therefore the calibration typically favours emissions over fuel economy, where there is a conflict. Thus, fuel injection timing is optimised for the NO_x /particulate matter (PM) trade-off and EGR is used to reduce the NO_x still further. (Increasing EGR levels also affects the operating AFR of the engine which can influence the PM emissions.) Therefore to improve fuel economy means addressing the pumping work, which is the area that VVA can influence.

5.2.3 Control strategies

As can be seen from the above discussion a modern light duty diesel engine has a number of control systems that can affect output, fuel consumption and emissions: Fuel injection timing (and rate shaping/multi shot), EGR valve and VGT setting. In this piece of work two more degrees of freedom are being added through intake and exhaust VVA. (In addition enrichment that is not detectable by the driver is also needed to regenerate the particle traps, but a detailed discussion of this is outside the current scope.)

It is known (Lancefield, *et al* 1996) that current engines use a mass air flow method for calculating and controlling EGR levels. This is based on the assumption that for a given amount of fuel, without EGR the engine will consume a given amount of air at a given VGT setting. Therefore, any short fall in measured mass air flow is assumed to be displaced by EGR, giving a notional EGR flow. But both EGR valve opening and VGT setting can influence the amount of EGR provided. So, some form of hierarchy of controls is needed in order that one is subservient to the other. In practice it appears that for fine control the VGT setting is made dominant, as this also allows control of boost pressure and thereby AFR, but in high rate transients the behaviour of the EGR control valve must take precedence, or large AFR excursions can result in un-wanted smoke. However, it is evident that the addition of two further control loops will only compound this hierarchy of controls problem. This is an interesting area for future work.

5.2.4 Interaction of Intake and exhaust VVA with the VGT, without EGR at 2000 rpm

Initially a set of simulations was run at 2000 rpm, 10mg/stroke fuelling, with no EGR, to investigate the underlying trends associated with VGT setting before the introduction of EGR. *Figure 5.2.4.1* (left) shows the effect of VGT setting on output and brake specific fuel consumption, with standard valve timing. It can be seen that maximum bmep and minimum bsfc are achieved with the VGT fully open. This is a consequence of minimised pumping work and minimum air flow. *Figure 5.2.4.1* (right) shows the corresponding effects of VGT setting on air flow, AFR and pmep (BDC to BDC).

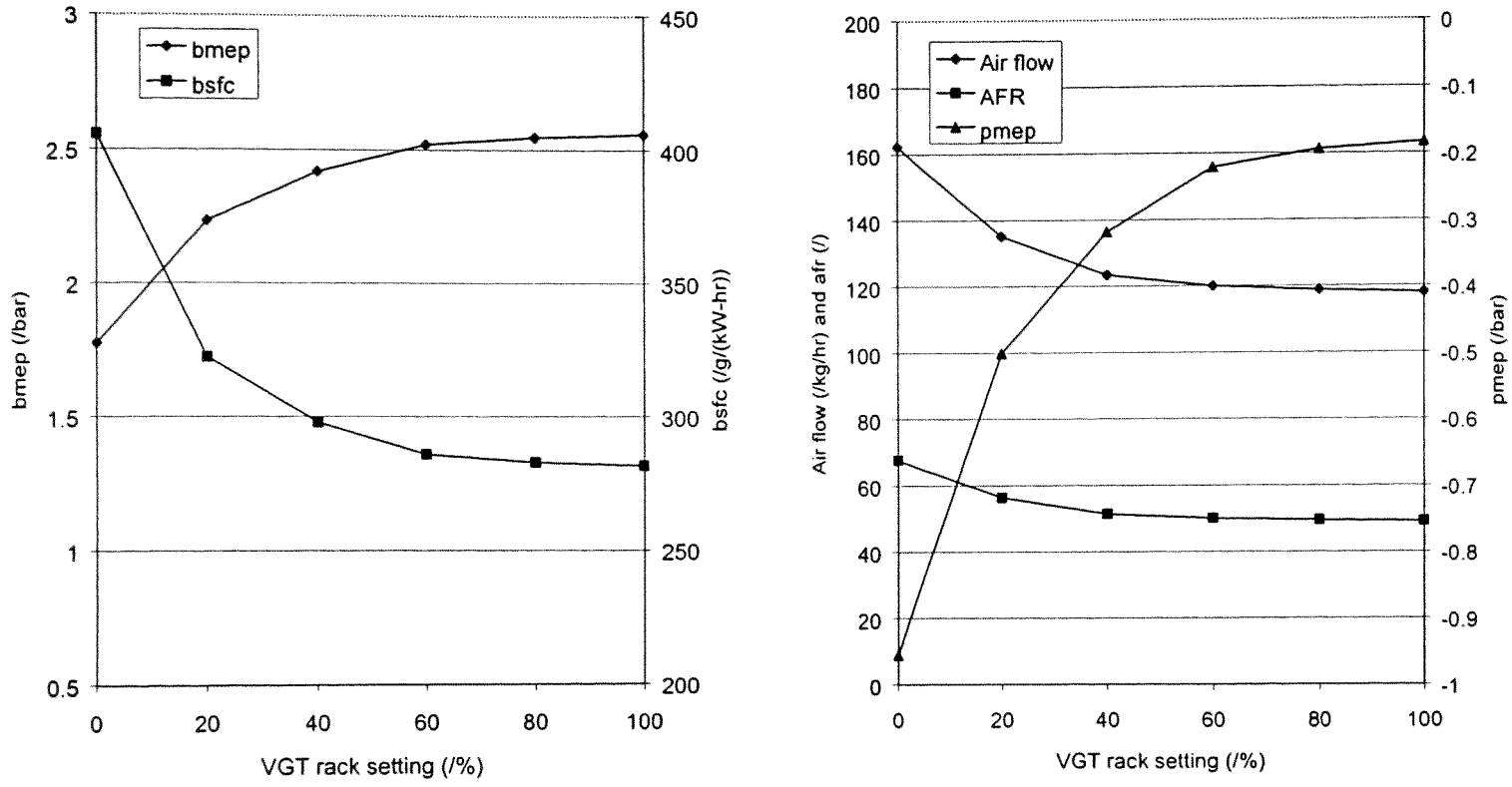


Figure 5.2.4.1. The effects of VGT setting on bmep and bsfc (left) and air flow, afr and pmep (BDC to BDC) (right) with 10mg/stroke fuelling, no EGR and standard valve timings

The rather obvious conclusion from this is that minimising air flow and reducing the restriction offered by the exhaust system are key to good part load fuel economy. To see how VVA could assist with this another set of simulations was run with zero EGR, fuelling at 10mg/stroke and several settings of the VGT. *Figure5.2.4.2* (left) shows the effect of VVA on the bmep with the VGT fully closed. The results are relative to the output with standard valve timings. *Figure 5.2.4.2* (right) shows the corresponding change in bsfc. It can be seen from *figures 5.2.4.2* that the greatest improvements in bmep and bsfc occur with the latest IVC. (It is worth noting that advancing IVC also increases bmep and improves bsfc, but not as much as retarding, within this range of timings.) The data shows, as illustrated by *figure 5.2.4.2,* (right) that exhaust VVA setting 3 is the other optimum integer setting. (True optimum lies between 3 and 4.) The improvements available with changing intake valve closing timing are larger than those with

exhaust valve opening timing, and improvements in bsfc of the order of 8% are available at this fuelling level with the VGT nozzles fully closed.

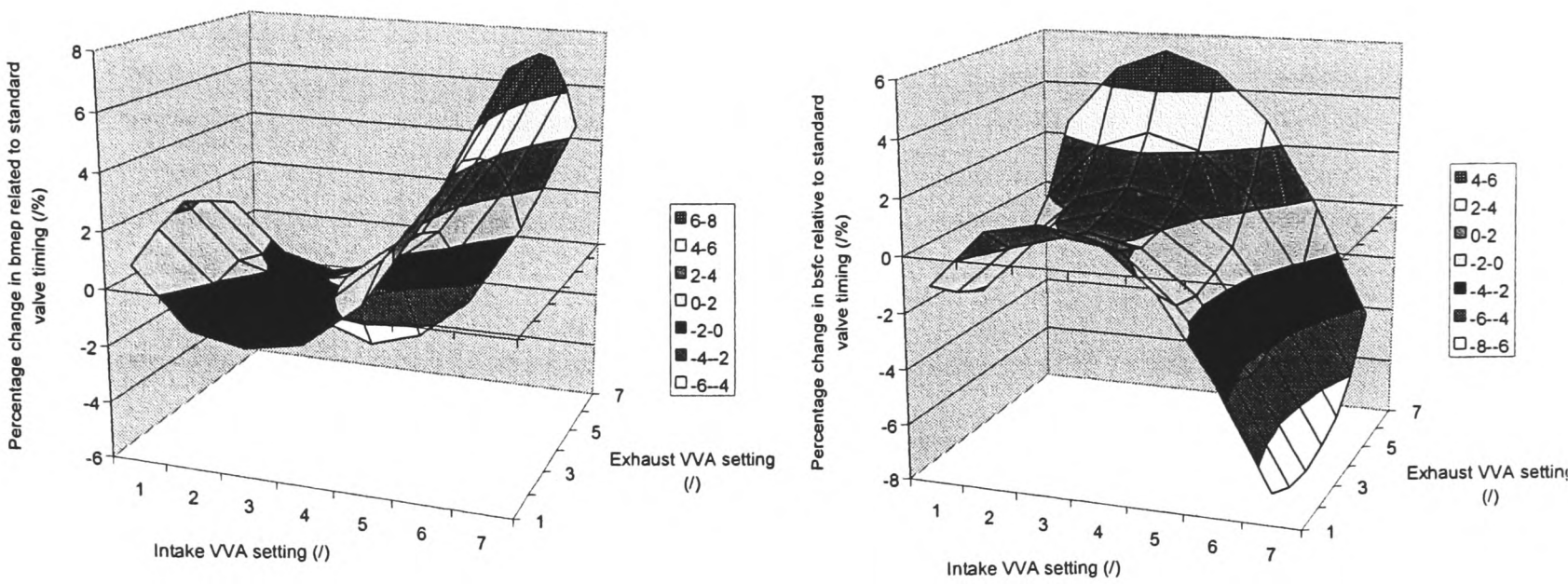


Figure 5.2.4.2. The effects of intake and exhaust VVA on bmep (left) and bsfc (right) with fully closed VGT setting and 10 mg/stroke fuelling

Further simulation was carried out at more open VGT settings. These revealed that the optimum valve timings did not change. Optimum fuel economy and corresponding bmep occurred at intake VVA setting 7 and exhaust VVA setting 3. The results presented hereafter refer to exhaust VVA setting 3 and show the effect of intake VVA.

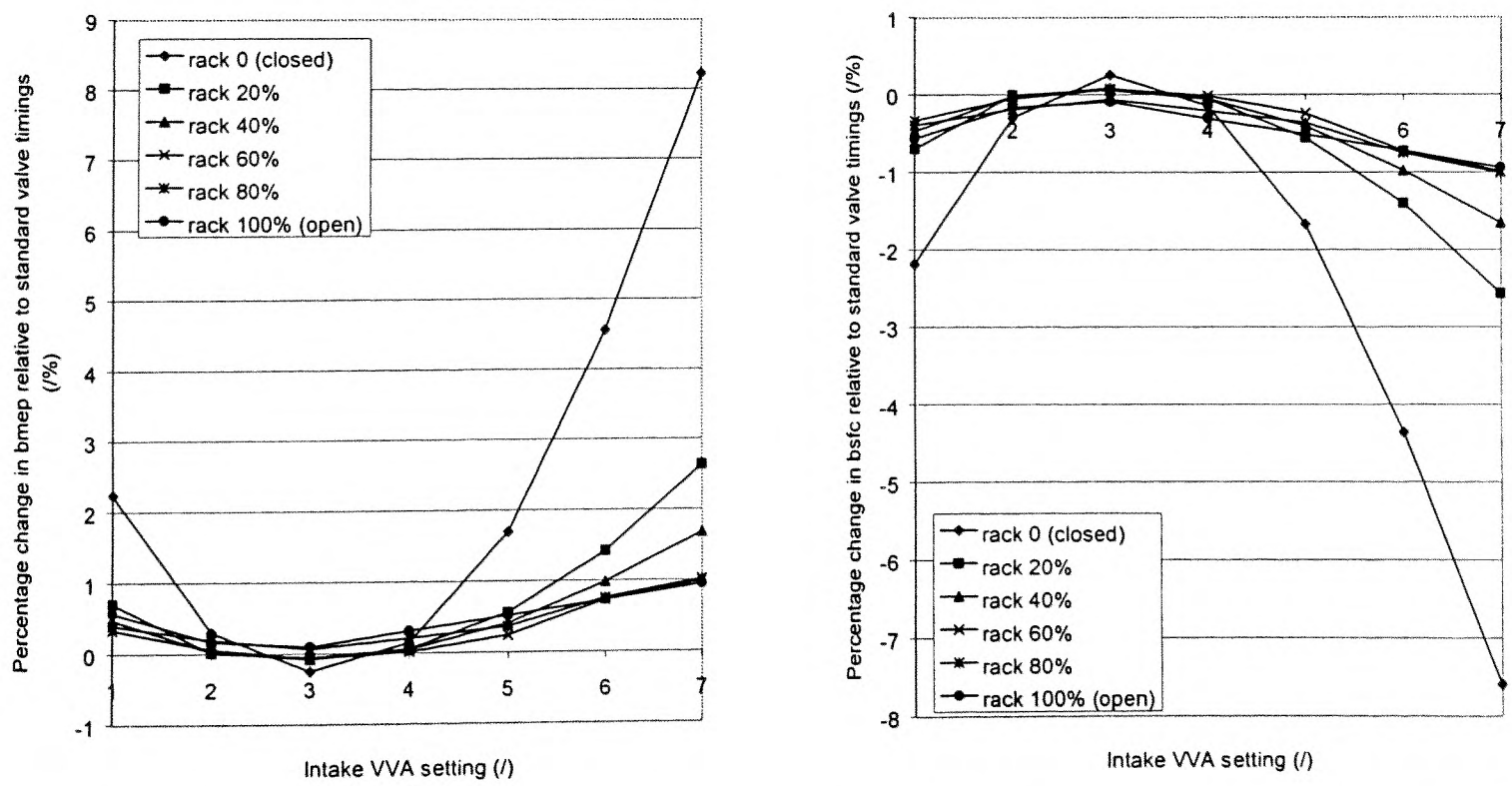


Figure 5.2.4.3. Effects of intake VVA setting on bmep (left) and bsfc (right) at various VGT settings (Zero EGR). Exhaust VVA setting 3.

It can be seen from *figure 5.2.4.3* that the benefits that can be generated by the use of VVA are strongly affected by the VGT setting, at 10 mg/stroke fuelling and zero EGR: with closed VGT

the improvement in bsfc can be as high as 8%, but at 60% open and beyond they only amount to 1% or less. This underlying behaviour needs to be kept in mind for the next section.

5.2.5 Interaction of Intake and exhaust VVA with Variable Geometry Turbine and EGR at 2000 rpm

It might be thought from the above that minimising fuel consumption at part load operation is only a matter of fully opening the turbine inlet guide vanes, to minimise boost and exhaust back pressures. However, as mentioned earlier the VGT setting is used to control the pressure differential across the EGR valve to manage the EGR flow. Therefore, this approach to minimising fuel consumption may not be possible when using EGR. To investigate this further a series of simulations runs, again at 2000 rpm, but with two levels of fuelling, 5mg and 10mg/stroke, each at three levels of EGR, 10%, 30% and 50%, (by mass) were made. Cylinder pressure data, which was translated into heat release curves, was available for the 0%, 30% and 50% EGR runs, but as no data was available for the 10% EGR setting it was assumed that the combustion characteristics were the same as the zero EGR case.

The EGR flow is governed, not just by the pressure difference across the engine, but also by the size of the EGR valve orifice. It was established, by simulation, that for 50% EGR it was necessary for the EGR valve to be fully open (effective orifice diameter 14mm) if the VGT setting were to be anything other than fully closed. But at the 30% and 10% settings a range of combinations of VGT and EGR valve settings could be used to provide the necessary levels of EGR. Therefore another "driver" was needed to govern the hierarchy of controls. In this case a major problem is the closing response time of the EGR valve when a positive load transient occurs, so to some extent there is a need to minimise the EGR valve opening. However, no data was available to define the EGR valve settings at 10% and 30%, so for the 10% operating point an EGR valve setting that required a relatively closed VGT setting was selected (6mm diameter orifice) and for the 30% an EGR valve setting that allowed a relatively open VGT (12mm diameter orifice) was used.

Figure 5.2.5.1 shows the range of control that VGT setting has over EGR levels at a range of EGR valve orifice diameters. It can be seen that for 50% EGR an effective diameter of greater than 12mm is needed and for 30% EGR an effective diameter of greater than 9mm is needed, if the VGT setting is to be anything other than fully closed. It should be noted that at values lower than these insufficient EGR results. For the 10% EGR case it can be seen that sufficient EGR

could be provided by effective diameters of less than 6 mm, but VGT settings of less than 0.2 would result. It can also be seen that for effective diameters of more than 9mm too much EGR results even with the VGT fully open. *Figure 5.2.5.2* shows the corresponding effects on isfc.

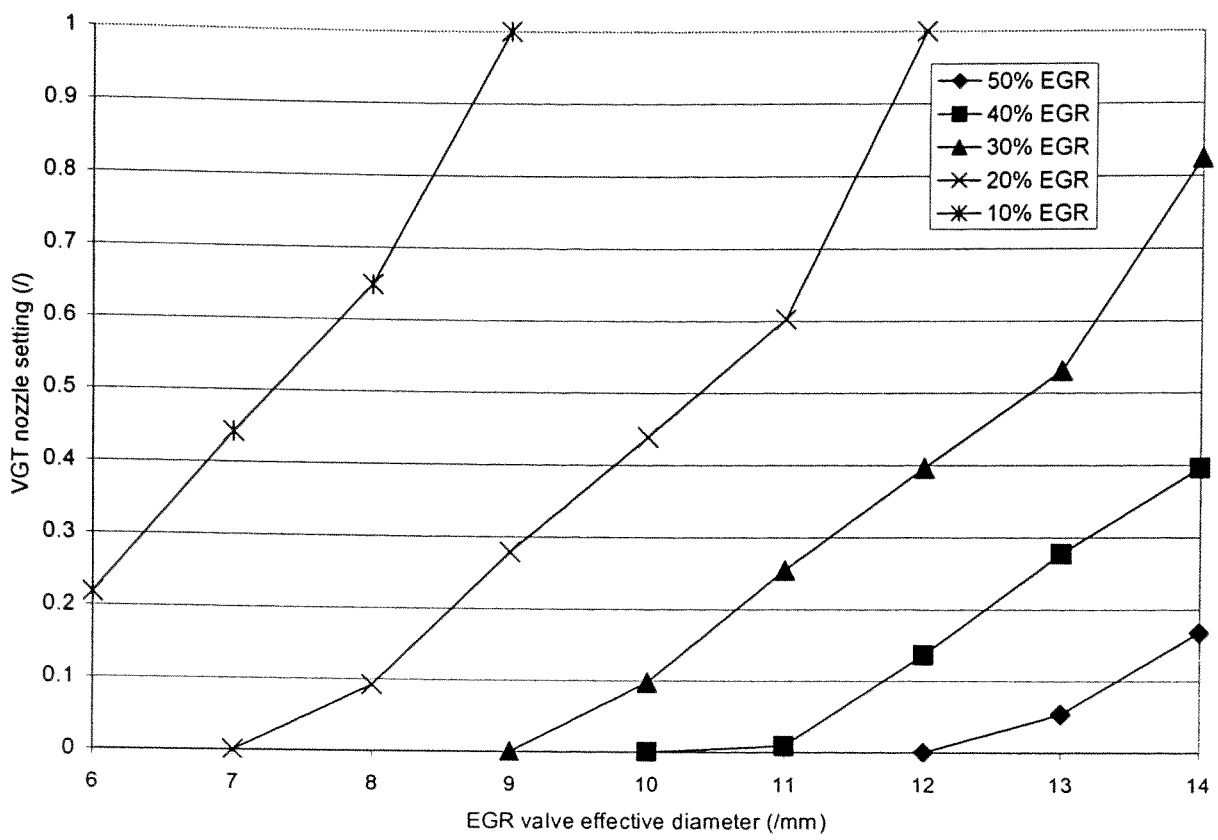


Figure 5.2.5.1 VGT settings required to produce specified EGR levels for a range of EGR valve effective diameters. 2000 rpm with 10 mg/stroke fuelling, standard valve timings

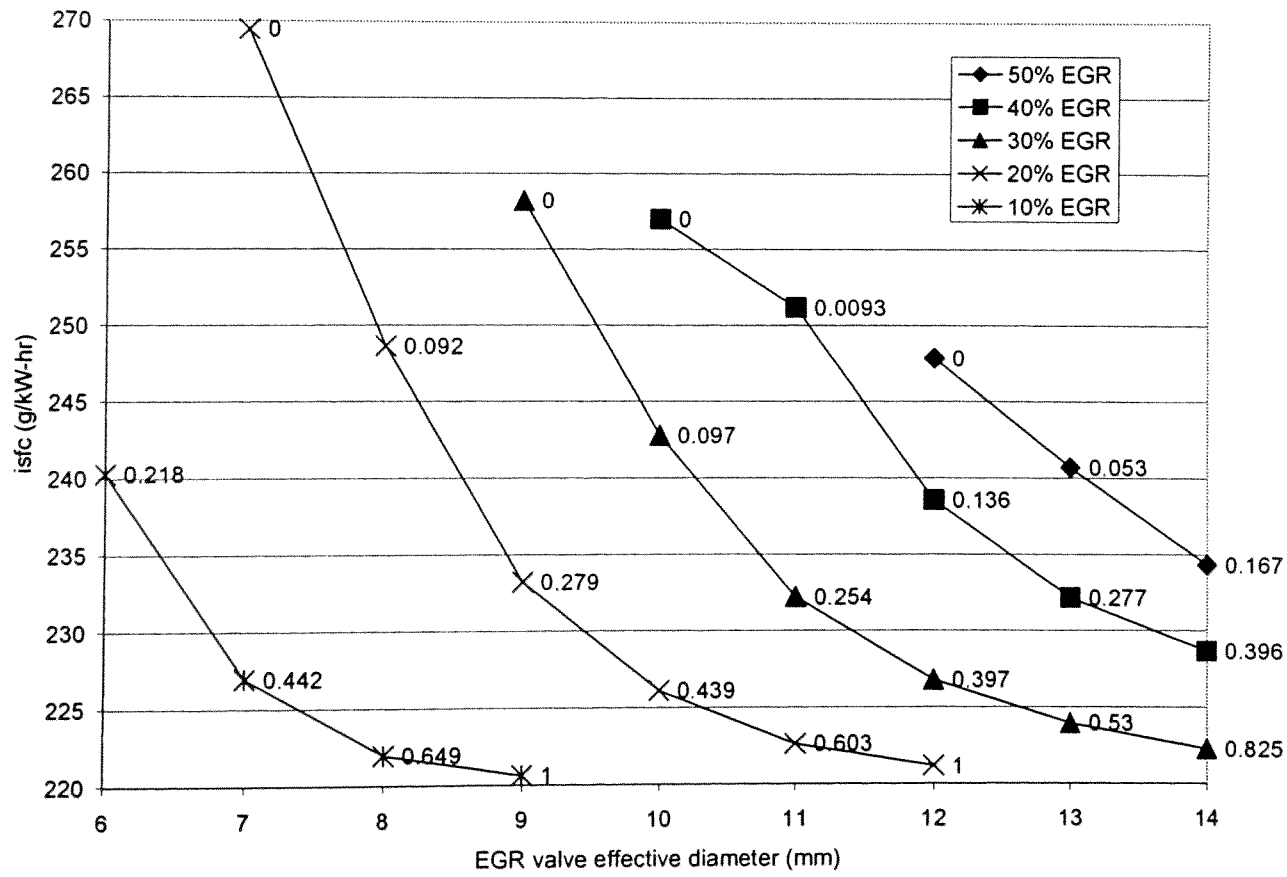


Figure 5.2.5.2 isfc at specified EGR levels for a range of EGR valve effective diameters. 2000 rpm with 10 mg/stroke fuelling, standard valve timings. (VGT nozzle settings as per *figure 5.2.5.1* numbers next to the data points are the VGT settings.)

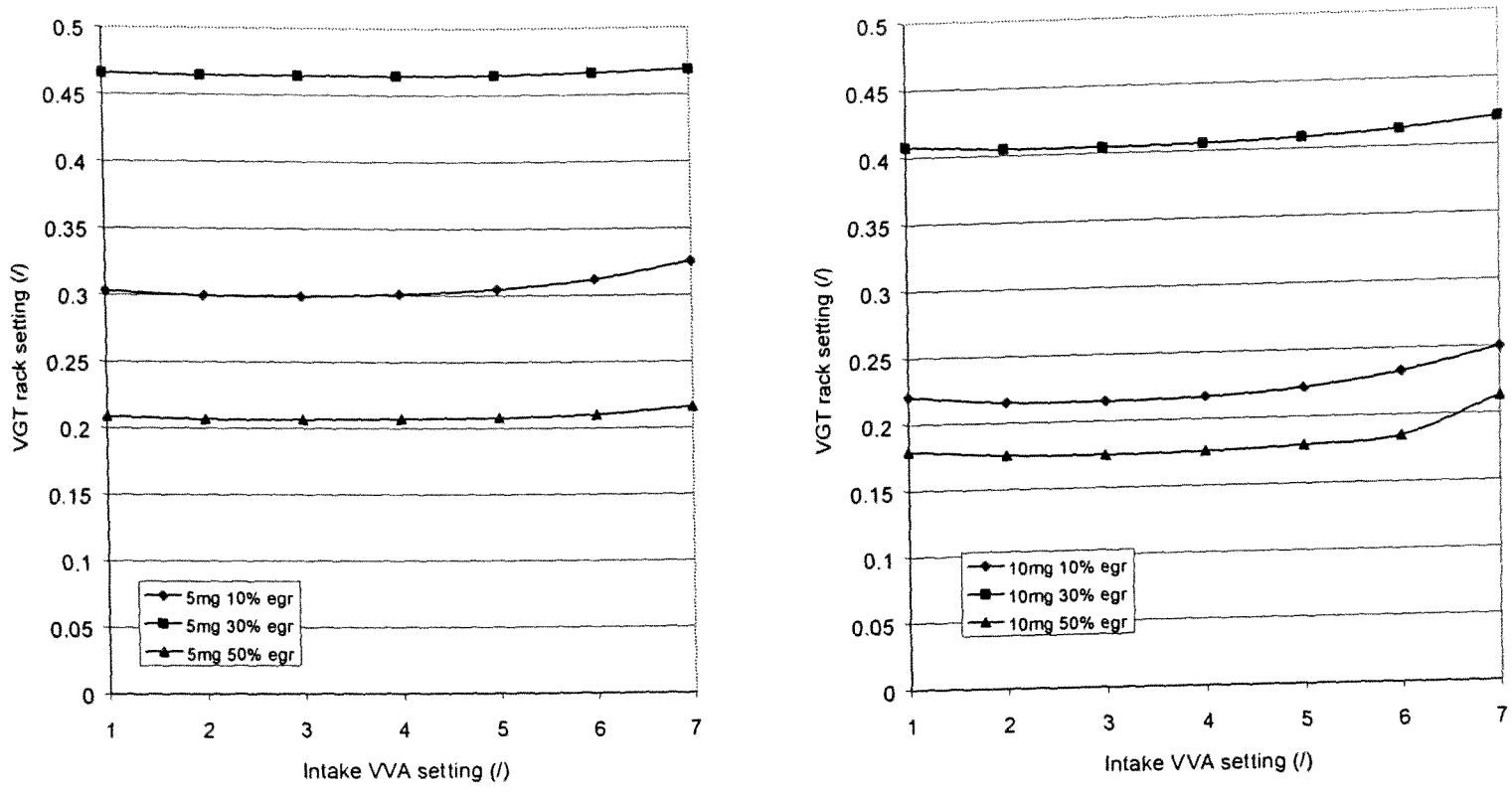


Figure 5.2.5.3 The VGT settings taken for 5mg/stroke (left) and 10mg /stroke fuelling (right) with exhaust VVA setting 3.

Figure 5.2.5.3 shows the VGT settings resulting from the 6 combinations of fuelling and EGR level tested with optimised exhaust VVA, setting 3, and intake VVA operated across its whole range. It may seem counter-intuitive that the higher fuelling rate cases required a more closed VGT setting, but this is explained by the fact that the turbo-charger produced more boost, with higher fuelling, so a more closed VGT was needed to restore the necessary pressure differential across the engine and EGR valve.

As with the zero EGR investigation, for all fuelling and EGR combinations tried, it was found that exhaust VVA setting 3, with later EVO than standard, was optimum

For the 10mg/stroke fuelling and 10% EGR case, *figure 5.2.5.4* (left) shows the optimum exhaust setting to be between 3 and 4, but the higher calculated output is at 3. It can also be seen from *figure 5.2.5.4*, (right) that both advancing and retarding EVO, relative to standard, reduced the amount of work done during the firing and exhaust strokes, (TDC(f) to TDC(o)), but the effects on the work done in the intake and compression strokes, (TDC(o) to TDC(f)), offered the ability to improve the work output with later EVO and in the region between exhaust VVA settings 3 and 4 a small increase in engine output, relative to standard, was possible.

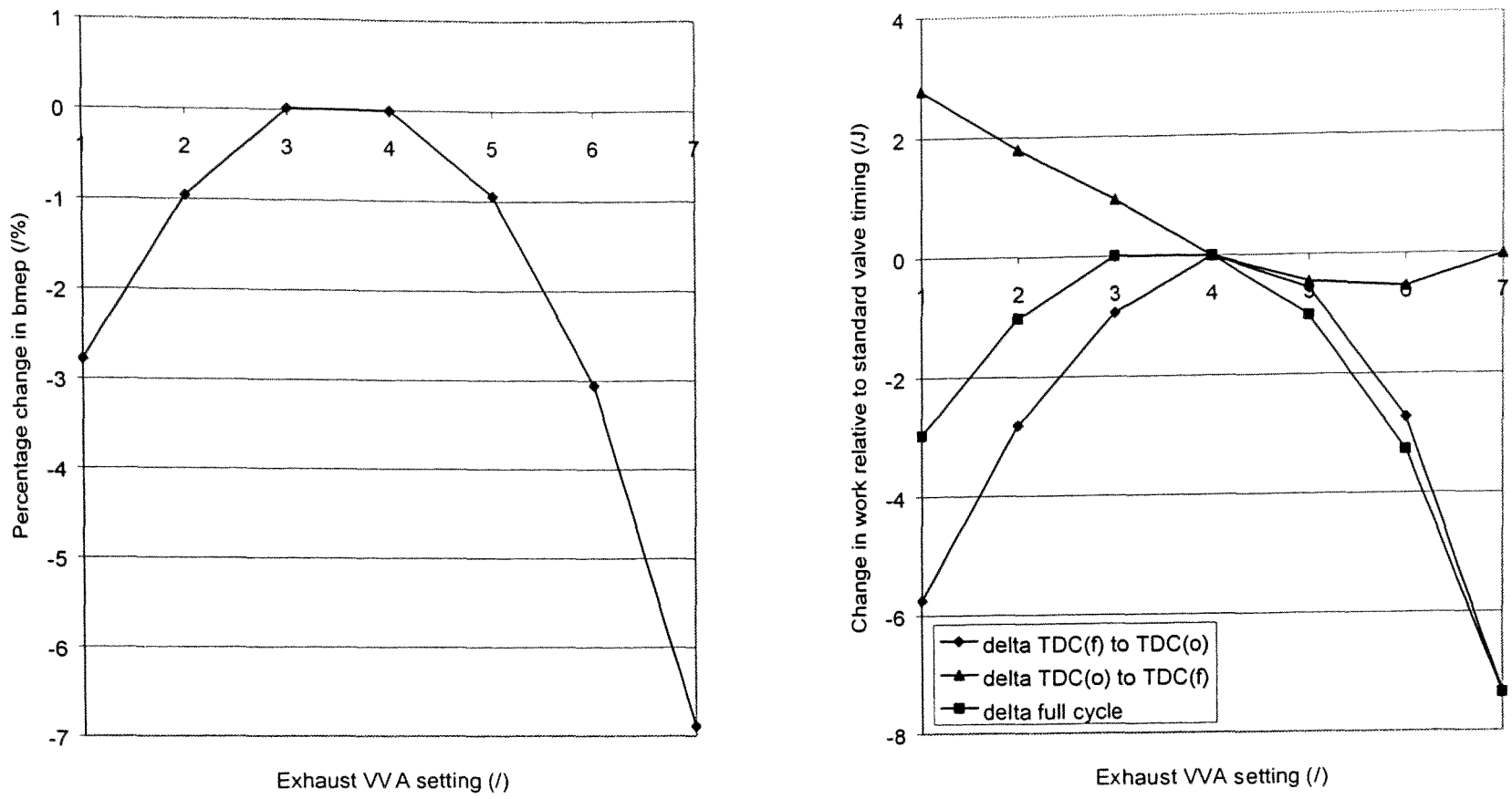


Figure 5.2.5.4 The effects of exhaust VVA on bmep (left) and the work done on the piston (right) at 10mg /stroke fuelling, 10% EGR and standard intake valve timing.

Examination of the behaviour of the system with exhaust VVA setting 3 and varying the intake valve timing over the full range showed that output and bsfc could both be improved. Consideration of the work distribution in the cycle and inspection of the changes that took place in the work in the various strokes highlighted the reasons for this. (Note for *figures 5.2.5.5* through to *5.2.5.8* the basis for reference is the standard intake valve timing, setting 4, but with exhaust VVA setting 3.)

Figure 5.2.5.5 shows the work done in the expansion and exhaust strokes, in absolute terms (left) and as changes from the standard intake valve timing value, (right) for the two fuelling cases 5mg/stroke, (top) and 10mg/stroke, (bottom). By summing the components of the work in these two strokes, it can be seen that for intake VVA settings 2 and 3 small improvements in work output could be achieved. These were of the order of 3 joules. (Note for this engine a 50 joule change is equivalent to 1 bar mep) For all other intake VVA settings the total output from these two strokes was worse than for standard intake timing as there was a more significant reduction in expansion work.

Figure 5.2.5.6, shows the same sets of data for the induction and compression strokes. It can be seen that intake valve timing only had a small effect on the (+ve) work in the intake stroke, (the changes in nominal value were caused by changes in boost pressure.) However, it had a

significant effect on the (-ve) work done in the compression stroke, being able to substantially reduce the work required to compress the trapped mass, by retarding IVC.

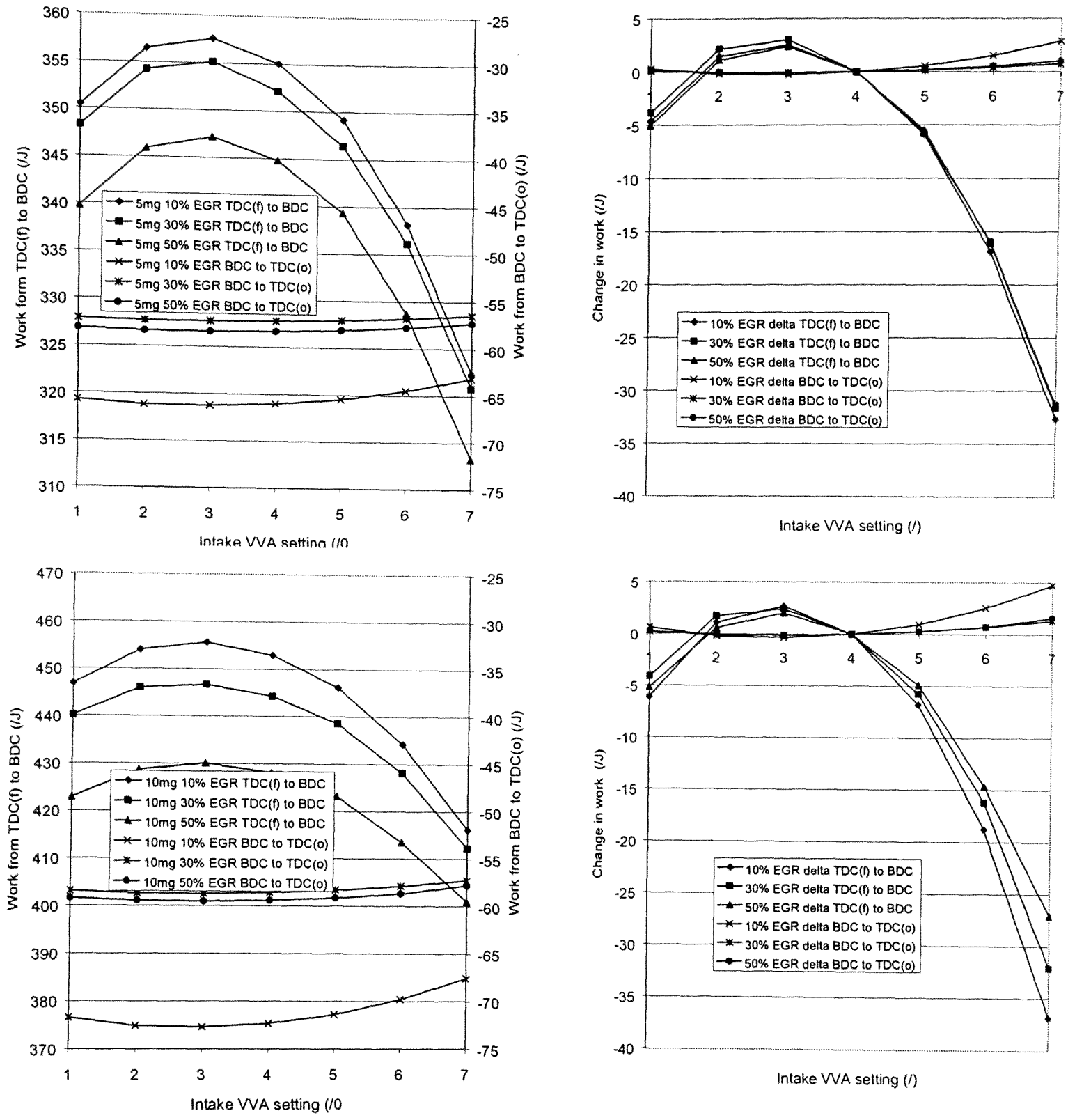


Figure 5.2.5.5 Work done between TDC(f) and BDC and BDC and TDC(o), (left) and changes in these values relative to intake VVA setting 4 (standard) (right) for 5mg/stroke (top) and 10mg/stroke fuelling (bottom)

This reduction in compression work occured because from BDC to IVC the pressure operative in the work calculation, $\int pdv$ was largely that of the intake manifold, rather than that of the compressed gas which it would have been after IVC. Also retarded IVC reduced the trapped mass, which in turn further reduced this work integral. The above also indicates that early intake valve closing (late IVC mirrored about BDC,) should have the same effect, but the valve dynamics implications of this make such early IVC difficult to achieve with acceptable valve lift and a cam operated valve train.

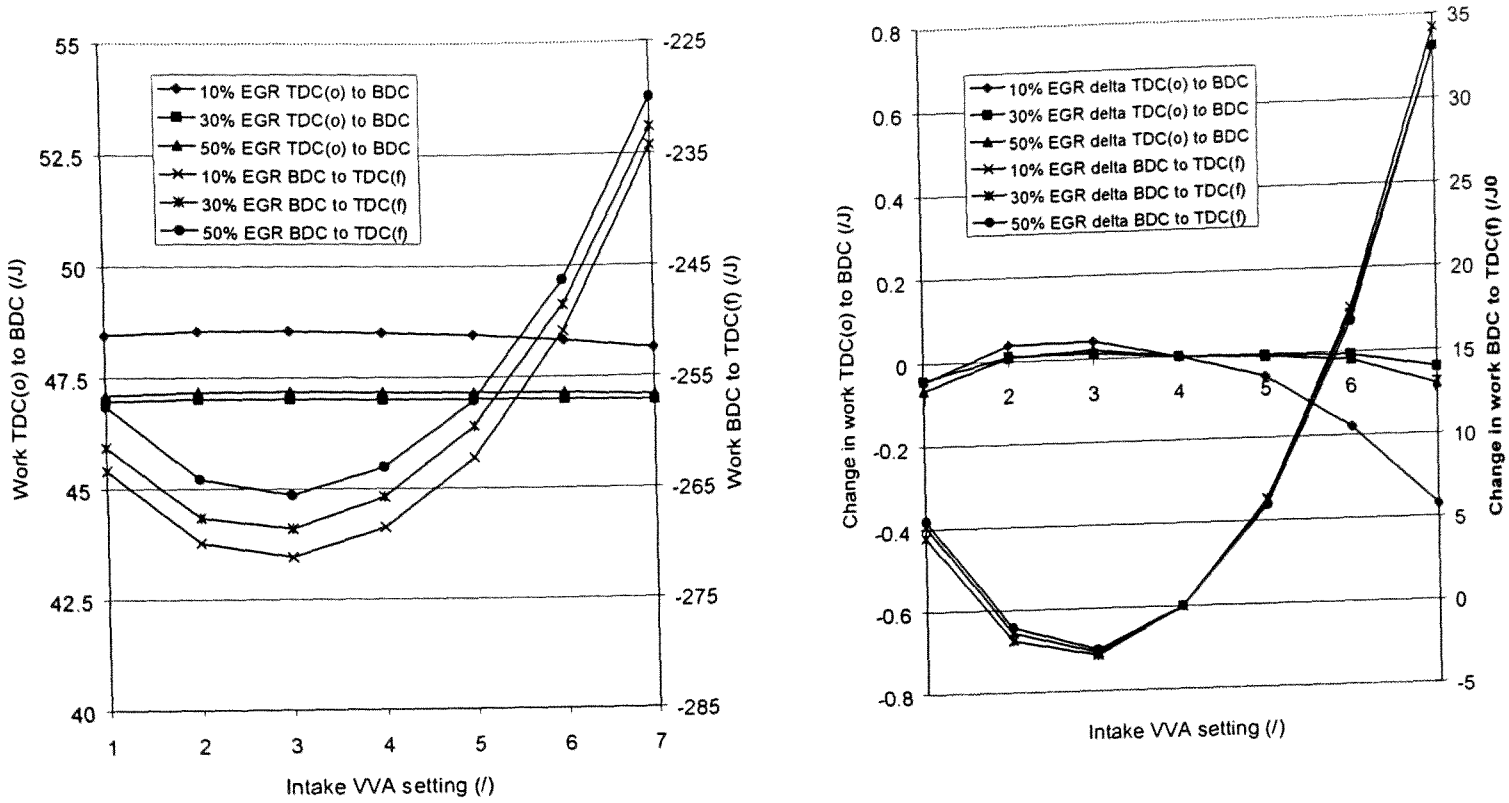


Figure 5.2.5.6 Work done between TDC(o) and BDC and BDC and TDC(f), (left) and changes in these values relative to intake VVA setting 4 (standard) (right) for 5mg/stroke (top) and 10mg/stroke fuelling (bottom)

From the above it can be seen that there were significant changes in expansion and compression work and small changes in induction and exhaust stroke work levels. *Figure 5.2.5.7* shows how these combine in the two half cycles and over the complete cycle. It can be seen that the net results of the latest intake valve timings were small single digit changes in work output. However, these need to be considered in the context of the overall work output of the cycle.

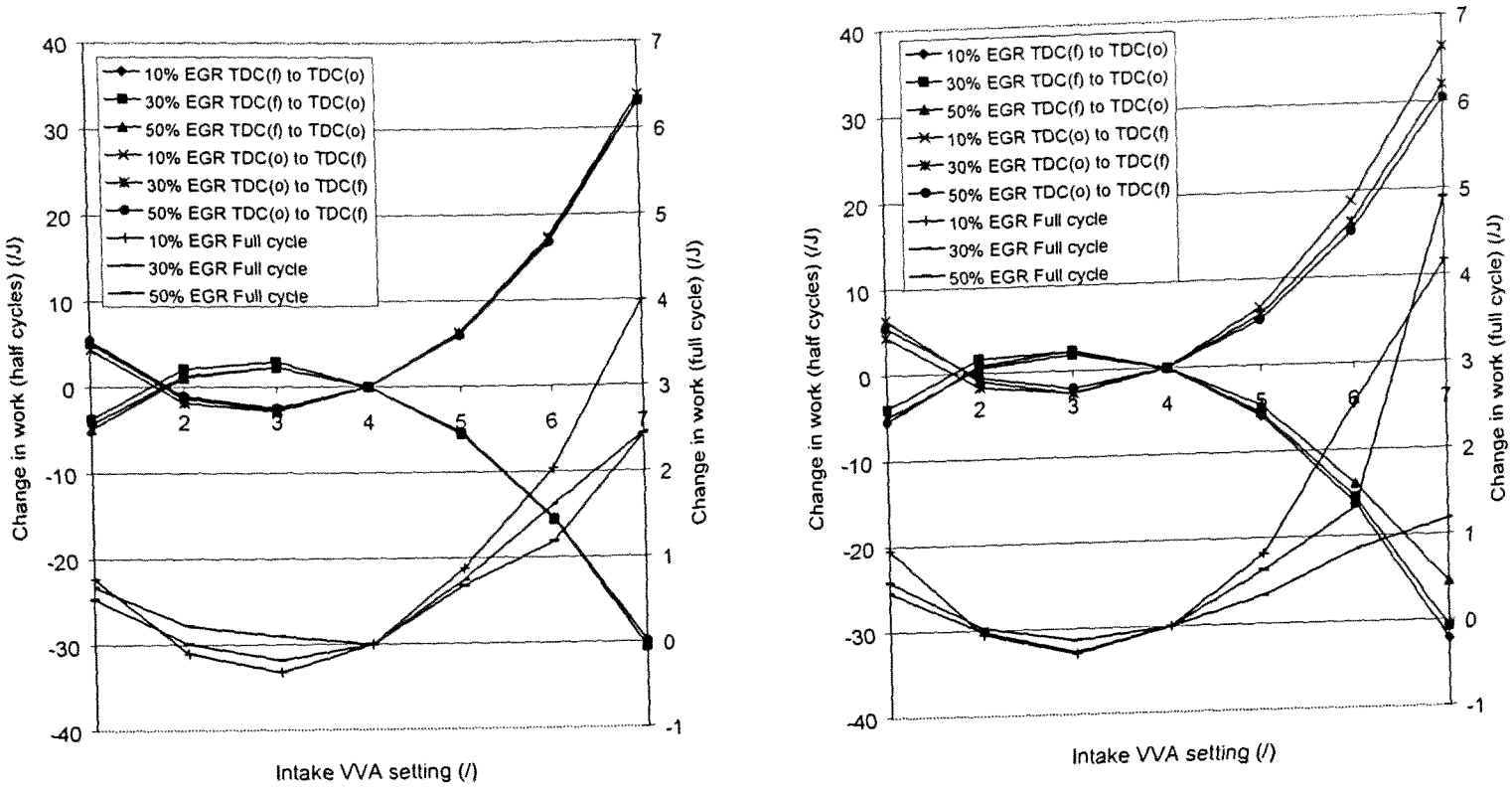


Figure 5.2.5.7 Changes in work done in the two half cycles TDC(f) to TDC(o) and TDC(o) to TDC(f) and the full cycle relative to intake VVA setting 4 (standard) for 5mg/stroke (left) and 10mg/stroke fuelling (right)

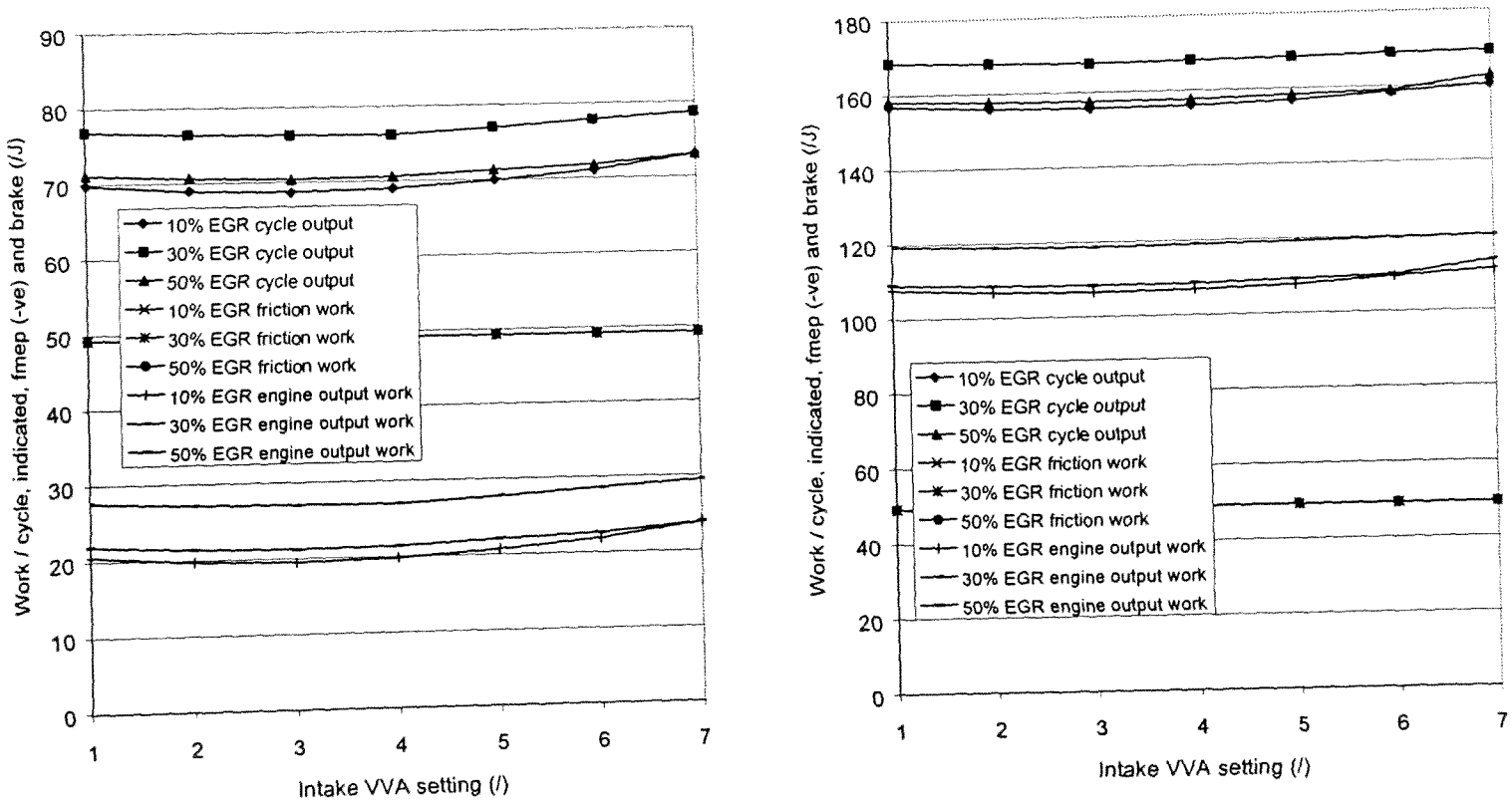


Figure 5.2.5.8 Indicated, friction and resulting work output for 5mg/stroke (left) and 10mg/stroke fuelling (right)

Figure 5.2.5.8 shows the full cycle work, the fmep converted to work/cycle and the resulting work available as output. In this context it can be seen that the changes in output from the intake valve timing variations were more significant, when considering brake output. In the 5mg case the change of approximately 4 Joule per cycle represents approximately 25% of the resultant output, and in the 10mg/stroke case the change was of the order of 4% although the actual change in work was greater. (Please note that for *figures 5.2.5.9* and *5.2.5.10*, the basis for comparison is the operation of the engine with standard intake and exhaust valve timings, and so the data represents the overall benefits available from intake and exhaust VVA.)

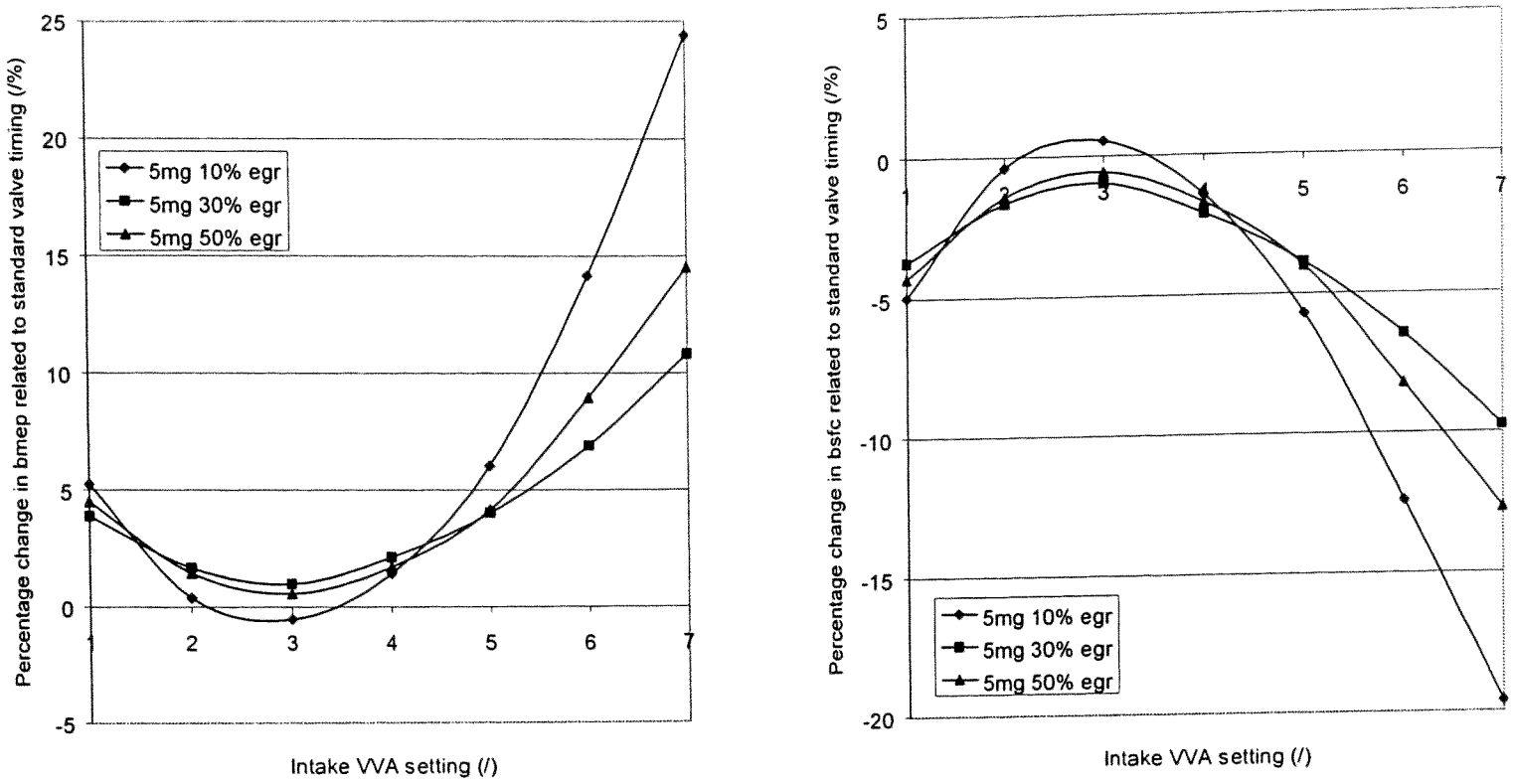


Figure 5.2.5.9 Changes in bmep (left) and bsfc (right) versus intake VVA setting, with exhaust VVA setting 3, 5mg/stroke fuelling at three EGR rates.

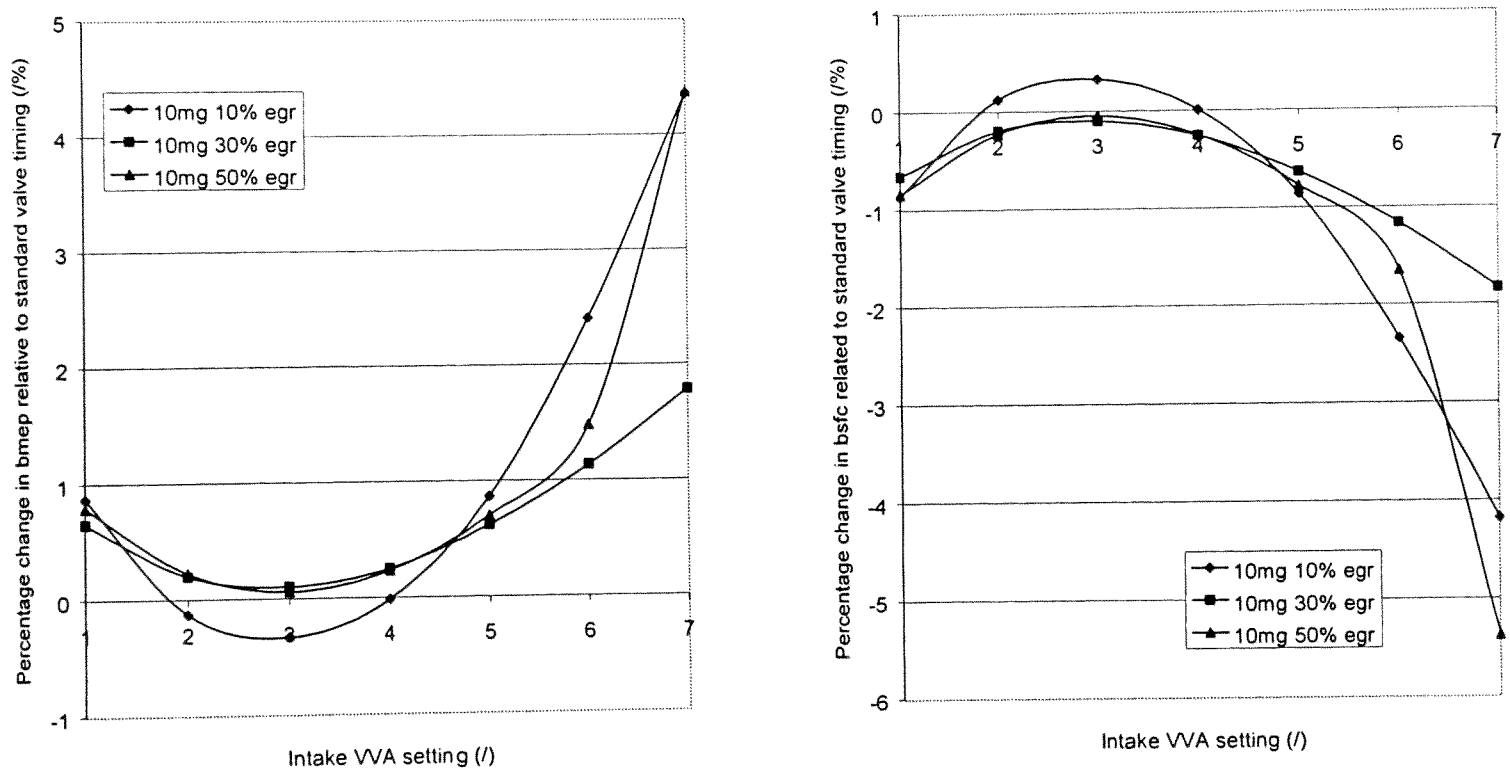


Figure 5.2.5.10 Changes in bmep (left) and bsfc (right) versus intake VVA setting, with exhaust VVA setting 3, 10mg/stroke fuelling at three EGR rates.

It can be seen from *figures 5.2.5.9* and *5.2.5.10* that significant increases in bmep and reductions in bsfc are possible with optimised (11° retarded) exhaust and optimised (33° retarded) intake valve timings at the operating conditions investigated, with improvements in bsfc of up to 19% and in bmep of up to 24% at 5mg/stroke fuelling. At the higher fuelling rate of 10mg/stroke these reduce to 5.5% and 4.5% respectively. However, care needs to be taken in the interpretation of bsfc values at very light loads, where a significant proportion of the fuel is used simply to overcome friction because small changes in output as calculated here with fixed fuelling can

produce large changes in bsfc. The use of isfc offers an alternative insight: *figure 5.2.5.11* shows these same operating conditions, but with the fuel consumption benefits in terms of isfc. It can be seen that the magnitude of the benefits is smaller for the reason outlined above, but these numbers approximately represent the improvements in fuel flow that might be expected if the bmep levels were restored to their nominal values by a reduction in fuel flow. These are also of the order of the fuel consumption benefits that might be expected at idle. Even at these levels the reductions in drive cycle fuel consumption would probably be significant.

As was mentioned earlier the EGR valve openings for the 10% and 30% EGR settings were somewhat arbitrarily chosen, with an EGR valve opening necessitating a relatively closed VGT setting for 10% EGR and one allowing a relatively open VGT setting for 30% EGR. From *figures 5.2.5.9* and *5.2.5.10* in combination with *figure 5.2.5.3*, showing VGT settings, it can be seen that the more closed the VGT setting, the greater the reduction in bsfc.

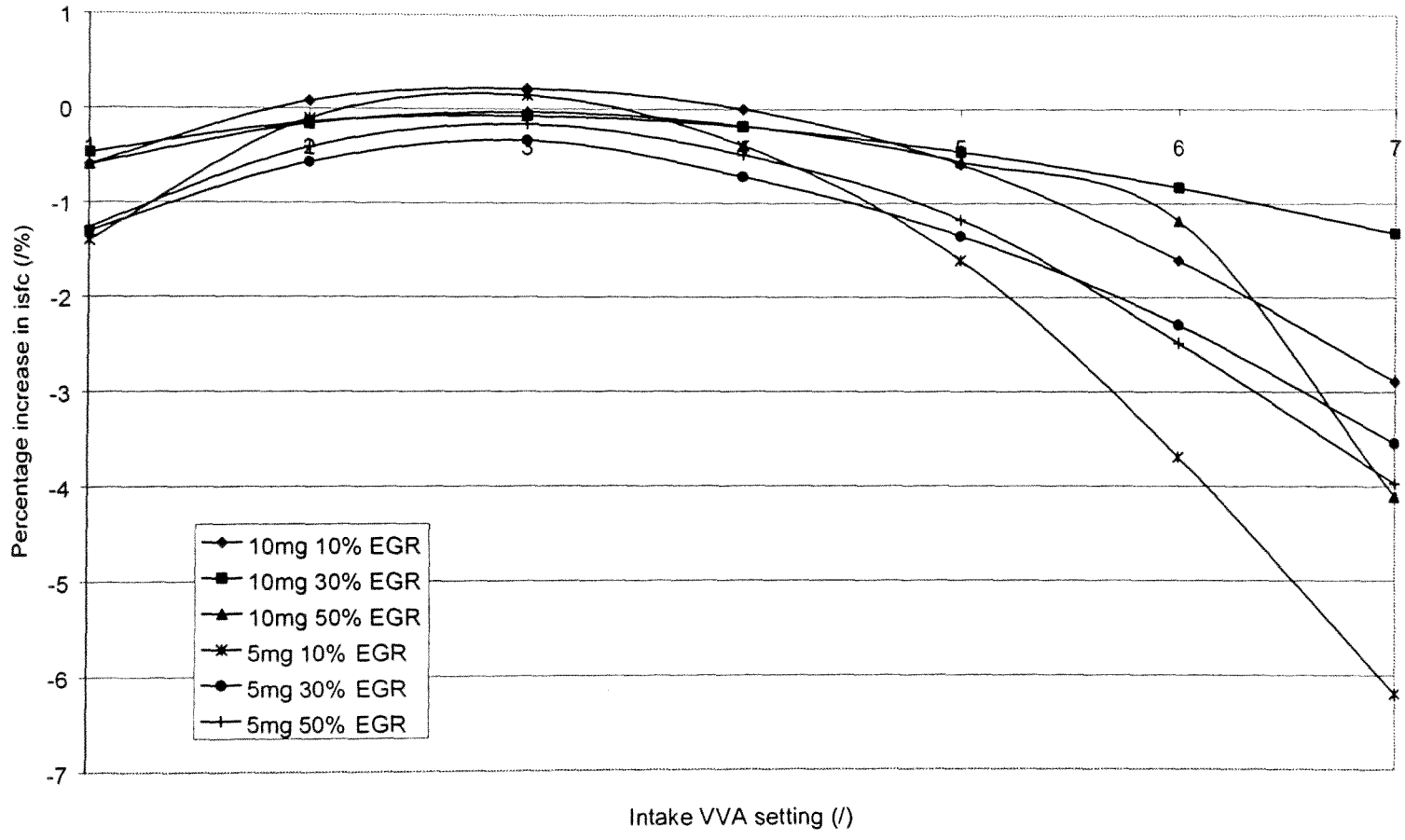


Figure 5.2.5.11 Percentage change in isfc from standard, for varying fuelling, EGR and intake VVA settings (Exhaust VVA setting 3)

There are three factors causing this: 1. The more closed the VGT the greater the exhaust pumping work, *figure 5.2.5.3*. 2. The more closed the VGT the greater the boost pressure and the greater the benefits of late intake valve closing in reducing compression work. 3. The underlying bsfc with the more closed VGT settings is higher. See *figure 5.2.5.12*

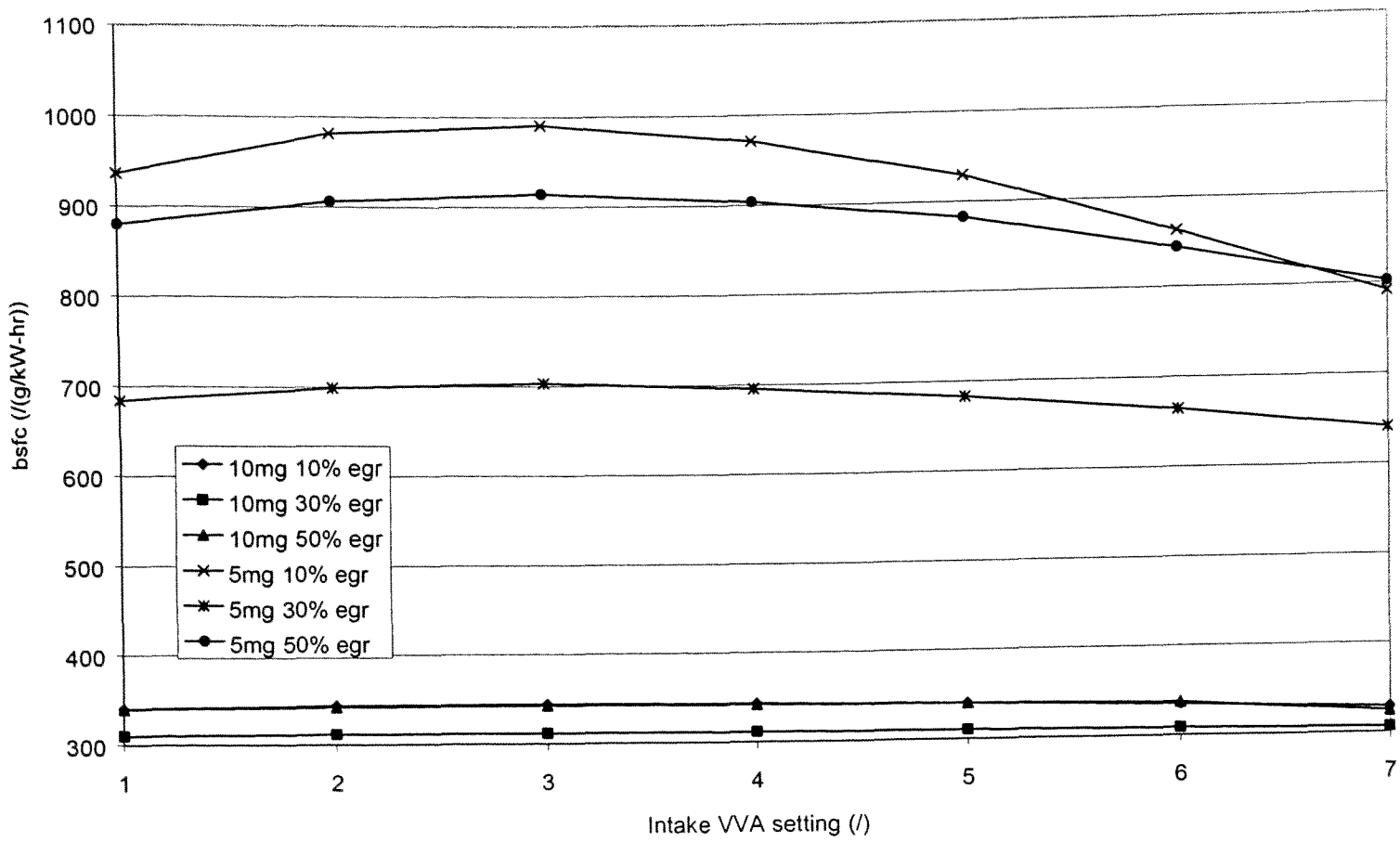


Figure 5.2.5.12 bsfc values for 5 mg/stroke and 10 mg/stroke at 2000 rpm and the three EGR rates, with varying intake VVA and exhaust VVA setting 3

From this the fuel economy penalties of running with high levels of EGR, a smaller than necessary EGR valve orifice or small VGT nozzle openings are apparent. Effectively, the use of EGR is mandatory as it is the most cost effective method of controlling NO_x, but the amount of EGR required is largely dictated by the engine characteristics and the applicable legislation. However, the combination of EGR valve and VGT settings used to implement it are a matter of calibration.

At present the majority of EGR valves and VGT controllers are vacuum operated. These have relatively slow response times of up to a second for full range operation. During positive (tip-in) load transients it is critical that the air-fuel ratio is controlled to avoid smoke. This requires that the EGR flow is quickly reduced to divert more mass flow to the turbo-charger in order that its speed rises rapidly to provide the air needed to allow an increase in fuelling, which in turn increases engine output, but all without the AFR falling below the smoke threshold. Typically this will require the EGR valve to be more closed than would be the case for minimum fuel consumption.

Thus it can be seen that there is a trade-off between minimised fuel consumption and VGT/EGR valve settings for best transient behaviour. The influence of intake and exhaust VVA on the

calibration of the EGR/VGT control systems and the transient operation of the light duty diesel engine is investigated in the next section.

5.3 TRANSIENT OPERATION

As with each of the investigations after the establishment of the baseline, it was necessary to extend the simulation model. The major extension was the implementation of the controllers needed to co-ordinate the operation of the VVA systems, the VGT setting and the EGR flow. But special attention was also given to the modelling of the combustion as the heat release characteristics were affected significantly by the level of EGR and fuelling over the transient from very light to full load.

Once the behaviour of these control systems had been adequately modelled, simulation was carried out to investigate the transient torque rise of the engine at a constant 2000 rpm from 5mg/stroke fuelling with 50% EGR to full load, zero EGR, with a target boost level. This was selected as being representative of the start of an overtaking manoeuvre in a high gear.

A base characteristic was established with standard valve timings and full load boost pressure . This was then compared with the behaviour of the system, starting with the VVA settings that produced the lowest fuel consumption at 5mg/stroke fuelling and 50% EGR and ending with the settings for maximum output at full load with the standard boost pressure. Whilst efforts were made to use representative controller time-response characteristics it was not certain that they were absolutely correct, so a sensitivity analysis was carried out to identify which controllers had the greatest influence in torque rise rate. This allowed comment on the significance of any errors that may have been made in the controller characteristics.

5.3.1 Changes to the model

The changes to the model fell into two areas:

1. The provision of a combustion correlation that could deal with the trends of ignition delay and heat release rate with varying engine load, EGR levels and boost conditions.

2. The provision of either time based controller characteristics or actual controllers for the various sub-systems (such as fuelling, VVA, VGT and EGR) that respond to the load transient.

The ways in which these were implemented are discussed in the next two sections. Besides these areas of significant work it was a matter of routine to provide the model with a new set of initial pipe wall temperatures that represented the converged steady state conditions at the start of the transient.

5.3.1.1 Combustion

As was stated at the beginning of section 5.2 on part load fuel economy, it was not found to be possible to adequately model the ignition delay and fuel burning rate curves that were derived from measured part load cylinder pressure data using the Wolfer correlation and the 3-term-Wiebe function used for the full load modelling. Therefore ignition delays and burn rate curves derived from measured data were used to deal with the steady part load operation. This method was extended to provide a "map" of combustion characteristics (including provision for the ignition delays) that covered the fuelling – EGR operating space.

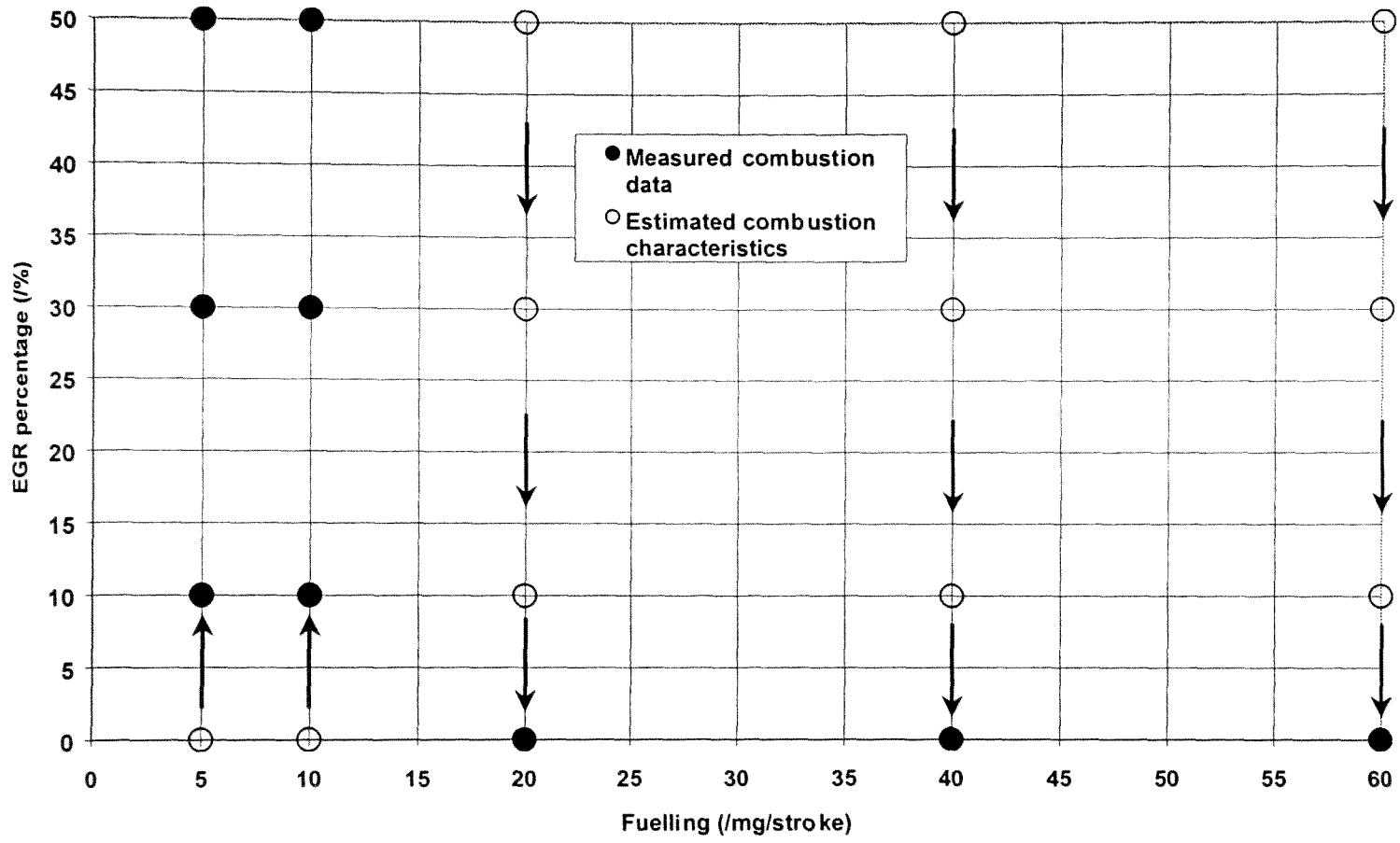


Figure 5.3.1.1.1 Combustion characteristic map in the fuelling - EGR space (Arrows point to the data used when measured data was not available) .

Figure 5.3.1.1.1 shows the way in which the map was populated, by indicating the actual test fuelling/EGR percentage conditions leading to the ignition delays and burn rate curves. However, as might be expected, measured pressure data was not available for all combinations of fuelling and EGR level needed to populate the map. This was particularly true at the higher levels of fuelling. After some consideration it was assumed that there would be little or no EGR at the higher fuelling levels, as the air flow required to use these amounts of fuel, with the prevailing air fuel ratio, would take sufficient time for the EGR valve to have shut. Therefore, the zero EGR burn curves have been propagated upwards across the maps to the higher EGR levels at the high fuelling values. The validity of this assumption will be discussed later in section 5.3.2 This map

was installed into the GT-Power model for use, where interpolation between the curves for intermediate values of both fuelling and EGR level was carried out automatically. (No extrapolation was allowed, if the operating point went off the edge of the map the value at the edge of the map was used)

5.3.1.2 Controller operation and characteristics

As already discussed the relative priorities and speeds of response of the various sub-system controllers is a major constraint on calibration of light duty diesel engines as there is a trade-off between fuel economy and transient drivability through the interaction of the VGT setting and EGR valve orifice settings. (In these discussions the term controller is used to describe the complete control system, software, electronics and actuators.) Fuelling systems can respond on a stroke by stroke basis and will, within measurement system accuracy, follow a prescribed air-fuel ratio trajectory very closely. Therefore, the limitations on transient operation are imposed by the air/EGR management. When using AFR fuelling control (as is common these days) transient torque rise is a function of how quickly the air flow can be increased. This is initially a problem of rapidly reducing the amount of EGR to increase turbine mass flow and then becomes a matter of achieving a target boost level, through management of the turbine and if present VVA, as quickly as possible to maximise volumetric efficiency throughout the transient.

From the foregoing it can be seen that five controllers were needed for this piece of work:

1. Fuelling/AFR
2. Intake VVA
3. Exhaust VVA
4. VGT setting (2 modes)
5. EGR valve

In order to discuss the operation of these controllers it is necessary to describe the sequence of events during the transient: In a real driving situation the transient from light load cruise to full load would be initiated by the driver pressing the accelerator pedal. In a modern diesel engine management system this would trigger a change of operating mode from minimised emissions and fuel consumption to maximised output. This would be achieved by lowering the target AFR

and providing adequate fuelling to achieve it, closing the EGR valve and reducing the VGT setting to maximise boost.

To replicate this sequence of events in the model, time based series were used to represent the changing inputs, with simultaneous step changes in AFR and available fuel representing the combination of driver input and engine management mode change. Up to the start of the transient the EGR valve is fully open and the VGT setting is controlled to manage the amount of EGR. At the time of the step change in fuelling and AFR, the controller for the VGT is switched to a boost pressure target from an EGR target and a time based series representing the EGR valve controller closing response is applied. (The strategy governing the operation of the VVA controllers is discussed later in section 7.4.3)

GT-Power provides a number of ways in which controllers can be imposed on system actuators, and in addition to the time based controller response series a PID controller was implemented to control the VGT setting. *Table 5.3.1.2.1* summarises the controller characteristics:

Variable controlled	Controller type	Comments
Fuelling / AFR	Time based series	Step changes (during one cycle)
Intake VVA	Time based series	Taken from measured controller response data
Exhaust VVA	Time based series	Taken from measured controller response data
Variable Geometry Turbine setting	PID – switches between EGR target and boost pressure target at the start of the transient	Tuned for response to match baseline model characteristics for speed, overshoot and stability
EGR valve orifice diameter	Time based series	Taken from simulation results of detailed study of complete EGR valve control system

Table 5.3.1.2.1 Summary of controller characteristics

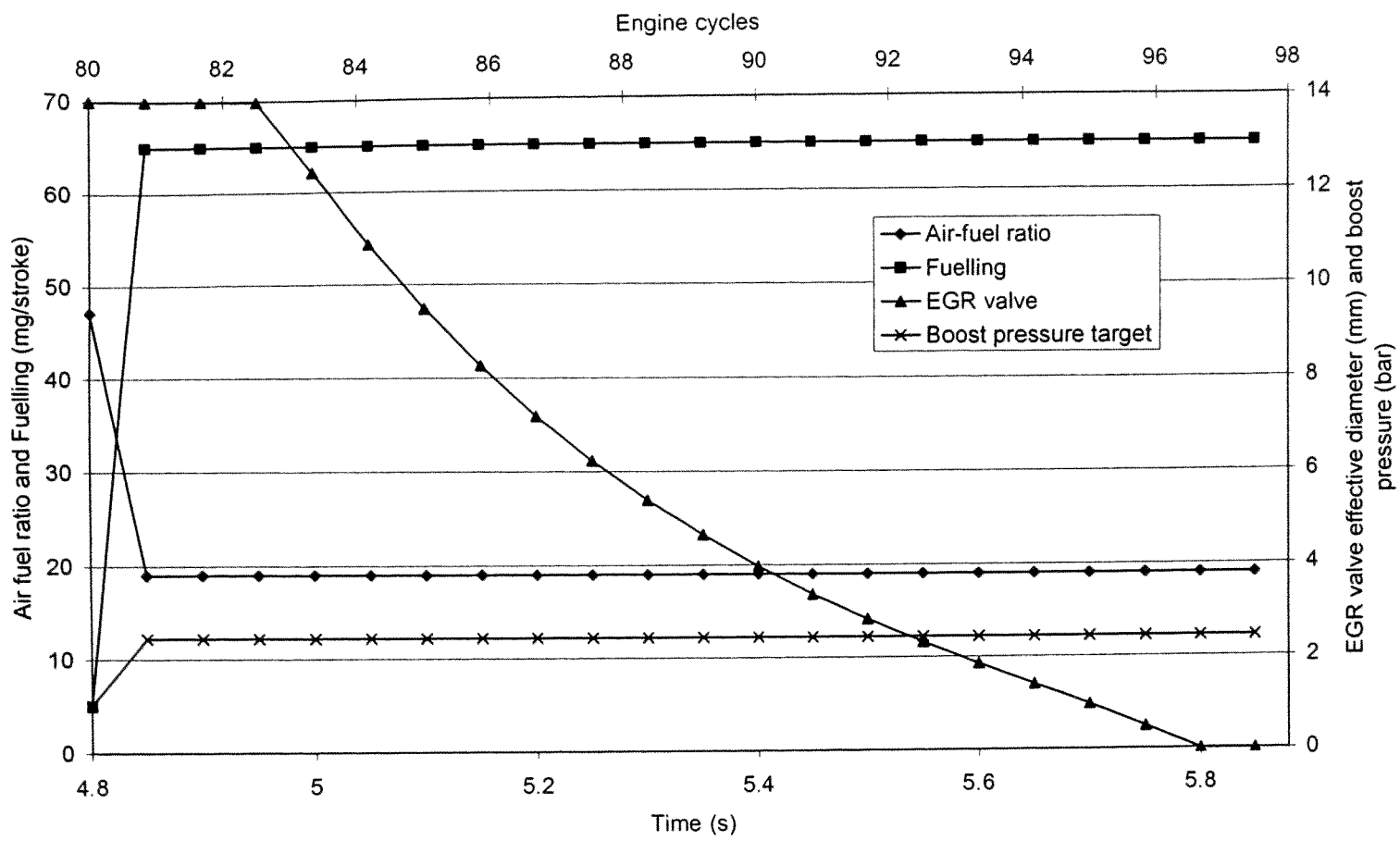


Figure 5.3.1.2.1 Time based controller characteristics used with the standard valve timing (The first 4.8 seconds is used to stabilise the low load operating condition).

Figure 5.3.1.2.1 shows the time based controller characteristics used during the standard valve timing run. The transient is set to start at t=4.8 seconds. The air-fuel ratio switches from 47:1 to 19:1, which is representative of very light cruising load to smoke limited full load. The available fuel switches from 5mg/stroke to 65mg/stroke, but the actual amount of fuel used is set by the AFR limit once the transient starts. As already mentioned the VGT controller switches from EGR control to boost control at the start of the transient, and this results in the target boost level changing from approximately 1 bar absolute to 2.44 bar absolute pressure. Inspection of *figure 5.3.1.2.1* also shows that there is a delay between the initiation of the transient and the EGR valve beginning to close. This time series was chosen to be representative of typical EGR valve response and includes the detailed behaviour of the valve, the controller and the vacuum actuation system and it is the vacuum actuation system that introduces the delay (Lancefield *et al* 1996). In this figure it will also be noted that the time series for the controllers finish at t=5.85s. This is because the last of the time series has stabilised and from then on GT-Power uses the last value in the series.

The behaviour of the PID controller implemented to control the VGT for boost pressure control can be seen later in *figure 5.3.2.1*, where the transient VGT setting is shown.

5.3.2 Behaviour with standard valve timing

At the end of section 5.2.5 the problems associated with calibration and control for good transient behaviour were mentioned in the context of the conflict between EGR and fuel economy for rapid torque rise. Also the advent of variable geometry turbines has made it possible to utilise larger compressors than would have been possible with wastegated systems. As a consequence the rotary inertia of the turbocharger has increased, increasing the torque required to accelerate it. The ability to alter the nozzle settings can reduce this problem, but the controller and actuator needed to alter the nozzle positions have their own time response characteristics. The latest electrical actuators for VGT systems can slew from end to end in approximately 0.5 second. This equates to an end to end time of approximately 8 complete engine cycles at the speed used for this investigation, 2000 rpm.

In all of the following figures the data presented is converged data for the end of a given cycle. The start of the transient is the end of cycle 80 at t = 4.8 s.

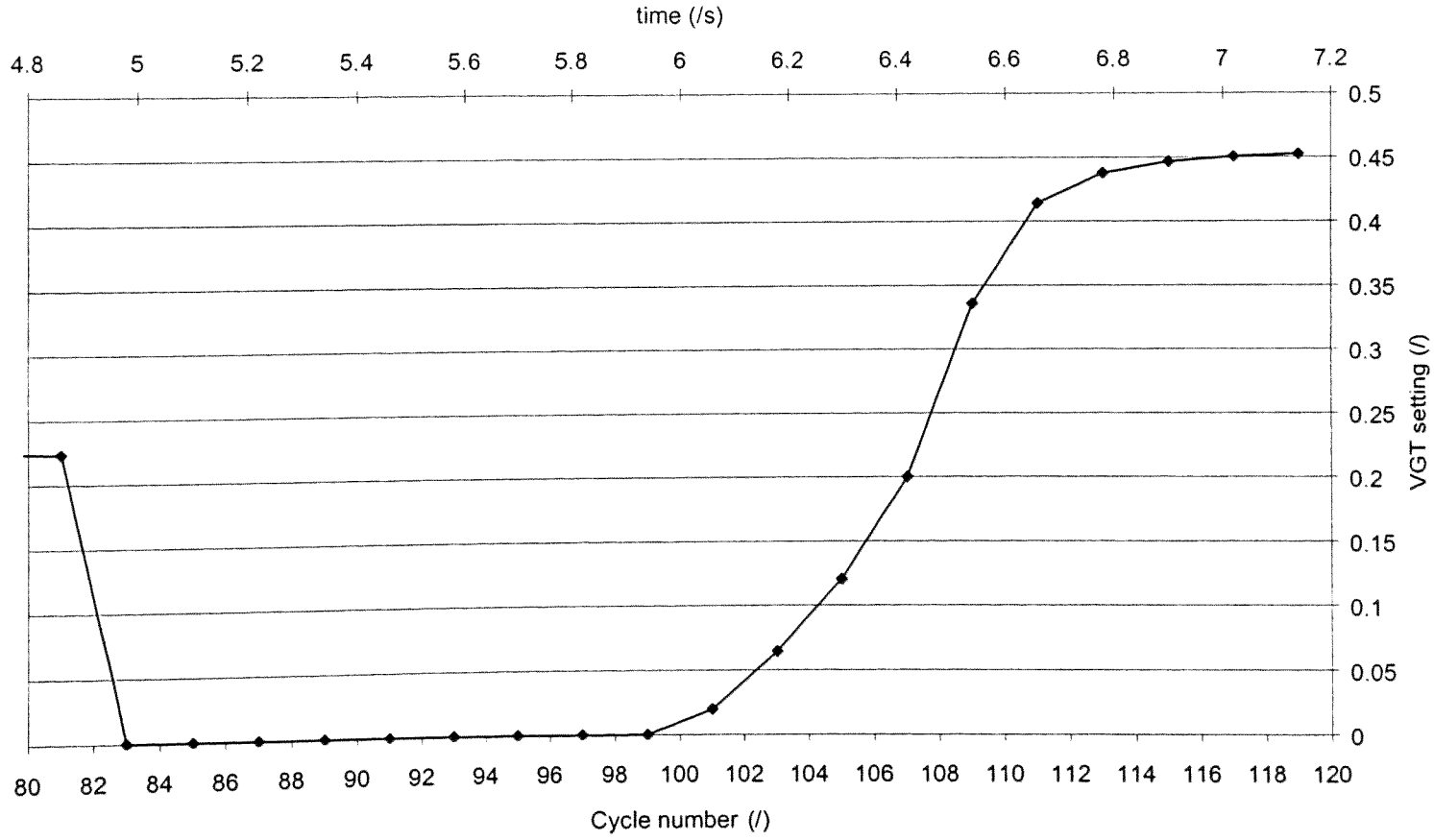


Figure 5.3.2.1 Transient VGT setting as a function of engine cycle number for the standard valve timings

Figure 5.3.2.1 shows the VGT behaviour throughout the transient. At the desired level of EGR, 50%, at 5mg/stroke fuelling the VGT setting is approximately 0.22, which generates the pressure differential to cause the desired EGR flow rate. At the switching time, the end of cycle 80, the priority becomes maximising boost and the error term in the PID controller becomes large

causing the nozzles to be rapidly closed. (The time taken in the above plot is consistent with the slew rate of an electrical actuator as described above.) As the error in boost pressure reduces so the controller opens the VGT nozzles, finally stabilising at 0.45 for the target boost level of 2.44 bar absolute. *Figure 5.3.2.2* shows the engine torque predicted during the transient. It will be seen from this that there is a small torque peak shortly after the transient begins. This is a consequence of the difficulty of reducing EGR and increasing boost pressure quickly and, whilst it might be thought that this is positive, fluctuations in torque of this nature are not good for the transmission and there is an emissions implication for a real application.

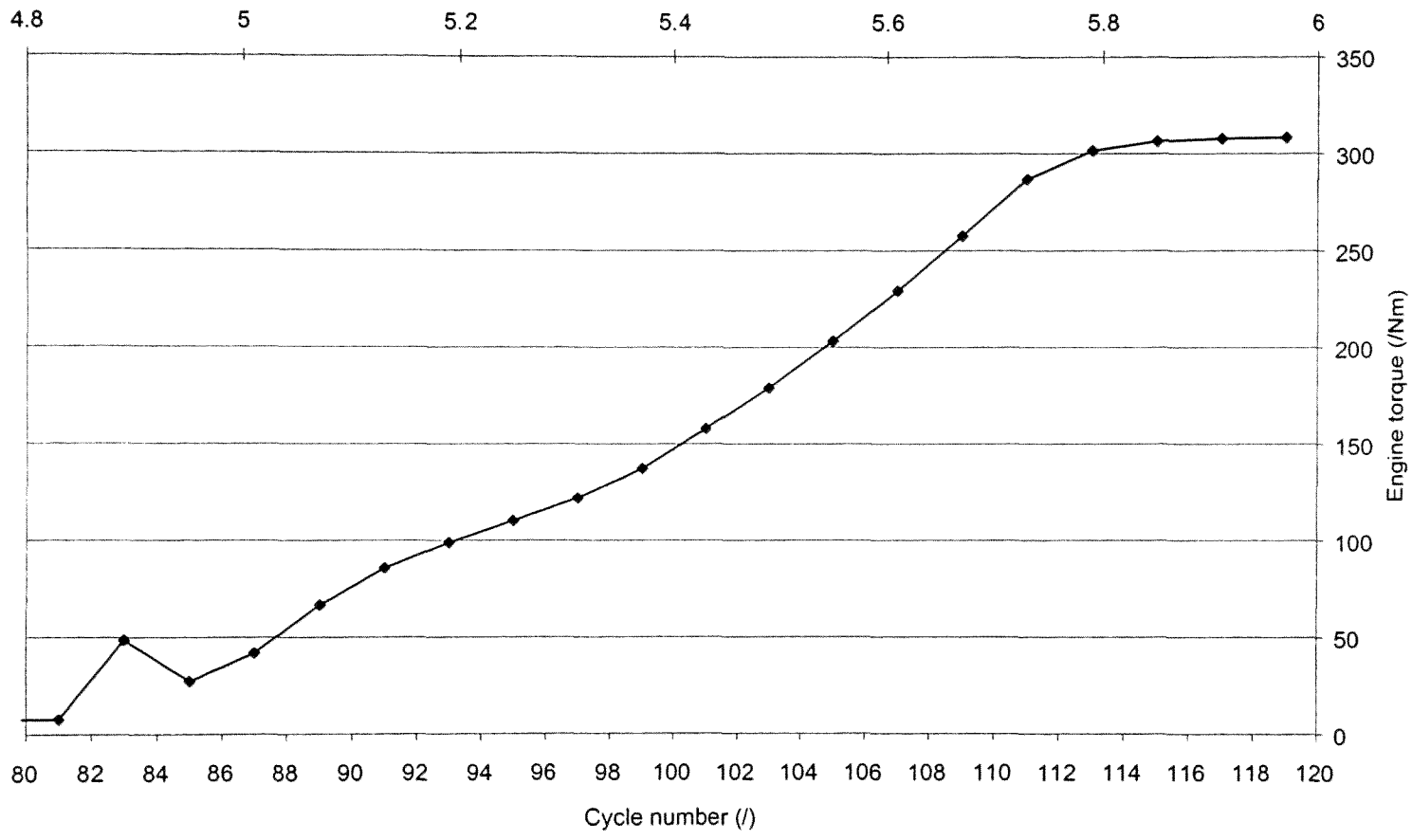


Figure 5.3.2.2 Transient torque rise with standard valve timing

Figure 5.3.2.3 shows the EGR-fuelling operating locus on the combustion characteristic map, initially shown in *figure 5.3.1.1.1*. It can be seen from this that during the transient, the model moves into operating regimes (combinations of fuelling and EGR level) that are not well populated with measured combustion data. In the region above 50% EGR the model simply uses the 50% EGR condition, for fuelling levels between 10 and 20 mg/stroke interpolated data provides some of the effects of the EGR, but probably not all, and for fuelling levels between 20 and 40 mg/stroke the data used does not include the effects of EGR, despite the locus showing that some is needed. It is not possible to comment on how important these excursions from measured data are, but it can be seen that for the majority of the transient the major effects of EGR are captured.

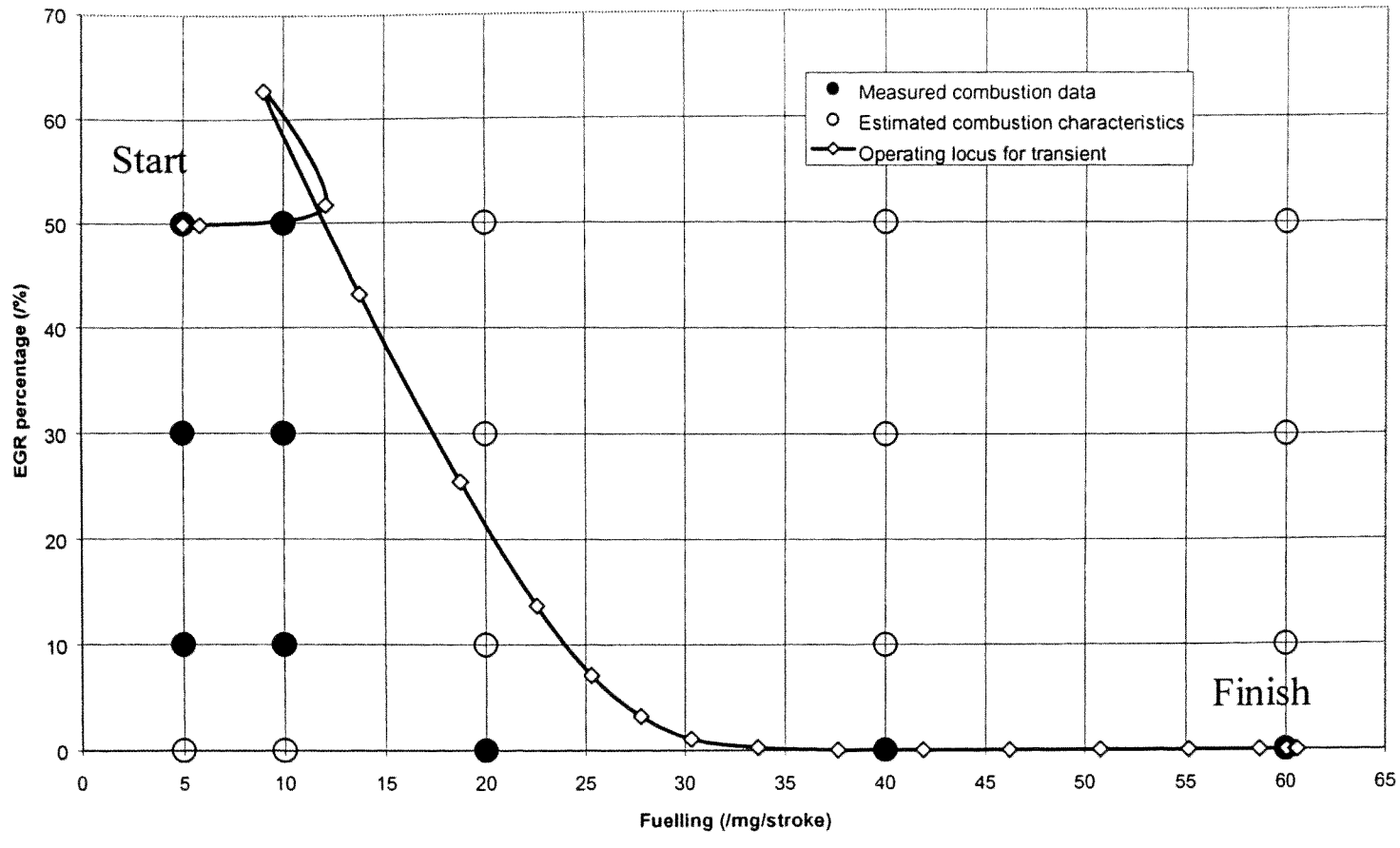


Figure 5.3.2.3 Transient EGR-fuelling operating locus with standard valve timing

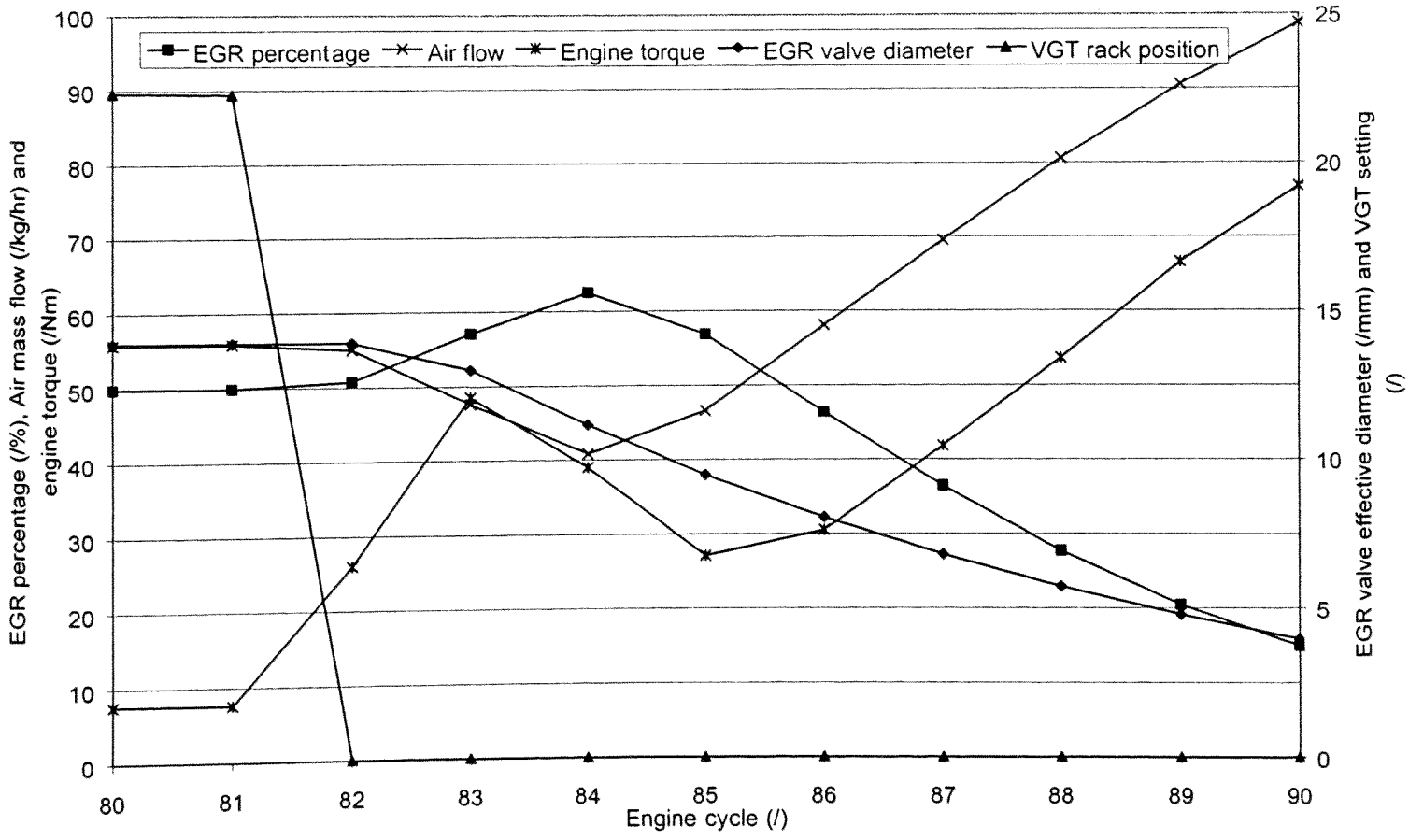


Figure 5.3.2.4 Cycle based response of the EGR orifice diameter and percentage, VGT setting, air flow and torque with standard valve timing.

Figure 5.3.2.3 also shows that the torque spike occurring around cycle 83 is associated with a combination of increased fuelling and increased EGR (from starting conditions). *Figure 5.3.2.4*, shows that a consequence of the increase in EGR is a dip in airflow. It also shows the explanation for the rise in EGR and reduction in air flow: It can be seen that, in comparison with the EGR

valve control the VGT control is fast, so the VGT starts to close, increasing the pressure driving the EGR across the engine, before the EGR valve starts to close to reduce the EGR level. However, by cycle 86 the EGR valve is closed sufficiently to reduce EGR flow and the air flow starts to increase again. Despite this dip in airflow, because of the implementation of the AFR controller, the amount of fuel injected into each cylinder is correct and the AFR remains correct. Thus if the dip in airflow could be avoided a step change (within 2 engine cycles) in torque at the start of the transient, and a smooth rise from there on, might be expected. This is discussed further in section 5.3.4.

It should be pointed out that the model uses a "smoke limiting" AFR controller that has access to the air mass trapped on a cylinder by cylinder basis to adjust the fuel injected for each cylinder. Thus there are no delays and accurate AFR control is possible with the simulation model. But, in a real system, the air mass flow data would be measured for the whole engine and would be historical, i.e. delayed, thus falling air flow would tend to result in a reduction in AFR below the target, possibly leading to smoke, and increasing air mass flow would result in an AFR above the target, leading to slower torque rise than would be achievable with more accurate fuel control. (However, at the expense of speed of torque rise the AFR control algorithm could be modified to compensate for this type of AFR excursion.)

Overcoming the shortcoming of the simulation model control system which produces this torque spike is practical in a real system, where the response of the VGT controller could be delayed to allow the EGR valve to partially close before the VGT setting reduced, but this would have taken considerable effort to implement in the simulation model. Therefore, since it was considered that the early torque rise and fall was unlikely to mask any underlying differences between the behaviour with and without VVA it was decided that this controller strategy would be retained for the comparison in torque rise rate.

5.3.3 Comparison of standard valve timing and VVA performance

The only difference between the models with standard valve timing and with VVA was the addition of controllers for both intake and exhaust VVA systems. The difficulty with these was that the actuators used in real VVA hardware systems are subject to the reversing loads imposed by the valve train events and as such are highly dynamic, often moving to their target positions in a stop-start manner in small high frequency steps. Within the scope of this piece of work it was

considered that it was not possible to replicate this type of behaviour for the controllers and a higher level approach was needed. The controller characteristics used were therefore based on measured data, sampled at a low speed, such that the high frequency stop start behaviour was filtered out. This data was measured from a hydraulically actuated VVA system on a test bench and is represented as time series in the model.

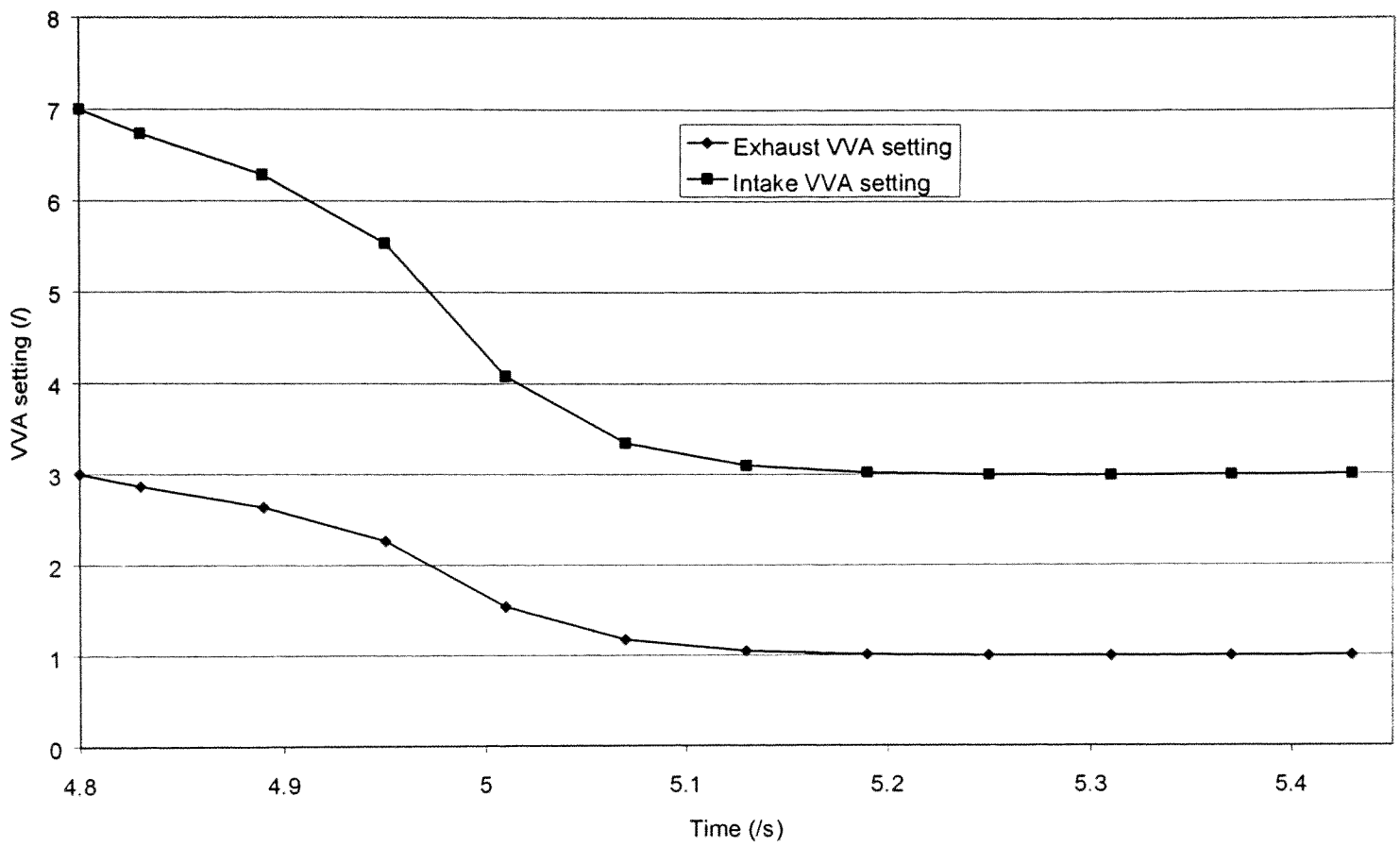


Figure 5.3.3.1 Time series of VVA controllers. t = 4.8 s (end of cycle 80) is the start of the transient.

It was shown in section 5.2.5 that at 2000 rpm, 5mg/stroke fuelling and 50% EGR, the initial condition for the transient, for minimum fuel consumption the intake valve closing setting would need to be 7 and the exhaust valve opening setting 3 and in section 5.1.4 it was shown that for maximum output, at 2000 rpm full load, these settings would need to be 3 and 1 respectively. Thus the intake VVA controller needed to change the setting from 7 to 3 and the exhaust VVA controller from 3 to 1. *Figure 5.3.3.1* shows these time series characteristics.

Figure 5.3.3.2 shows the transient torque rise characteristics for the model with fixed, standard, valve timing and with VVA operating according to the strategy outlined above. It can be seen that whilst the initial characteristics in the region of the torque spike, discussed earlier, show the two curves to be very similar, beyond cycle 87 the model with VVA has a notably higher rate of torque rise. *Figure 5.3.3.3* shows the difference between the two torque levels, a positive difference indicating greater torque with VVA. It can be seen that initially the torque output is marginally higher with VVA, as the fuelling is fixed at 5mg/ stroke in both cases, but the VVA

reduces pumping work. But this situation reverses as soon as the AFR controlled fuelling starts at the end of cycle 80. The situation again reverses after cycle 85, beyond which the engine model with VVA predicts greater torque. The reason for this behaviour is shown by *figure 5.3.3.4* which shows that after cycle 85 there is greater air flow through the engine with VVA (and because the fuelling is AFR controlled) a greater output results.

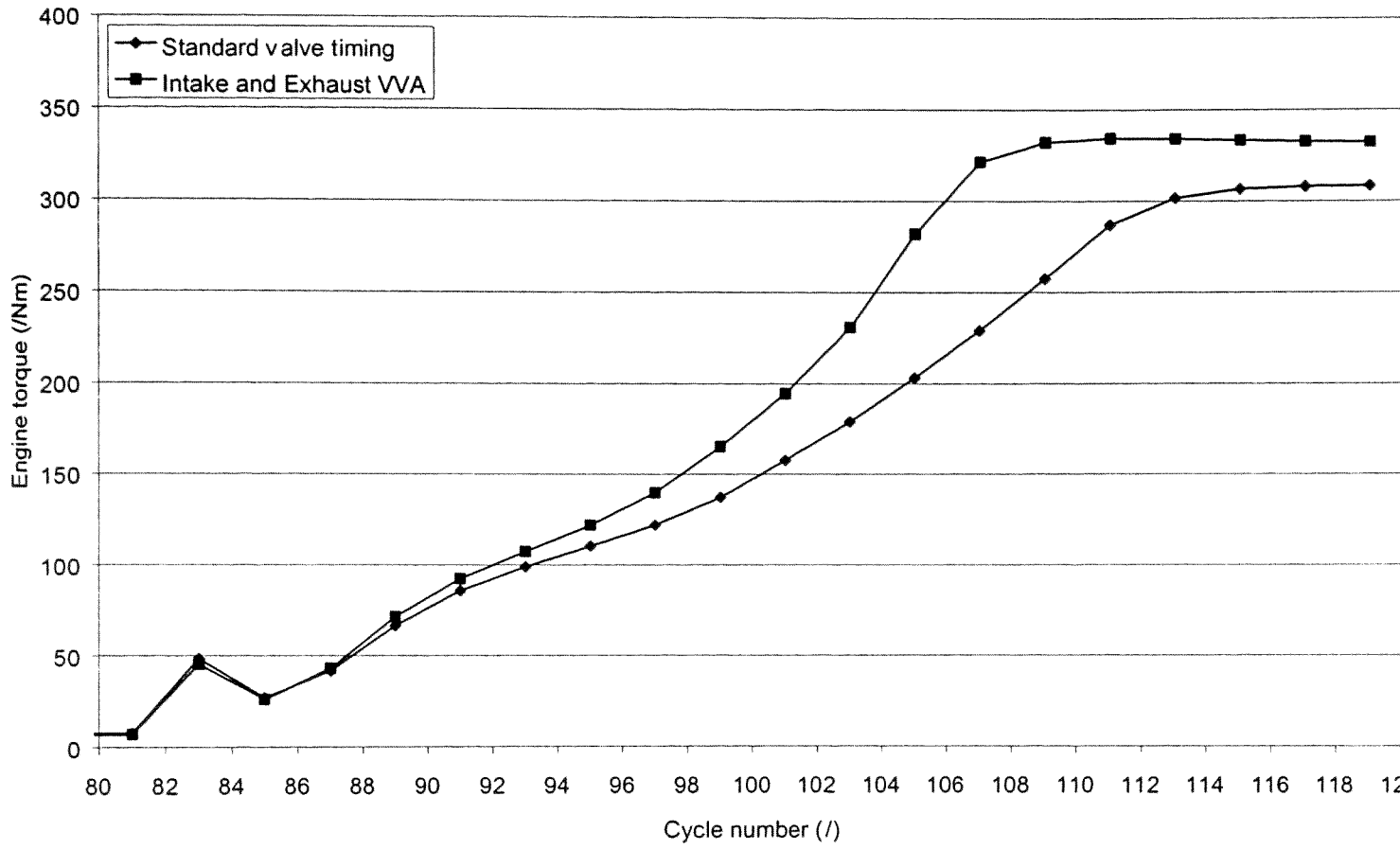


Figure 5.3.3.2 Transient torque rise with and without VVA

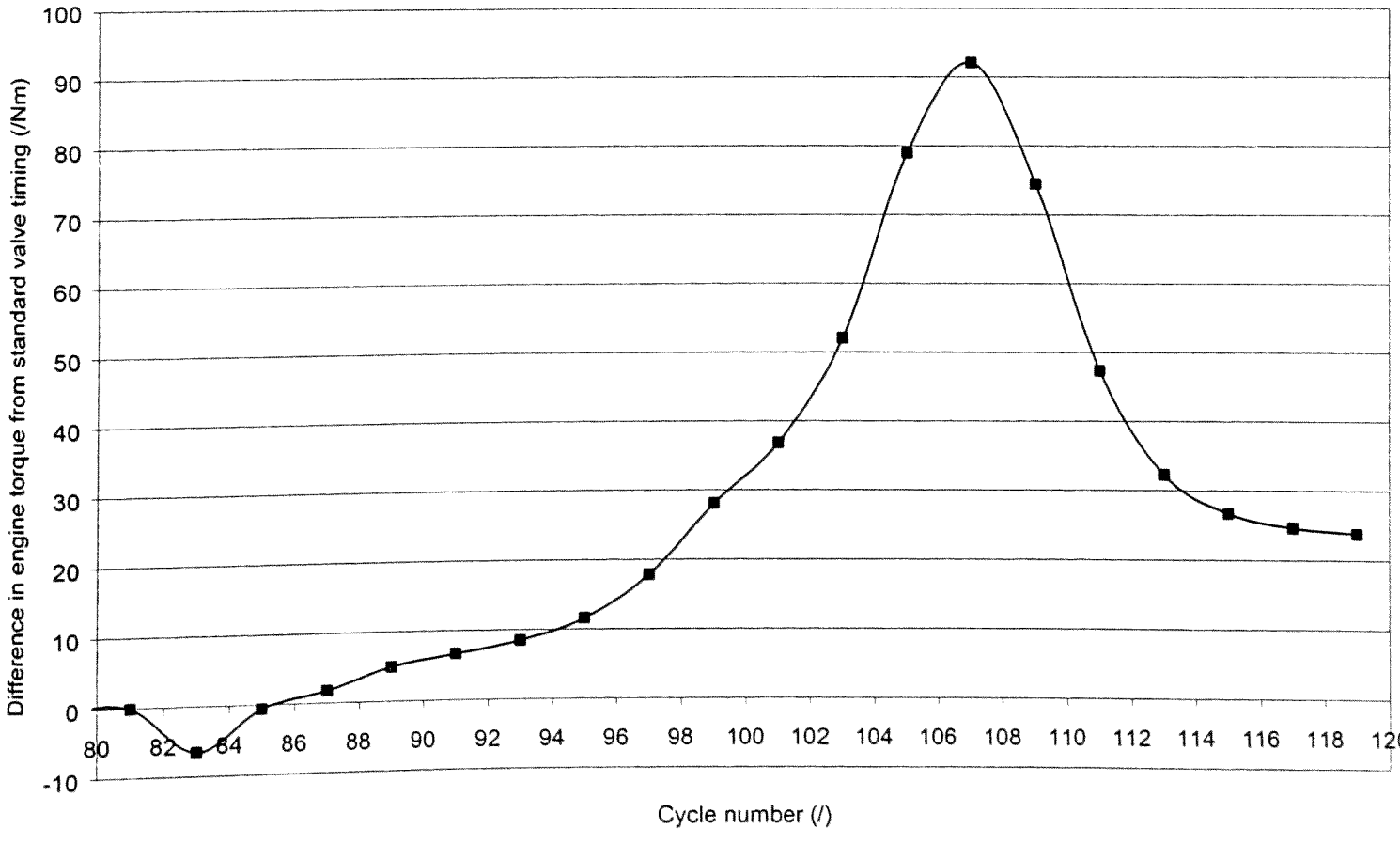


Figure 5.3.3.3 Increase in torque levels when using VVA compared to those with fixed standard valve timings.

The factors that lead to this greater airflow are greater volumetric efficiency, greater power from the turbine (partly from increased efficiency and partly from increased mass flow) and increased compressor efficiency, all of which result from the use of VVA. *Figure 5.3.3.5* shows the turbine and compressor cycle averaged efficiencies for the transient and it can be seen that from cycle 87 onwards the efficiencies of both are higher with VVA than standard valve timing until the transient is over and the models have stabilised at maximum torque. (It should be noted that with VVA the stabilised torque output is higher as the volumetric efficiency of the engine is higher.)

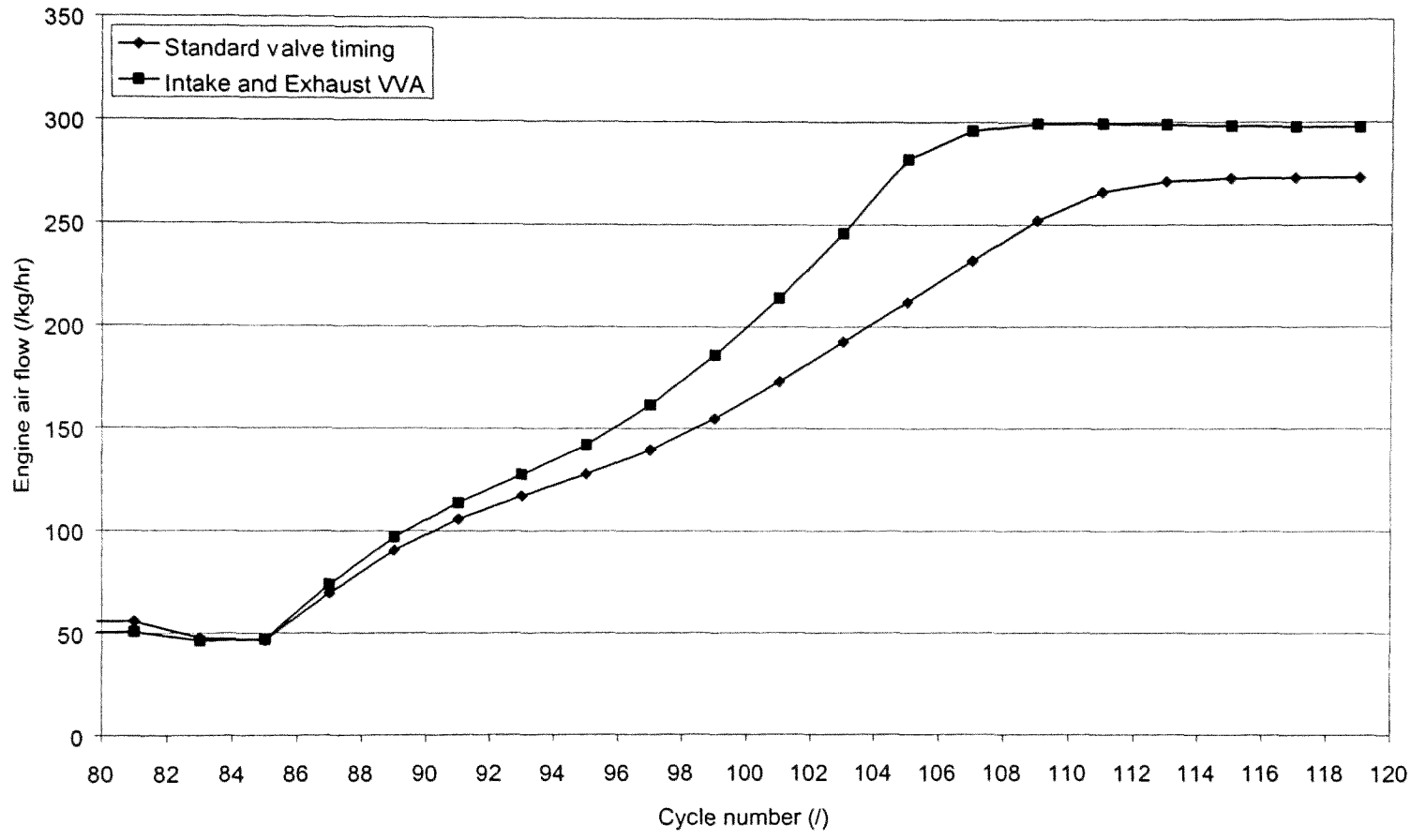


Figure 5.3.3.4 Air flows with fixed standard valve timing and VVA

Figure 5.3.3.6 shows the effect of the VVA on the volumetric efficiency. It also shows the time based characteristics of the VVA controllers as well as the standard valve timing settings. From this it can be seen that the VVA systems are already at their target positions by the end of the dip in the volumetric efficiency caused by the EGR level excursion (cycle 85.) It should be noted that on the basis of the work carried out in the full load investigation, the exhaust VVA system starts the transient, and remains, at settings that are superior to the standard, while for the intake VVA system the transient starting condition is worse than standard for volumetric efficiency. However, since they both reach their final positions before the air flow actually starts to rise the disadvantageous intake starting point appears not to be a problem, but slower VVA control systems might reduce the benefits.

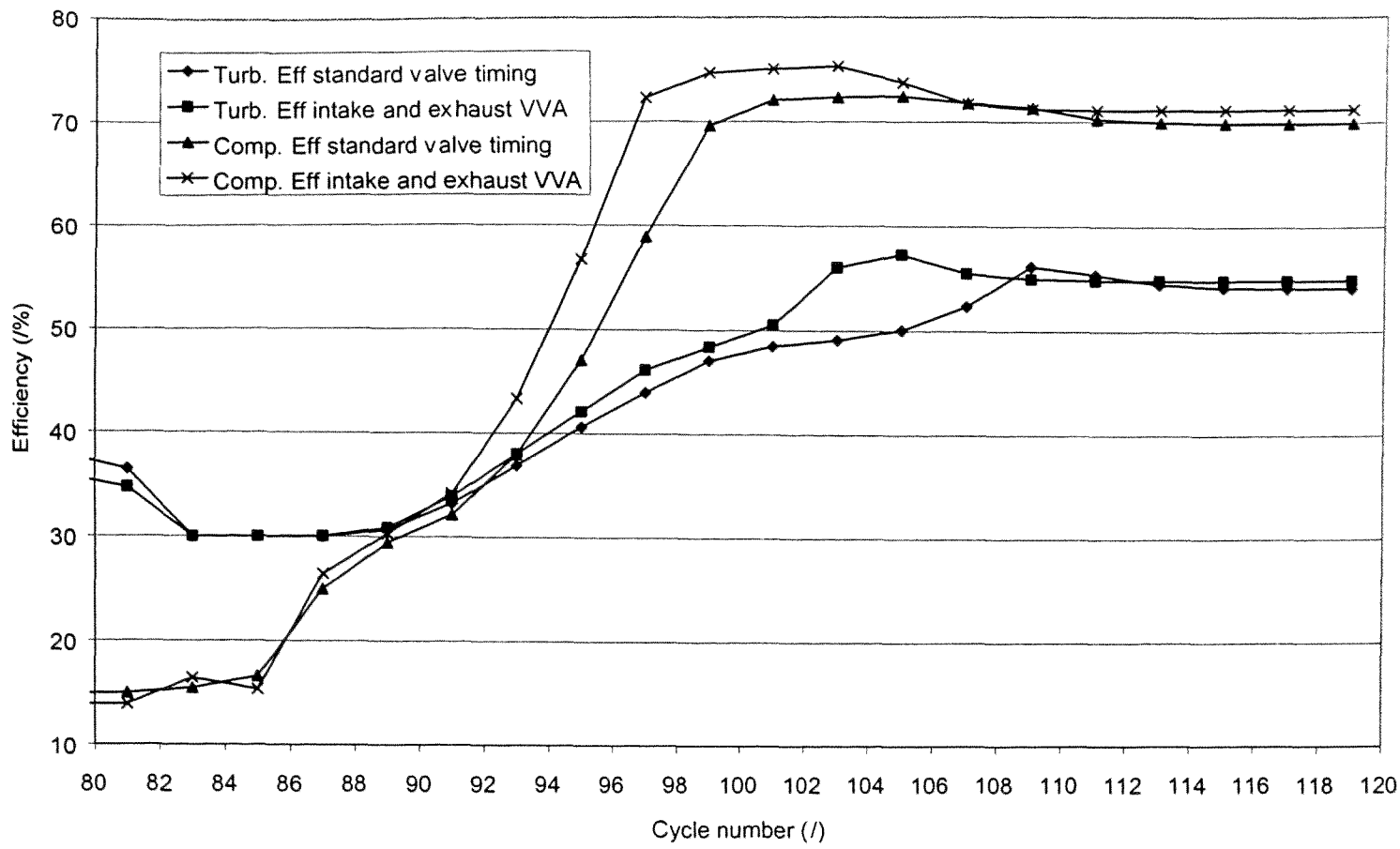


Figure 5.3.3.5 Turbine and compressor efficiencies for standard fixed valve timing and with VVA

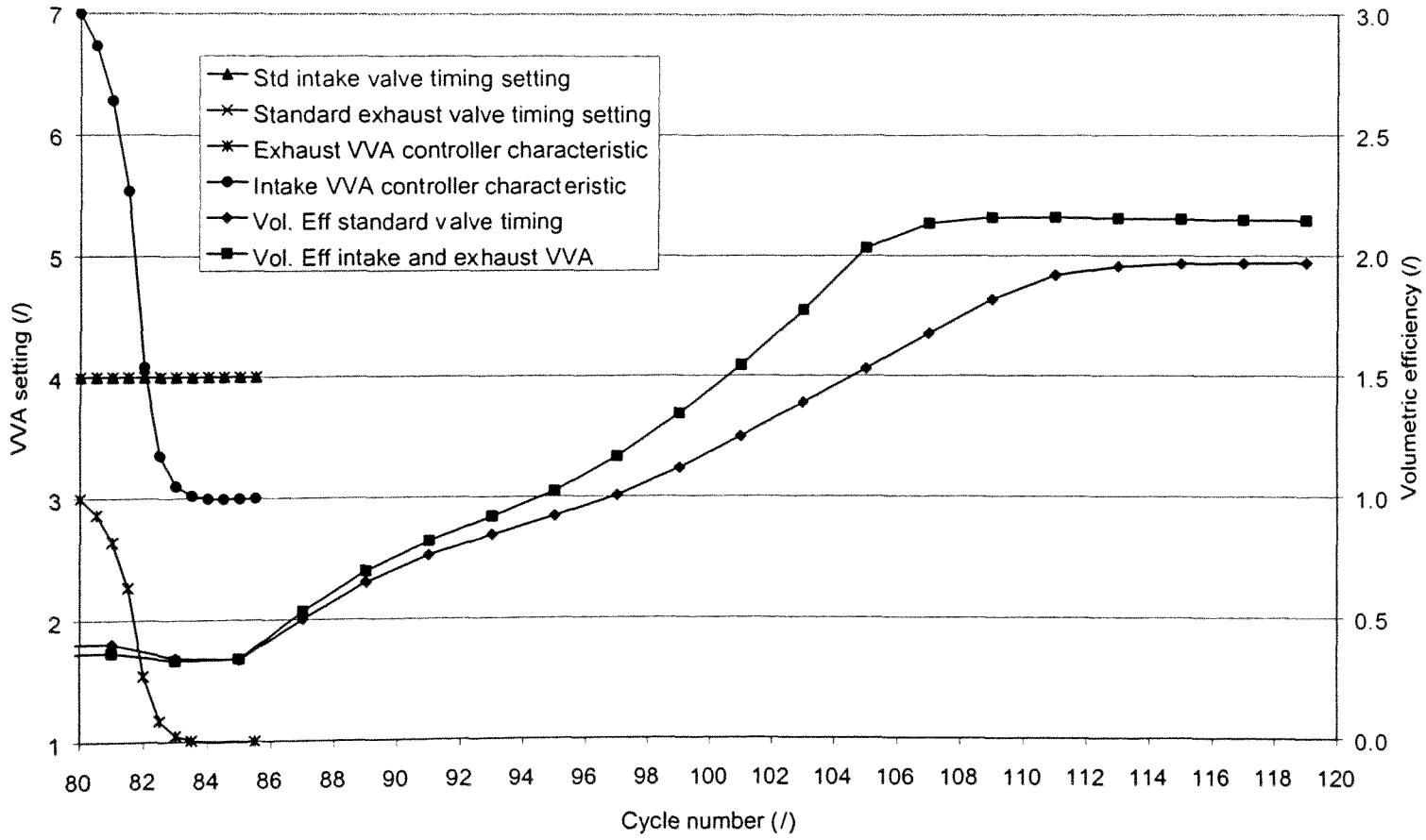


Figure 5.3.3.6 Volumetric efficiency referred to ambient conditions and valve timing settings (4 is standard)

Figure 5.3.3.7 shows the effects of the VVA on available torque for accelerating the turbo-charger. It is not clear if the 200+% greater available torque around cycle 83 is significant overall, but the availability of 15% to 25% greater torque to speed up the device, from cycle 87 until the boost pressure is achieved, (cycle 107) is significant and demonstrates another reason why the improved transient operation is achieved.

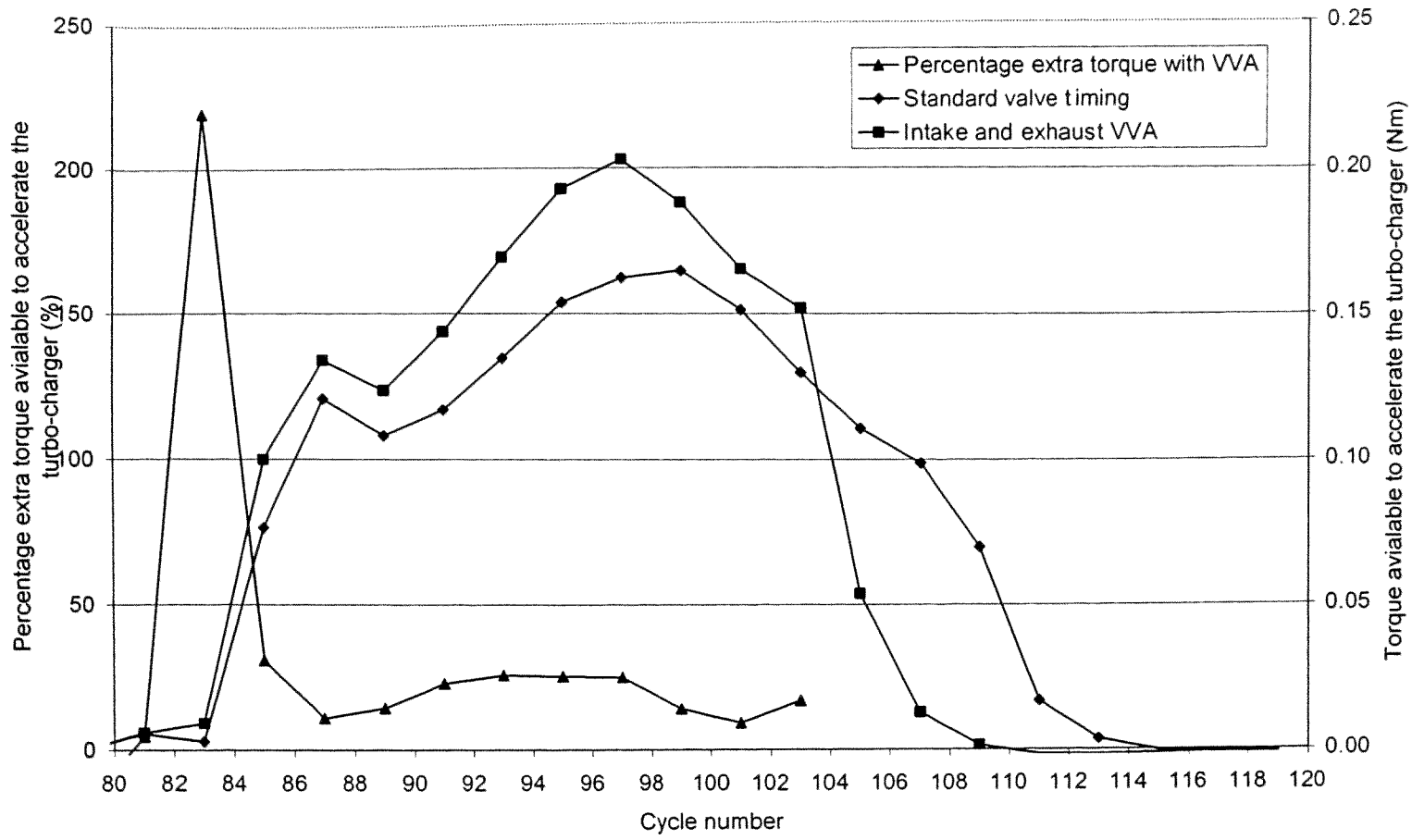


Figure 5.3.3.7 Mean torque available to accelerate the turbo-charger and percentage greater torque available with VVA

The fact that there is still torque to accelerate the turbo-charger at cycle 107, despite boost pressure being achieved is symptomatic of overshoot of the boost pressure controller. This can be seen in *figure 5.3.3.8*, which shows the VGT settings, the boost pressure target and actual boost pressure characteristics for the transients, the later demonstrating the overshoot. (It is interesting to note that despite greater airflow and output the model with VVA has a less restrictive VGT rack setting at the full load operating point because the volumetric efficiency of the engine is predicted to be higher.)

Thus it can be seen that VVA offers faster transient torque rise capability by maximising volumetric efficiency and thereby mass flow through the engine. This increased mass flow and the improved interaction between the turbine and the flow through it produce greater turbine net torque to accelerate the turbo-charger, leading to a faster rise in boost pressure. However, with the controller characteristics investigated here the application of VVA has no impact on the torque spike and air flow dip early in the transient.

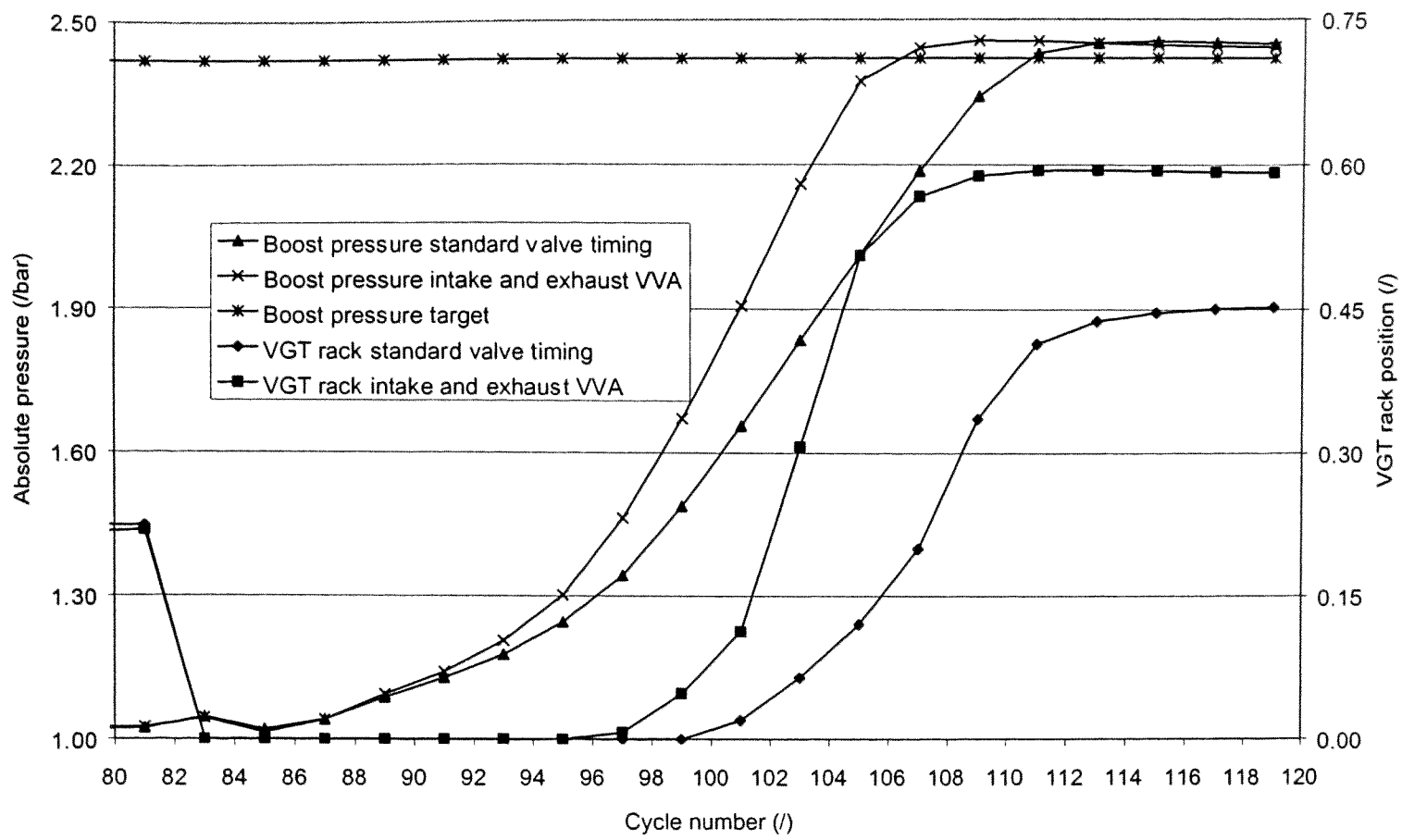
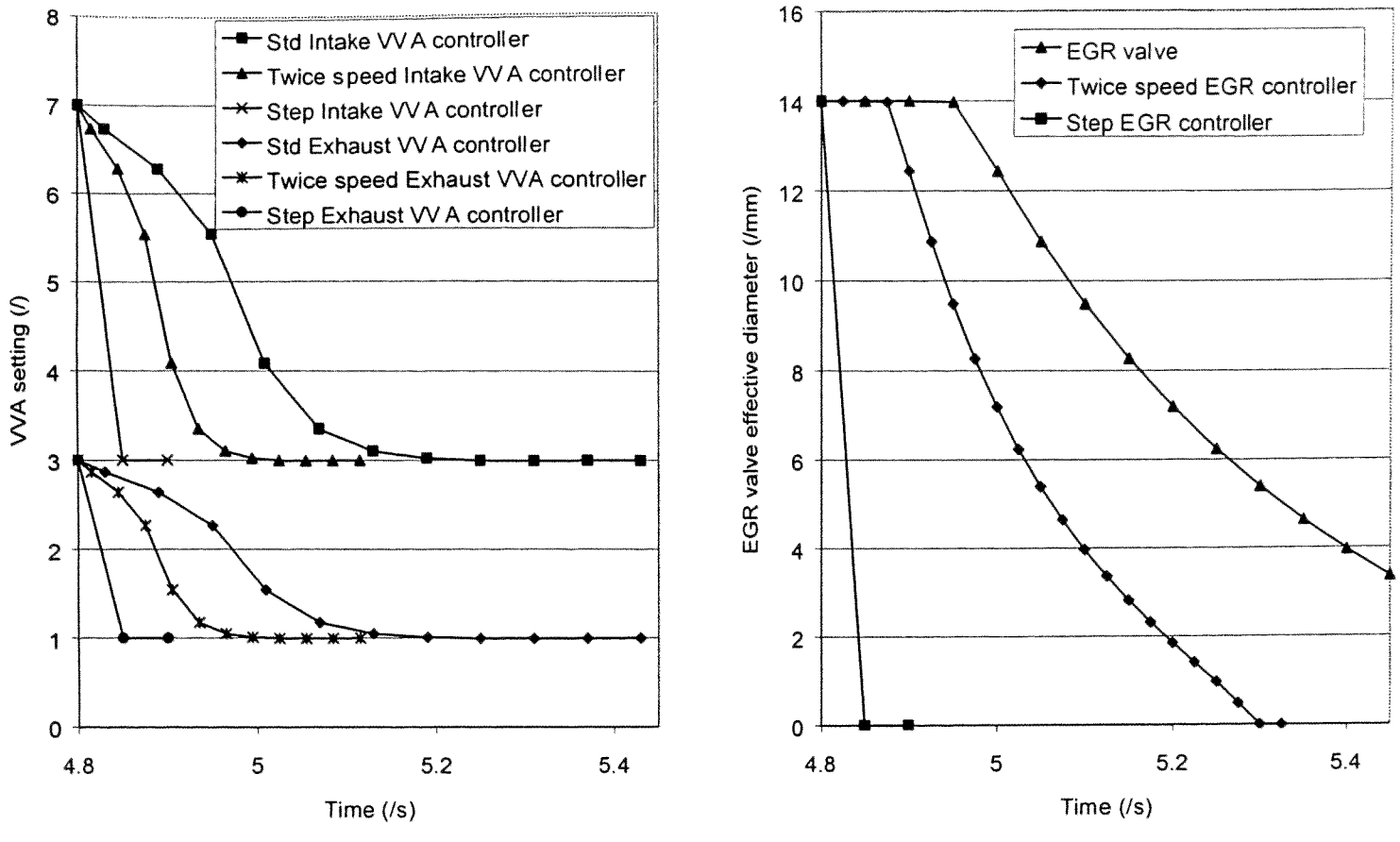


Figure 5.3.3.8 VGT settings and boost pressure during the transient.

Analysis of the above indicates that slowing the initial response of the VGT controller could remove the EGR spike and consequent air flow dip. However, it seems likely that this will be at the expense of slower and therefore less accurate control of EGR and less rapid transient response. Therefore consideration of the effects of a faster EGR valve and VVA controllers might provide alternatives that do not cause reductions in other aspects of the engine's performance.

5.3.4 Sensitivity to controller speed

An investigation was carried out into the effects of faster VVA and EGR controllers. For each of them a controller that was twice as fast, i.e. took half the time to complete the movement and a step response controller i.e. one that changed instantaneously were implemented. *Figure 5.3.4.1* shows the time characteristics of these controllers.



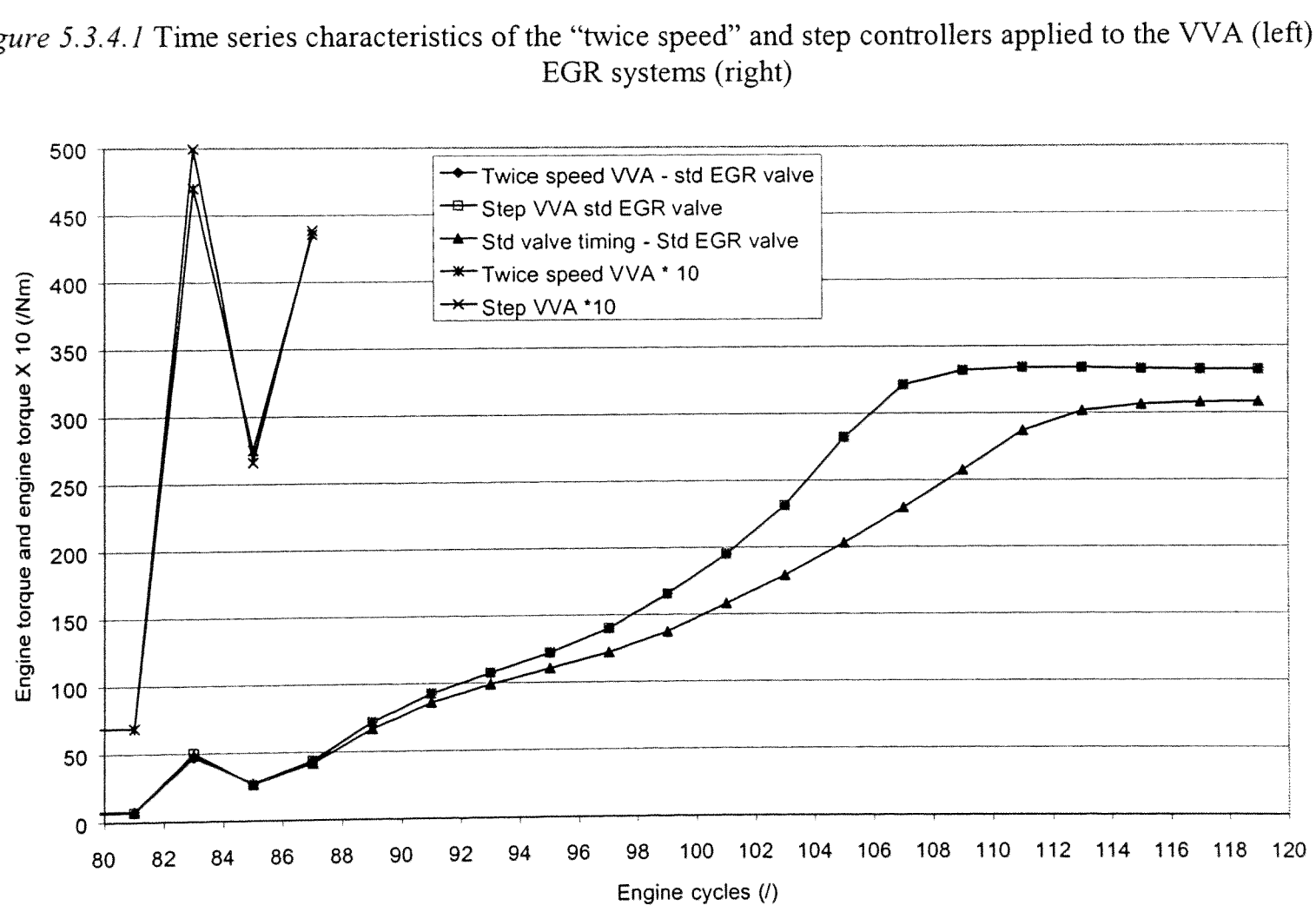


Figure 5.3.4.2 The effect of faster VVA controllers on torque rise.

Figure 5.3.4.2 shows the effects of the faster VVA controllers. It can be seen that the controller with the step characteristic offers only very small improvements over the twice speed and standard controllers in the early cycles. This is because it offers the possibility to optimise the intake VVA setting earlier in the transient. However, the advantages of the faster controller are so small as to offer little incentive to implement faster, and necessarily more expensive, controllers

for the VVA systems. (It is worth noting that direct valve actuation systems are capable of implementing these step changes.)

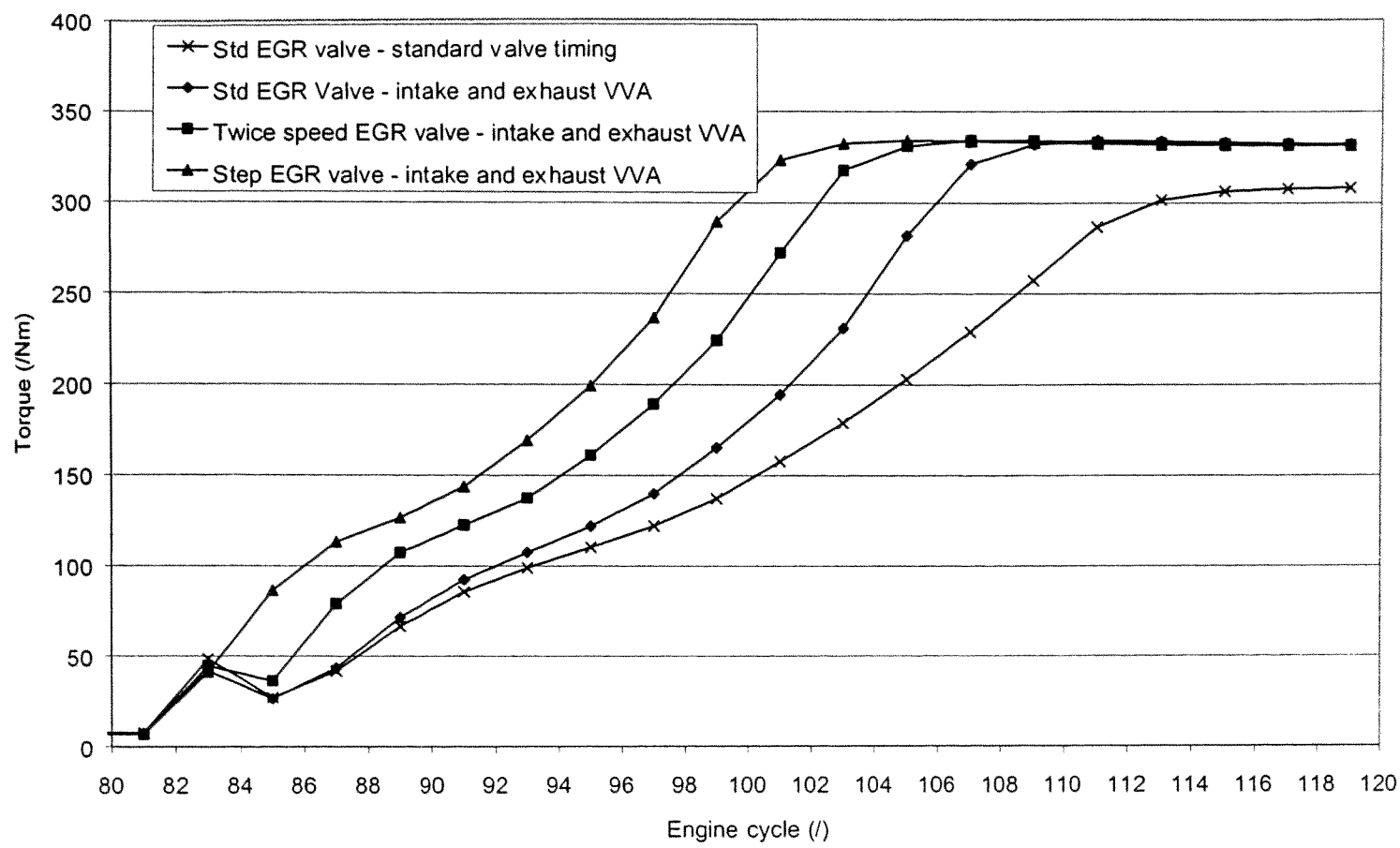


Figure 5.3.4.3. The effect of faster EGR valve controllers on torque rise.

From *figure 5.3.4.3*, it can be seen that EGR valve speed is very influential in the rate of torque rise. With a step characteristic EGR valve and VVA, approximately 100% more torque is available 10 engine cycles (0.6s) after the start of the transient when compared to standard and maximum torque is achieved 10 cycles earlier. From the above it is possible to comment on the validity of the assumptions made in the implementations of the controllers: it can be seen that faster VVA controllers offer little advantage, and provided they are faster than the EGR valve, making them slower is unlikely to affect the results of this type of work significantly. But faster EGR valve control does have a significant effect on torque rise. Therefore in investigations such as this it is important to have representative data for the response of the EGR valve.

In summary it has been found that the use of intake and exhaust VVA can improve the transient torque rise of a turbo-charged diesel engine, despite offering the potential to start the transient from an operating condition that offers improved fuel consumption, but reduced air flow. In a transient at 2000 rpm from 5mg/stroke fuelling and 50% EGR to full load at the same speed it has been shown that up to 40% more engine torque is available and standard engine full load torque is available 14 engine cycles earlier (0.84 seconds). Maximum torque is also improved with VVA as volumetric efficiency is higher.

The improved volumetric efficiency with VVA leads to significantly more excess turbine torque (between 15% and 25% for the majority of the transient) to accelerate the turbo-charger and turbine and compressor efficiencies that are also higher for a given time in the transient.

Investigation of the importance of controller speed has indicated that the system with greatest sensitivity to controller speed of response is the EGR valve, with even more significant improvements in transient torque rise available if a step closing characteristic can be achieved. However, it appears that provided the VVA controllers are not slower than that of the EGR valve making them faster is of little benefit.

5.4 CONCLUSIONS

Three areas of engine operation that are of major importance to the engine manufacturers have been examined through simulation. These were: 1) full-load torque, 2) part-load fuel economy, and 3) transient torque rise. For these investigations the model had to be extended to reproduce the effects of intake and exhaust VVA. In addition the investigation of part load operation required the provision of a closed loop controller to allow the VGT to modulate the pressure differential across the EGR valve and control EGR flow. A part load operating condition was the start of the torque transient investigated, but to implement the full transient, controllers for fuelling and AFR, intake and exhaust VVA systems, a second mode for the VGT setting (to control boost pressure) and for EGR valve opening were required.

The primary results presented here are the high level quantities that would be of interest to the engine manufacturer, the underlying effects that lead to these results and important considerations about the model are summarised in the conclusions section 6:

(As with all measured and predicted data there is a level of uncertainty attached to the results presented. Potential error bands are enumerated and explained in Appendix 2)

Full load torque

1. The increases in imep associated with just changes to IVC were: 4.8% at 1000 rpm, 7.6 % at 1500 rpm, 3.5% at 1800 rpm and 1.9% at 2000 rpm. At speeds above this they were 1% or less. (See table 5.1.3.1 for details)

2. The increases in imep associated with optimized IVC and EVO were: 9% at 1000 rpm, 23.2% at 1500 rpm, 19.8% at 1800 rpm, 14.1% at 2000 rpm, 6.3% at 2500 rpm, and 2.98% at 3000 rpm. At speeds above this the increases were 1% or less. (See table 5.1.4.1 for details)

Part load fuel economy

3. It was found that light part-load bsfc could be improved:

   - by up to 13% by retarding intake valve closing by 33° at 5mg/stroke fuelling and 50% EGR.

- by up to 4.5% by advancing intake valve closing by 33° at 5mg/stroke fuelling and 50% EGR.

- by up to 19% by retarding intake valve closing by 33° at 5mg/stroke fuelling and 10% EGR (It should be noted that this operating point may not be consistent with acceptable emissions.)

Transient torque rise

4. It was demonstrated that the use of variable duration VVA systems applied to both intake and exhaust valves could lead to improved transient torque rise. For the transient from 5mg/stroke fuelling and 50% EGR to full load at 2000 rpm the improvements shown by simulation were:

   - 10 cycles into the transient 6.6 Nm or 7.8% more torque was available

   - 20 cycles into the transient 37 Nm or 23% more torque was available

   - The equivalent of standard full load torque was achieved after 26 cycles, with VVA, 11 cycles or .66 seconds sooner than without. (Total transient time was reduced from 2.3 to 1.6 seconds)

6 CONCLUSIONS AND FUTURE WORK

6.1 CONCLUSIONS

6.1.1 Drivers for the adoption of VVA in light-duty diesel engines

Legislation

The relationships between the legislative pressures on fuel economy and emissions and the benefits provided by VVA in gasoline engines are well understood and are driving the application of VVA in these engines. However this relationship is not so clear with diesel engines as they are already very fuel efficient, but the effects VVA can have on their emissions are not well understood (although the potential for reductions in NO_x emissions has been identified, if the compression ratio can be lowered).

Corporate average fuel economy requires the vehicle manufacturers to reduce fuel consumption across their product range and the increasing market penetration of diesel engines is helping them achieve this. But the agreed future CO_2 levels require not just more diesels but smaller engines in general. Since diesels have higher specific torque than gasoline engines the use of smaller diesel engines seems likely, but increases in specific rating will be needed to help with customer perceptions. VVA is able to help with increasing specific rating and making diesels more efficient thus helping the manufacturers to meet legislated limits.

Customers demands

It is widely known that diesel engines exhibit significantly higher levels of low speed torque and exceptional fuel economy when compared with gasoline engines. However, they are perceived as inferior to gasoline engines in terms of maximum power and low speed transient drivability.

Diesel engine maximum power is limited by combustion speed, something that can probably only be addressed through fuelling system development. However, various methods of improving transient acceleration are under investigation, including electrically assisted turbo-chargers, variable geometry turbines and VVA. But, of these VVA is the only device that is able to influence turbo lag, significantly improve specific torque and part load fuel economy, and offer the potential for reduced emissions, and is thus able to help improve customer perceptions about diesel engines.

Manufacturer's economics

The economic equation for the adoption of VVA is not clear with diesel engines. With gasoline engines removal of EGR systems provides partial, or in some cases complete, funding of the VVA application, whereas with diesels this sort of direct exchange of function does not appear to be feasible. But there may be opportunities for the partial substitution of, or cost reduction of, some systems that form part of the exhaust system. Some modern diesel engines are fitted with lean "De-NO_x" catalysts and are likely, in the future, to be fitted with particulate traps. It is likely that in future VVA will be able to influence the operation of diesel engines to an extent where significant cost reductions can be achieved on these external systems, particularly through advanced combustion systems such as homogeneous charge compression ignition (HCCI).

These (currently) limited opportunities for cost offset perhaps make it less likely that this factor will influence the adoption of VVA on already relatively expensive engines. The main drivers to the adoption of VVA on diesel engines will be improved part load fuel economy, increased specific output and improved low speed transient drivability.

6.1.2 Necessary features for VVA in diesel engines

The fact that diesel engines have very high compression ratios means that they have very little clearance between the piston and the cylinder head face and valves when the piston is at TDC. This dictates that the valves can have little or no lift at overlap TDC. As a consequence, for conventional diesel engine operation, any VVA system employed is restricted to altering only EVO and IVC, leaving EVC and IVO in more or less standard positions. This requires VVA systems that can alter the open period of the valves

A review of many types of VVA systems has been carried out to assess their suitability for application to diesel engines. Whilst several system types were identified that can control valve open period, the majority of them altered the valve lift as well as period. For conventional diesel operation this is not desirable. The unsuitability of these systems left devices classified as "non-constant angular velocity" VVA systems as the most applicable. Two groups of devices in this general classification were reviewed and only those that retained full, direct, control of the valve motion were considered suitable.

A number of mechanisms within this classification were identified and from these a system was selected on the basis that it was well developed and had been successfully applied to gasoline engines. This design was investigated and shown to be able to provide appropriate control of EVO and IVC, and its dynamics and motion were analysed to allow investigation of its impact on valve train design. Subsequently, the behaviour of the mechanism was shown to have the potential to help in the optimisation of the complete valve train design in terms of cost, stress, valve spring design and space requirements.

6.1.3 Creation and correlation of the simulation model.

The conclusions in this section are reproduced from section 4.3.3 The objective of this work was to investigate the effects of VVA on those aspects of the operation of light duty diesel engines that are of interest to the engine and vehicle manufacturers, such as full load torque, part load fuel economy and increasing load transient operation. In all of these the quality of the simulation of combustion and the turbo-charger was very important.

A simulation model was constructed using a commercially available code, GT-Power and with the exception of the turbo-charger and combustion, the model used a high level of theory and physics and did not need any adjustment to achieve good correlation with baseline data. However, production of the turbine and compressor maps relied on extrapolation of manufacturer's data to cover the necessary operating regions. This was a manual process, reliant upon estimation of trends in the measured data and was the only area of model development where matters of judgement had the potential to significantly influence the results of the simulation.

The combustion modelling, implemented through the use of normalised fuel burning rate curves was adjusted (for each known steady state operating point) to be as near as possible, the same as the baseline, so good correlation was to be expected at the correlated operating points, but since the fuel burning rate characteristics were not responsive to trapped conditions there was the possibility that where predicted operating points (with VVA) were far from the correlated points, errors due to incorrect combustion characteristics could have occurred.

The full-load correlations between the model and the baseline for bmep, imep, fmep and pmep values and trends were good (maximum errors of 5% but typically less than 3%) and since the comparative simulations were carried out using the same fixed fuelling, the quality of bsfc and isfc correlation carried over. There were more significant differences in cylinder heat transfer, but it was known that GT Power used a modified Woschni, whereas the baseline results were produced using standard Woschni, however this only had a minimal impact on output.

The sub-systems that were least well correlated were the turbine and compressor, particularly at low speeds: The overall air flow through the engine correlated well (maximum error of 12% at 1000 rpm, less than 3.5% from 1500 rpm to 4000 rpm, and 4.4% at 4500 rpm). It should be remembered that for this comparison the boost pressure was controlled, so the only discrepancy was at 1000 rpm where the turbo-charger could not achieve the required boost.

More detailed inspection of the results revealed that turbine efficiency was being under-predicted and compressor efficiency slightly over-predicted, and these effects were to some extent cancelling each other out.

It is significant that at 1000 rpm engine speed, both the turbine and compressor were operating in areas of their maps that were the result of extrapolation of manufacturer's measured data, whilst at 4500 rpm the turbine was right at the edge of the measured data and the compressor was in an extrapolated region. This highlights the importance of the techniques used to extrapolate these operating maps as errors in this process can significantly affect the predicted engine performance.

Another potential problem with predicting compressor operation occurred when its operating locus ran off the edge of the compressor efficiency map, as happened at the lower engine speeds at full load. GT-Power truncated the efficiency at the value found at the edge of the map, but it is known that compressor efficiency falls rapidly after its operating point crosses the surge line. However it is not known by how much. It is possible that this truncation of the efficiency may have led to an over-prediction of the average compressor efficiency.

These potential problems at high and low speed are symptomatic of the problems associated with the extrapolation of the compressor maps. A different set of efficiency values for the very low speed and mass flow regions and extension further into the soft surge region would probably overcome these deficiencies, but there is no rigorous basis for this. Similar differences in the data

extrapolation for the turbine maps is likely to have occurred and may have led to differences in its predicted operation.

Despite these concerns, overall the model predicted trends and values well over the full load operating speed range and was considered adequate for use for the investigation of the effects of VVA.

6.1.4 Predicted engine performance improvements

As with all measured and predicted data there is a level of uncertainty attached to the results presented and whilst it is not usual to provide error bands for simulation results it was thought desirable to propose some for this piece of work. These error bands are enumerated and explained in Appendix 2 and should be applied as percentages of the percentage improvements quoted as results, such that if a predicted improvement is 20% and the error band is ±5% then the improvement ranges from 19% to 21%.

6.1.4.1 Full load torque

In interpreting the results of this section, several characteristics of the model and its operation should be kept in mind:

a. The VVA settings used were only discrete points and more detailed investigation would probably generate slightly greater improvements in torque.

b. The VGT settings used were those established during the baseline runs to produce the specified boost pressure. Detailed optimisation is likely to provide greater improvements in torque.

c. Fixed fuel burning rate characteristics were used for each speed. These did not respond to changes in trapped conditions, such as pressure and temperature at start of injection. At the low speed operating points the trapped conditions did vary considerably as trapped mass was significantly increased by the application of VVA.

d. No account was taken of the maximum cylinder pressure structural limitations of the base engine and at the lower speeds (1500 rpm to 2500 rpm) the P_{max} values exceeded the acceptable limit. This was not considered to be a constraint for this investigation.

Summarising the trends and results for full load operation:

1. With fixed, standard exhaust valve timing, advancing IVC by up to 33° crank improved imep at speeds up to 2500 rpm. At 3000 rpm the standard IVC was optimum and at speeds of 3800 and above retarding IVC by up to 22° crank increased output marginally.

2. The increases in imep associated with just changes to IVC were: 4.8% at 1000 rpm, 7.6 % at 1500 rpm, 3.5% at 1800 rpm and 1.9% at 2000 rpm. At speeds above this they were 1% or less. (See *table 5.1.3.1* for details)

3. With IVC at values that optimized output with standard exhaust timings: at 1000 rpm, imep could be increased by retarding EVO by up to 33°, with small increases in output available by advancing it by up to 22°; at speeds from 1500 to 2000 rpm the imep could be increased by retarding EVO by up to 33°, and by advancing EVO by 11° or more, up to 33° (a small reduction in imep occurred between std and 11° advanced); at 2500 and 3000 rpm imep could only be increased by retarding EVO by up to 22°; at 3800 rpm and above no significant change in output could be achieved over the whole range of EVO.

4. The increases in imep associated with optimized IVC and EVO were: 9% at 1000 rpm, 23.2% at 1500 rpm, 19.8% at 1800 rpm, 14.1% at 2000 rpm, 6.3% at 2500 rpm, and 2.98% at 3000 rpm. At speeds above this the increases were 1% or less. (See *table 5.1.4.1* for details)

5. At speeds up to 3000 rpm the greatest improvements in imep were achieved with retarded EVO, when it was found that the increase in expansion work (up to 360J/stroke at 1800 rpm) was far larger than the consequent increase in exhaust pumping work (up to 57J/stroke at 1800 rpm).

6. At engine speeds of 3800 rpm and above it was found that the pressure in the cylinder and that in the exhaust manifold remained similar for much of the period from EVO to TDC(o). Detailed investigation of the work distribution in the expansion and exhaust strokes showed that at 4500 rpm EVO had very little authority over either.

7. Inspection of the compressor operating points showed that at speeds of 3800 rpm and above, any increase in compressor speed and mass flow tended to reduce its efficiency, thus becoming to some extent self regulating and preventing increases in output.

8. A limited investigation showed that increasing the mass flow capability of the turbine and compressor by 10% allowed improvements in high speed output (7.4% at 4500 rpm, 4.8% at 4000 rpm and 4.3% at 3800 rpm). At 3000 rpm the effect was negligible but at the lower speeds it made the output worse. (All tests used the same VGT setting and optimized valve timings as with the standard turbine and compressor at these operating speeds.)

9. It was demonstrated that even at their minimum periods the exhaust valve open periods of consecutive firing cylinders overlapped. At high speeds this caused an increase in cylinder pressure towards the end of the exhaust stroke, which did not decay substantially before EVC. Earlier EVO made this worse. The use of a twin entry turbine would allow more effective use of advanced EVO by avoiding the interaction between cylinders.

6.1.4.2 Part load fuel economy

In interpreting the results of this section of work several characteristics of the part load model operation should be kept in mind:

a. The part load investigation was carried out at 2000 rpm, 2 fuelling levels (5mg/stroke and 10 mg/stroke), each at 10% 30% and 50% EGR.

b. Fixed fuel burning rate characteristics were used for each operating condition. These were derived from measured cylinder pressure data, and did not respond to changes in trapped conditions in terms of pressures and temperatures at start of injection. The use of VVA altered the trapped mass significantly.

c. The pressure differential across the EGR valve was modulated by the VGT nozzle setting controller to provide the required EGR level.

Summarising the findings for 2000 rpm part load operation.

1. It was demonstrated that whilst the required EGR levels can be achieved with a range of combinations of VGT setting and EGR valve orifice sizes, there are limits to these ranges. For instance at 30% EGR an effective EGR valve diameter of greater than 9mm was needed, if the VGT setting were to be anything other than fully closed, and smaller orifice sizes than these produced insufficient EGR irrespective of the VGT setting. For 10% EGR it was shown that sufficient EGR could be provided by effective diameters of less than 6 mm, but it was

also shown that for effective diameters of more than 9mm too much EGR resulted even with the VGT fully open.

2. Within the workable limits, it was demonstrated that the smaller the EGR valve orifice, then the more closed the VGT setting to achieve the required EGR flow and the higher the fuel consumption. It was also demonstrated that the higher the required EGR flow the higher the resulting fuel consumption.

3. This trend for increased fuel consumption with decreased EGR valve orifice size and higher level of EGR was shown to be in conflict with good transient drivability which requires minimised EGR valve orifice size, in order that it can close quickly to provide maximum torque rise rate on "tip-in" transients.

4. It was found that at light part-load, fuel economy could be slightly improved by retarding exhaust valve opening by up to 11° from standard.

5. It was found that outside the range of standard EVO to 11° retarded, changing EVO reduced output because:

   - Advancing EVO reduced expansion work more than it reduced exhaust pumping.
   - Retarding EVO further than 11° increased exhaust pumping work more than it increased expansion work.

6. It was found that light part-load bsfc could be improved:

   - by up to 19% by retarding intake valve closing by 33° from standard
   - by up to 5% by advancing intake valve closing by 33° from standard.

7. These improvements were produced by minimizing the mass flow through the engine, which reduced work done in the compression stroke and pumping work in the exhaust stroke.

8. The greater improvements associated with lighter loads highlight the potential for significant fuel economy benefits during the standard drive cycles, where large percentages of the cycle time are spent at light load and idle.

6.1.4.3 Transient torque rise

The investigation of transient torque rise was carried out at a constant 2000 rpm from 5mg/stroke fuelling with 50% EGR to full load, zero EGR, with the target boost level for the standard engine. This was selected as being representative of the start of an overtaking manoeuvre in a high gear. Combustion again relied on fuel burning rate data derived from measured cylinder pressure data. Controllers were implemented to co-ordinate the activities of the VGT, EGR valve and VVA settings.

The sequence of events modelled during the transient would be initiated by the driver pressing the accelerator pedal, which would trigger a change of operating mode from minimised emissions and fuel consumption to maximised output. This would be achieved by lowering the target AFR and providing adequate fuelling to achieve it, closing the EGR valve, and reducing the VGT setting to maximise boost. To replicate this sequence of events in the model, time based series were used to represent the changing inputs, with simultaneous step changes in AFR and available fuel representing the combination of driver input and engine management mode change. Up to the start of the transient the EGR valve was fully open, and the VGT setting was controlled to manage the amount of EGR. At the time of the step change in fuelling and AFR the controller for the VGT was switched to a boost pressure target from an EGR flow target, and a time based series representing the EGR valve controller closing response was applied.

Summarising the results of the transient torque rise investigation:

1. It was demonstrated that when a variable geometry turbine is used to modulate engine pressure differential to control the flow of EGR, if the VGT actuation is substantially faster than the EGR valve actuation, the interaction between the two systems can lead to short term increases in EGR levels at the beginning of "tip-in" transients.

2. It was demonstrated that the use of variable duration VVA systems applied to both intake and exhaust valves could lead to improved transient torque rise. For the transient from 5mg/stroke fuelling and 50% EGR to full load at 2000 rpm the improvements shown by the simulation were:

   - 10 cycles into the transient 6.6 Nm or 7.8% more torque was available
   - 20 cycles into the transient 37 Nm or 23% more torque was available

- The equivalent of standard full load torque was achieved after 26 cycles, with VVA, 11 cycles or .66 seconds sooner than without. (Total transient time was reduced from 2.3 to 1.6 seconds)

3. The reasons for these improvements were:

   - The VVA increased the engine's volumetric efficiency which in turn increased engine mass flow.

   - The efficiencies of the turbine and compressor were increased.

   - The improved volumetric efficiency and operating efficiencies with VVA led to significantly more excess turbine torque (between 15% and 25% for the majority of the transient) to accelerate the turbo-charger

4. An investigation into the sensitivity of the transient operation to controller speeds demonstrated that:

   - Provided the VVA controllers were faster than the EGR valve, then making them faster had little impact on transient torque rise rate.

   - A faster EGR valve controller had a significant effect on torque rise rate and could overcome the initial EGR excursion referred to in 1, above.

6.2 FUTURE WORK

The suggestions for future work fall broadly into three areas: those that arise from the findings of the research, those that arise from concerns about the modelling, and those that are prompted by recent developments in the field of VVA and diesel engines.

Future work arising from the findings of the research

As was pointed out earlier the optimisation of the VVA settings was carried out using a relatively coarse integer setting scale with only 7 positions covering the continuous 70° crank ranges available on EVO and IVC. Also the VGT settings used for the full load output simulations were chosen to be those that provided the required boost level with standard valve timings. It is

probable that re-optimisation of the VVA and VGT settings making use of their continuous variability would produce even larger improvements in imep.

In some cases the optima were achieved with extreme settings of the VVA, but trends of continued improvement were displayed. In these areas extended VVA ranges might provide more insight into the limits of these trends.

It was noted that at the lower engine speeds advancing EVO produced increases in full load imep, but the gains were not as significant as with retarded EVO. It was demonstrated that even at their minimum period the exhaust valve open periods of consecutive firing cylinders overlapped. At high speeds this caused an increase in cylinder pressure towards the end of the exhaust stroke, a problem that earlier EVO made worse. An investigation into the use of twin entry turbines and early EVO might yield results that help with the high speed output limitations.

It was noted that at the lower speeds where VVA produced large increases in imep the structural cylinder pressure limit of the engine investigated (P_{max}) had been exceeded. With modern fuel injection systems sophisticated injection profiles that alter timing and rate shape can be used to limit P_{max} whilst not losing significant imep. It would be instructive to investigate the extent of the trade-off between P_{max} and imep. This problem could also be addressed in an alternative way by investigation of the effects of reduced compression ratio on P_{max} and output.

A consequence of reduced compression ratio is inferior cold starting, if the standard valve timings are retained. However, advancing IVC towards BDC increases the effective compression ratio and is known to help with cold starting. An investigation of cold starting performance with a lowered compression ratio and intake VVA would provide insight into the extent to which a reduced compression ratio could be used to help with P_{max} limitations, at high imeps, with VVA utilised to restore the starting characteristics.

Future work arising from concerns about the modelling

A number of concerns were identified with the simulation model in those areas where "tuning" on the model, such as in the combustion model, was necessary, or extrapolation of measured data was needed, as with the compressor and turbine maps.

The tuning required to match the fuel burning rate characteristics to data was valid at the specified operating conditions, but when the operating conditions are perturbed from these

nominal points the validity of the combustion characteristics comes into question. This was the case when large increases in imep were predicted and during the transient simulations where interpolation between fuel burning rate characteristics was needed to deal with changing load and EGR content. It is desirable to carry out investigations into the uncertainty introduced by these approximations either by the use of a more physically based and sophisticated combustion simulation, or preferably by measurement of actual engine operation.

It has been shown that at the low and high engine speeds simulated the compressor and turbine operated in regions of their maps that were produced by extrapolation of manufacturer's measured data. It is desirable to carry out an investigation into the operation of the compressor and turbine at the extremities their maps to verify that the extrapolation of the maps is valid. Of particular interest are compressor operation in areas of extrapolation at low pressure ratios and mass flow, high speed and high mass flow, and into surge. For the turbine the areas of primary interest are low mass flows and pressure ratios and high mass flows and pressure ratios. It is unlikely that rig testing could be used to exercise the turbo devices into these regions under the correct conditions (pulsating flows usually yield lower efficiencies than steady flow) but careful measurement of their use on running engines should provide useful data.

At the highest level it is very important that the overall engine performance predictions are corroborated by measurements. Not only would this allow confirmation of the magnitude of the benefits, but would also provide insight into the extent of the errors caused by the less rigorous model elements.

Future work prompted by recent developments in the field of VVA and diesel engines

The discussion of the transient operation of a modern diesel engine has indicated the number of control systems that are needed for its correct operation and has highlighted their interactions and identified potential conflicts in their operation. The introduction of new after-treatment systems such as Lean NO_x catalysts and particulate traps, with their attendant control requirements, significantly increases the complexity of control strategy development and calibration. The investigation of a "hierarchy of controls" for these engines is an extremely challenging, but necessary piece of future work.

The introduction of the BMW "ValveTronic" variable valve lift and duration system has indicated that this type of VVA system might become cost effective over the next few years.

These systems operate over much larger duration ranges than the system discussed in detail here, but have a reduction of lift associated with a reduction in duration. With the very short valve open periods that can be achieved with this type of VVA it would be practical to investigate Miller cycle operation, the area of interest being to understand at what level of lift reduction does the engine start to lose the benefits of the Miller cycle.

The last area of significant future work is in the application of VVA for implementation of advanced combustion systems such as Homogeneous Charge Compression Ignition "HCCI." It has become apparent that control over cylinder composition through EGR and temperature and pressure history, through modulation of (effective) compression ratio are key factors in controlling and extending the operating area of this type of combustion system. Internal EGR can be generated, even in diesel engines, if negative overlap can be implemented, and control of IVC can modulate effective compression ratio; thus advanced VVA is potentially influential in the implementation of HCCI. It would be instructive to investigate the extent to which internal EGR and effective compression ratio can be modulated using advanced VVA.

7 APPENDICES

7.1 APPENDIX I

7.1.1 Miller and Atkinson cycles

A detailed discussion of these cycles is outside the scope of this thesis, but a brief discussion of each is provided in order to explain how they are defined. Comment on how they relate to the actual cycles implemented with the VVA system applied for this investigation is also provided.

It is important to note that these cycles, as strictly defined, are typically used in large medium speed diesel engines which have little residual wave action in the manifold systems and therefore IVC is typically very close to BDC and EVO is optimised to give the best balance between expansion work and energy flux to the turbine. These valve timings are very different to those used in high-speed light-duty diesel engines, and therefore the references to these cycles in the body of the thesis relate to valve timing strategies that have the same asymmetric valve timings, but are not used for the same reasons as the properly defined cycles.

7.1.1.1 Miller cycle

The "Miller" cycle, or system of engine operation relies on closing the intake valve before BDC to reduce the pressure and/or temperature at the end of the compression stroke. This is achieved because from IVC to BDC the charge is cooled by expansion, and thus relative to an engine with IVC near to BDC, the temperature and pressure at the start of compression are lower. It can be seen that without pressure charging this will result in a reduction of volumetric efficiency, but since this cycle is used with turbocharged engines an increase in boost pressure is provided to restore the mass flow through the engine. (Boost temperature is assumed to be held constant; a perfectly reasonable assumption since the engine would be intercooled.) Watson and Janota, (1982 – 1)

In this thesis the term Miller cycle is used to conceptually refer to valve timings that have IVC before BDC, but with the additional proviso that boost pressure is maintained or reduced and thus volumetric efficiency is reduced leading to reduced mass flow and compression work in part load operation.

7.1.1.2 Atkinson cycle

This name is frequently used to describe cycles that have a larger expansion ratio than compression ratio i.e. EVO is closer to BDC than is IVC. The relatively later EVO allows the piston to extract more useful work from the cylinder contents. (Stone, 1992 – 3). *Figure 7.1.2.1* shows an idealised air standard Atkinson cycle, with the shaded area representing the increased work output. It should be noted that in this diagram EVO is at point A, which as can be seen is only approximately half way down the expansion stroke. Real engines, particularly modern light duty diesel engines have relatively later EVO than shown and the potential benefits of this strategy are therefore reduced as the amount of extra expansion work that can be extracted is limited.

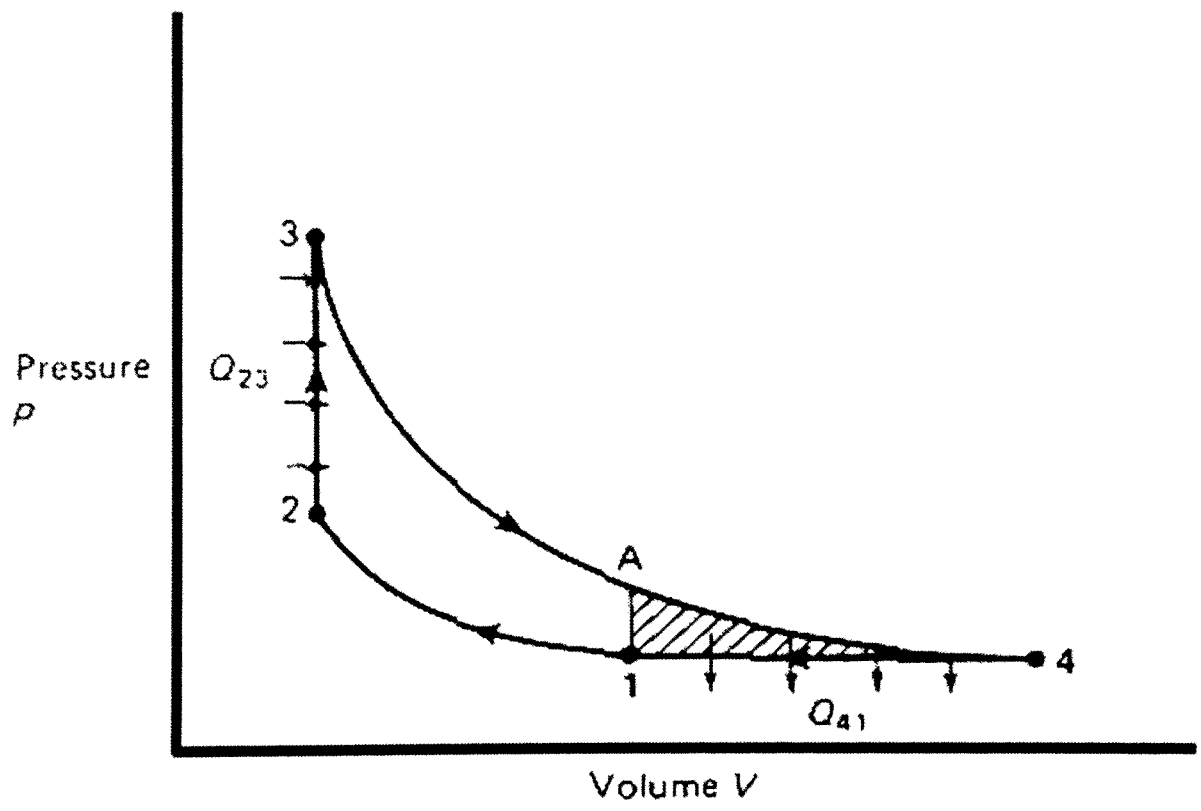


Figure 7.1.1.2.1 Ideal air standard Atkinson cycle (Stone, 1992-3)

However there is a variant of the Atkinson cycle, the so called "Otto-Atkinson" cycle (Blakey *et al* 1991) where the real engine Otto cycle remains, but late intake valve timing is used (to control air mass flow) providing substantially different compression and expansion ratios, and leading to the appended Atkinson part of the name. Blakey also mentions that late intake valve closing reduces the effective compression ratio. In the discussions of part load operation of the light duty diesel engine in this thesis the term Atkinson cycle is used to describe a cycle where late intake valve timing is used to reduce volumetric efficiency (and thereby mass flow) and also reduces compression work.

7.2 APPENDIX II

7.2.1 Simulation error band estimation

In experimental science it is normal to state anticipated levels of error and statistical significance (eg standard deviation) associated with the experimental processes and instrumentation, but this is typically only carried out when one variable is of particular interest and many measurements are required to obtain a reliable averaged result. With multivariate systems, such as an engine, estimating the errors in any particular measurement can be achieved by similar techniques. But when simulation is involved it is not conventional to state error bands or values for statistical significance. However, in order to try to put the results identified in this thesis into perspective a brief discussion of the causes and magnitudes of errors that might be expected in engine simulation is provided.

The results presented in this thesis are entirely the product of simulation. But whilst significant effort was made to correlate the simulation model against a mixture of output data from another simulation code, with a well correlated model, and limited measured data, there is clearly the potential for error in the output from the model.

The major sources of potential error in predicted engine output fall into the following system areas:

1. Pipe and junction (i.e. mixing or dividing) flows (this includes the effects of heat transfer in the manifold systems).
2. Orifice flows (particularly poppet valves).
3. Combustion and cylinder heat transfer.
4. Turbine and compressor operation.

The discussions below present the features of greatest significance to the accuracy of the simulation results and the estimates of the error bands are based on the experiences of the author and a "straw poll" of a small number of very experienced engine simulators as well as the originator and main developer of the GT-Power code. Percentages, unless otherwise stated, relate to the effect of errors on imep as this is the model output that most fully reflects the key aspects of engine operation discussed in this thesis.

7.2.1.1 Pipe flows.

Pipes are generally modelled using simplified Navier-Stokes equations in which flow property gradients are represented in one dimension along the pipe axis. Transverse gradients are assumed to be zero. Since

the equations used for calculating the flows through pipes are exact it is the quality of the data provided by the user that determines the accuracy of the predicted flows. Of particular significance are correct "boundary conditions" for the estimation of the surface friction and heat transfer, correct data describing pressure losses (i.e. irreversible compressions and expansions) in bends, convergent or divergent sections and junctions. The majority of this data is empirical in origin but readily available and an error band of ±2% is estimated for pipe flows.

7.2.1.2 Orifice flows.

The modelling of flows through orifices is based on the assumption of "Sharp edged orifice" flow. However, there are few orifices in an engine that really conform to this, whilst there are several of great significance to engine operation that do not, such as throttles and poppet valves. Therefore, these important orifices are typically modelled using measured flow coefficient data, which allow for changes in flow regime (as occurs with varying lift in poppet valve flow). For these important orifices the error bands are affected by measurement accuracy and a consistent definition of the pressure ratio at which the flows are measured. Estimated error bands are ±3-4% for intake valve and throttles with an additional ±2% for the exhaust valves because of deviations between the measured and actual operating conditions.

7.2.1.3 Combustion and cylinder heat transfer.

In this piece of work, as is often the case in engine simulation, under the standard operating conditions the combustion characteristics were adjusted to provide what amounts to the correct integral under the cylinder pressure-volume curve (i.e. the IMEP) to produce the required output. Thus the main source of error is the data processing error, which is estimated to produce an error band of ±3%

However, in both the full load and part load investigations, the effects of the VVA were such that the trapped masses deviated substantially from those at which the combustion characteristics were correlated. These departures from the correlated conditions could lead to changes in ignition delay and heat release profile. However, modern multi-shot fuel injection systems have the capability to tailor the shape of the heat release curve and it is considered that their use will minimise the error between predicted and achievable results.

In the case of increased mass flow, as was typically achieved with full load operation, the ignition delay could be expected to reduce and heat release rate to be controllable with multiple shot injection. Thus it is considered that for the full load case the departures in mass flow are not likely to cause large errors and an additional ±1% might be allocated to this.

In the part load case, where the mass flows were reduced, the situation may not be as controllable by the fuel injection characteristics and slightly larger differences between prediction measurement might result. An additional ±3% might be allocated to this.

7.2.1.4 Turbine and compressor operation.

The main feature of both the turbine and compressor that affects engine output is efficiency. Although, as discussed in earlier sections (4.2.3.2 and 4.3.3.3), the efficiency predictions are based on measured data, the accuracy of the overall predictions is affected by the use of steady flow data to represent highly pulsating flows and the need for extrapolation for operating points well outside the measured data. Thus the scale of the errors depends on the operating point of the turbocharger. At maximum efficiency these errors are of the order of ±3% and at very low mass flows they may be as great as ±10%. These errors are of most significance to full load operation, where the greatest error could therefore be anticipated, and indeed were found to be at very low speed. However, it should be noted that for the part load results presented there is little or no boost and the turbine and compressor are acting largely as flow restrictions. therefore the errors introduced are small despite the fact that the turbocharger is operating well outside the measured data.

7.2.1.5 Full system errors

There are a number of approaches that could be taken to producing "full system errors" based on the above constituent errors: the percentages could be summed, or they could be multiplied together in the $(1+a_1)*(1+a_2)*(1+a_3)$ ……$(1+a_N)$ form, where a_I represent the error bands scaled from unity. These two approaches give maximum errors bands of ±14% (summed) and ±14.7% (product) with a turbocharger operating well within its maps and ±21% (summed) and ±22.5% (product) with the turbocharger well outside its maps.

However, it is probably an invalid assumption that all errors are maximum at the same time, as the actual errors typically change in magnitude and sign, within their bounds, with speed and load and it is therefore likely that the actual total error band is smaller than calculated above. (An alternative that might be considered if the errors are thought to be random is to take the square root of the sum of the squares)

Typical error bands expected are imep ±5%, isfc ±7% but a very experienced user might achieve ±3% in imep. Gamma Technologies expect GT-Power to be able to predict the volumetric efficiency of a naturally aspirated engine to within ±3% and at full load would expect a model of a turbocharged engine

to predict results within ±5%. It is considered that ±2% for a full load torque curve is the best that can be expected. (Smith, 2003)

7.2.1.5.1 Full load.

Since the fuelling was AFR controlled for the full load simulations the results depended heavily on the predicted volumetric efficiency and it is considered from the above that this should be expected to be within ±5% taking account of the pipe and orifice flows and turbocharger. In addition the effects of the combustion errors are thought to be ±4% (±3% for processing error plus ±1% for increased mass flow) giving a total of ±9% for the full load results.

7.2.1.5.2 Part load

At the light part load operating points investigated in this piece of work, the turbocharger was not producing any significant boost and was acting primarily as a restriction to flow. The combustion characteristics were processed from measured cylinder pressure data, but the operating conditions were at lower mass flows. From this basis it is considered that errors are those associated with combustion (±6% worst case for processing errors and reduced mass flow), valve head flows (±6% worst case for intake and exhaust valves) and pipe flows (± 2%) as the major impact of the part load work was seen in pumping work. On the basis of this the error band is thought to be ±14% for the part load results.

8 REFERENCES / BIBLIOGRAPHY

Ahmad, T. and Theobald, M.A. (1989) A Survey of Variable-Valve-Actuation Technology. *SAE paper 891674.*

Alkidas, A.C. and In-Soo, S. (1991) The effects of intake flow configuration on the heat release and heat transfer characteristics of a single cylinder four valve SI engine. *SAE paper 910296.*

Annand, W.J.D. (1963) Heat transfer in the cylinders of reciprocating internal combustion engines. *Proc. I. Mech. E. Vol. 177, No36, pages 973 to 990.*

Annand, W.J.D. and Ma, T. (1971) Instantaneous heat transfer rates to the cylinder head surface of a small compression ignition engine. *Proc. I. Mech. E. Vol. 185, No72, pages 976 to 987*

Annand, W.J.D. and Roe, G.E. (1974) Gas flow in the internal combustion engine. *G.T Foulis and Co.*

Anon, (1999) *Financial Times Automotive Environment Analyst. Issue 54, page 12, July 1999.*

Asmus, T., (1991) Perspectives on Applications of Variable Valve Timing. *SAE paper 910445.*

Bassett, M.D., Winterbone, D.E. and Sierens, R. (1999) Steady flow loss-coefficient estimation for the exhaust manifold pulse-converter type junctions. *SAE paper 1999-01-0213*

Bassett, M.D., Winterbone, D.E. and Pearson R.J. (2000) Modelling engines with pulse converted exhaust manifolds using one dimensional techniques. *SAE paper 2000-01-0290*

Bazari, Z. (1992) A Diesel combustion and emissions predictive capability for use in cycle simulation. *SAE paper 920462.*

Bazari, Z. and French, B. (1993) Performance and emissions trade-offs for a HSDI diesel engine - An optimisation study. *SAE paper 930592.*

Beier, A., Distler, D. and Adamis, P., (1994) *German patent specification 4406968, entitled*: Knockenwellenanordnung mit einem auf einer nockenwelle begrenzt schwenkbar gelagerten schwenknocken.

Benajes, J., Reyes, E. and Lujan, J.M., (1996) Intake valve pre-lift effect on the performance of a turbocharged diesel engine. *SAE paper 960950.*

Benson, R.S., Garg, R.D. and Woolatt, D. (1964) The numerical solution of unsteady flow problems. *BSRA Report No. 375, and the International Journal of Mechanical Sciences, Vol. 6, no. 1, pages 117-144.*

Benson, R.S. (1982) The thermodynamics and gas dynamics of internal combustion engines. Volume 1. Edited by Horlock, J.H. and Winterbone, D.E. *Oxford University Press.*

Bickford, J.H., (1926) Mechanisms for intermittent motion. *Industrial Press, New York. Reprinted 1972.*

Birmann, R. (1946) *US Patent specification number 2406656, entitled:* Exhaust energy converting means for internal combustion engines.

Blair G.P. (1996) Design and simulation of Two-Stroke Engines. *Society of Automotive Engineers.*

Blakey, S.C., Saunders, R.J., Ma, T.H and Chopra, A. (1991) A design and experimental study of an Otto Atkinson cycle engine using late intake valve closing. *SAE paper 910451.*

Bohac, S.V., Baker, D.M. and Assanis, D.N. (1996) A global model for steady state and transient S.I. Engine heat transfer studies. *SAE paper 960073.*

Bull, G.L., (1924) *UK Patent Specification number 221,699, entitled:* Valve operating means for internal combustion engines.

Charlton, S.J., Stone C.R., Leonard, H.K., Elliott, C. and Newman, M.J. (1991) Transient simulation of a highly turbocharged diesel engine with variable valve timing. *Paper C430/016, Conference "Computers in engine technology. September 1991, Cambridge, UK. Institution of Mechanical Engineers.*

Chen, S.K. and Flynn, P.F. (1965) Development of a single cylinder compression ignition research engine. *SAE paper 650733.*

Church, W. and Farrell, P.V. (1998) Effects of intake port geometry on large scale in-cylinder flows. *SAE paper 980484.*

Colburn, A.P., (1933) A method of correlating forced convection heat transfer data and a comparison with fluid friction. *Trans. AIChE, vol. 29 pages 174-210.*

Dammers, W.A., (1997) A chronology of hydraulic lash compensation in the United States. *ASM. Paper 4, session 1. Proceedings of the international symposium on valve train system design and materials. Detroit 14-15th of April 1997.*

De Haller, R. (1945) The application of a graphic method to some dynamic problems in gases. *Sulzer technical Review 1, 6.*

Demmelbauer-Ebner, W., Dachs, A. and Lenz, H-P., (1991) Variable valve actuation systems for the optimisation of engine torque. *SAE paper 910447.*

Dent, J.C. and Sulaiman, S.J. (1977) Convective and radiative heat transfer in a high swirl direct injection diesel engine. *SAE paper 770407.*

Dresner, T. and Barkan, P (1989) A Review and classification of Variable Valve Timing Mechanisms. *SAE paper 890674.*

Earnshaw, S. (1910) On the mathematical theory of sound. *Proceedings of the Royal Society, 84*

Eichelberg, G. (1939) Some new investigations on old combustion engine problems. *(Originally published in German ZDVI, Vol 67, 1923)*

Fox, R. and McDonald, A., (1992) Introduction to Fluid Mechanics. *4th Edition, John Wiley and Sons Inc.*

Freudenstein, F., Maki, E.R. and Tsai, L.W. (1988) The synthesis and analysis of variable valve timing mechanisms for internal combustion engines. *SAE paper 880387.*

Frost, D., (1986) *UK Patent application number 2166842, entitled*: Drive mechanism for variable valve timing.

Frost, D., (1987) *UK Patent application number 2186939, entitled:* Cam drive mechanism.

Frost, D., (1992) *UK Patent application number 2247061, entitled:* Variable event valve timing.

Frost, D and Lancefield, T.M., (1996) *European patent specification 733154, entitled:* Variable valve timing.

Fuenmayor, J., Suarez, D.B. and Camarena, E. (1982) Synthesis of four-bar mechanisms with 2 variable parameters: application to total intake angle variation in an internal combustion engine. *Proc. 6th world congress on theory of machines and mechanisms, pages 209-212.*

Gamma Technologies (2001) GT-Suite CAE simulation tools for engines, powertrains and vehicles. GT-Power Version 5.1 engine simulation code used for this piece of work.

Gosman, A.D. (1985) Multi-dimensional modelling of cold flows and turbulence in reciprocating engines. *SAE paper 850344.*

Gosman, A.D., Hill, C., Marooney, C.J. and Sarantinos, M. (1991) Interactive computational fluid dynamics tools for engine design. *Institution of Mechanical Engineers. Paper C430/023, pages 1 to 6.*

Gray C., (1988) A Review of Variable Engine Valve Timing. *SAE paper 880386.*

Griffiths P. J. and Mistry K.N., (1988) Variable valve timing for fuel economy improvement, the Mitchell system. *SAE paper 880392.*

Han, Z., Henein, N.A. and Bryzik, W. (2000) A new ignition delay formulation applied to predict misfiring during cold starting of diesel engines. *SAE paper 2000-01-1184.*

Hara, S., (1993) *UK patent specification 2263529, entitled:* Device for controlling timing intake and exhaust valves of internal combustion engine.

Heath, (1988) Valve train design for multi-valve automotive gasoline engines. *SAE paper 885133.*

Hardenberg, H.O. and Hase, F.W. (1979) An empirical formula for computing the pressure rise delay of a fuel from its cetane number and from the relevant parameters of Direct–Injection diesel engines. *SAE paper 790493.*

Heywood, (1988 - 1) Internal Combustion Engine Fundamentals. (Valve timings.) *Section 6.3.1, pages 223-4 . McGraw-Hill.*

Heywood, (1988 - 2) Internal Combustion Engine Fundamentals. (Atkinson cycle.) *Section 5.6, pages 183-186 . McGraw-Hill.*

Heywood. J.B. (1988 - 3) Internal Combustion Engine Fundamentals. (Cylinder heat transfer.) *Section 12.4, pages 676 to 696. McGraw-Hill.*

Hiroyasu, H. and Kadota, T. (1976) Models for combustion and formation of nitric oxide and soot in direct injection diesel engines. *SAE paper 760129.*

Hiroyasu, H. Kadota, T. and Arai, M. (1983) Development and use of a spray combustion modelling to predict diesel engine efficiency and pollutant emissions. Part 1 Combustion modelling and part 2 Computational procedures and parametric studies. *Papers No. 214-12 and 214-13, Bulletin of the JSME, Vol. 26, No. 214, pages 569-583.*

Hollingworth, P. and Hodges, R.A, (1991) The history and mathematical development of cam profile design in Rover. *Institution of Mechanical Engineers, Autotech Conference, Birmingham, 1991, paper C427/1/107.*

Holmer, E. and Haggh, B., (1969) The turbo-charged diesel as a road transport power unit. *Proceedings of the Institution of Mechanical Engineers, Vol. 184 part 3P, pages 55 to 62, 1969-70.*

Horrocks, R.W. and Robertson, P.S. (1996) Light duty diesel developments for low emissions and low fuel consumption. *4th Internat'l Conference on the Automotive Industry and the Environment, Brussels, September 1996. Session 3, Paper 3.*

Hu, H., Israel, M.A. and Vorih, J.M. (1997) Variable Valve Actuation and Diesel Engine Retarding Performance. *SAE paper 970342.*

Hummel, K., Krieger, K. and Hansen, N., (2000) Evolution of the Bosch common rail system for passenger cars. *Paper 20A2012, International Symposium - The future of diesel engine technology for passenger cars. Oct 12-13, Costa Smeralda, Italy.*

Itoyama, H., Uchida, M. and Miwa, N., (1997) A Study of an EGR Control System for Diesel Engines Based on an Intake/Exhaust System Model. *SAE paper 970621.*

Jacques, B., (1997) Market place requirements and their impact upon valvetrain systems and architecture. *ASM. Paper 2, session 1. Proceedings of the international symposium on valve train system design and materials. Detroit 14-15th of April 1997.*

JANAF Thermochemical tables. (1971) NSRDS-NB537, *US National Bureau of Standards, June 1971.*

Jenny, E. (1950) Unidimensional transient flow with consideration of friction, heat transfer and change of section. *Brown Boveri Review, 37, 11, 447.*

Johns, R.J.R. and Jones, P.M. (1991) Computer modelling of the flow in a lean burn natural gas engine. *Institution of Mechanical Engineers. Paper C430/058, pages 21 to 26*

Kent, J.C., Mikulec, A., Rimal, L., Adamczyk, A.A., Mueller, S.R., Stein, R.A. and Warren, C.C. (1989) Observations of the effects of intake generated swirl and tumble on combustion duration. *SAE paper 892096.*

Kim, S.H., Huh, K.Y. and Fraser, R.A. (2000) Numerical prediction of the autoignition delay in diesel-like environment by the conditional moment closure model. *SAE paper 2000-01-0200.*

Knibb, Gormezzano and Partners (1998) Section 8, Legislation – Vehicle emissions and fuels. *Report commissioned by Mechadyne Ltd. KGP , Derby UK.*

Kohketsu, S., Mori, K. Sakai, K. and Hakozaki, T. (1997) EGR technologies for a turbocharged and intercooled heavy duty diesel engine. *SAE paper 970340.*

Krieger, R.B. and Borman, G.L. (1966) The computation of apparent heat release for internal combustion engines. *ASME paper 66-WA/DGP-4.*

Kreith, F. and Bohn, M.I. (1993) Principles of heat transfer. *5th edition. West Publishing Company, St Paul, MN, USA.*

Krüger, H., (1984) *German patent specification 3234640, entitled*: Ventiltrieb, insbesondere fur eine Brennkraftmaschine.

Lancefield, T.M., Gayler, R.J. and Chattopadhay, (1993) The practical application and effects of a Variable Valve Timing System. *SAE paper 930825.*

Lancefield, T.M., Bazari, Z., Smith, L.A., Pratt, R.W. and Brunt, M.J, (1995) An enhanced representation of the Four Valve Pent Roof Combustion Chamber for the calculation of flame area and flame intersections with the chamber surfaces and valve heads. *Paper number C498/15/113, Autotech Conference, Birmingham, 1995. Published by the Institution of Mechanical Engineers.*

Lancefield, T.M., Cooper, L. and French, B. (1996) Designing the control and simulation of EGR. *Automotive Engineer February/March 1996*

Lancefield, T.M. (1999) Control of residuals and pumping work in internal combustion engines using variable valve timing. *Transfer Report, Department of Engineering Science, University of Oxford*

Lancefield, T.M., Methley, I., Räse, U. and Kuhn, T. (2000) The application of variable event valve timing to a modern diesel engine. *(Draft SAE paper for the 2000 Congress in Detroit)*

Lax, P.D. and Wendroff, B. (1964) Difference schemes for hyperbolic equations with high order of accuracy. *Communications in Pure and Applied Maths, 17, 381-398.*

Lee, K., Yoo, S.C., Strueken, T., McCarrick, D., Shock, H., Hamady, F., Lapointe, L.A., Keller, P. and Hartmann P. (1993) An experimental study of in-cylinder air flow in a 3.5L four valve SI engine by high speed flow visualisation and two-component LDV measurement. *SAE paper 930478.*

LeFeuvre, T., Myers, P.S. and Uyehara, O.A. (1969) Experimental instantaneous heat fluxes in a diesel engine and their correlation. *SAE paper 690464.*

Leonard, H.J., Stone, C.R, Charlton, S.J, Johnstone, D., elliot, C. and Newman M. (1993) Design and analysis of a roller follower variable valve timing system. *SAE paper 930824.*

Lowe, A.S.H. and Morel, T. (1992) A new generation of tools for accurate thermo-mechanical finite element analyses of engine components. *SAE paper 920681.*

Ma, T., (1981) *UK Patent specification number 2096695, entitled:* IC Engine camshaft drive mechanism.

Ma, T., (1988) Effect of variable engine valve timing on fuel economy. *SAE paper No. 880390.*

McLaren, J.F.T., Tramschek, A.B., Sanjines, A. and Pastrana, O.F. (1975) A comparison of numerical solutions of the unsteady flow equations applied to reciprocating compressor systems. *Proceedings of the Institution of Mechanical Engineers, Vol. 17, No. 5.*

Meier, E. (1971) New exhaust systems for turbocharged internal combustion engines. *Brown Boveri Review, pages 161 to 166, Vol 58, Nos.4/5 April/May.*

Meistrick, Z. D., (1993) Auxiliary retarders compliment service brakes. *Truck Technology International. Pages 191 to 194. Sterling Publications International Ltd, London.*

Mews, H., Brehler, H., Maas, G., Seiffert, J. and Lehmann, J., (1994) The dynamic simulation of valve trains with hydraulic lash adjustment. *MTZ, March 1994, No. 3, published by Franckh-Kosmos Verlags-GmbH.*

Miller, D.S. (1990) Internal flow systems. *2nd Edition. BHR Group Ltd.*

Mitchell, S.W., (1978) *UK Patent specification number 1522405, entitled:* Improvements in or relating to valve timing mechanisms.

Mitchell, S.W., (1980) *UK Patent specification number 2066361, entitled*: Improvements in or relating to the valve timing mechanisms of internal combustion engines.

Morel, T., Fleming, M.F. and LaPointe, L. (1990) Characterisation of Manifold dynamics in the Chrysler 2.2 S.I. Engine by measurement and simulation. *SAE paper 900679.*

Morel, T. and Keribar, R. (1985) A model for predicting spatially and time resolved convective heat transfer in bowl-in-piston combustion chambers. *SAE Paper 850204.*

Morel, T., Keribar, R. and Blumberg, P.N. (1988 – 1) A new approach to integrating engine performance and component design analysis through simulation. *SAE Paper 880131.*

Morel, T., Rackmill, C.I., Keribar, R. and Jennings, M.J. (1988 – 2) Model for heat transfer and combustion in spark ignited engines and its comparison with experiments. *SAE paper 880198.*

Morel, T., Wahiduzzaman, S. (1996) Modelling of diesel combustion and emissions. *FISITA 1996.*

Muller, M., Hendricks, E. and Sorenson, S. C. (1998) Mean value modeling of turbocharged spark ignition engines. *SAE paper 980784.*

Nagle, J. and Strickland-Constable, R.F. (1962) Oxidation of Carbon between 1000-2000 °C. *Proceedings of the 5th Carbon Conference, Vol 1, pp 137-164, Pergamon Press, 1962.*

Oehling, K-H, Teichmann, R. and Unger, H. (1995) Requirements and potentials of future valve train concepts. *Institution of Mechanical Engineers. Paper C498/15/207, Autotech 1995.*

Olikara, C. and Borman, G.L. (1975) A computer program for calculating properties of equilibrium combustion products with some applications to IC engines. *SAE paper 750468*

Olree, R.M. and Lenane, D.L. (1984) Diesel combustion cetane number effects. *SAE paper 840108.*

Osborne, R.P. and Morris, T. (2002) Aspects of EGR control on turbocharged light-duty diesel engines. *Paper C602/013/2002 from the seventh International conference on Turbochargers and Turbocharging Published by the Institution of Mechanical Engineers. London May 2002.*

Parker, P.H., (1992) *UK Patent Specification Number 2252130, entitled:* An internal combustion engine camshaft drive mechanism.

Parker, P.H., (1994) UK Patent Specification Number 2268570, entitled: I.C. engine camshaft drive mechanism.

Parker, D.A. and Kendrick, M. (1974) A camshaft with variable lift-rotation characteristics; Theoretical properties and application to the valve gear of a multicylinder piston engine. *Fisita congress 1974, Paris, p224-232*

Paulmier, C., (1974) Variable valve timing for poppet valve internal combustion engines. *Ingens De L'Auto paper number M24909, pages 1-19, June/July 1974.*

Peters, B. and Gosman, A.D. (1993) Numerical simulation of unsteady flows in engine manifolds. *SAE paper 930609.*

Pethers P. (1997) The business perspective – Engineering affordable solutions to the HSDI Diesel Euro IV challenge. *I. Mech. E. Conference: Euro IV challenge – Future technologies and systems. 3-4 December 1997, London.*

Phlips, P and Schamel, A. (1991) The dynamics of valve trains with hydraulic lash adjusters and the interaction with the gas exchange process. *SAE paper 910071.*

Phoenix L. and Phoenix J., (1991) A camshaft mechanism for synchronous phasing valve timing. *SAE Paper 910448.*

Poloni, M., Winterbone, D.E. and Nicholls, J.R. (1987) Calculation of pressure and temperature discontinuity in a pipe by the Method of Characteristics and the two-step differential Lax-Wendroff method. *International Symposium on Flows in Internal Combustion Engines, FED, Vol. 62. ASME Winter Annual Meeting, Boston, 13-18 December.*

Poulos S.G. and Heywood, J.B (1983) The effect of chamber geometry on spark ignition engine combustion. *SAE paper 830334.*

Rayleigh, Lord (1910) Axial plane waves of finite amplitude. *Proceedings of the Royal Society 84.*

Reimann, B. (1885) Uber die fortpflanzung ebener luftwellen von endlicher schwingungsweiße. *Bott. Abh. 8 (Math)*

Roe, G.E. (1972) Variable valve timing unit suitable for internal combustion engines. *Proc. Inst. Mech. Engineers Vol. 186, 23/72.*

Scott, D. and Yamaguchi, J. (1980) Eccentric cam drive varies valve timing. *Automotive engineering October 1980. Published by the Institution of Mechanical Engineers, UK.*

Shapiro, A.H. (1954) The dynamics and thermodynamics of compressible fluid flow. *Vol II, The Ronald Press.*

Sihling, K. and Woschni, G. (1979) Experimental investigation of the instantaneous heat transfer in the cylinder of a high speed diesel engine. *SAE paper 790833.*

Smith, L.A. (1999) Evaluation of Exhaust Brakes as Back Pressure Simulators on Engine Testbed. *GT-Power User's Conference, Frankfurt, October1999.*

Smith, L.A. (2003) Private communication. *Contact details MIRA, Watling Street, Nuneaton, Warks. Tel 02476 355 365.*

Spalding, D.B. (1976) Mathematical models of turbulent flames: A review. *Combustion Science and Technology, Vol 13, Nos 1-6, pages 3-25.*

Stein, R.A., Galietti, K.M. and Leone, T.G., (1995) Dual equal VCT – A variable camshaft timing strategy for improved fuel economy and emissions. *SAE paper 950975.*

Stone, C.R. (1992-1) Introduction to Internal Combustion Engines. Second Edition. (Wiebe functions) *Pages 96 to 100. Society of Automotive Engineers Inc. USA..*

Stone, C.R. (1992-2) Introduction to Internal Combustion Engines. Second Edition. (Cylinder heat transfer) *Pages 377 to 381. Society of Automotive Engineers Inc. USA.*

Stone, C.R. (1992-3) Introduction to Internal Combustion Engines. Second Edition. (Cylinder heat transfer) *Pages 32 to 33. Society of Automotive Engineers Inc. USA..*

Stone, C.R. and Kwan, E. (1985) Variable valve timing for IC engines. *Intitution of Mechanical Engineers. Automotive Engineer, August/September 1985, pages 54-58.*

Stone, C.R. and Kwan, E. (1989) Variable Valve Actuation mechanisms and the potential for their application. *SAE paper 890673.*

Stojek I.D. and Stwiorok A., (1983) Valve Timing with Variable Overlap Control. *Fisita paper 845026.*

Tai, C., Tsao, T., Schörn, N. and Levin, B. (2002) Increasing torque output from a turbodiesel with camless valvetrain. *SAE paper 2002-01-1108.*

Takeyama, S., Ishizawa, S., Yoshikawa, Y. and Takagi, Y. (1987) Gas exchange simulation model for improving charging efficiency of a four-valve internal combustion engine. *Paper C28/87 The Institution of Mechanical Engineers.*

Wallace, F.J. and Adgey, J. (1967-8) Theoretical assessment of the non-steady flow performance of inward radial flow turbines. *Proc. Instn. Mech. Engineers, Vol 182, part 3H, pages 22-36.*

Walter, G.A. and Chapman, M. (1979) Numerical simulation of the exhaust flow from a single cylinder of a two cycle engine. *SAE paper 790243.*

Wampler, C., (1993) Type synthesis or mechanisms for variable valve timing. *SAE paper 930818.*

Watkins, A.P, Lea, C.J, and Gül, M.Z. (1991) Development of advanced turbulence models for the calculation of flows in internal combustion engine cylinders. *Institution of Mechanical Engineers. Paper C430/025, pages 7 to 20*

Watson, H.C. and Chow, H.C., (1991) Inclusion of hydraulic lash adjuster behaviour and gas dynamic forces in camshaft design. *Institution of Mechanical Engineers. Paper C430/064, pages 251 to 258.*

Watson, N. and Janota, M.S., (1982) Turbocharging the internal combustion engine.. *Macmillan Press, 1982.*

Watson, N. and Janota, M.S., (1982 - 1) Turbocharging the internal combustion engine.. *Macmillan Press, 1982, Section 11.2 pp 380-386.*

Watson, N. and Marzouk, M., (1977) A non-linear digital simulation of turbo charged diesel engines under transient conditions. *SAE paper 770123.*

Watson, N., Pilley, A.D. and Marzouk, M., (1980) A combustion correlation for diesel engine simulation. *SAE paper 800029.*

Whitely, F., (1995) VVC for Rover K series. *Automotive Engineer April/May 1995. Published by the Institution of Mechanical Engineers. UK.*

Wiebe, I., (1956) Habempirische formel für die verbrennungsgeschrwindigkeit. *Verlag der Akademie der Wissenschaften der VdSSR, Moscow.*

Williams, C. (1997) New Beetle boasts revolutionary VVT. *Autocar 27 August 1997.*

Winterbone, D.E., Nikpour, B. and Alexander, G.I. (1990) Measurement of the performance of a radial inflow turbine in conditional steady and unsteady flow. *Paper C405/015, from the 4th international conference "Turbocharging and Turbochargers", Institution of Mechanical Engineers.*

Winterbone, D.E., Pearson, R.J. and Zhao, Y. (1991) Numerical simulation of intake and exhaust flows in a high speed multi-cylinder petrol engine using the Lax-Wendroff method. *Paper C430/038, from the international conference "Computers in Engine Technology", Institution of Mechanical Engineers.*

Winterbone, D.E. and Pearson, R.J., (1999) Design techniques for engine manifolds: Wave action methods for IC engines. *Professional Engineering Publications, page 368.*

Winterbone, D.E. and Pearson, R.J., (2000) Theory of engine manifold design: Wave action methods for IC engines. *Professional Engineering Publications.*

Wolfer, H.H., (1938) Der zünderzug im dieselmotor. *CDI-Forschungsheft.*

Woschni, G., (1967) A Universally applicable equation for the instantaneous heat transfer coefficient in the internal combustion engine. *SAE paper 670931*

Yamada, T,. Ikeya, N. and Kondoh, N., (1998) New EGR system for heavy duty diesel engines. *SAE paper 980775.*

Yeo, J.H. and Baines, N.C. (1990) Pulsating flow behaviour in a twin-entry vaneless radial-inflow turbine. *Paper C405/004, from the 4th international conference "Turbocharging and Turbochargers", Institution of Mechanical Engineer*

Yoshizaki, T., Nishida, K. and Hiroyasu, H. (1993) Approach to low NO_x and smoke emission engines by using phenomenological simulation. *SAE paper 930612.*

Zappa, G. and Franca, T. (1979) A 4-stroke high speed diesel engine with two stage of supercharging and variable compression ratio. *13th Congres International des Machines a Combustion, Vienna 1979. Paper D19, session B3.*

Ziegler, J. and Nichols, N.B. (1942) Optimimum settings for automatic controllers. *Trans ASME* 64, *page 759.*